ERANET SEAS-ERA

Towards Integrated Marine Research Strategy and Programmes

EMoSEM Final Report

Ecosystem **Mo**dels as **S**upport to **E**utrophication **M**anagement In the North Atlantic Ocean (EMoSEM)

FINAL REPORT

31/08/2015

Funding agencies:

ANR belspo

CONTRACT NUMBER SD/ER/11

CONTACT INFORMATION

COORDINATOR
Geneviève Lacroix
Royal Belgian Institute of Natural Sciences (RBINS)
Operational Directorate Natural Environments (DO Nature)
Gulledelle 100 – 1200 Brussels (Belgium)
Phone: +32 2 7732100, email: glacroix@naturalsciences.be

OTHER PARTNERS
Christiane Lancelot
Ecology of Aquatic Systems (ESA)
Free University of Brussels (ULB)
Avenue Franklin Roosevelt, 50 – 1050 Brussels (Belgium)
Phone: +32 2 6505988, email: lancelot@ulb.ac.be

Alain Ménesguen
Department of Coastal Environment Dynamics (DYNECO)
French Research Institute for Exploration of the Sea (IFREMER)
Centre de Brest, B.P. 70 – 29280 Plouzané (France)
Phone : +33 2 98224334, email : amenesg@ifremer.fr

Gilles Billen
UMR METIS
Pierre.et Marie Curie University (UPMC)
Place Jussieu 4 – 75005 Paris (France)
Phone: +33 1 44275019, email: gilles.billen@upmc.fr

Ramiro Neves
Institute of Marine Research (IMAR)
Instituto Superior Técnico
Av. Rovisco Pais 1 – 1049-001 Lisboa (Portugal)
Phone : +351 21 8417397, email : ramiro.neves@ist.utl.pt

AUTHORS
Xavier Desmit, Geneviève Lacroix, Valérie Dulière (RBINS)
Christiane Lancelot, Nathalie Gypens (ULB),
Alain Ménesguen, Bénédicte Thouvenin (IFREMER), Morgan Dussauze (ACTIMAR)
Gilles Billen, Josette Garnier, Vincent Thieu, Marie Silvestre, Paul Passy, Luis Lassaletta, Gabriel Guittard, Sylvain Théry (UPMC)
Ramiro Neves, Francisco Campuzano, Carla Garcia, Ligia Pinto, João Sobrinho, Marco Mateus, Isabella Ascione Kenov (IMAR)

PROJECT WEBSITE: http://odnature.naturalsciences.be/emosem/

Table of content

Abbreviations used in this report

BE	Belgium
Chl	Chlorophyll *a* concentration (µgChl L^{-1})
Chl P90	90^{th} percentile of Chlorophyll *a* concentration (µgChl L^{-1})
DA	Diatom phytoplankton concentration (µgC L^{-1})
DIN	Dissolved Inorganic Nitrogen concentration (µmol L^{-1})
DIP	Dissolved Inorganic Phosphorus concentration (µmol L^{-1})
DONUTS	Database of Observed NUTrients in riverS
Ecozone	Ecological zone, i.e. sub-area determined on the basis of RS Chl P90
EEZ	Exclusive Economic Zone (national maritime boundary definition)
FR	France
GAP	Good Agricultural Practices (also a model scenario combining UWTD & GAP)
GEnS	Good Environmental Status (MSFD)
GES	Good Ecological Status (WFD)
Inhequ	Inhabitant equivalent
LocOrgDem	Local production, Organic farming, Demitarian diet (name of a model scenario)
MSFD	Marine Strategy Framework Directive
MS	Member States of the European Union
NDA	Non-diatom phytoplankton concentration (µgC L^{-1})
NDAChl	Non-diatom chlorophyll *a* concentration (µgChl L^{-1})
NEA	North-East Atlantic
OSPAR ICG-EMO	OSPAR Intersessional Correspondence Group on Eutrophication Modelling
P90	Percentile 90 (i.e. value below which 90% of the data may be found)
PDF	Probability Distribution Function
PFT	Phytoplankton Functional Type (e.g. diatom, dinoflagellate etc.)
Pristine	The pristine situation (also the name of a model simulation)
PT	Portugal
PyNuts	New generic modelling platform supporting the Riverstrahler model (nutrients transport and biogeochemistry in river systems)
RS	Remote Sensing (satellite-borne)
SBNS	Southern Bight of the North Sea
UWTD	Urban Wastewater Treatment Directive (also the name of a model scenario)
WFD	Water Framework Directive

Executive Summary

One of the leading challenges in marine science and governance is to improve scientific guidance of management measures to mitigate eutrophication nuisances in the EU seas. Too few approaches integrate the eutrophication process in space (continuum river-ocean) and in time (past, present and future status). A strong need remains for (i) knowledge/identification of all the processes that control eutrophication and its consequences, (ii) consistent and harmonized reference levels assigned to each eutrophication-related indicator, (iii) identification of the main rivers directly or indirectly responsible for eutrophication nuisances in specific areas, (iv) an integrated transboundary approach and (v) realistic short term and long term nutrient reduction scenarios. As a step in this direction (ou in agreement), the main objective of EMoSEM was to link the eutrophication nuisances in specific marine regions of the North-East Atlantic (NEA) to river anthropogenic inputs, trace back their sources up to the watersheds, then test nutrient reduction options that might be implemented in these watersheds and propose consistent indicators and reference levels to assess Good Environmental Status (GEnS).

To achieve this objective, the state-of-the-art modelling tools describing the river-ocean continuum in the NEA continental seas have been developed and combined. Three marine ecological models (BIOPCOMS, ECO-MARS3D, MIRO&CO) have been adapted and coupled to a newly developed generic ecological model for European river-basins (PyNuts-Riverstrahler). The modelling tools have been validated against observations. Numerical methods have been included in the marine models to track the origin of nutrients at sea from different sources (riverine, oceanic and atmospheric). State-of-the-art tools based on the transboundary nutrient transport (TBNT) and the distance-to-target (DTT) methods have been improved to estimate the riverine nutrient reductions necessary to reach the GEnS in the sea. Scenarios have been designed to estimate natural and anthropogenic nutrient contributions to the watersheds for the pristine conditions (simulated from a situation where Europe is covered in forests without human impact), for the contemporary situation, and for future realistic nutrient reduction scenarios (e.g. waste water treatment plants, good agricultural practices and conversion to local, organic farming and demitarian diet).

Maps of common eutrophication indicators (e.g. winter DIN, winter DIP and percentile 90 of chlorophyll concentrations (Chl P90)) have been computed from model results integrated over the whole NEA. Background values of the same indicators have been estimated and mapped, based on model results obtained for the pristine scenario. Areas subjected to anthropogenic eutrophication in the NEA have been identified from differences between contemporary and pristine situations. Based on Chl P90, these areas cover the French coastal zone of the Bay of Biscay, the Seine Plume and the Belgian and Dutch coastal zones. Less intense eutrophication is found along the coasts of Portugal and offshore in the English Channel and the Southern Bight of the North Sea.

Mitigating the current eutrophication requires the implementation of nutrient reduction options at the level of the river watersheds. Three scenarios of nutrient reduction were

examined based on realistic adaptations of human activities in the watersheds. (1) The scenario corresponding to the full implementation of the *Urban Wastewater Treatment Directive* showed that most Wastewater Treatment Plants required by the UWWTD (Directive 91/271/EEC) are already operational. (2) The *Good Agricultural Practice* scenario showed that a change to reasoned agricultural practices results in better quality drainage waters but is not sufficient to mitigate marine eutrophication nuisances. (3) The *Local Organic Demitarian* scenario implies radical changes in the agro-food system. The effect of this scenario is considerable in terms of nitrogen surplus reduction and results in significant improvement of water quality along the drainage network as well as a strong reduction of the nitrogen fluxes to the sea which in turn results in significant improvement of the marine eutrophication status.

Relative contributions from different sources of nitrogen and phosphorus to the marine ecosystem have been computed. Along the Iberian Peninsula, significant river-borne nutrient transport may be observed along the coastal zone in the south-west direction during the wet season in summer, though there is hardly any transboundary exchange of nutrients between Member States in that marine region. In the Bay of Biscay, the Loire river brings nitrogen along the coasts of Brittany and up to the English Channel. The transboundary nutrient transport is significant in the English Channel and the Southern Bight of the North Sea (SBNS), due to the combination of high nutrient loads from the rivers (e.g. Seine, Scheldt, Rhine, Meuse and Thames) and the patterns of water transport. Any marine area within the NEA would generally count different contributors in terms of nutrient enrichment. Surprisingly, in the Bay of Biscay, English Channel and SBNS, nitrogen atmospheric depositions account for about 10 to 20% of the nitrogen present in phytoplankton.

The DTT exercise provided useful information regarding the river load reductions necessary to reach the GEnS in target areas. DTT results showed that (1) dual-nutrient reduction (N,P) in the rivers is necessary to reduce the transboundary contamination and mitigate eutrophication and (2) the reduction needed to reach the GEnS depends on the target area (WFD or MSFD) and chosen threshold values for indicators. Two sets of threshold values have been tested. In the "rigorous" case, threshold values (8 µgChl L^{-1}, 9.0 µmol L^{-1} and 0.56 µmol L^{-1} for Chl P90, winter DIN and winter DIP, respectively) are representative of background values close to the pristine situation, and in the "lenient" case, threshold values (15 µgChl L^{-1}, 19.5 µmol L^{-1} and 0.65 µmol L^{-1} for Chl P90, winter DIN and winter DIP, respectively) are close to values recommended by the WFD/MSFD. Necessary dual-nutrient reductions in rivers have been computed and showed significant differences between both cases. . The optimal river loads reductions required to achieve the GEnS in the sea were compared to the nitrogen reductions in the river loads estimated by PyNuts for the *Local Organic Demitarian* scenario. The latter are generally in the range of the reductions calculated by the DTT between the rigorous and lenient cases. This suggests that the status of marine eutrophication will be significantly improved across the NEA if such a scenario is implemented in the future.

The EMoSEM project stimulated the rational to more universal and transboundary approaches to estimate the GEnS in large areas like the NEA and led to design transboundary **Ecozones** across the NEA. New sub-areas have been defined based on ecological criteria (e.g. highly eutrophic vs. oligotrophic) instead of usual political boundaries. A **new indicator** ("non-diatom chlorophyll *a"*, NDAChl) was proposed to complement the Chl P90 indicator. This new indicator reflects the phytoplankton composition and provides indications on potential nuisance or

toxicity due to the presence of undesirable species. **Background values** of the ratio between winter DIN and winter DIP obtained from model results for the pristine situation equals 30 molN $molP^{-1}$ in some coastal zones, whereas the reference ratio value which is commonly accepted (OSPAR, MSFD, WFD) is set to 16 molN $molP^{-1}$. This suggests that further work is required to ensure consistency between winter DIN and winter DIP thresholds.

The EMoSEM project outcomes suggest that

- Further analysis is needed to define consistent thresholds for winter DIN, winter DIP and Chl P90 in the light of the new estimation of background values
- Significant progress towards the GEnS across the NEA will require major changes in the agro-food systems
- A reduction of the atmospheric N depositions is required in parallel to any future riverine nutrient reduction (no reduction in N depositions was tested in this study)
- Eutrophication should be assessed on areas defined on the basis of ecological criteria instead of political boundaries
- The proposed novel indicator ("non-diatom chlorophyll *a*") should be verified based on phytoplankton measurements over the whole NEA.

1 INTRODUCTION

1.1 Assessment of current marine eutrophication

Human-induced nutrient enrichment (cultural eutrophication) is one of the most important anthropogenic pressures that affect estuarine and coastal waters worldwide (e.g. Nixon 2009). In US and European countries, undesirable eutrophication started after the Second World War due to the synergetic effect of increased human population and socio-economic development (the so-called Great Acceleration). Even if due to similar causes (increased nitrogen and phosphorus with respect to silicon delivery) the related eutrophication symptoms (high-biomass non-siliceous algal blooms with potential oxygen depletion, toxic phytoplankton…) in the coastal waters can be quite different, depending on the chemical speciation of added nutrients, the local phytoplankton community and the hydro-geomorphological characteristics of the receiving coastal zones. The North-East Atlantic (NEA) Ocean offers between Portugal and Denmark, a succession of coastal ecosystems, all affected by river inputs but that respond differently in terms of dominant phytoplankton communities and impact on trophic structures and the related goods and services.

The Portuguese Continental Shelf (PCS) typically shows a width smaller than 30 km. As a consequence, the ecological processes are influenced by both terrestrial nutrient loads and ocean-margin exchanges (upwellings). The relative influence of both nutrient sources follows the hydroclimatic seasonal pattern. In winter, river discharges are high and they enhance the northern flow generated by density gradients. Terrestrial nutrient loads to the coastal zone are also higher. In summer, the river discharges are lower by one order of magnitude compared to winter, and nutrients discharged by rivers tend to be consumed locally. Then, the coastal circulation is mostly influenced by the northern wind, which is responsible for upwelling events. These coastal upwellings enhance the importance of exchanges across the shelf border, and act as a significant source of nutrients to the coastal zone. Eutrophication-related problems have not yet been reported in the coastal zone. However, amongst the estuaries, the Sado estuary is considered eutrophied and the Mondego estuary is potentially under eutrophication threat. The Tagus and the Douro estuaries, that generate the highest terrestrial loads, are not considered eutrophied.

The French Celtic Sea and the western English Channel have seen the nitrate fluxes from Brittany to coastal waters increase ten times during the last four decades. Eutrophication has become obvious along beaches invaded by mass strandings of *Ulva* sp. Also on the continental shelf, episodic massive blooms of phytoplankton (diatoms or sometimes dinoflagellates as the green *Lepidodinium*) occur in the plumes of the Loire and Vilaine rivers (Ménesguen 1990), where they create massive organic settlements in bottom waters, which sometimes result in lethal anoxia events (Chapelle et al. 1994). The nitrogen enrichment of the coastal zone in excess with regard to phosphorus (P) and silica (Si) is also suspected to have triggered the toxicity of some phytoplankton species as the production of the amnesic shellfish poisoning (ASP) toxin by diatoms belonging to the *Pseudo-Nitzschia* genus. *Karenia mikimotoï* is another toxic dinoflagellate, which can produce red to dark-brown waters and induce widespread mortality events of wild fishes and benthic invertebrates (Jones et al. 1982). Blooms of this species may occur in eutrophication-free places (Holligan 1979, Rodriguez et al. 2000), but

man-made coastal enrichment of river plumes in nitrogen may also trigger coastal blooms of this species that turn out to be nuisance. In the Bay of Brest, they caused a loss of 4,000,000 individuals in scallop nurseries and culture trays (Erard-Le Denn et al. 2001), and along the French Atlantic coast, the mortality of 800-900 tons of mussels and many fishes coincided with an exceptional bloom of 48 million cells L^{-1} (Arzul et al. 1995), following very high flow rates of Loire river. The Bay of Seine receives, in a naturally confined embayment, the important nitrogen loadings from the Seine river. This induces a high primary production during spring and summer in the river plume, and every year, chlorophyll *a* concentrations reach values between 30 and 70 µgChl L^{-1} (Aminot et al. 1997). Diatoms are dominant, but flagellates can become abundant in late summer*: Lepidodinium* (e.g. *Gymnodinium*) *Chlorophorum* reached 120 million cells L^{-1} along the Calvados coast in August 2009. *Dinophysis* sp. blooms can also reach 10^6 cells L^{-1} and induce acute diarrhetic shellfish poisoning (DSP) toxicity (Le Grand 1994).

The English Channel and Southern Bight of the North Sea (SBNS) are submitted to the nutrient inputs by large rivers (Seine, Somme, Scheldt, Rhine/Meuse, Ems, Elbe and Thames) that cumulate along the SW-NE direction (Lancelot et al. 1987). The combination of South Atlantic water inflows, freshwater discharge and wind patterns results in a variety of salinity and nutrient distributions (Ruddick and Lacroix 2006), which in turn effect the spatial distribution of the phytoplankton bloom. The spatial distribution of chlorophyll *a* concentrations in Belgian and Dutch waters typically shows high values in the coastal zone and a decreasing gradient towards the offshore (De Vries et al. 1998, Los and Bokhorst 1997, Rousseau et al. 2006, Baretta-Bekker et al. 2009). These nutrient inputs show a large excess of nitrates that is beneficial to *Phaeocystis* colonies (Lancelot 1995, Gypens et al. 2007). Due to their large size, these colonies are inedible to zooplankton (Weisse et al. 1994, Rousseau et al. 2000, Daro et al. 2006), constitute a loss for secondary production, and decrease trophic efficiency (Rousseau et al. 2000, Lancelot et al. 2009). Deprived of grazing control, *Phaeocystis* colonies grow rapidly in the water column and their disruption causes large foam accumulation and bottom oxygen deficiency in some enclosed areas. N-reduction should be prioritized to limit *Phaeocystis* colonies in the Belgian and Dutch coastal zone, with target winter DIN:DIP ratios below 34.4 molN $molP^{-1}$ in the Belgian Continental Shelf (BCS), or 28.6 molN $molP^{-1}$ in the Dutch Continental Shelf (DCS) (Desmit et al. 2015).

1.1.1 Spatial heterogeneity of chlorophyll *a*

Along the coastal zones of the North-East Atlantic waters, high chlorophyll *a* blooms occur in the period between March and October (Figure 1).

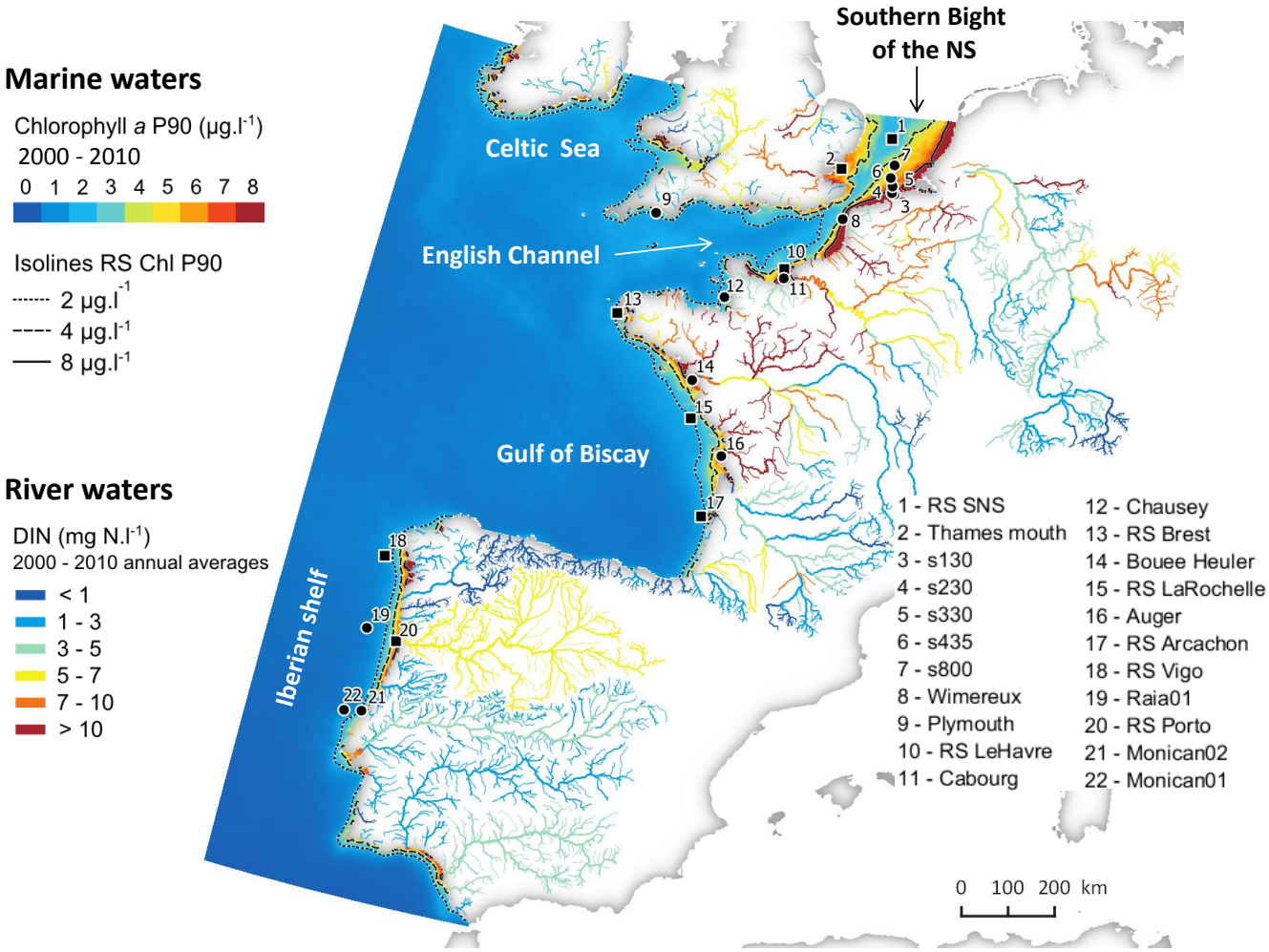

Figure 1: Marine waters: multiyear average of chlorophyll a percentile 90, i.e. the value below which 90 percent of the chlorophyll a observations may be found (SeaWiFS remote sensing 2000-2010, F. Gohin). River waters: multiyear average of winter dissolved inorganic nitrogen (DIN) (PyNuts-Riverstrahler model 2000-2010, M. Silvestre). The main validation stations of the marine ecosystem models used in EMoSEM are represented (black circle dots). Additional stations (black square dots) were used to analyse the long-time series of RS chlorophyll a (see Figure 2)

The onset of the spring biomass bloom is often determined by the light availability (i.e. 12 µmol quanta m^{-2} s^{-1}, Rousseau et al. 2006), while the magnitude of the chlorophyll *a* maximum is commonly considered to be limited by the nutrient availability (Riegman et al. 1992, Muylaert et al. 2006). The nutrient-enriched river waters cause nutrient imbalances at sea that allow not only coastal chlorophyll *a* blooms but also changes in species dominance, some of them being toxic (Jickells 1998, Philippart et al. 2007, Lancelot et al. 2009, 2014). The relative importance of terrigenous nutrients delivery into the sea increases with the degree of freshwater eutrophication that is sensitive to agricultural practices and water treatment policies at the level of the watersheds (Thieu et al. 2010, Passy et al. 2013).

1.1.2 Patterns of chlorophyll *a* temporal variability across the NEA

Beside differences in the intensity and geographical extent of Chl P90 across the NEA, there are also differences in the patterns of temporal variability of chlorophyll *a*. The method of chlorophyll *a* signal decomposition proposed by Cloern and Jassby (2010) allows identifying these patterns. The decomposition model was applied on RS Chl (see method in Appendix) at several stations representative of phytoplankton dynamics. The seasonal vs. interannual variability in Chl signal is shown for 22 stations and allows distinguishing different systems in a structural way (Figure 2).

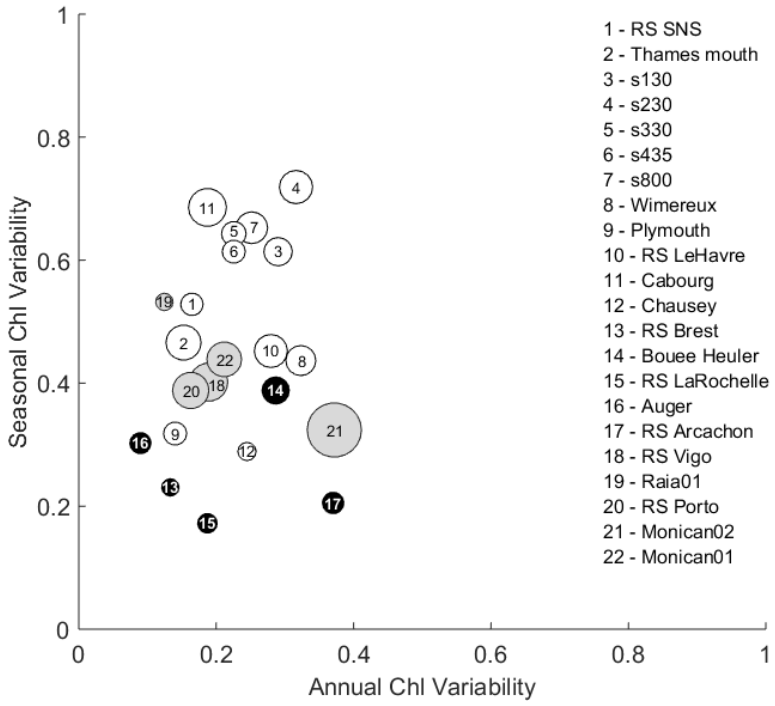

Figure 2: Bubble plot comparing patterns of chlorophyll a variability across 22 stations within the NEA (remote sensing MERIS data, courtesy of D. Van der Zande). Seasonal and interannual variability components are derived in each marine station from the decomposition of the long-term (2003-2013) chlorophyll a signal (see Appendix for chlorophyll a signal decomposition, Cloern and Jassby 2010). X-Axis measures variability of the annual component, hypothesized to be an index of regime shifts in the climate system or punctual disturbance from human actions. Y-Axis measures variability of the seasonal component, hypothesized to be an index of the importance of the annual climate cycle. Circle size measures variability of the residual component, hypothesized to be an index of irregular nutrient enrichment. White dots represent stations in the English Channel and southern North Sea, black dots are stations in Bay of Biscay, and grey dots are stations along the Iberian Peninsula (see Figure 1 for locations).

Figure 2 shows the differences and the similarities between stations regarding Chl temporal variability. The Chl signal in the SBNS stations (3 to 7) is strongly dominated by its seasonal variability while the stations in the Bay of Biscay (13 to 17) show relatively much less seasonal variability, except for station (14). A station like Monican02 (21) in the Portuguese shelf seems to be particularly subjected to irregular nutrient enrichment, as depicted by the relatively high residual component of its Chl signal. The fact that some remote stations like Raia01 (19) and a station in the middle of the SBNS (1) show comparable patterns of Chl variability suggests

defining ecologically-based subareas in the NEA (Ecozones), in which similar stations would be assembled despite their geographical distance.

1.1.3 State-Members metrics to assess eutrophication

Three directives and conventions govern the environmental status of European waters with a focus on different geographical areas: (i) the Water Framework Directive (WFD) that concerns all ground and surface waters (rivers, lakes, transitional waters, and coastal waters) including marine waters up to one nautical mile from shore (Directive 2000/60/EC), (ii) the Marine Strategy Framework Directive (MSFD) focusing on national marine waters (Exclusive Economic Zone, EEZ) (Directive 2008/56/EC), and (iii) the OSPAR Convention that extends to the whole North-East Atlantic (1992 OSPAR Convention). A comparison of eutrophication metrics proposed by Belgium, France and Portugal in the scope of WFD, OSPAR and MSFD was conducted. Special attention was paid to eutrophication parameters and metrics that could be used for model assessment of geographical areas affected by eutrophication. These are winter (Dec-Feb) nutrient (N, P) concentrations, phytoplankton biomass during the vegetative period – March-October – (max, mean or 90th percentile) and harmful species (e.g., *Phaeocystis* cells).

Four main categories of area-specific criteria were recommended by OSPAR (OSPAR commission 2008).

Category I – Degree of nutrient enrichment

	Winter nutrient enrichment					
	Winter DIN (µmol/l)			Winter DIP (µmol/l)		
	Offshore	Coast	Estuary	Offshore	Coast	Estuary
Belgium	12	15	--	0.8	0.8	--
France	--	--	--	--	--	--
Portugal	--	--	66	--	--	--

In the absence of eutrophication problem in Portuguese marine waters, metrics were proposed for estuarine waters. France proposed no criterion owing to the extremely complex relationship existing between eutrophication and nutrient concentrations.

Category II – Direct effects of nutrient enrichment during growing season (including Chl concentration and phytoplankton indicator species)

	Chlorophyll a (µg/l)								
	Offshore			Coast			Estuary		
	Mean	Max	90^{th} per	Mean	Max	90^{th} per	Mean	Max	90^{th} per
Belgium	4.2	--	8.4	7.5	--	15	--	--	--
France	--	--	15	--	--	15	--	--	15
Portugal	--	--	--	--	--	--	7.4	56	15

For harmful species indicator, no data are available for Portugal.

Belgium has defined a threshold of 10^7 cells L^{-1} during a period of 30 days for *Phaeocystis spp* and France has proposed a cell density metric for scaling blooming densities. The threshold was set to 40% above the percentage of samples with at least one bloom defined by category and taxon size: small (<20µm): 250.000 cells L^{-1} and large (>20 µm +colonial species): 100.000 cells L^{-1}.

Category III – Indirect effects of nutrient enrichment (during growing season)

	Oxygen deficiency (mg/l)
Belgium	6
France	3 (10^{th} percentile)
Portugal	8.4 (6mg/l, 10^{th} percentile)

Category IV – Other possible effects of nutrient enrichment (during growing season) as algal toxins: Not considered in this project.

In the scope of the WFD implementation, three metrics were chosen for scaling water quality based on phytoplankton biomass or cell counts (Carletti and Heiskanen 2009):

- Chlorophyll *a*: phytoplankton biomass indicator calculated based on the 90th percentile of monthly (or once a fortnight) samplings over a 6 year period.

	90^{th} percentile Chl a (µg/l)				
	High	Good	Mod	Poor	Bad
Belgium	<= 10	10-15	15-30	30-45	>45
France (except North)	<=5	5-10	10-20	20-40	>40
France (North)	<=10	10-15	15-20	20-40	>40
Portugal	< 8	8-12	>=12		

The Chl threshold values set by Belgium, France and Portugal to determine the moderate status from which remediation measures are required vary between 10 and 15 µgChl L^{-1}.

- Frequency (%) of *Phaeocystis* cell counts above 10^6 cells L^{-1} over a 6 year period (for Belgium)

- Frequency (%) of microphytoplankton cell counts above 10^5 cells L^{-1} (for France and Portugal)

	% of samples exceeding threshold				
	High	Good	Mod	Poor	Bad
Belgium	< 10%	10-17%	>17%	>33%	>80%
France	<20%	20-40%	40-70%	70-90%	>90%
Portugal	<30%	30-50%	>=50%		

Finally the MSFD implementation by State Members appears as a combination criteria proposed in compliance with OSPAR and WFD, for defining the 'eutrophication descriptor' of the GEnS (Good Environmental Status) of coastal waters. For Belgian waters, the Environmental Targets (ETs) and associated indicators are:

1. Direct effects of nutrient enrichment
- A) 90th percentile of chlorophyll *a* concentration (in the growing season[1] and over 6 years) is less than 15 µgChl L^{-1} (Commission Decision 2008/915/EC).
- B) If target A is reached, less than 17% of monthly samples contain more than 10^6 *Phaeocystis* cells L^{-1} (Commission Decision 2008/915/EC).

2. Nutrient levels
- Complementary target: winter[2] DIN concentrations are less than 12 µmol L^{-1} (S>34.5 PSU) or 15 µmol L^{-1} (30<S<34.5 PSU) and winter DIP concentrations are less than 0.8 µmol L^{-1} (OSPAR COMP).

For French and Portuguese waters, criteria are not yet defined.

[1] March-October

[2] December-February

1.2 Characteristics of the river system in NE Europe

The terrestrial watershed of the NE Atlantic area covered by the marine EMoSEM domain represents an area of more than 1 million km², with 174 individual fluvial basins of area over 300 km² (Figure 3). Smaller basins were not modelled, but the point sources located in these areas (e.g. coastal cities) are documented and their nutrient content directly released into the sea, without any riverine filter.

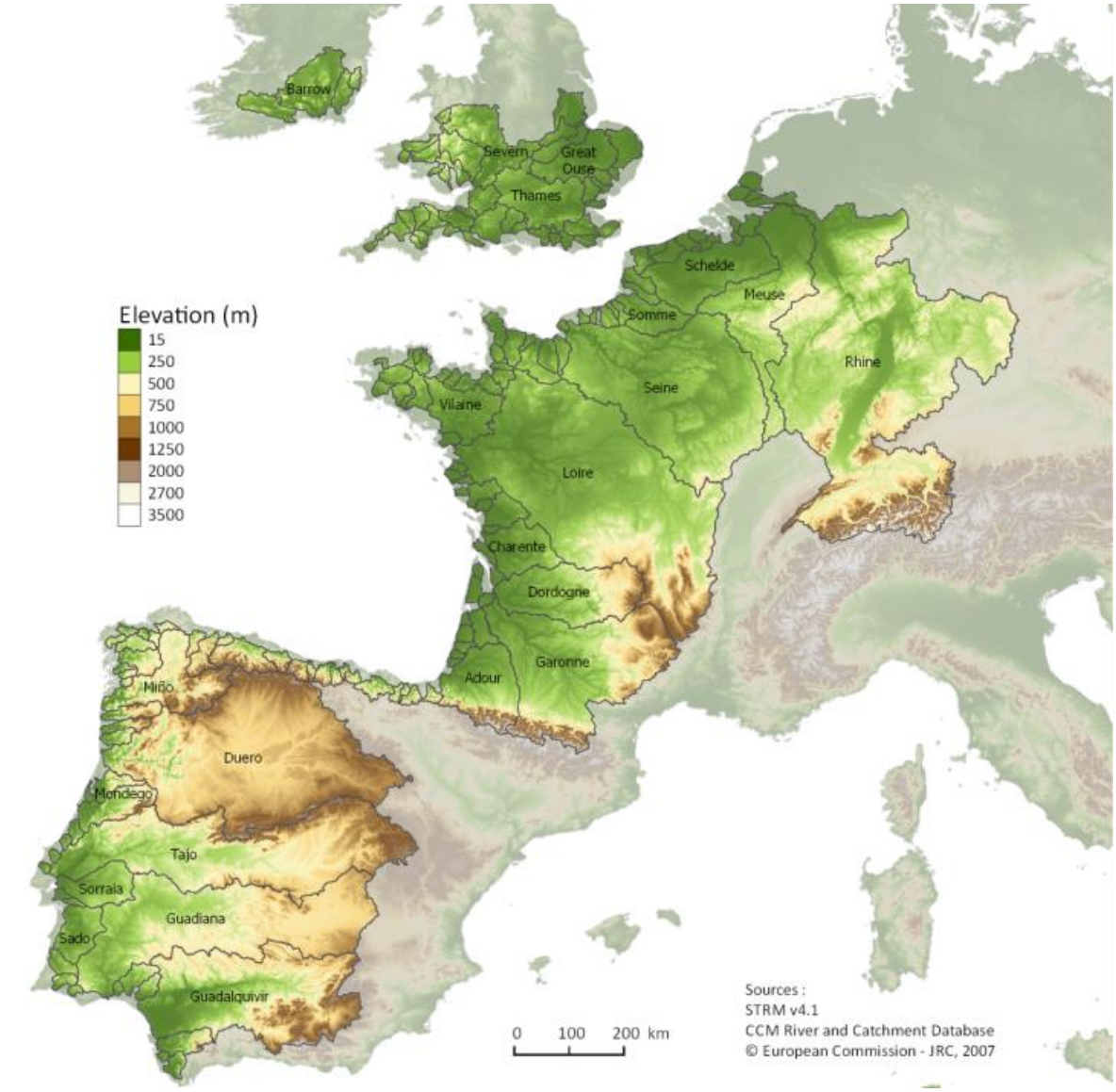

Figure 3: Physical boundaries of the 174 NEA catchments

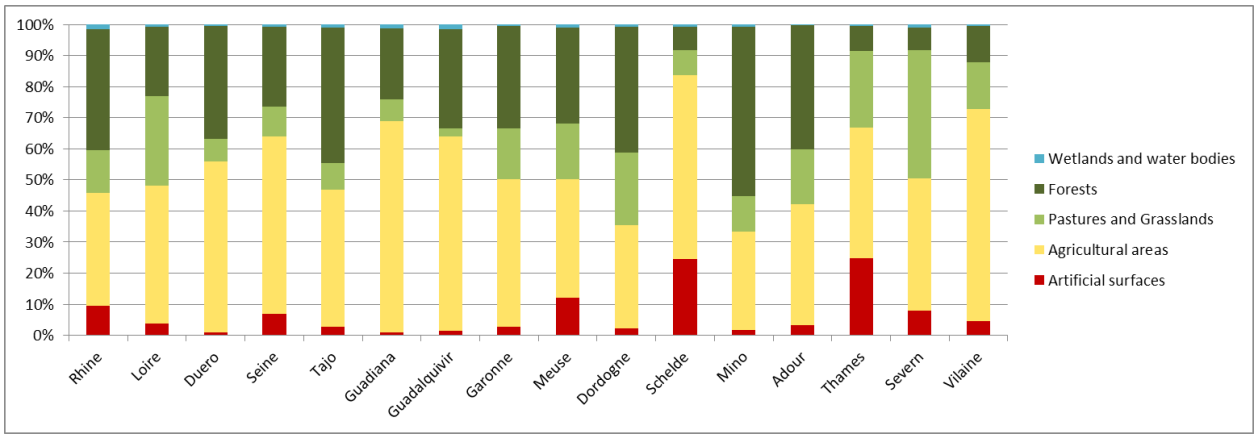

Figure 4: comparison of land use distribution within the main NEA river basins (based on the simplified Corine Land Cover database)

As a whole, the NEA domain covers a wide gradient of climate, population density, land use and hydrological conditions (Figure 4 and Table 1). Among the main river systems, the Rhine, the Scheldt and the Thames rivers are textbook examples of highly impacted river-basins, dominated by agricultural land, with extended urban area and low proportion of natural forest. Within these rivers basins, agglomerations are more numerous and proportionally bigger compare to other NEA basins. The Seine and the Meuse rivers have quite similar importance but they concentrate their population in a few big agglomerations. The Mino is the only main basin where forest dominates.

In a large part of the NEA watershed area severe problems of ground- and surface water quality deterioration arise. These include nitrate contamination of drinking groundwater resources (over 800 drinking water wells closed in France during the last decade because of agricultural contamination, Direction Générale de la Santé 2012), as well as loss of biodiversity and increased eutrophication because of excessive nitrogen and phosphorus concentration in rivers and lakes. This advocates for an integrated approach of the nutrient management covering the whole aquatic continuum from upstream river systems to the sea; the management scenarios to be proposed in relationship to marine eutrophication issues should also answer the freshwater problems occurring in the terrestrial watershed.

Table 1: Morphological information and importance of agglomeration in the main NEA river basins

Basin	Area (km²)	Cumulated river length (km)	Drainage density (km / km²)	Strahler order	Nb of agglo. (> 2000 PE)	Cumulated inhequ generated (in milions)	Yearly avg flow (m3/s) 2000-2010
Rhine	160 221	62 992	0,393	8	2 097	59,9	2 654
Loire	116 981	34 986	0,299	8	481	7,5	1 046
Duro	97 419	35 635	0,366	8	248	5,4	527
Seine	75 990	20 742	0,273	7	414	16,6	715
Tagus	71 202	25 559	0,359	7	383	14,6	592
Guadiana	67 063	20 391	0,304	6	237	3,0	641
Guadalquivir	57 053	21 062	0,369	7	282	5,7	551
Garonne	55 703	21 190	0,380	7	183	2,9	621
Meuse	32 047	9 325	0,291	6	288	12,6	434
Dordogne	23 902	8 011	0,335	7	72	0,8	428
Scheldt	18 949	4 550	0,240	6	326	9,8	201
Mino	16 985	8 951	0,527	7	40	0,6	335
Adour	16 861	7 280	0,432	6	73	0,7	377
Thames	13 514	3 426	0,254	5	166	15,1	127

1.3 Foreword to EMoSEM

The marine governance requires "to improve assessment capabilities and thus the potential success of management measures" (Ferreira et al. 2011). Numerous monitoring programs and modelling tools have been developed in recent years to carry out the assessment of the eutrophication status (e.g. Lenhart et al. 2010) and to propose recommendations towards achieving the GEnS. However, knowledge gaps remain at many levels, and the existing approaches still do not integrate the eutrophication in space (river-ocean continuum) and in time (past, present and future eutrophication status). A strong need remains for:

- knowledge/identification of all the processes that determine eutrophication and its consequences
- consistent and harmonized reference levels assigned to each eutrophication-related indicator
- identification of the main rivers directly or indirectly responsible for eutrophication nuisances in specific areas
- integrated transboundary approach across the North-East Atlantic waters

- implementation of the atmospheric depositions
- realistic and scientific-based nutrient reduction options to mitigate eutrophication nuisances in European seas

The EMoSEM project aimed at filling in these gaps.

1.4 Objectives in EMoSEM

A major challenge in EU marine governance is to reach the "Good Environmental Status (GEnS)" in the North-East Atlantic (NEA). This area is facing several eutrophication problems that have been linked to the growing human pressure in the watershed. Human activity delivers nitrogen and phosphorus to the river system, in excess to silica naturally issued from rock weathering, that reach the coastal zone after having been processed along the river system. Mitigating coastal eutrophication problems needs to identify the major sources of anthropogenic N and P nutrients, their transformation paths along their transfer to the coastal sea and the ecological response of the coastal ecosystem to these nutrient alterations. The objective of EMoSEM is to develop and combine the state-of-the-art modelling tools describing the river-ocean continuum in the NEA continental seas, in order to link the eutrophication nuisances in specific marine regions to anthropogenic inputs, and trace back their sources up to the watersheds. More specifically, the four objectives are:

1. **To develop and combine modelling tools describing the river-ocean continuum** in the NEA continental seas in order to link eutrophication nuisances in marine regions to anthropogenic inputs, and trace back their sources up to the watersheds (Figure 5).

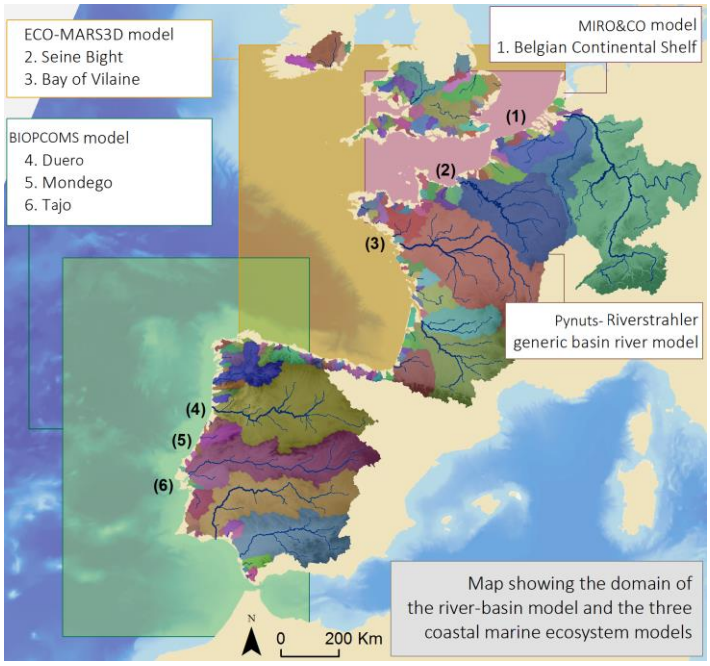

Figure 5:Map showing the domain of the NEA river-watershed (PyNuts-Riverstrahler) and the geographical extension of the three marine ecosystem models.

2. **To suggest novel indicators of eutrophication** based on the analysis of a reconstructed pristine-like NEA watershed and marine ecosystem. More specifically, it is proposed first to define a new «ecologically-based» indicator from pristine-like situation (ex: N:P ratio, Non-diatoms chlorophyll *a* concentration), and second to propose the associated reference levels for the marine GEnS assessment.

3. **To scale the current coastal eutrophication problems against a reconstructed natural status** (pristine-like situation) across the NEA. More specifically, it is proposed to integrate the marine model results in a common map, to determine transboundary Ecozones (i.e. sub-area determined on the basis of the satellite Chl P90 across the NEA), and to compare the integrated results of the current situation with those of the pristine situation.

4. **To identify "realistic" future scenarios of nutrient reduction in the river watersheds** of NEA and assess the impact of these scenarios in the sea. This will allow to check the adequacy between «optimal river loads» (DTT) and «realistic future river loads» (best "realistic" PyNuts-Riverstrahler scenarios).

EMoSEM's outcomes will be transferred to MS responsible for WFD & MSFD operations, and to the OSPAR Commission.

2 METHODS

2.1 Description of models and model improvements

2.1.1 PyNuts-Riverstrahler

2.1.1.1 The Riverstrahler model: an ecological model for river functioning

The Riverstrahler model (Billen et al. 1994, Garnier et al. 1995) is based on a comprehensive description of microscopic processes occurring within the water column and involved in the transfer and retention of nutrients in the entire drainage network. A simplified algorithm is taken into account for calculating benthic sediment fluxes (Billen et al. 2015).

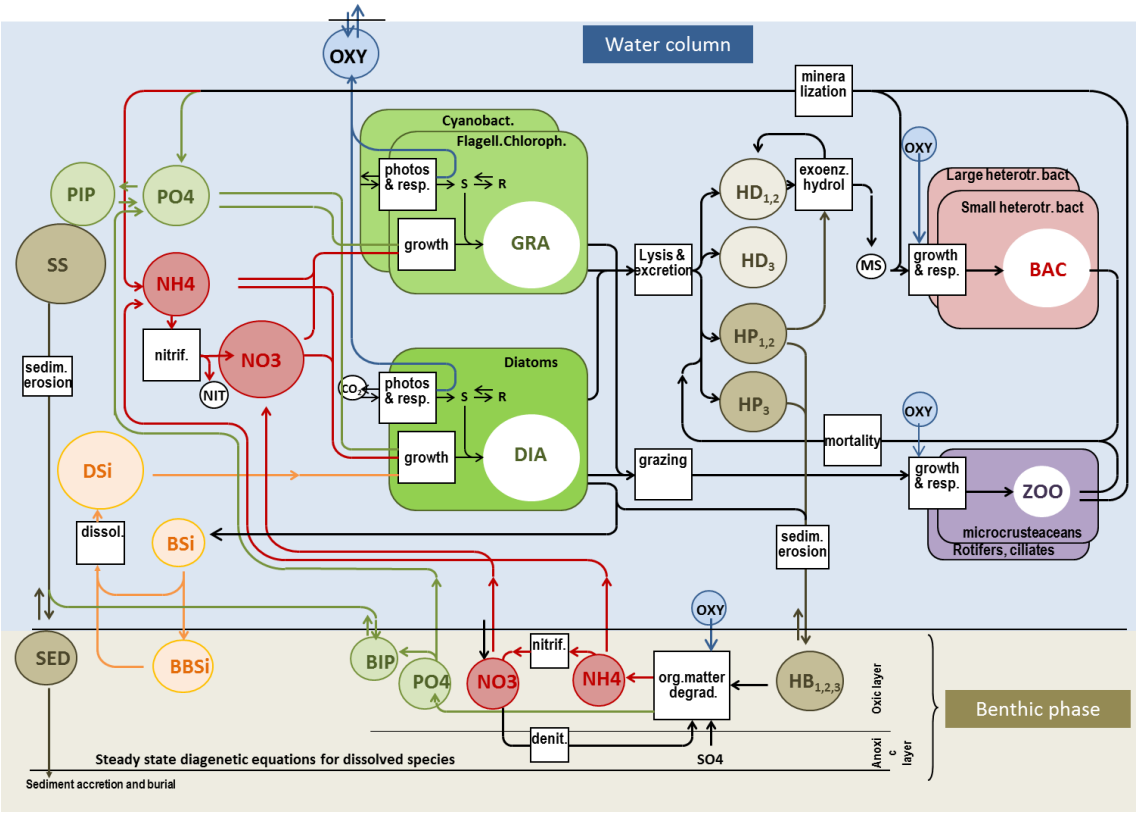

Figure 6. Schematic representation of the ecological Riverstrahler model (Billen et al. 1994, Garnier et al. 1995).

In agreement with the river continuum concept, the ecological Riverstrahler model (Figure 6) takes into account the physiology of algae (three groups, one diatoms and two non-diatoms) and zooplankton (two groups) for the calculation of their biomass and simulates the biogeochemical cycles of carbon, oxygen, nitrogen, phosphorus and silica in the drainage network, taking also explicitly into account heterotrophic and nitrifying bacterial communities. Most of the processes important in the transformation, elimination, and/or immobilization of nutrients during their transfer in-streams are explicitly calculated at the seasonal scale (at a ten days resolution). Interestingly, the description of the ecological module of Riverstrahler, and the ones of marine systems has greatly converged through previous collaboration (see below).

Considering that the same processes operate in all aquatic ecosystems and obey to the same biological or physical kinetics, the Riverstrahler approach also assumes that the singular functioning of aquatic ecosystems is directly related to the variety of constraints applied to the aquatic continuum. Kinetics and parameters of Riverstrahler model were estimated from experimental works or obtained from literature reviews, and the generic Riverstrahler has already been successfully applied to several river systems across the world (Table 2). In this way, the Riverstrahler model does not require any calibration and could be applied to any river system.

Table 2: coverage of the Riverstrahler modelling approach with associated publications

River basin	Publications
Temperate systems:	
• Seine	• Billen et al. 1994, 1999, Garnier et al. 1995, 2005, Ruelland et al. 2007
• Somme, Scheldt	• Thieu et al. 2009, Passy et al. 2013
• Mosel	• Garnier et al. 1999
• Loire	• Calens et al. 2010
Continental systems:	
• Danube	• Garnier et al. 2002
Sub-tropical systems:	
• Red River	• Le et al. 2007, 2014, Luu et al. 2012
Sub-arctic systems:	
• Kalix, Lule	• Sferratore et al. 2008

2.1.1.2 Modelling units and spatial resolution

The generic Riverstrahler model is applicable at various scales, from few square kilometres to several tens of thousands square kilometres, with the distinctive feature to adapt it spatial resolution according to the modelling objectives.

The elemental spatial unit of the Riverstrahler model is the incremental watershed area drained by a river reach between two confluences (Figure 7). Accordingly, these units can be described as a set of river axis with a spatial resolution of 1 km, or they can be aggregated to form upstream basins that are idealized as a regular scheme of tributary confluences (Strahler 1957) where each stream order is described by mean characteristics. A third kind of object are stagnant systems (ponds and reservoirs), represented as perfectly mixed reactor (not yet implemented in the framework of the EMoSEM project) connected either to axis-object or stream-order-object.

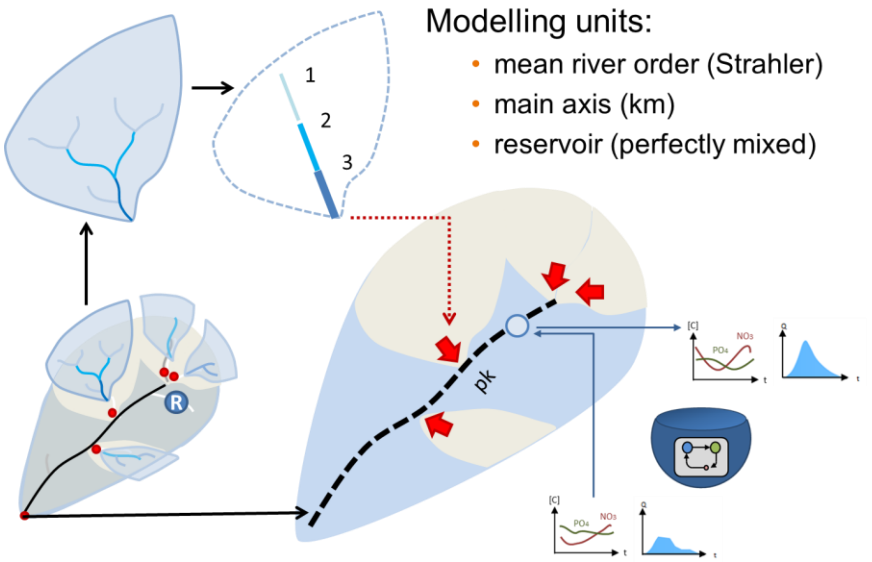

Figure 7: Principle of idealized objects taken into account by the Riverstrahler model to form modelling units with variable spatial resolution

For the EMoSEM project, river- basins ranging from 300 to 3000 km² within the NEA domain have been systematically considered as single basin (idealized as a regular scheme of tributaries of increasing stream order). Larger river basins where subdivided into smaller objects (either axis or basins) following the principle of the Pfafstetter hierarchy (Pfafstetter 1989) as long as the subdivision process provided (sub-)objects of at least 3000 km² in size. Results of the subdivision process are provided in Table 3.

Table 3: subdivision of the most important river basins in the NEA domain

Name	Area km²	Strahler	Num. sub-objects
Rhine	160 221.4	8	159
Loire	116 981.0	8	110
Seine	75 989.5	7	77
Garonne	55 703.1	7	67
Meuse	32 047.2	6	26
Dordogne	23 902.0	7	25
Scheldt	18 949.0	6	22
Adour	16 860.9	6	24
Thames	13 513.7	5	6
Vilaine	10 490.4	6	6
Barrow	9 224.3	6	6
Great Ouse	8 442.7	6	6

Some important Iberian rivers (namely the Douro, Tagus, Guadiana, Guadalquivir and Minho rivers) were initially sub-divided into numerous modelling features. However, such high spatial resolution (kilometric) was not compatible with the availability of hydrological data in this

region. It thus forced our modelling approach to consider a lower resolution (one single river basin described by stream order) for these specific river systems.

2.1.1.3 The PyNuts modelling framework (newly constructed platform for EMoSEM)

EMoSEM's ambition for the terrestrial domain aims at enabling a large scale modelling (1 million km²) of nutrient cycling in all watersheds based on a detailed description of the processes operating from headwaters down to coastal areas and with a sufficient temporal resolution to represent the seasonal variability.

The Riverstrahler approach considers that an accurate description of natural and anthropogenic constraints is the key to understand the biogeochemical functioning of any hydrosystems, raising the issue of harmonizing the necessary inputs information available under various formats with different spatial and temporal resolutions across the NEA domain. Such modelling exercise also asks for specific solution to address the problem of calculation time and data management.

For this reason and because of the great number of watersheds involved in the study domain a new modelling platform "PyNuts" has been specifically designed for enabling a large scale application of the Riverstrahler model. While the platform was developed in Python language, the Riverstrahler model, previously in Visual Basic has also been here completely recoded in Python too.

The PyNuts modelling platform (Figure 8) aims at:

- Sub-dividing the domain of interest (zonation) to create an idealized representation of the drainage network, defined for each river system as a combination of the Riverstrahler modelling units (see 2.1.1.2).
- Calculating all inputs required by the Riverstrahler approach for each idealized object (modelling units) based on a set of heterogeneous GIS data describing natural and anthropogenic constraints gathered for the whole continental domain, and storing them within a harmonized databases structure.
- Managing a modelling project. This implies to provide appropriate inputs data to the Riverstrahler model following the storylines of a specific scenario, to enable multi-year simulations (keeping memory of benthic variables).
- Piloting the Riverstrahler model itself, ensuring its propagation following a regular scheme of confluence between all modelling units from up to downstream.
- Organizing all inputs and outputs data in an object-relational database management system (PostgreSQL) to enable (i) large storage capacities, (ii) efficient access to simulations results (iii) facilitate post-processing of simulation (extract synthetic figures, maps etc.).

The development of PyNuts, was a real challenge, particularly because it was located 'upstream' of most of the other tasks in EMoSEM.

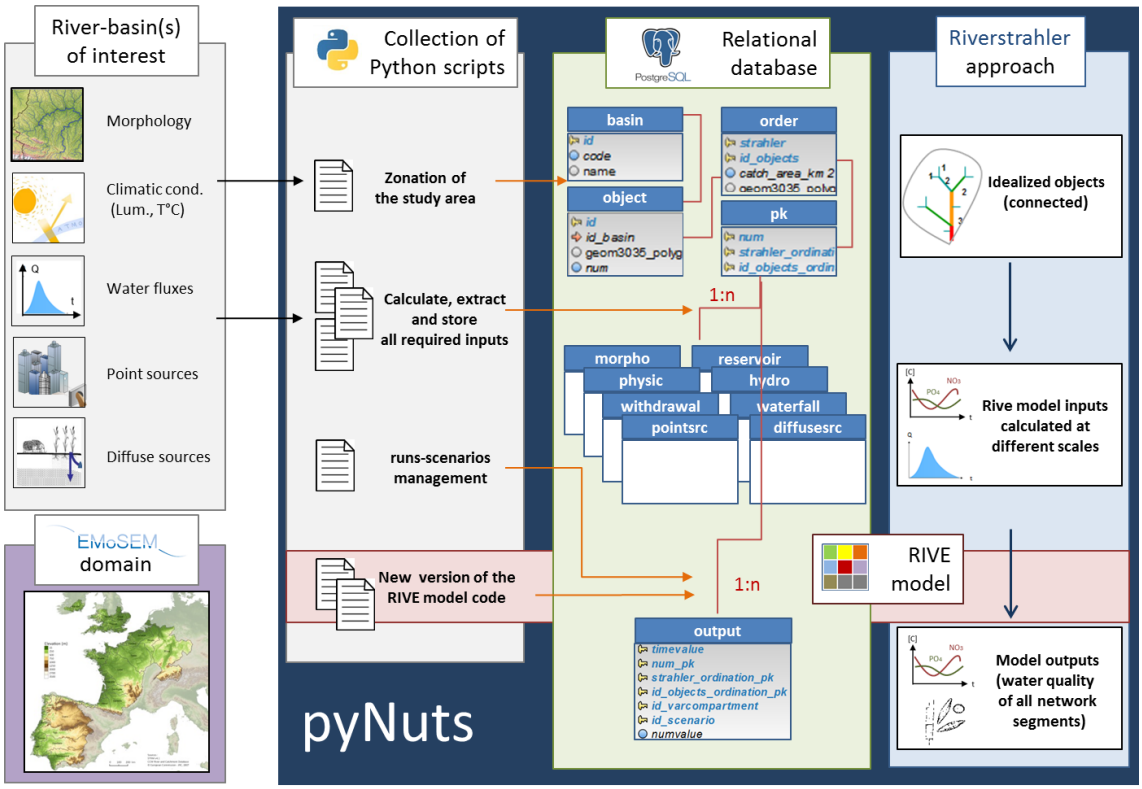

Figure 8: Schematic representation of the PyNuts-Riverstrahler modelling framework

2.1.2 BIOPCOMS

2.1.2.1 The Portuguese Coast Operational Modelling System (BIOPCOMS)

The study area covers the western Iberian coast that is simulated by the Biological version of the Portuguese Coast Operational Modelling System (hereafter referred as BIOPCOMS, Mateus et al. 2012). The operational system is providing forecasts and analysis of hydrodynamics since 2009 (PCOMS) and ecology since 2012 (BIOPCOMS). The BIOPCOMS model application consists in two nested domains: West Iberia (2D) and Portugal (3D) (Figure 9) that run the MOHID Water Modelling System (Neves 2013, http://www.mohid.com) covering the Iberian Atlantic coast and its contiguous ocean (Longitude: 12.6W-5.1W; Latitude: 34.38N-45N). The BIOPCOMS is 3D full baroclinic hydrodynamic and ecological regional application with a horizontal resolution of 5.6 km and with 50 vertical levels with a resolution of down to 1 m near the surface. The application is a downscale of the Mercator-Océan PSY2V4 North Atlantic solution (Drillet et al. 2005) that provides daily values for water levels and 3D values for horizontal currents, temperature and salinity. Tides are included in the BIOPCOMS application by forcing the West Iberia domain open ocean boundary with tidal components obtained from the FES2004 global tide solution (Lyard et al. 2006). For the atmospheric conditions, the system is one-way coupled with the MM5 atmospheric forecast model for the west Iberian coast (http://meteo.ist.utl.pt). The ocean boundary condition of the model domain was initialised and forced by monthly climatological profiles of oxygen, nitrate and phosphate obtained from the World Ocean Atlas 2009 (Garcia et al. 2010a and 2010b) at the coordinates 12.5W and 38.5N. This modelling system was used to simulate the period between 2010 and 2012.

In order to simulate the primary production in the coastal area of West Iberia, the Water Quality module has been coupled to the MOHID model. This module is a nutrient-phytoplankton-zooplankton (NPZ) model adapted from a model initially developed at USEPA (U.S. Environmental Protection Agency) (Bowie et al. 1985). The model simulates inorganic and organic forms of nitrogen and phosphorus as nutrients in its dissolved and particulate forms. It also calculates oxygen, phytoplankton and zooplankton concentrations (Figure 10). In this application the phytoplankton growth has not been limited by temperature considering the maximum optimum interval for phytoplankton growth between 10°C and 25°C.

Regarding the land boundary conditions and in order to simulate the input of nutrients in the Western Iberian coasts, the discharges obtained from the PyNuts modelling framework during the EMoSEM project were incorporated. The PyNuts properties included in the discharges are flow, oxygen, nitrite, nitrate, ammonia and inorganic phosphorus. Additionally, salinity concentration was included as a constant value of 32 and temperature values were obtained by the MOHID Land applications for the Iberian Peninsula and Western Iberia (Campuzano et al. 2014).

The 27 rivers included as surficial direct discharges were: Alcobaça, Anllons, Arade, Arnoia, Ave, Cavado, Douro, Eo, Esva, Eume, Guadalquivir, Guadiana, Lima, Lis, Minho, Mira, Mondego, Navia, Odiel-Tinto, Piedras, Sado, Sizandro, Tagus, Ulla, Umia, Vouga and Xallas.

2.1.2.2 Model improvements during EMoSEM

During the EMoSEM project two main improvements were made in the model: the inclusion of river discharges in the BIOPCOMS model calculated by the MOHID-LAND model (http://www.mohid.com/MOHIDLand.htm) and the implementation of the atmospheric depositions of nitrogen in the MOHID model. A total of 47 river discharges were included in the model, 24 rivers located along the Portuguese continental coast and 23 rivers located in the Spanish coast (Figure 11). Two approaches were used to implement the rivers discharges in the BIOPCOMS model depending on the existence or not of an estuarine model. If the estuarine model exists a 2D or 3D section is extracted and imposed in the coastal area. In the case of absence of estuarine model a continuous discharge is imposed. In both methodologies hourly river discharges are imposed in the BIOPCOMS model domain.

For the atmospheric depositions of nitrogen (N), the model considers the inclusion of NH_4 (ammonium) and NO_3 (nitrate) as direct input in the biological state variables, and the Oxidized (wet+dry depositions) and Reduced (wet+dry depositions) nitrogen. The monthly atmospheric depositions of nitrogen (wet and dry, reduced and oxidized) come from the EMEP program. Finally, the BIOPCOMS application has been coupled to the PyNuts model results.

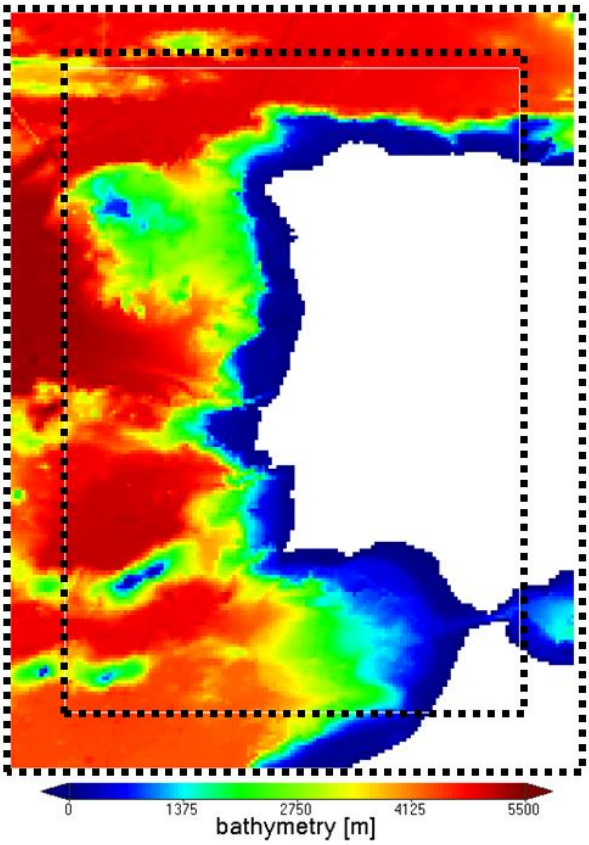

Figure 9: Model domains (dot lines) and bathymetry.

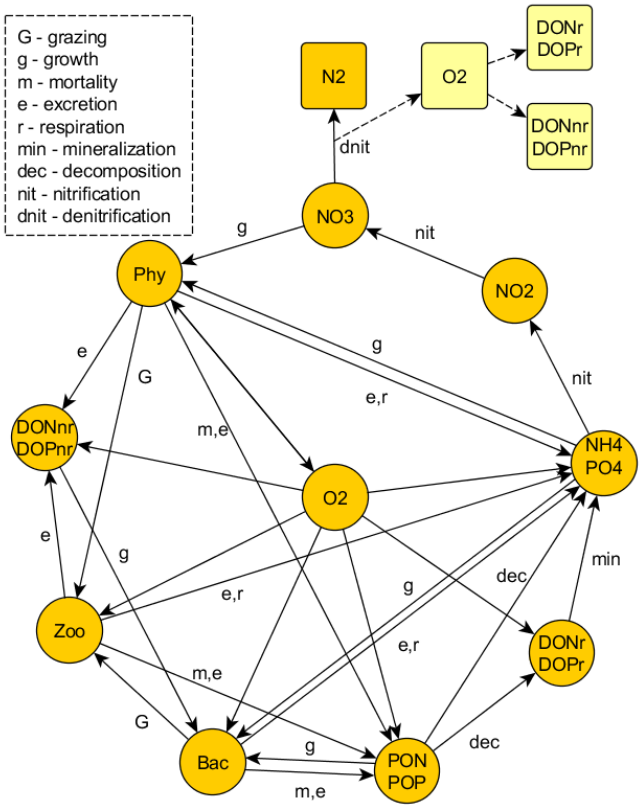

Figure 10: Conceptual diagram of the MOHID ecological model.

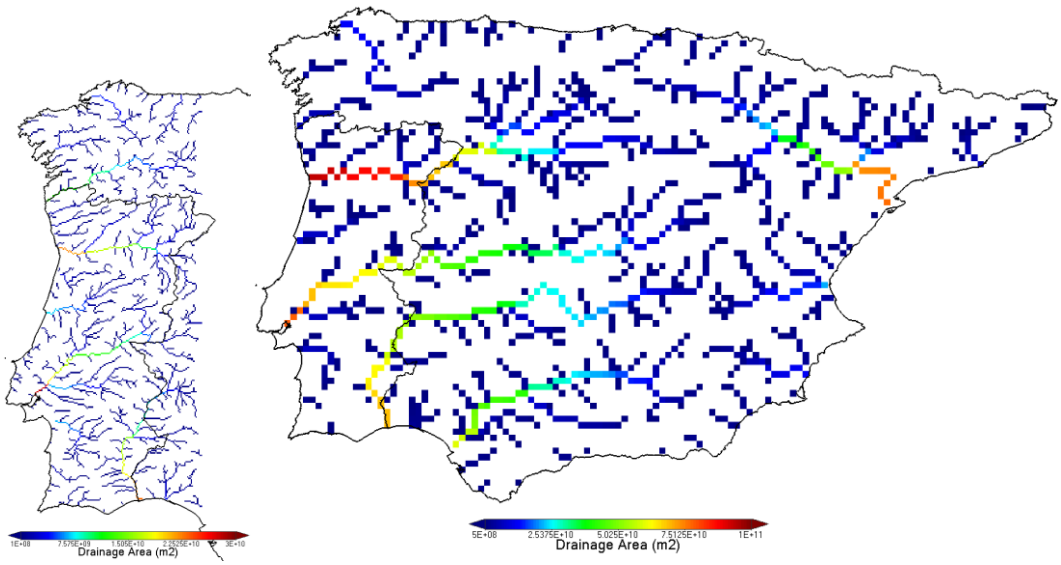

Figure 11 : Main water lines in the Western Iberian Peninsula (WI domain, left) and in the complete Iberian Peninsula (IP domain, right) indicating the drainage area obtained with the MOHID Land for the 2 and 10 km resolutions respectively.

2.1.3 ECO-MARS3D

2.1.3.1 Structure of the model

The French ECO-MARS3D model is based on the IFREMER's MARS3D hydrodynamical code (Lazure and Dumas 2008). The current application to the French Atlantic shelf is based on the so-called "small MANGA" domain, with a regular grid with 4x4 km meshes and 30 sigma levels covering the Bay of Biscay, the English Channel and the southern part of the North Sea, up to the Rhine estuary; it extends from 8.13°W to 5.0°E, and from 43.17°N to 52.75°N (Figure 12, black square). In order to improve the oceanic currents and the biogeochemical fluxes at the western boundary of this "small" domain, and to avoid local artificial enrichment through zero derivative boundary conditions, this grid has been embedded in a wider one, the so-called "large MANGA" domain extending from 41°N to 55°N and 18°W to 9°30'E, with also 4x4 km meshes and 30 sigma levels. This large domain is used for computing the hydrodynamic forcing (sea surface elevation and 3D currents) at the small domain boundaries at every moment during the 2000-2010 decade, and has also been used to generate a kind of "climatological year" of biogeochemical fluxes at the boundaries of the small domain.

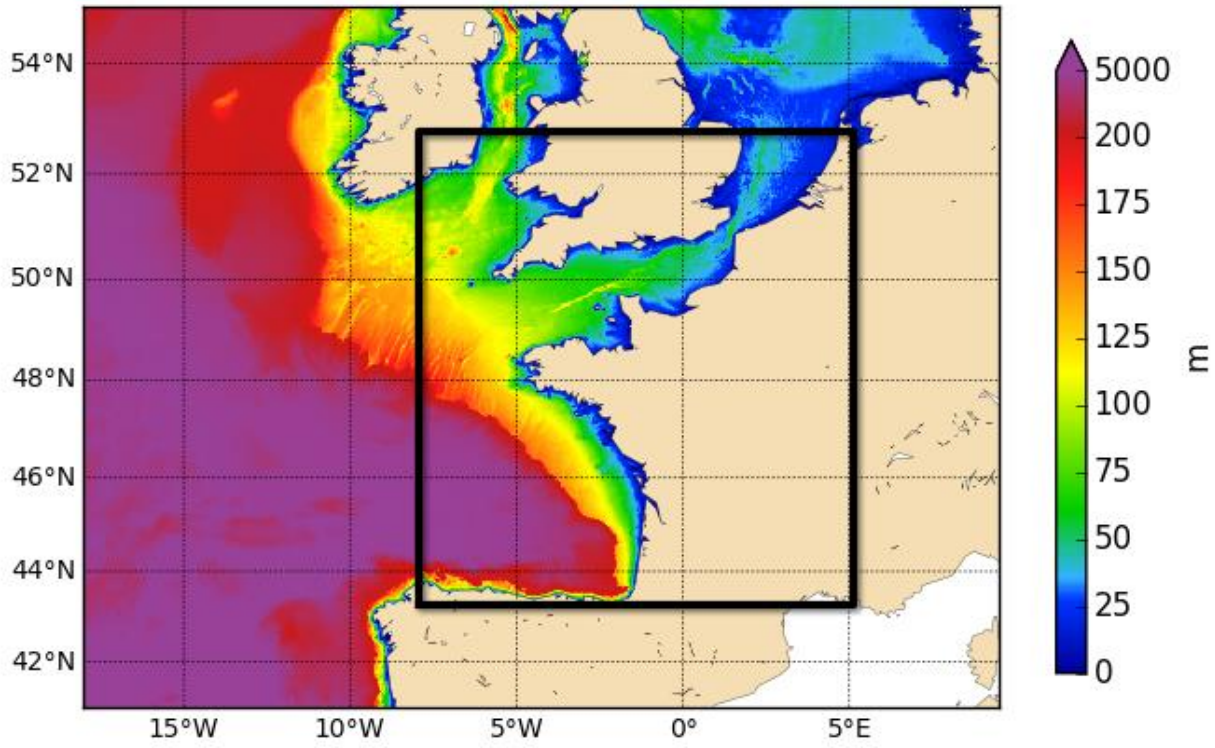

Figure 12. Bathymetry of the "small MANGA" and "large MANGA" domains used by the ECO-MARS3D model.

Wind, atmospheric pressure and thermal fluxes at the sea surface are provided by the Arpege model of Météo-France with a 30 km and 6 h space-time resolution. Simulated daily discharges as well as 10-day river temperatures and biogeochemical concentrations are provided by the PyNuts-Riverstrahler model. Suspended particulate matter is set to the maximum of ambient climatological fortnightly mean distribution derived from satellite data (Gohin et al. 2011) and the suspended matter brought by the rivers, which is simply simulated as a particulate conservative tracer, with uniform and constant settling velocity.

The basic biogeochemical model (Figure 13) contains 17 state variables, describing the nitrogen, phosphorus and silicon cycles and the dissolved oxygen in the pelagic ecosystem. Three limiting dissolved inorganic nutrients are considered: nitrogen, with nitrate and ammonium separately, phosphorus, and silicon. Phytoplankton is divided into three groups: diatoms, dinoflagellates and nanoflagellates, with concentrations expressed in nitrogen currency. Especially for assessing specific consequences of eutrophication in EMoSEM project, a module simulating the single-cells, colonial forms and mucus of the haptophyte *Phaeocystis* (inspired from the MIRO&CO model) has been added in competition with the bulk phytoplanktonic variables. Total chlorophyll is deduced from the nitrogenous state variables of the model by an empirical Chl/N ratio, computed as a Smith-like formula depending on the local extinction coefficient. There are two zooplanktonic components, expressed in nitrogen currency: the microzooplankton, which feeds on nanoflagellates, dinoflagellates and detrital particulate matter everywhere, along with diatoms in oceanic regions (depth>200m), and the mesozooplankton, which grazes diatoms, dinoflagellates and microzooplankton. So, in this

model, diatoms do sink, whereas nanoflagellates and dinoflagellates do not (they are considered as able to maintain at any depth in calm water, thanks to motility). Three particulate detrital variables (detrital N, detrital P, detrital Si) close the biogeochemical cycles, and settle in the water column; in the bottom layer, each settling fraction is partially transferred to a fixed state variable, which can give back to the water layer some particulate material through erosion by currents, and some dissolved equivalent after remineralisation.

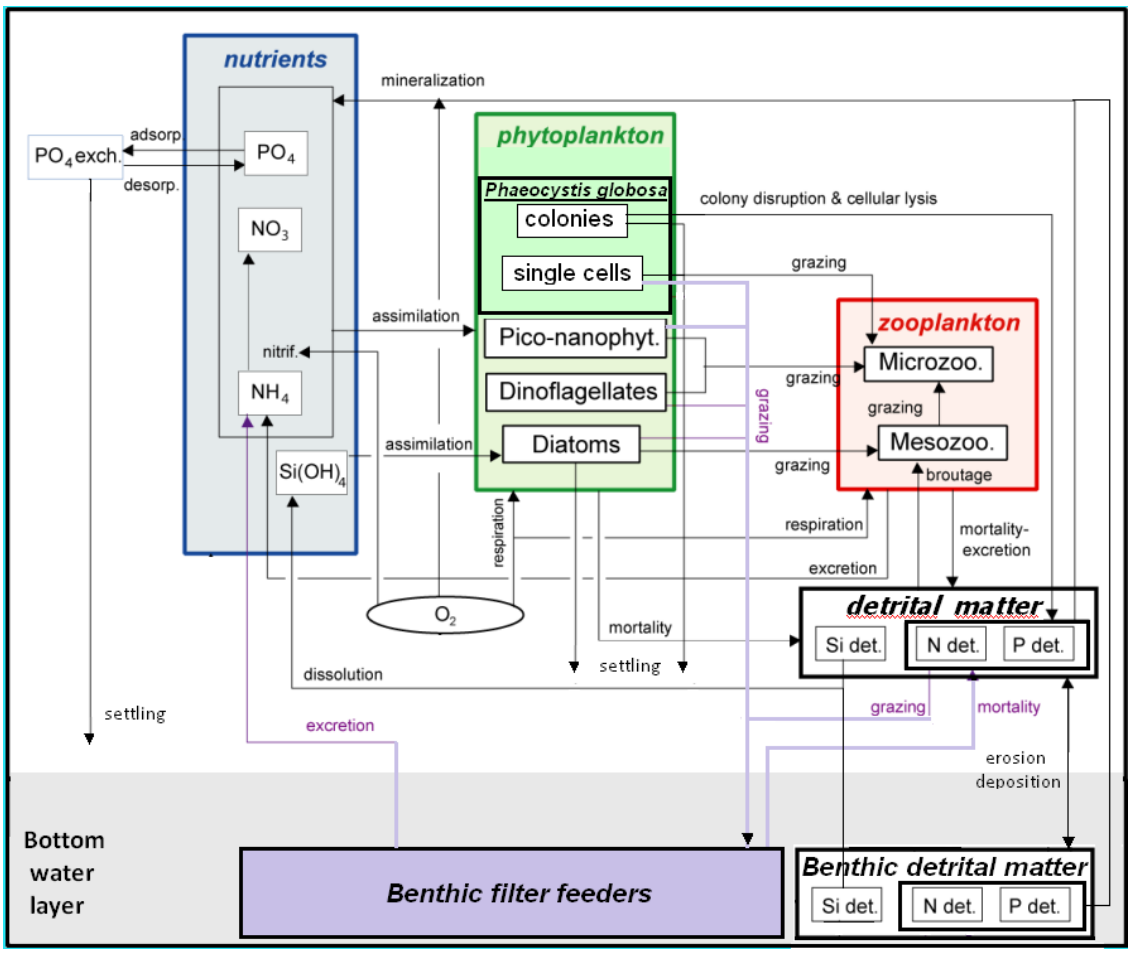

Figure 13. Conceptual diagram of the biogeochemical component of the ECO-MARS3D model.

Useful Links: http://www.previmer.org/previsions/production_primaire

2.1.3.2 Model improvements during EMoSEM

In order to take into account the atmospheric depositions of nitrogen (wet and dry, oxidized and reduced) computed by the "European Monitoring and Evaluation Program (EMEP)", ECO-MARS3D has been adapted to include the atmospheric depositions after re-interpolation on its grid. In order to perform the so-called "transboundary approach" (TBNT tracers), the tagging technique has been applied in ECO-MARS3D to nitrogen and to phosphorus (see details in section 2.3.2.1). Finally, the ECO-MARS3D model has been coupled to the outputs of the PyNuts-Riverstrahler model.

2.1.4 MIRO&CO

2.1.4.1 Structure of the model

MIRO&CO-V2 (hereafter called MIRO&CO) results from the coupling of the 3D hydrodynamic COHERENS v2 model (Luyten 2011) with the biogeochemical MIRO model (Lancelot et al. 2005). COHERENS (COupled Hydrodynamical Ecological model for REgioNal Shelf seas) is a modelling system based on a 3D numerical hydrodynamical model. It is a three-dimensional multi-purpose numerical model, designed for application in coastal and shelf seas, estuaries, lakes, reservoirs MIRO is a biogeochemical model that has been designed for *Phaeocystis*-dominated ecosystems. A schematic representation of MIRO is presented in Figure 14. It integrates 4 modules describing: (i) the dynamics of phytoplankton [diatoms, autotrophic nanoflagellates and *Phaeocystis* colonies], (ii) zooplankton [microzooplankton and copepods], (iii) bacteria and dissolved and particulate organic matter degradation and, (iv) nutrients [nitrate, ammonium, phosphate and dissolved silica] regeneration in the water column and the sediment. *Phaeocystis* free-living cells are included in nanoflagellates, while *Phaeocystis* colonies are described by the sum of 2 components: colonial cells and the polysaccharide matrix in which the cells are embedded and which serves as a reserve of energy. Phytoplankton growth is described according to the AQUAPHY model of Lancelot et al. (1991), which considers three intracellular pools: monomers (S); reserve material (R, [OPM]); functional and structural metabolites (F). The degradation of organic matter by planktonic bacteria is described according to the HSB (High polymers, Small substrates and Bacteria) model of Billen and Servais (1989), considering two classes of biodegradability for DOM (DC1, DN1, DP1 and DC2, DN2, DP2) and POM (PC1, PN1, PP1 and PC2, PN2, PP2). The hydrolysis of these polymers produces dissolved monomers (BSC, BSN) that can be taken up by bacteria. Benthic organic matter degradation and nutrient (N, P, Si) recycling are calculated by the algorithms developed by Lancelot and Billen (1985) and Billen et al. (1989). A full description of the modules and a schematic representation of the MIRO model can be found in Lancelot et al. (2005). State variables, processes and conservation equations are detailed in Lancelot et al. (2005, Appendices available at www.int-res.com/journals/suppl/appendix_lancelot.pdf).

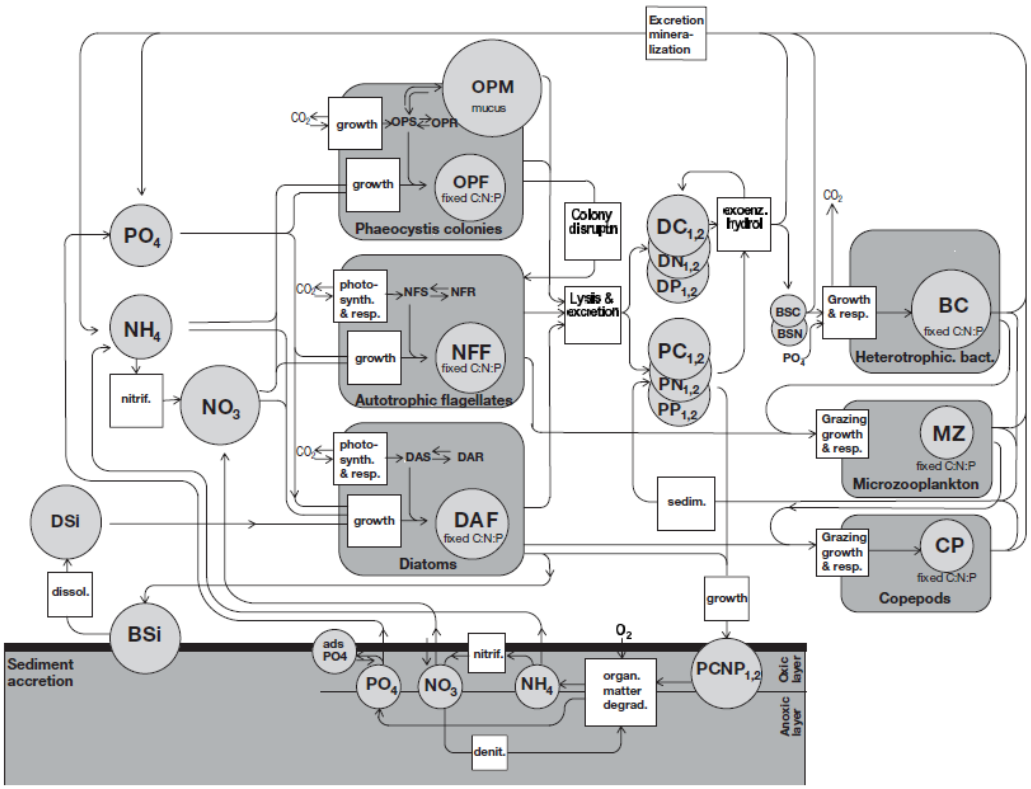

Figure 14: Structure of the MIRO model (source: Lancelot et al. 2005)

2.1.4.2 Model improvements during EMoSEM

During the EMoSEM project, MIRO&CO has been implemented with the second version of COHERENS and the code has been adapted to include the atmospheric depositions of nitrogen (wet and dry, oxidized and reduced) after a grid conversion. This new version of the model has been recalibrated and validated. The transboundary approach (TBNT tracers) has been adapted from Ménesguen et al. (2006) and implemented in the model. This approach allows tracking the nutrients from their respective sources whether they are oceanic (from the northern or western open boundaries), atmospheric or riverine (see Figure 46 in section 2.3.2.2). For computational reasons and common sense, the rivers have been gathered into 4 groups so that the TBNT implementation allows tracking nitrogen from what is here called the *Seine and small French rivers*, *the Scheldt and small Belgian rivers*, the *Rhine and Meuse* and the *Thames* (see details in section 2.3.2.2). Several tests have been carried out to test the tracking method and its implementation. Finally, the MIRO&CO model has been coupled to PyNuts assuming that planktonic organisms present in rivers die instantaneously as they reach marine salty waters.

2.1.4.3 Simulation setups

Five different simulation setups have been implemented: Reference situation, Pristine situation, UWTD scenario, GAP scenario and LocOrgDem scenario.

Reference situation

MIRO&CO has been set up for the region between 48.5°N-4°W and 52.5°N-5°E (cfr. Figure 15) with a horizontal grid resolution of about 5 km and 5 vertical sigma coordinate layers. Initial conditions have been generated from 12-year model simulations (1999-2010) and a 6-year spin up was used. At the western and northern open sea boundaries the time series of water currents and sea surface elevation are provided by a 2D implementation of COHERENS V2 over the North Sea continental shelf. This 2D model is forced by 6-hourly surface wind and atmospheric pressure fields from the analysed/forecast data of the UK Meteorological Office. The same wind and atmospheric pressure fields are used to force MIRO&CO in addition to 6-hourly precipitation rate, cloud cover, specific humidity and air temperature fields from the same data provider. For years previous to 2004, the last 4 atmospheric variables were not available and climatology computed from years 2004 to 2007 was used. The spatially variable temperature imposed at the surface is derived from the weekly sea surface gridded temperature (on a grid of 20 km×20 km) obtained from the BSH (Bundesamt fuer Seeschiffahrt und Hydrographie) (Loewe 2003). For periods without Sea Surface Temperature (SST) data (1991–1995), a weekly climatological SST (computed from 1996–2000 BSH data) is imposed. In addition to the two open sea boundaries, the main rivers are taken into account. The transport is imposed at these boundaries by daily river discharges simulated by the PyNuts model. At the two open sea boundaries, the vertical current structure is determined by imposing the condition of zero normal derivative of the deviation of current from the vertically-averaged horizontal current (Deleersnijder et al. 1989), while at river boundaries a condition of zero vertical gradient of current is applied.

At the English Channel and Central North Sea (West of 4°E) open sea boundary nutrient concentrations are specified as concentrations derived from climatological databases compiled by the European Union NOWESP and ERSEM projects (Radach and Lenhart 1995) and from ICES data, while East of this longitude a zero horizontal cross boundary gradient of nutrients is specified. At the English Channel open sea boundary, phytoplankton concentrations from SOMLIT[3] (station Roscoff ASTAN) are imposed. The distribution of chlorophyll *a* concentrations between the different phytoplankton species biomasses is made according to the species assemblage given by the MIRO model in this area (Lancelot et al. 2005). At the English Channel and Central North Sea open sea boundaries a zero horizontal cross boundary gradient is specified for the other biological state variables. 10-day dissolved (NO_3, NH_4, PO_4, DSi) and particulate (Norg, Porg) nutrient discharges from the rivers have been estimated by the PyNuts model. Monthly atmospheric depositions of nitrogen (wet and dry, oxidized and reduced), for the period 2000-2010, are taken from the "European Monitoring and Evaluation Program (EMEP)" (http://www.emep.int/, courtesy of Semeena Valiyaveetil and Jerzy Bartnicki, met.no).

The DINEOF methodology has been applied to the MODIS-Aqua Total Suspended Matter (TSM) images to reconstruct daily time series of TSM (Sirjacobs et al. 2011) for the period 2003-2006. A daily climatology has then been built and is used as input to compute the light attenuation with the kparv1 model (detailed in Lacroix et al. 2007).

[3] Service d'Observation en Milieu LITtoral, somlit.epoc.u-bordeaux1.fr/fr

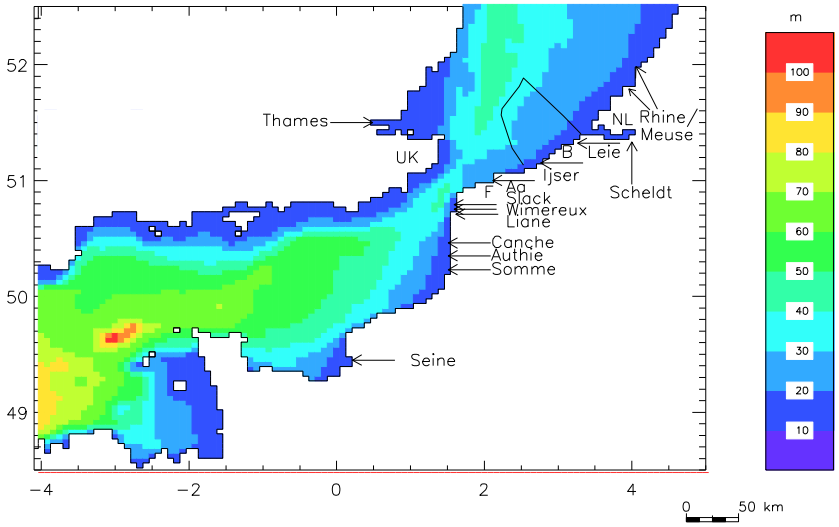

Figure 15: The MIRO&CO model domain covering the southern North Sea and the English Channel. Colors represent the bathymetry (Lacroix et al. 2004).

Pristine situation

MIRO&CO setup for the Pristine situation is similar to the setup for Reference situation described here above with some differences summarized in Table 4.

Nitrogen atmospheric depositions are set to zero values. River loads and discharges are taken from PyNuts for Pristine situation. Nitrogen forcing at the western open sea boundary also differs from the one used in Reference situation. They were estimated based on (1) the proportion between oceanic and riverine waters computed from past model simulations using the tagging approach, (2) the assumption that the oceanic biological conditions remain similar in time, and (3) PyNuts estimations of the N loads for the Loire during Pristine situation. No information is available to us about the biological conditions at the northern open sea boundary during pristine, therefore biological conditions are used as in Reference situation. Initial conditions are produced from a 12-year model simulation using Pristine situation setup of MIRO&CO.

Reduction scenarios

MIRO&CO setups for UWTD, GAP and LocOrgDem scenarios are similar to the Reference situation one. Model setup differences between Reference situation and reduction scenarios are summarized in Table 4.

River forcing is taken from the respective PyNuts simulations (UWTD, GAP and LocOrgDem). Nitrogen concentrations at the western open sea boundary are estimated using the same approach as described in the section here above for Pristine situation. Initial conditions are also produced from a 12-year model simulation using the respective model setup.

Table 4: MIRO&CO model setup differences between Reference situation, Pristine situation, and UWTD, GAP and LogOrgDem scenarios

	Initial conditions	N atmospheric depositions	River discharges and loads	Nitrogen concentration at western ocean boundary
Reference situation	Generated from a 12-year model simulation	From EMEP	From PyNuts Reference	Climatology + ICES data (1)
Pristine situation	Generated from a 12-year model simulation	None	From PyNuts Pristine	Adapted from (1) and PyNuts Pristine
UWTD scenario	Generated from a 12-year model simulation	From EMEP	From PyNuts UWTD	Adapted from (1) and PyNuts UWTD
GAP scenario	Generated from a 12-year model simulation	From EMEP	From PyNuts GAP	Adapted from (1) and PyNuts GAP
LocOrgDem scenario	Generated from a 12-year model simulation	From EMEP	From PyNuts LocOrgDem	Adapted from (1) and PyNuts LocOrgDem

2.2 Model validation

2.2.1 PyNuts-Riverstrahler

Application of the PyNuts-Riverstrahler model to the terrestrial NEA domain has to be supported by both water quality and discharge measurements. Indeed, the PyNuts-Riverstrahler model does not yet include a proper hydrological module and water fluxes are directly derived from observed daily discharge values by a procedure that allows to distinguish surface runoff and base-flow using the Eckhardt recursive filter (Eckhardt 2008). Additionally water quality measurements have to be collected to validate the simulations over the time period 2000-2010.

For this reason during EMoSEM, a Database of Observed NUTrients in riverS (DONUTS) has been specifically designed and built to collect water quality and quantity information among official concerned national Water Authorities and other institutions listed in Table 5.

Table 5: List of data producers of the DONUTS database (upper for water discharges, lower for water quality)

Country	Producer
PT	SNIRH (Serviço Nacional de Informação de Recursos Hídricos) – INAG (Instituto da água)
ES	CEDEX (Centro de Estudios y Experimentacion de Obras Publicas)
FR	Banque Hydro
BE	Hydronet - Vlaamse Milieumaatschappij
	Aqualim - Région wallonne
	Voies hydrauliques - Région wallonne
LU	-
NL	Waterbase - Ministry of infrastructure and the Environment
DE	GRDC (Global Runoff Data Centre)
	German Federal Institute of Hydrology (BfG)
CH	Federal Office for the Environment (FOEN)
UK	CEH (Centre for Ecology and Hydrology)
IE	Hydronet - Environmental Protection Agency (EPA)
	Office of Public Work (OPW)

Country	Producer
PT	SNIRH (Serviço Nacional de Informação de Recursos Hídricos) – INAG (Instituto da água)
ES	ICA Duero
	ICA Guadiana
	CH Norte
FR	AEAG - Adour Garonne
	AELB - Loire Bretagne
	AESN - Seine Normandie
	AEAP - Artois Picardie
	AERM - Rhin Meuse
BE	Vlaamse Milieumaatschappij
	Aquaphyc DGO3
LU	-
NL	Waterbase - Ministry of infrastructure and the Environment
DE	International Commission for the Protection of the Rhine
CH	-
UK	Environment Agency
IE	Hydronet - Environmental Protection Agency (EPA)

More than 12 000 monitoring stations have been listed within the NEA domain with more than 12.5 millions of records for water quality (see Figure 16b) and 34.1 millions of records for discharge (see Figure 16a).

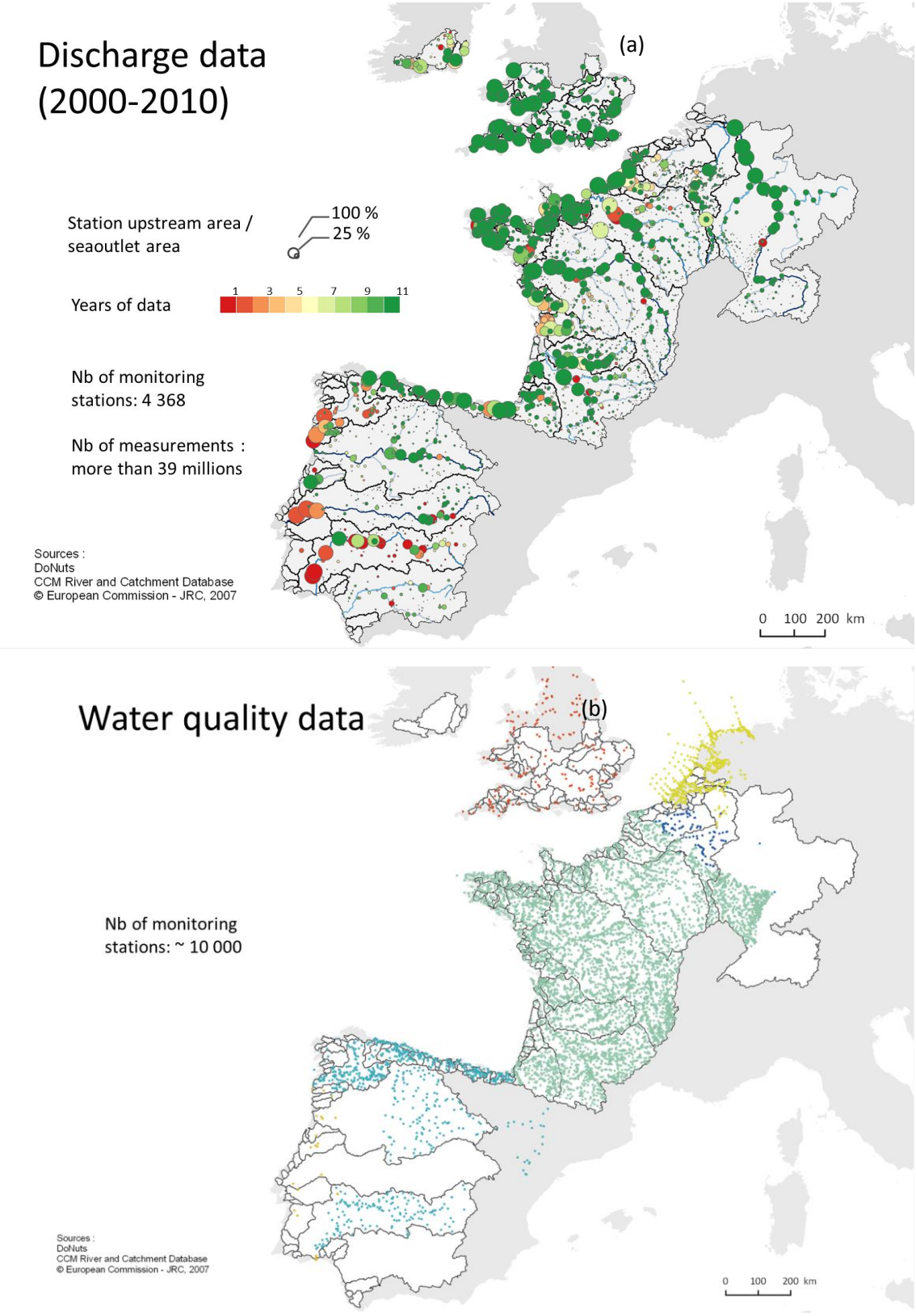

Figure 16: Spatial census of water discharge (a) and water quality (b) monitoring stations listed in the Donuts database.

The comparison of the results from the PyNuts-Riverstrahler approach compared to the observed nutrient concentrations for the recent period 2000-2010 directly represents a validation of the model as kinetics and associated parameters have been determined independently (see section 2.1.1.1).

The simulation of recent years is based on a set of national and European database describing respectively the current morphology, point sources, diffuse sources and water fluxes (see 3.1.1.1). Except for the hydrology where long time series were available, all other constraints refer to different time periods within the time frame 2000 – 2010. The time period where most of the constraints overlap is clearly the most recent (2007-2010). Figure 17 shows an example of comparison between PyNuts-Riverstrahler simulations and observed nutrient concentrations at the outlets of the main EMoSEM river basins. Because the constraints are those for the 2007-2010 period, true validations must be considered for the same period (cf. Figure 17)

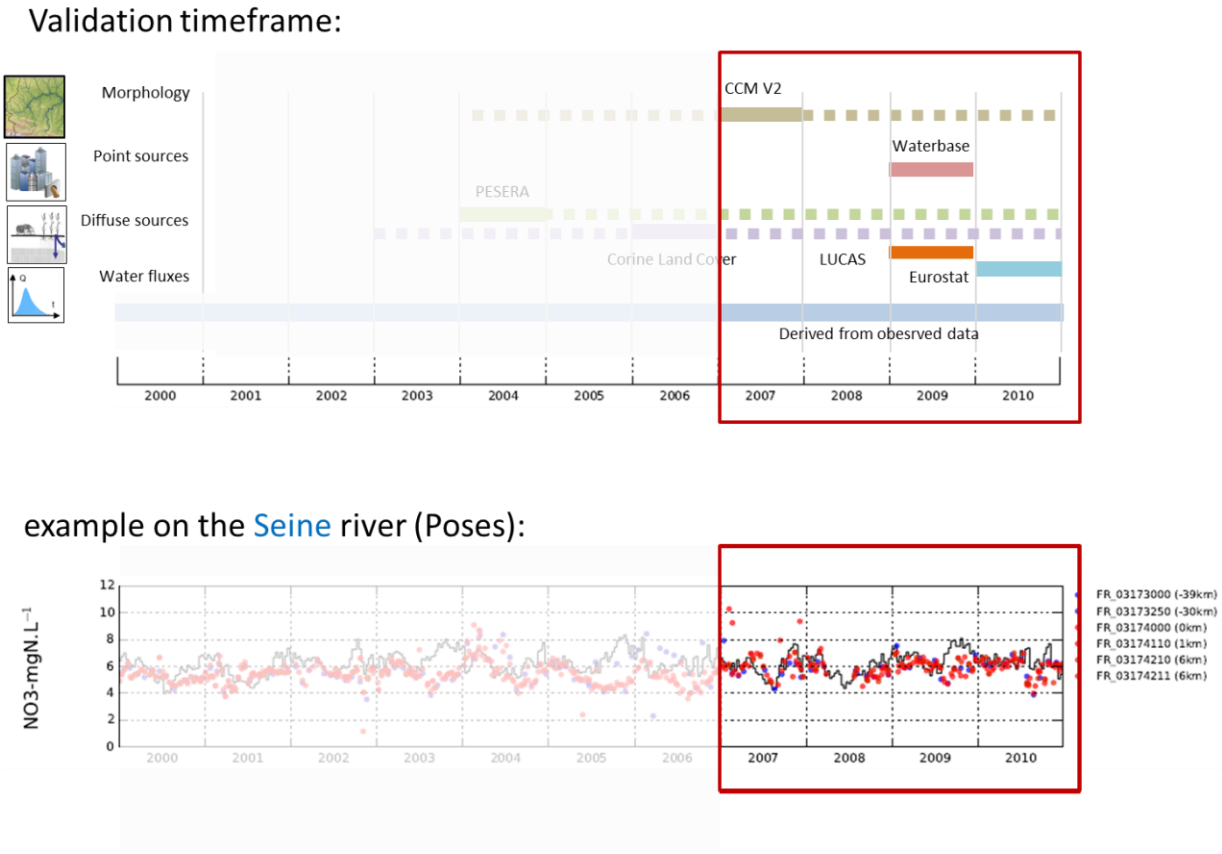

Figure 17: Identification of the suitable time frame (Red windows) to evaluate the PyNuts-Riverstrahler model performance against observed data (bottom panel). Black line: model results, red dots: observed data close to or upstream of the simulation station, blue dots: observed data downstream from the simulation station.

As shown in the examples of Figures 18 to 23, the PyNuts-Riverstrahler model, using the same set of kinetic parameters, succeeds in capturing the correct level and seasonal dynamics of nutrient concentrations at the outlet of most river systems in the NEA domain, in spite of the large range of variation of these concentrations, namely 1-5 mgN L^{-1} for nitrate, 0-5 mgN L^{-1} for ammonium, 0-2 mgP L^{-1} for ortho-phosphate, 0-6 mgSi L^{-1} for silica, 2-10 mgC L^{-1} for total organic carbon and 2-400 mg L^{-1} for suspended solids.

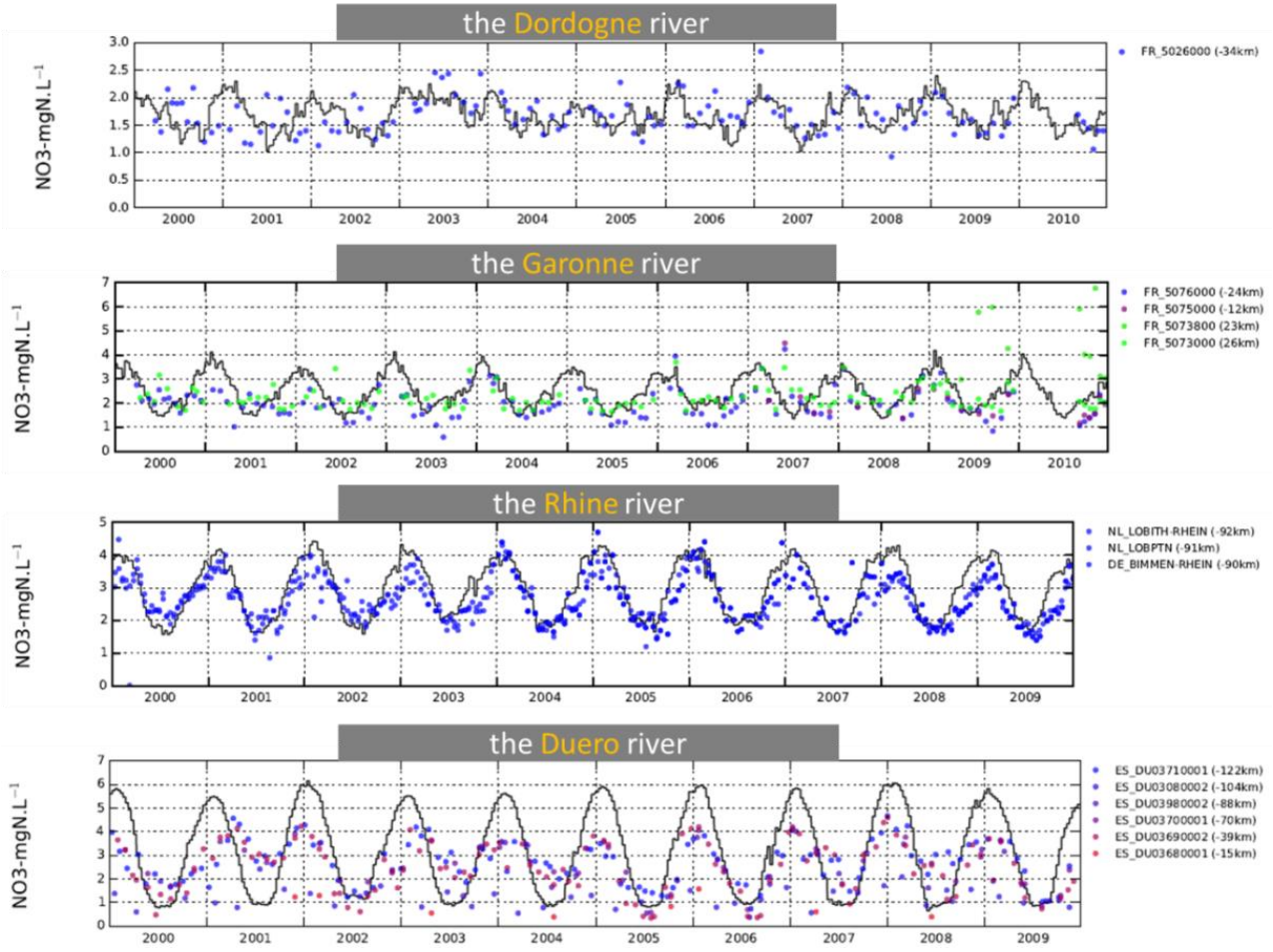

Figure 18: PyNuts-Riverstrahler simulations for NO_3 (black lines) at the outlets of some EMoSEM river systems. Natural and anthropogenic constraints refer to current situation and simulations are forced with 10 years of hydrological condition referring to the time period 2000-2010. Observed values (dots) are colored according to their position either upstream (blue) or downstream (red) the simulation pK ("kilometer point", distance indicated in km).

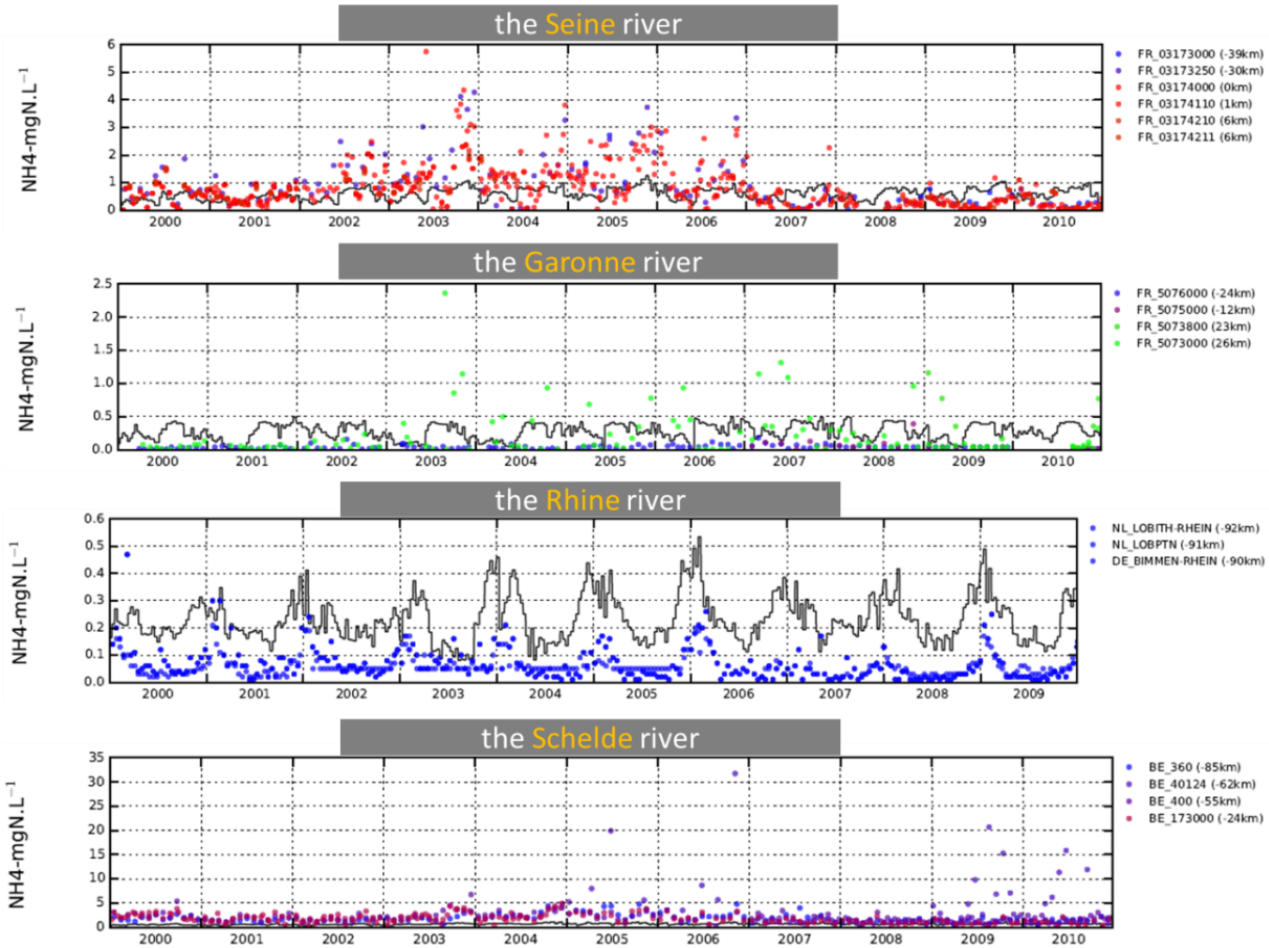

Figure 19: PyNuts-Riverstrahler simulations for NH_4 (black lines) at the outlets of some EMoSEM river systems. Natural and anthropogenic constraints refer to current situation and simulations are forced with 10 years of hydrological condition referring to the time period 2000-2010. Observed values (dots) are colored according to their position either upstream (blue) or downstream (red) the simulation pK ("kilometer point", distance indicated in km).

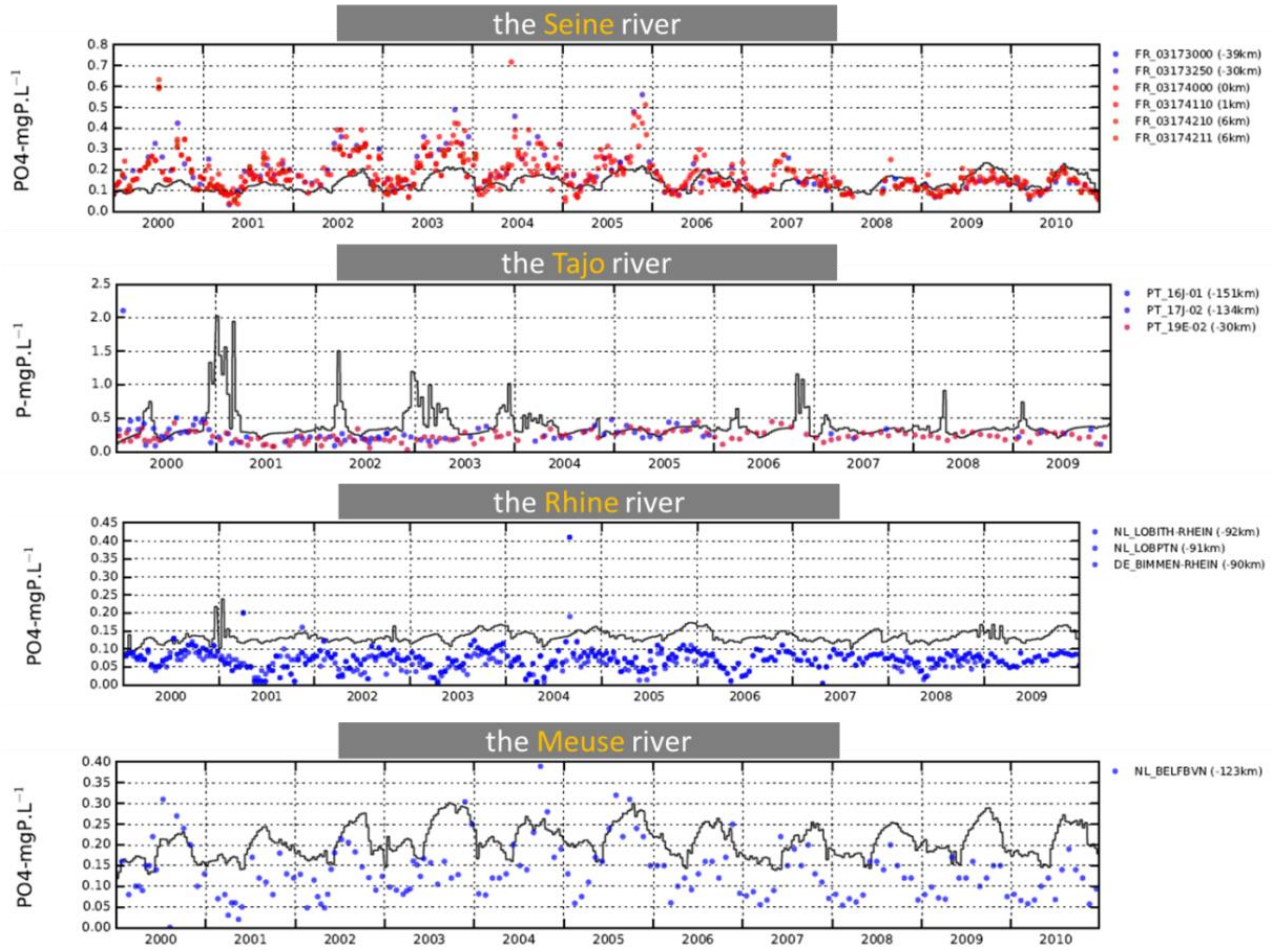

Figure 20: PyNuts-Riverstrahler simulations for Total P and PO_4 (black lines) at the outlets of some EMoSEM river systems. Natural and anthropogenic constraints refer to current situation and simulations are forced with 10 years of hydrological condition referring to the time period 2000-2010. Observed values (dots) are colored according to their position either upstream (blue) or downstream (red) the simulation pK ("kilometer point", distance indicated in km).

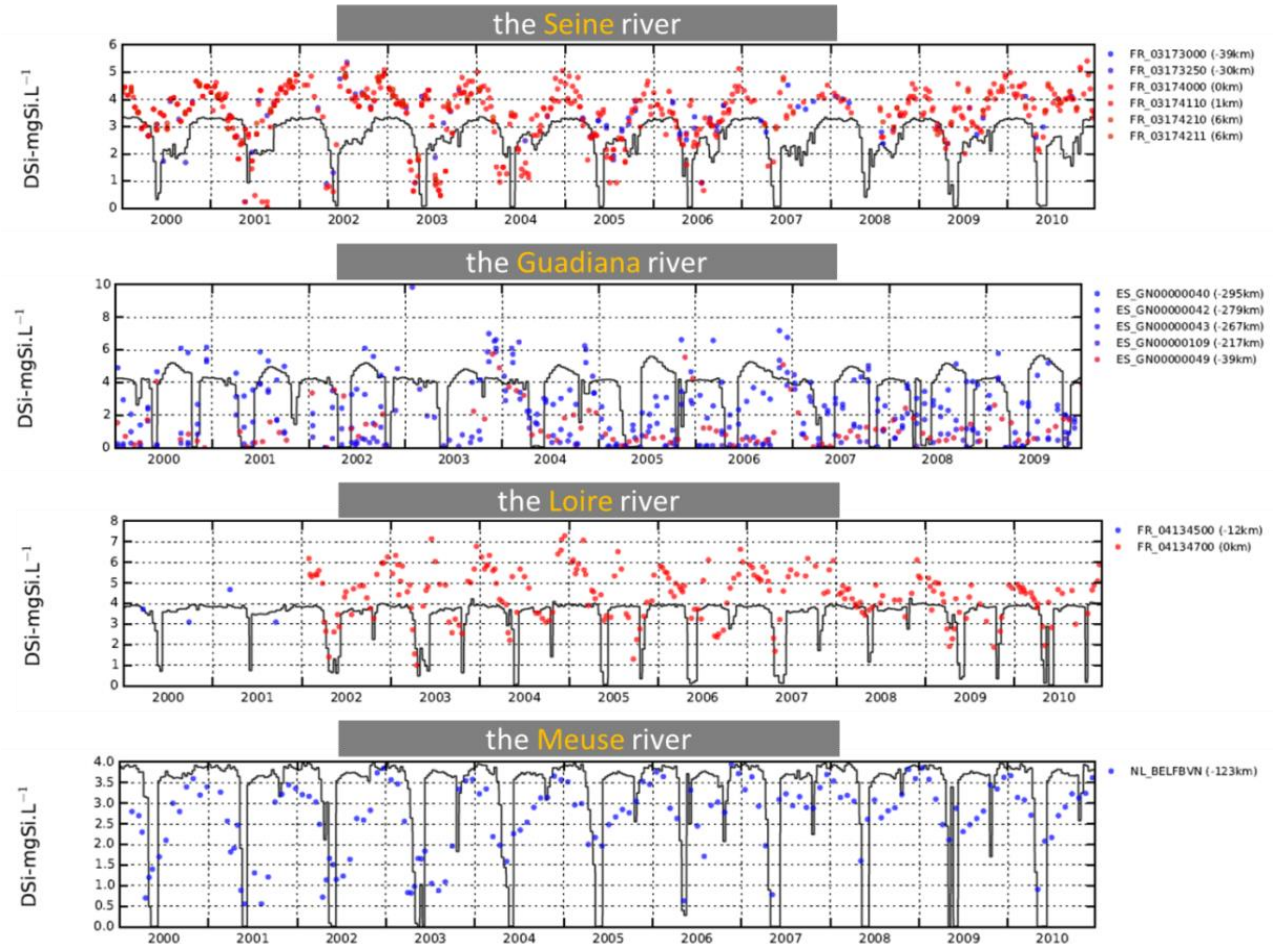

Figure 21: PyNuts-Riverstrahler simulations for DSi (black lines) at the outlets of some EMoSEM river systems. Natural and anthropogenic constraints refer to current situation and simulations are forced with 10 years of hydrological condition referring to the time period 2000-2010. Observed values (dots) are colored according to their position either upstream (blue) or downstream (red) the simulation pK ("kilometer point", distance indicated in km).

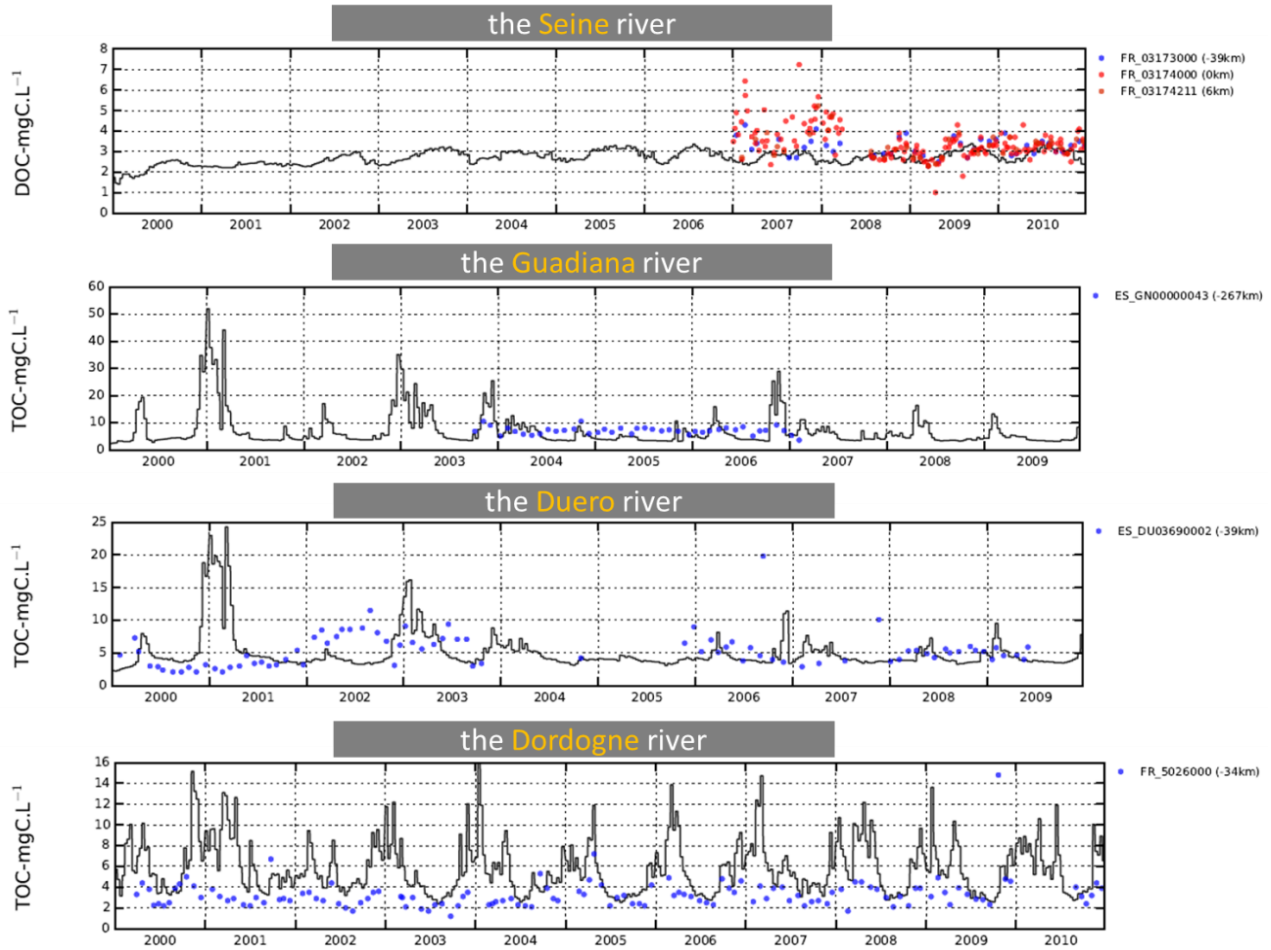

Figure 22: PyNuts-Riverstrahler simulations for Dissolved Organic Carbon (DOC) and Total Organic Carbon (TOC) (black lines) at the outlets of some EMoSEM river systems. Natural and anthropogenic constraints refer to current situation and simulations are forced with 10 years of hydrological condition referring to the time period 2000-2010. Observed values (dots) are colored according to their position either upstream (blue) or downstream (red) the simulation pK ("kilometer point", distance indicated in km).

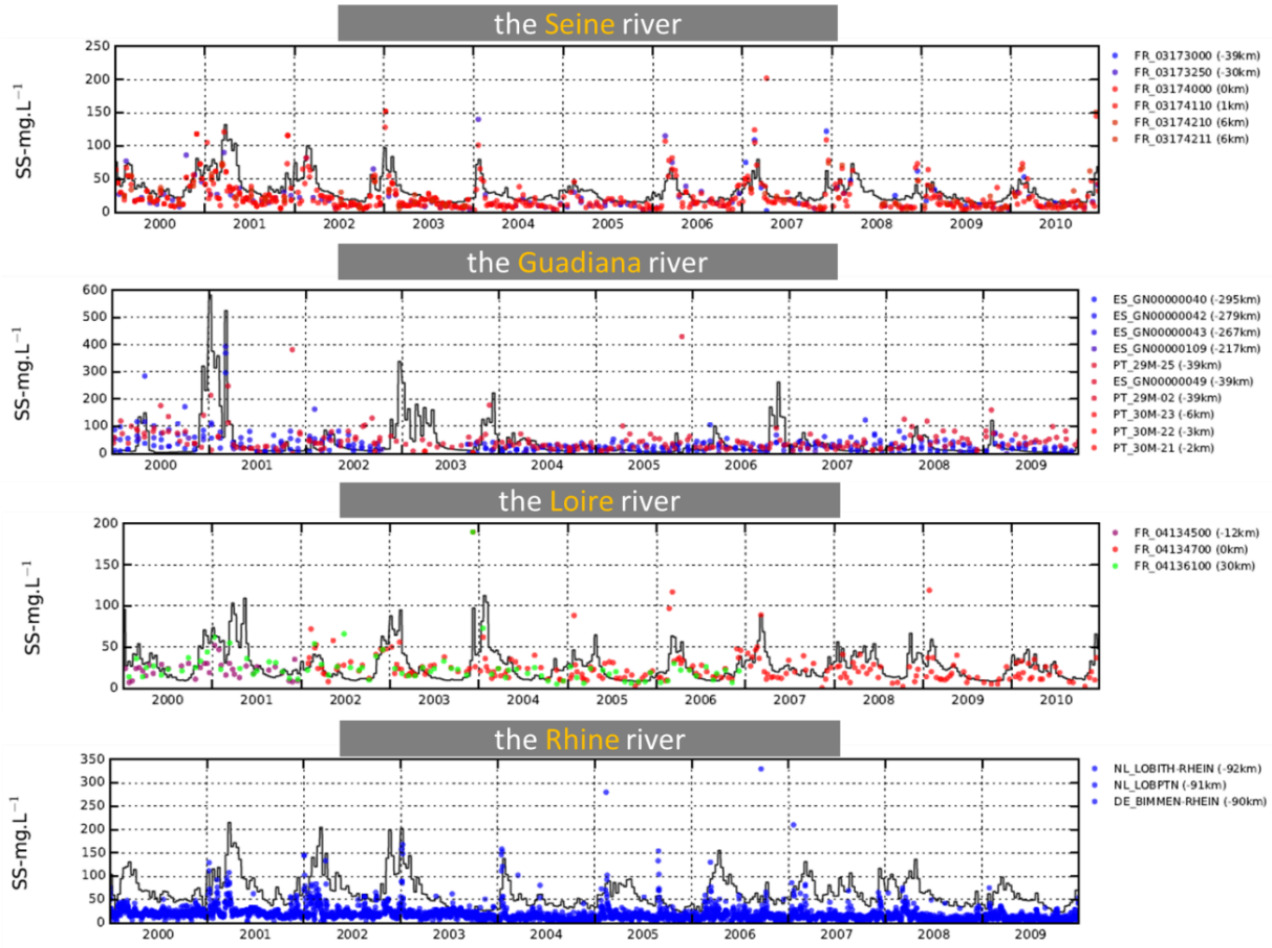

Figure 23: PyNuts-Riverstrahler simulations for Suspended Solid (black lines) at the outlets of some EMoSEM river systems. Natural and anthropogenic constraints refer to current situation and simulations are forced with 10 years of hydrological condition referring to the time period 2000-2010. Observed values (dots) are colored according to their position either upstream (blue) or downstream (red) the simulation pK ("kilometer point", distance indicated in km).

2.2.2 BIOPCOMS

2.2.2.1 Validation of the ecological module of the BIOPCOMS using remote imagery

The validation of a 3D-numerical model covering the Portuguese coastal area in terms of ecology is documented and discussed hereafter. One of the difficulties for achieving validation is related to the scarcity of direct and continuous observations available for the scientific community with dense temporal and spatial components. In order to validate the model results, satellite-borne remote observations covering large areas with a high regularity were the main source of observed data.

2.2.2.2 Satellite products

In order to evaluate the modelling results and due to the scarcity of long time series of in situ observations along the Portuguese coast, several satellite products are used to validate SST and Chl concentrations. RS SST products are quite evolved and with a relatively small error when compared with the chlorophyll *a* products. For that reason, a single product was used to validate the SST, the Microwave (MW) and Infrared (IR) OI SST (http://www.remss.com) with 9 km horizontal resolution and available since 2002 (hereafter referred as MW_IR_SST). For the Chl validation, several satellite Chl products were compared with the model results including: SeaWiFS, MODIS-Aqua, GSM V6 and GlobColour. Climatology and monthly data for MODIS-Aqua, SeaWiFS and GSM data were obtained from the Giovanni online data system, corresponding to the Giovanni-3 Level 3 monthly data at 9 km resolution. The GSM bio-optical products are derived from SeaWiFS and MODIS-Aqua data, processed by ICESS at the University of California - Santa Barbara. The GlobColour L3 data global (product GC-UM-ACR-PUG-01) corresponds to the Merged MERIS/MODIS/SeaWiFS/VIIRS global level-3 ocean with a horizontal resolution of 4 km. The GlobColour data and the modelling results have been interpolated to the same 9 km grid as the one used by the Giovanni products to allow inter-comparison.

Sá (2013) analysed 820 water samples during the period 2005-2012 and found Chl concentrations comprised between 0.01-10.15 µgChl L^{-1}. Values higher than 10 µgChl L^{-1} were eliminated from all the RS datasets. Additionally, only cells considered as water cells in all the different Chl sources were considered for this analysis, thus avoiding data located very close to the coast where many values out of the range have been detected.

2.2.2.3 Validation

The main processes affecting the primary production in the coastal areas are related with the delivery of the nutrients needed for the phytoplankton growth to the surface areas where nutrients are scarce and there is light availability. The two main pathways that transport those nutrients to the surface waters are mainly the river discharges and the upwelling processes.

The western Iberian coast shows a main N-S orientation and the northern winds prevailing mainly during the summer favour the upwelling of nutrient-rich waters to the surface areas. This process presents a signature also in the temperature as the upwelled waters are colder than the surrounding waters.

Modelling results are compared with remote sensing data with focus on the March-October period, when the main photosynthesis activity takes place in western Iberian Peninsula. Average surface temperature values for the period March-October for the year 2010 and 2011 obtained with the BIOPCOMS model are comprised between 15°C and 22°C (Figure 24). A clear latitudinal gradient can be observed in Western Iberia coastal waters, from the warm waters in the South (Gulf of Cadiz) to the colder waters in the northern part of the peninsula. Regarding the Atlantic front, the temperature is lower all along the coast than in the open ocean at the same latitude. However, this gradient between the coastal and the open ocean temperature is sharper north to the Tagus estuary area. The coastal band of low temperatures is generated by upwelling processes due to the North-south orientation of the coast and the prevailing winds coming from the north during the summer period that bring cold, nutrient rich waters to the coastal surface waters.

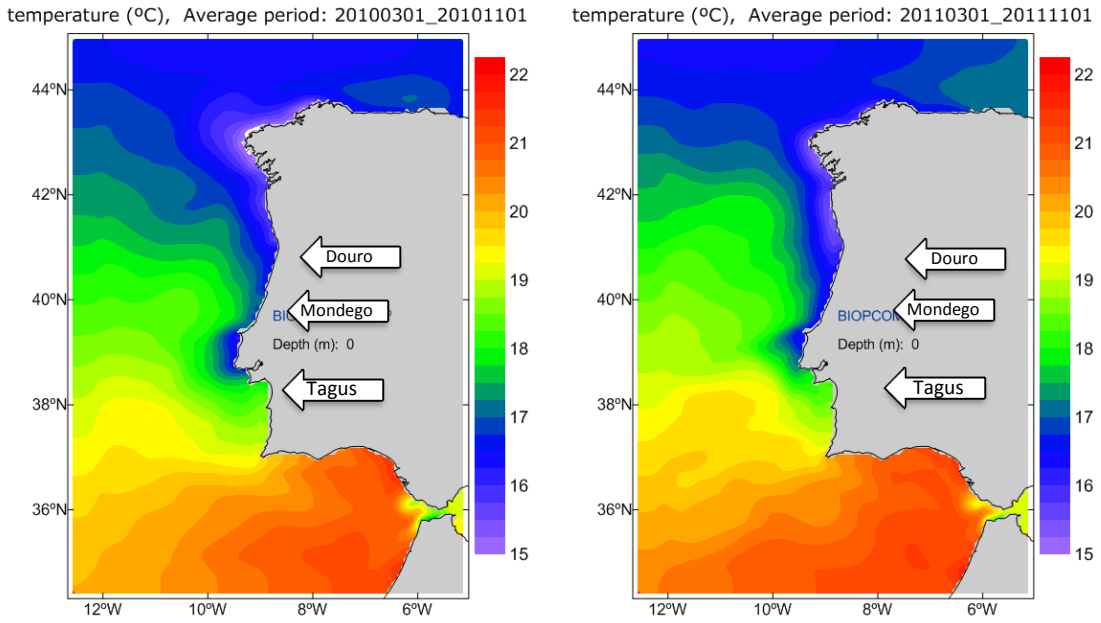

Figure 24: BIOPCOMS sea surface temperature for the period March-October 2010 (left) and March-October 2011 (right).

A comparison between daily temperatures obtained from the MR_IR_SST and model results for the year 2010 shows coefficient of determination above 0.75. Figure 25 presents a comparison between observed (satellite) and modelled SST for 3 dates (1 March 2010, 1 July 2010 and 1 November 2010).

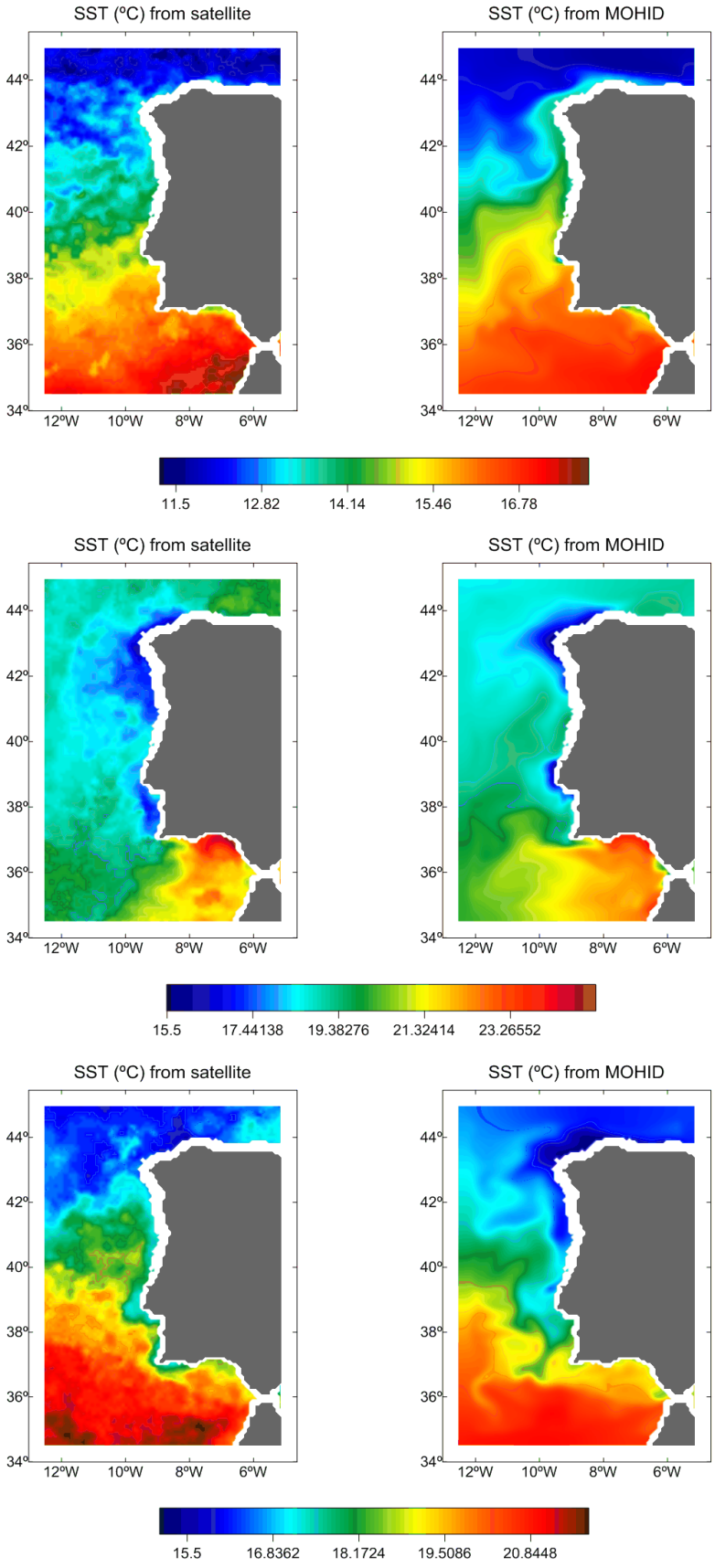

Figure 25: BIOPCOMS domain sea surface temperature obtained from the MR_IR_SST data (left) and modelling results (right) for the 1st March 2010 (top), the 1st July 2010 (middle) and the 1st of November 2010 (bottom).

In Figure 26 the distribution of phytoplankton along the western coast of the Iberian Peninsula for the March-October period can be observed for the years 2010 and 2011. These two years contrast in terms of precipitation, 2010 being a wet year while 2011 was a dry year. However, the phytoplankton distribution presents a similar pattern in the Atlantic front with surface maximum concentrations located in the vicinity of the discharge areas of the Douro, Tagus and Guadalquivir rivers. A continuous front of high primary production is located along the coastal area of Portugal associated to upwelling period and extending to the northwest of the Iberian Peninsula with a larger extension in 2010 probably due to the greater river input during that year. These results are in agreement with Alvarez et al. (2012) that identified the Chl concentration differences occurring in the northwestern part of the Iberian Peninsula between the high productive west coast associated with the northerly winds along the continental shelf in contrast to the low productive north coast.

It is important also to note here that the values presented correspond to chlorophyll concentration at the surface while the existence of a Subsurface Chlorophyll Maximum (SCM) associated to upwelling processes has been documented for this coastal area (Rossi et al. 2013) especially during the periods of stratification that takes place between upwelling and downwelling events (Crespo et al. 2008).

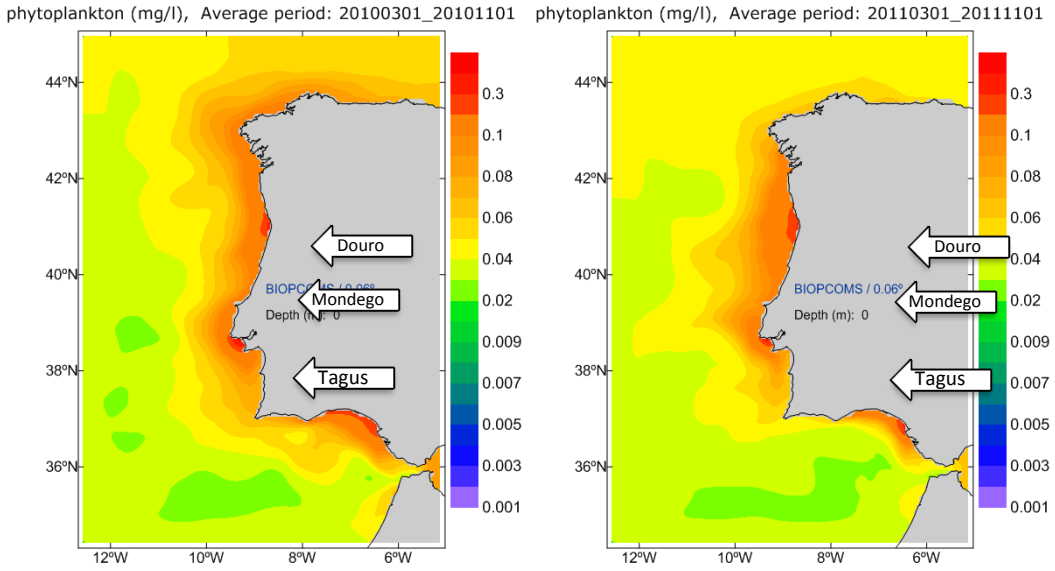

Figure 26: BIOPCOMS surface Chlorophyll a for the period March-October 2010 (left) and March-October 2011 (right). Color contouring corresponds to Chl concentration on a logarithmic scale.

In order to evaluate the model performance, phytoplankton model results have been converted into chlorophyll a (Chl) using a phytoplankton carbon to chlorophyll (C:Chl) ratio of 100 $gC.gChl^{-1}$. This value is in agreement with the values considered by Sathyendranath et al. (2009) where the ratio ranges from 10 to 150 being low in high-biomass areas and high in low-biomass areas. As the daily and eight-day GlobColour Chl products can be very patchy due to the cloud cover, we decided to compare surface results against monthly products from March to October months (Figure 27) and climatological chlorophyll values (Figure 28). The data analysis covers the period between March to October 2010. Figure 27 shows the Chl concentrations for the summer period (June, July and August) obtained by the BIOPCOMS simulations and the monthly GlobColour data.

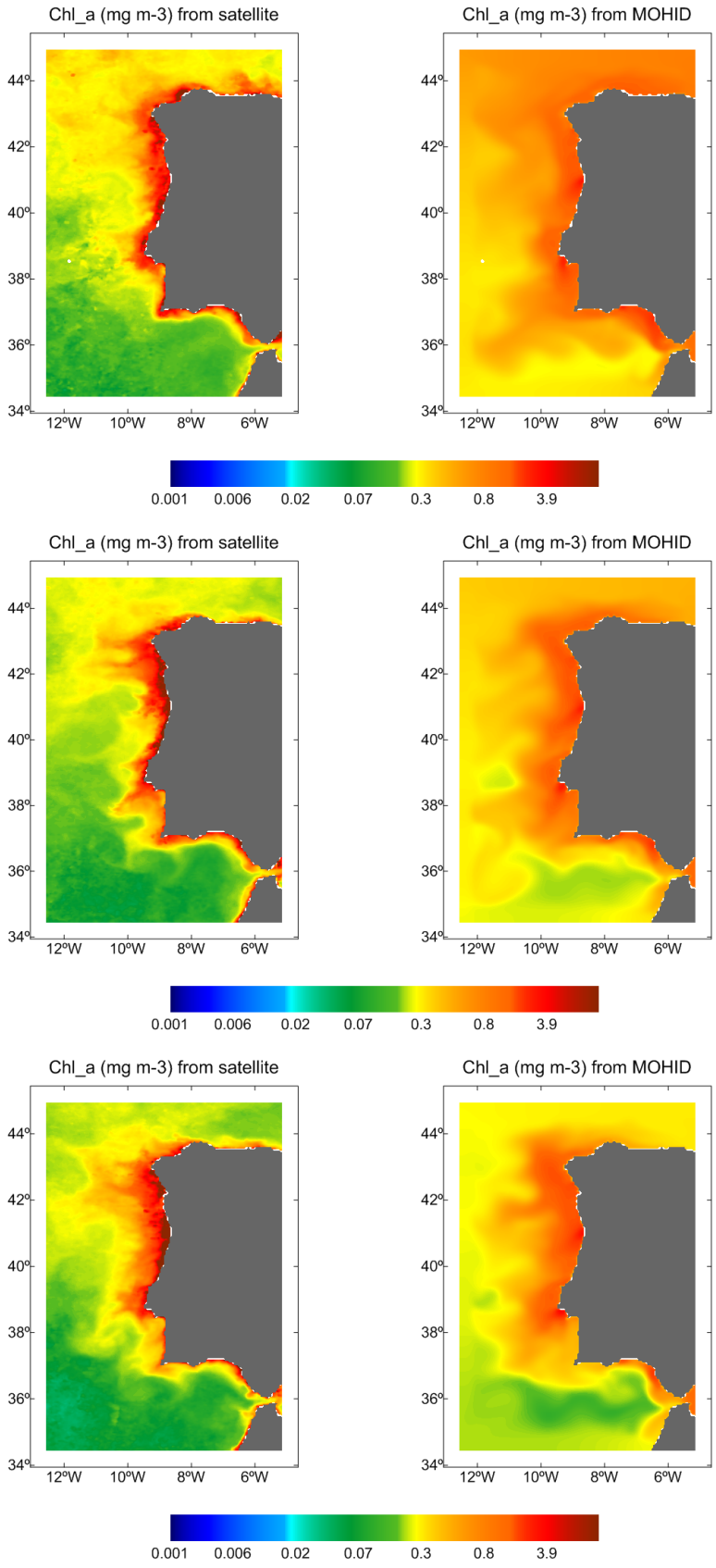

Figure 27: BIOPCOMS domain surface chlorophyll a concentrations obtained from the GlobColour product (left) and modelling results (right) for June (top), July (middle) and August (bottom) 2010. The scale is logarithmic.

March-October averaged climate data from SeaWifs (monthly binned files from September 1997 to August 2007) and MODIS-Aqua (monthly binned files from July 2002 to June 2012) products were compared with the BIOPCOMS model results averaged over March-October for the years 2010 and 2011. The model results were interpolated to the 9 km grid used by the Giovanni - Interactive Visualization and Analysis products (http://disc.sci.gsfc.nasa.gov/giovanni). Figure 28 shows the correspondence between these three sets compared two by two and the linear regression through the origin for each couple of datasets once the outliers (Chl concentrations over 10 µgChl L^{-1}) are removed. All the dataset averages present a similar value around 0.45 µgChl L^{-1} while maximum values and Percentile 90 values (within brackets) were 9.873 (0.746), 9.028 (0.651) and 6.866 (1.192) µgChl L^{-1} for the MODIS-Aqua, SeaWiFS and BIOPCOMS products. The coefficient of determination between MODIS-Aqua and SeaWiFS climatology is 0.85 while the values obtained for the BIOPCOMS results is 0.69 and 0.81 when compared with the MODIS-Aqua and SeaWiFS climatologies respectively.

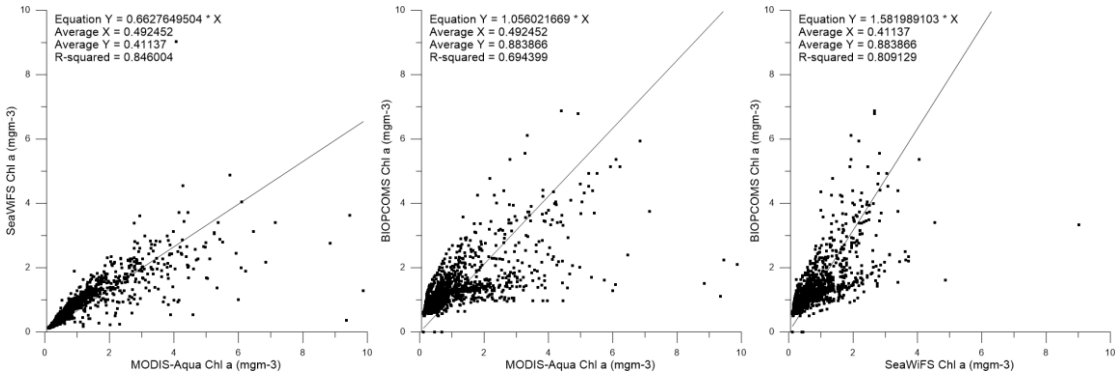

Figure 28: Chlorophyll a concentrations linear regressions obtained for the following products: SeaWiFS climatology vs MODIS-Aqua climatology (left), BIOPCOMS 2010-2011vs MODIS-Aqua (centre) and BIOPCOMS 2010-2011 vs SeaWiFS climatology (right).

In order to compare the data corresponding to the same year for several sources of satellite images, the period of March-October 2010 was selected as it is the last year with SeaWiFS data available. The selected Chl datasets for this comparison were: SeaWiFS, MODIS-Aqua, GSM, GlobColour and the BIOPCOMS results. Figure 29 shows an identical comparison to the one performed for the climatology but for the period Mar-Oct 2010, and includes also the GSM and GlobColour products. The coefficient of determination between the SeaWiFS and MODIS-Aqua (0.82) decreases compared with the climatology data (0.85) and so does the relation between SeaWiFS and the BIOPCOMS results (0.62 instead of 0.81). In any case, the coefficient of determination is higher than 0.6 for any Chl satellite product. The best results are obtained with the GSM and GlobColour products with R^2 around 0.7.

Minor differences between the coefficients of determination presented in Figure 29 and the linear regressions above (Figure 28) are related to the fact that the fitting lines were not forced to intersect the zero in the latter.

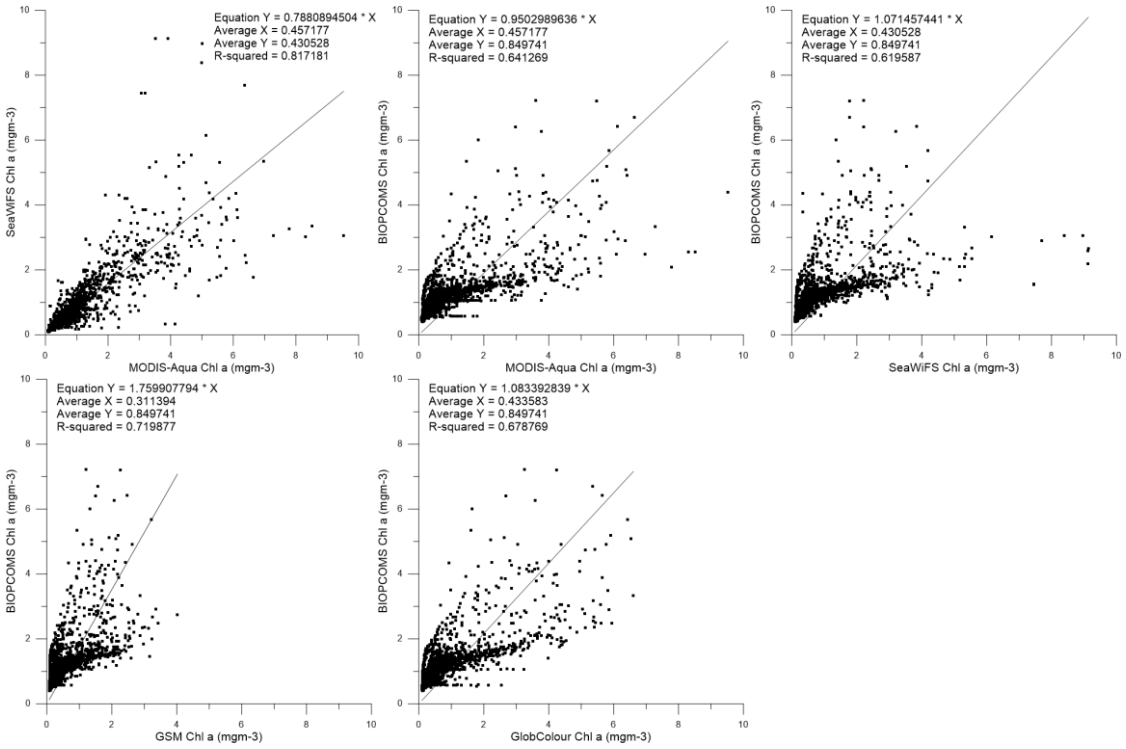

Figure 29: Chlorophyll a concentrations linear regressions obtained for Mar-Oct 2010 for the following products: SeaWiFS vs MODIS-Aqua (top left), BIOPCOMS vs MODIS-Aqua (top centre), BIOPCOMS vs SeaWiFS (top right), BIOPCOMS vs GSM (bottom left), BIOPCOMS vs GlobColour (bottom centre).

The similarity between RS Chl products and the BIOPCOMS model results is better observed through a Taylor diagram (Taylor 2001). The Taylor diagram characterizes the statistical relationship between model results and observations in terms of their correlations, their centered root-mean-square (RMS) difference and the amplitude of their variations, represented by their standard deviations. Each point in the 2D space of the Taylor diagram represents the three different statistics simultaneously. Figure 30 shows that the GSM product is closer to the numerical simulations than the three other products which are grouped in the same area of the graph.

In summary, the surface temperature and Chl concentration of a model covering the western Iberian Peninsula coast were evaluated by remote sensing products. While the surface temperature seem to be a reliable product in terms of range of values and horizontal resolution, the Chl product probably needs further calibration and processing to be a more reliable source for regional ocean model validation. The spatial distribution seems to be relatively satisfactory but the range of values resulted in a strong post-processing effort in order to compare quantitatively the model outputs with the satellite-born Chl. For that reason local knowledge and observations are crucial to filter the results and detect outliers.

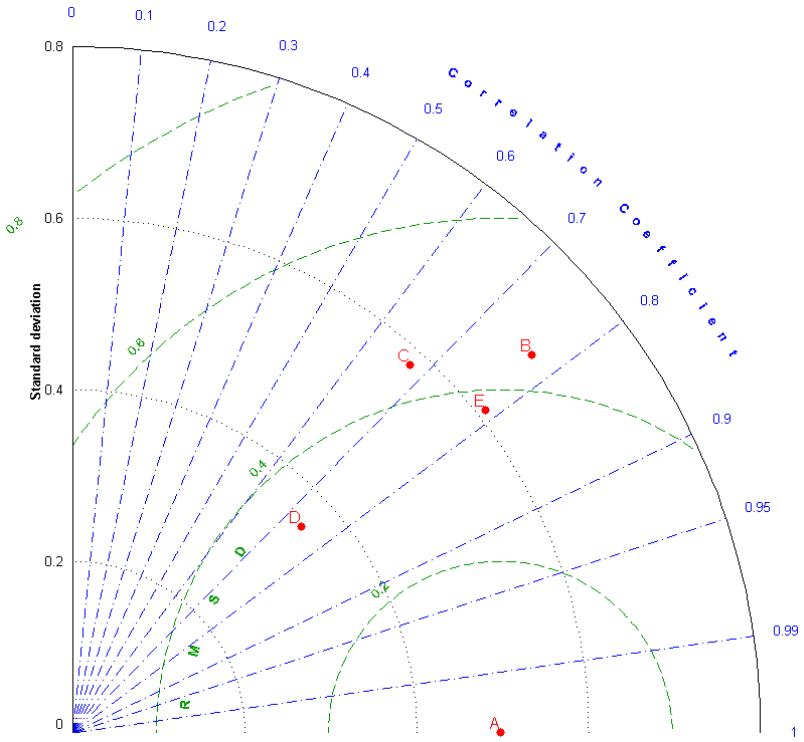

Figure 30: Taylor diagram for Chlorophyll a concentrations during the period Mar-Oct 2010 obtained from the following products: A: BIOPCOMS, B: MODIS-Aqua, C: SeaWiFS, D: GSM and E: GlobColour.

2.2.3 ECO-MARS3D

The ECO-MARS3D model has been run for the eleven years 2000-2010, using the historical data of meteorological forcing, as well as measured flow rates and nutrient concentrations of the rivers.

Figure 31 shows a very good simulation of sea surface temperature in every coastal station along the English Channel and the Bay of Biscay and a satisfactory simulation of salinity, which reproduces the local decreases of salinity induced by river plumes after floods.

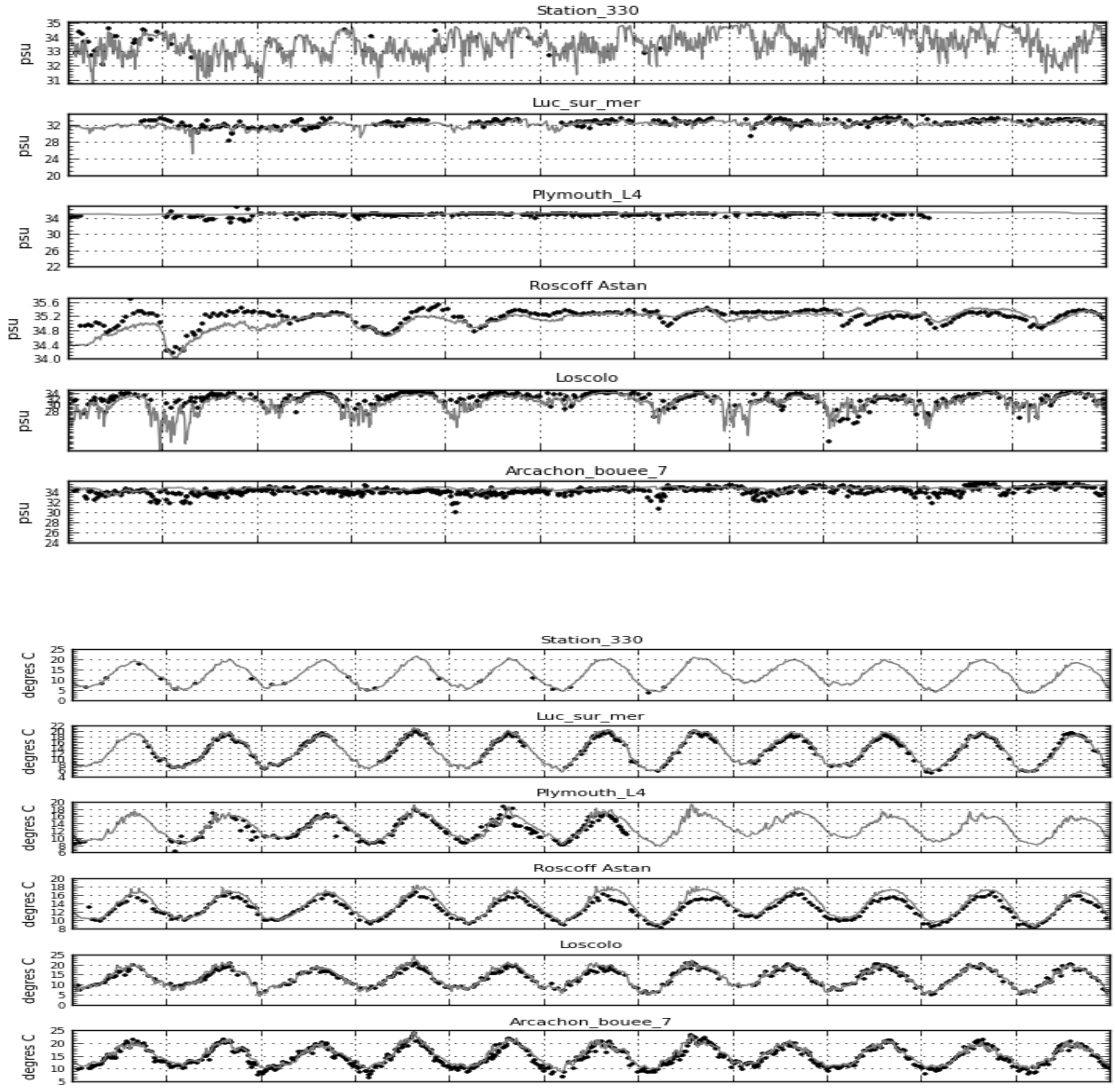

Figure 31: Comparison of simulated (solid line) vs measured (dots) salinity (top) and temperature (bottom) at 6 coastal stations (Belgian Station 330, Luc-sur-mer, Plymouth, Astan, Loscolo, Arcachon).

Figure 32 shows a high correlation (0.95) and a good standard deviation for temperature in French stations, and a medium correlation for salinity (0.7).

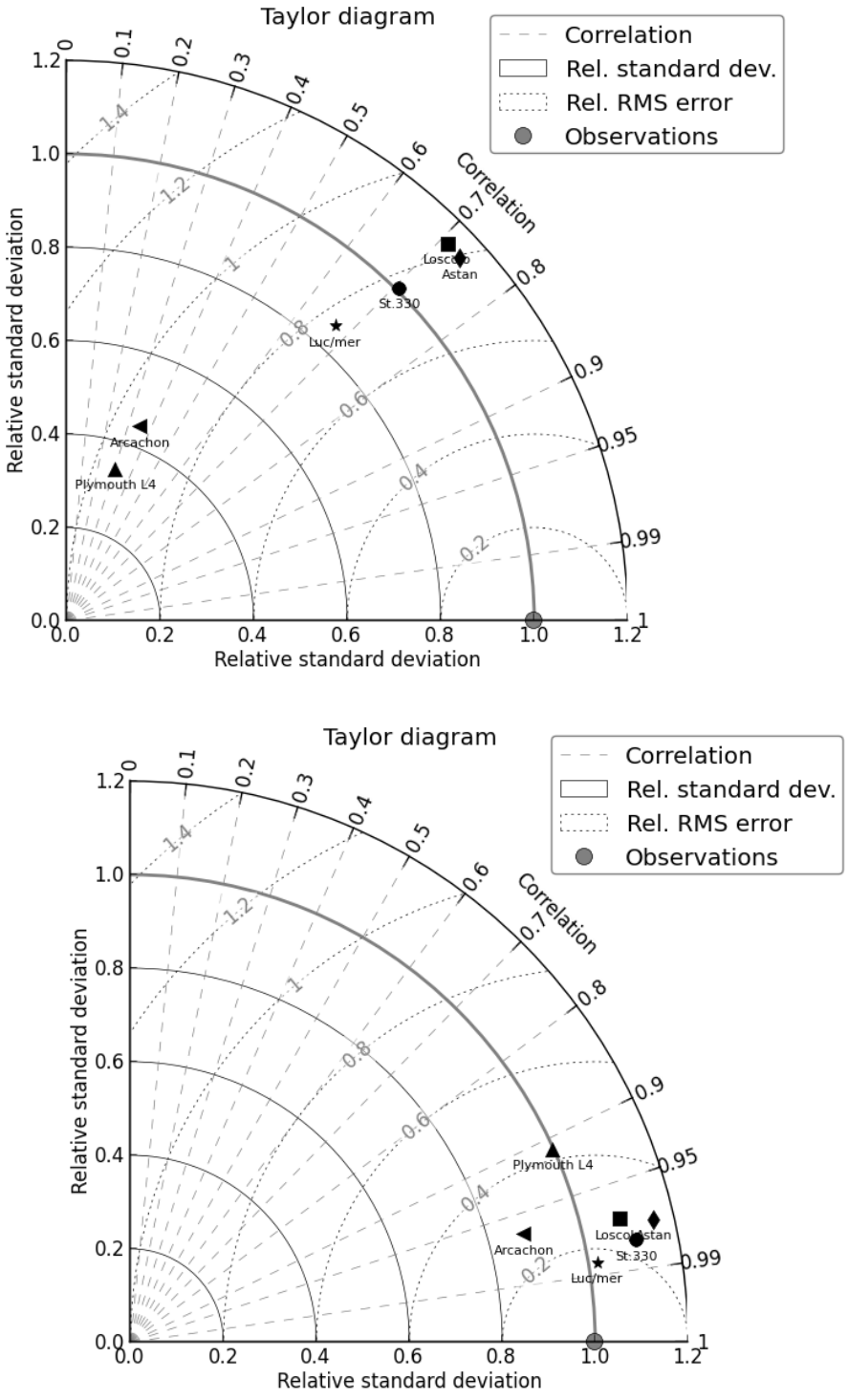

Figure 32. Taylor's diagrams for salinity (top) and temperature (bottom) at 6 coastal stations (Belgian Station 330, Luc-sur-mer, Plymouth, Astan, Loscolo, Arcachon).

Figure 33 and Figure 34 show a rather good agreement of model vs measurements in coastal stations for nutrients, and an acceptable fit for chlorophyll concentrations in terms of biomass levels and bloom phasing.

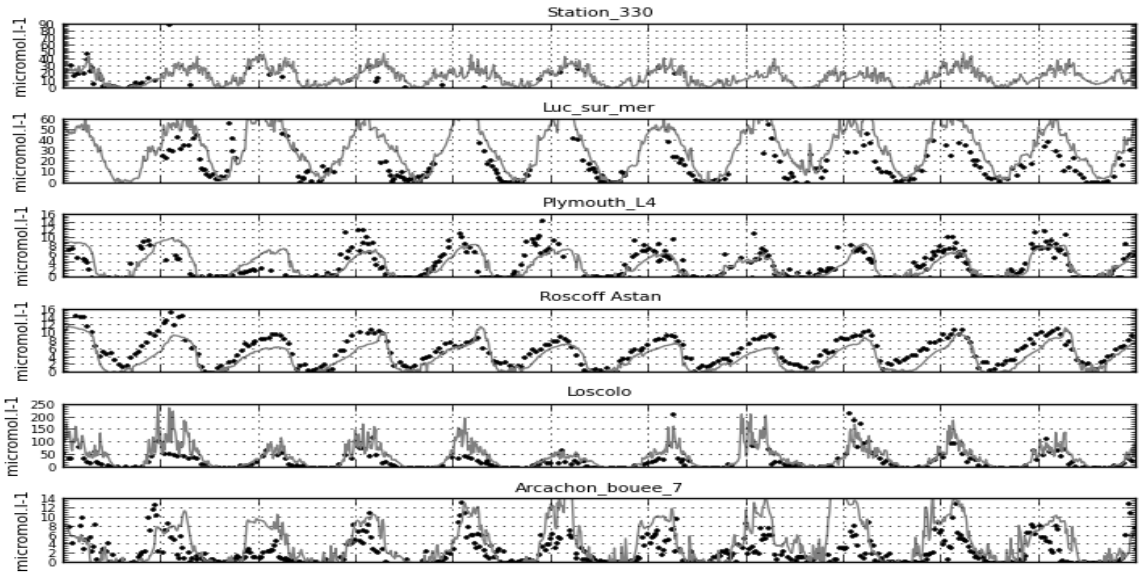

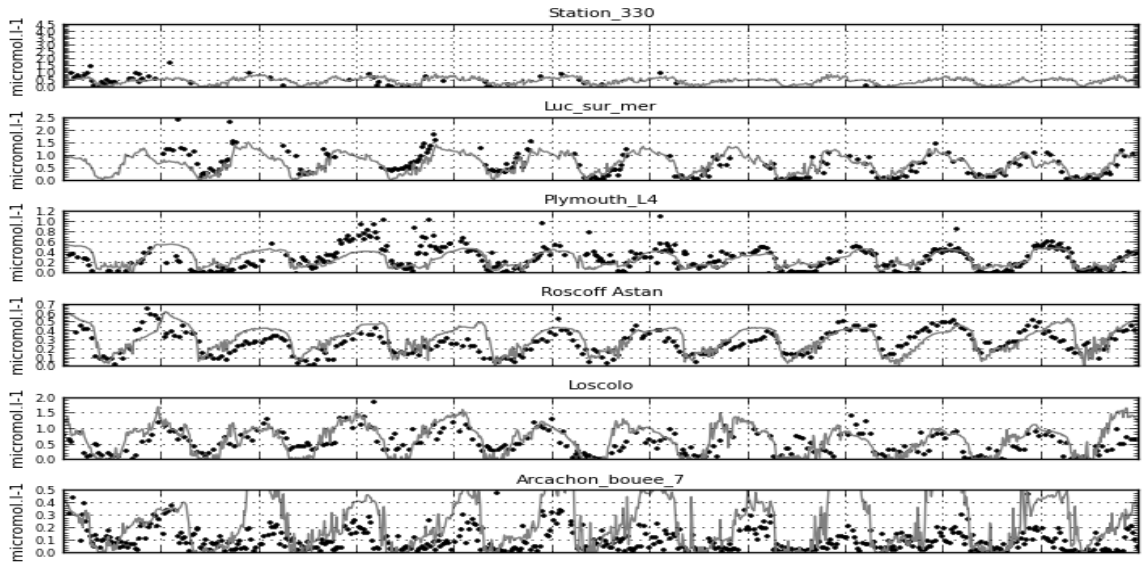

Figure 33: Comparison of simulated (solid lines) vs measured (dots) nutrients (1st group: NO_3 and 2nd group: PO_4) at 6 coastal stations (Belgian Station 330, Luc-sur-mer, Plymouth, Astan, Loscolo, Arcachon).

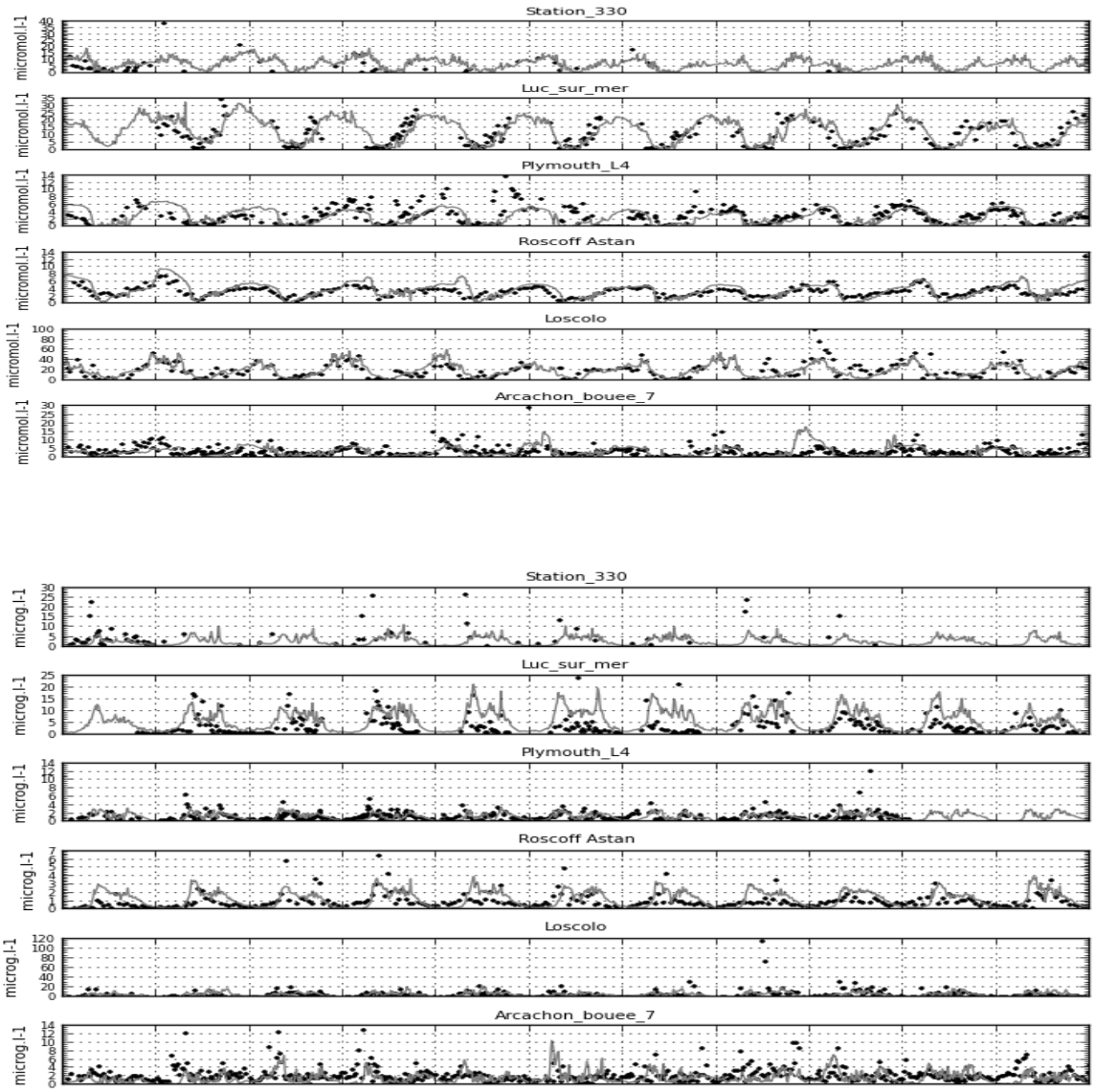

Figure 34: Comparison of simulated (solid lines) vs measured (dots) nutrients (1st group: Si(OH)4) and total chlorophyll (2nd group) at 6 coastal stations (Belgian Station 330, Luc-sur-mer, Plymouth, Astan, Loscolo, Arcachon).

Figure 35 and Figure 36 show that correlation between simulation and observations remains weak for chlorophyll and silicate (about 0.3) but seems better for nitrate and phosphate (0.5-0.6). In the simulations of nitrate and phosphate, Arcachon appears to be more variable than in the measurements.

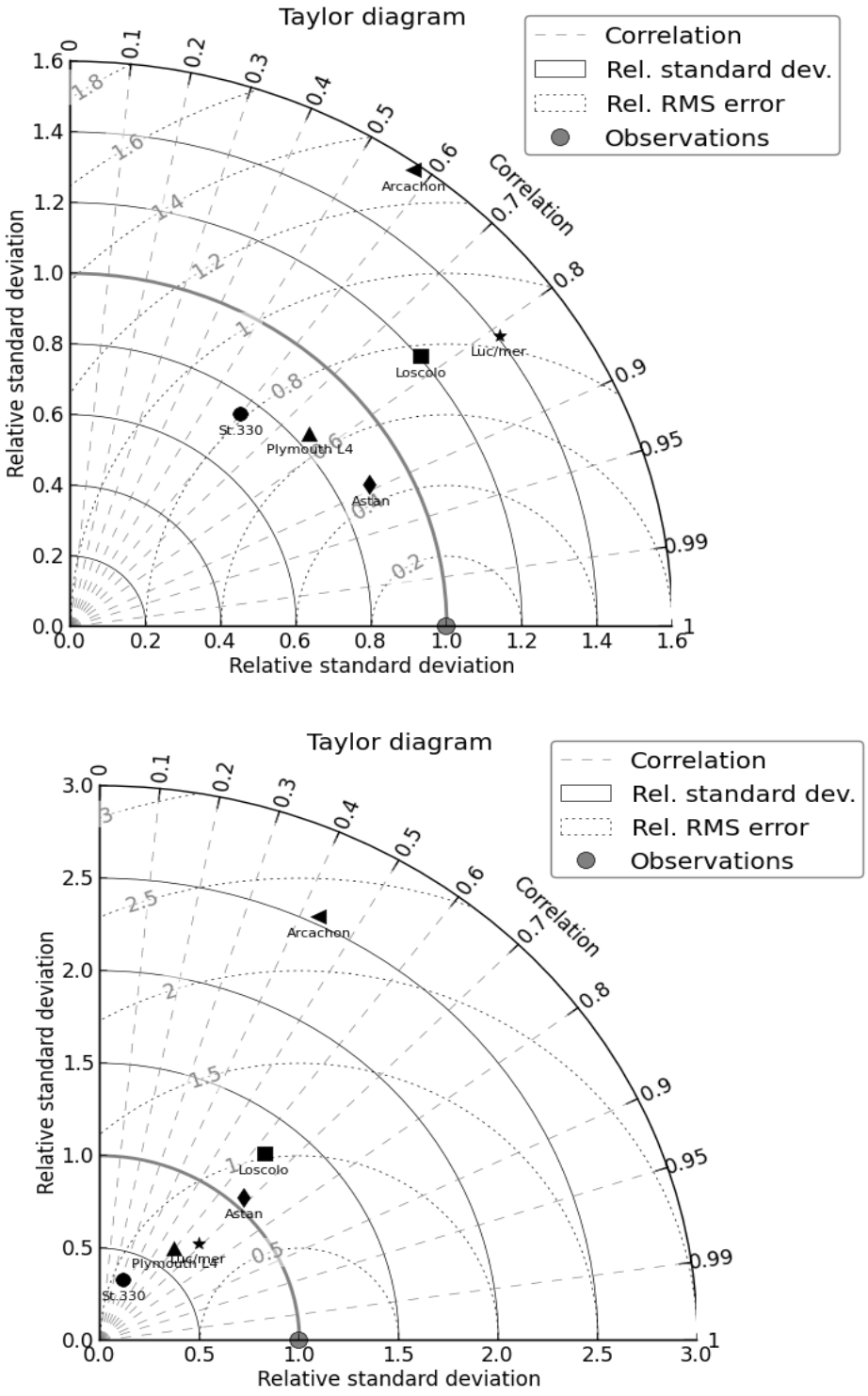

Figure 35. Taylor's diagrams for nitrate (top), phosphate (bottom) at 6 coastal stations (Belgian Station 330, Luc-sur-mer, Plymouth, Astan, Loscolo, Arcachon).

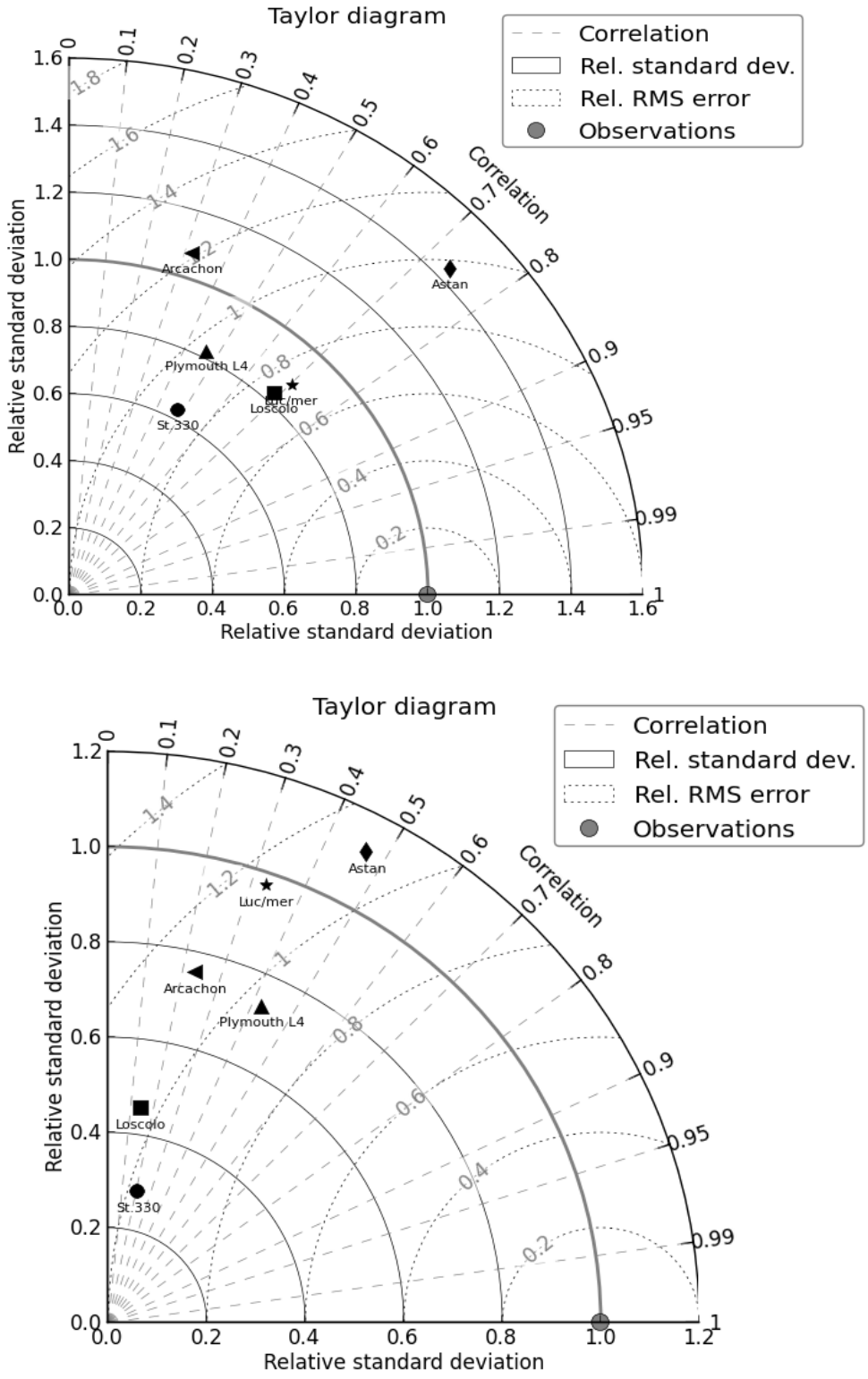

Figure 36. Taylor's diagrams for silicate (top) and chlorophyll (bottom) at 6 coastal stations (Belgian Station 330, Luc-sur-mer, Plymouth, Astan, Loscolo, Arcachon).

Over the whole domain, the comparison of simulated values to remotely-sensed surface values by satellites (SeaWiFS, MODIS) shows a global agreement for the mean annual chlorophyll *a* of a meteorological "mean" year such as 2007 (Figure 37), but reveals some discrepancies in the time-course of chlorophyll *a*, depending on the bathymetric stratum under consideration (Figure 38): whereas the model underestimates the spring bloom in the shallow coastal strip (0-25m), it overestimates it in the oceanic stratum (200-5000m).

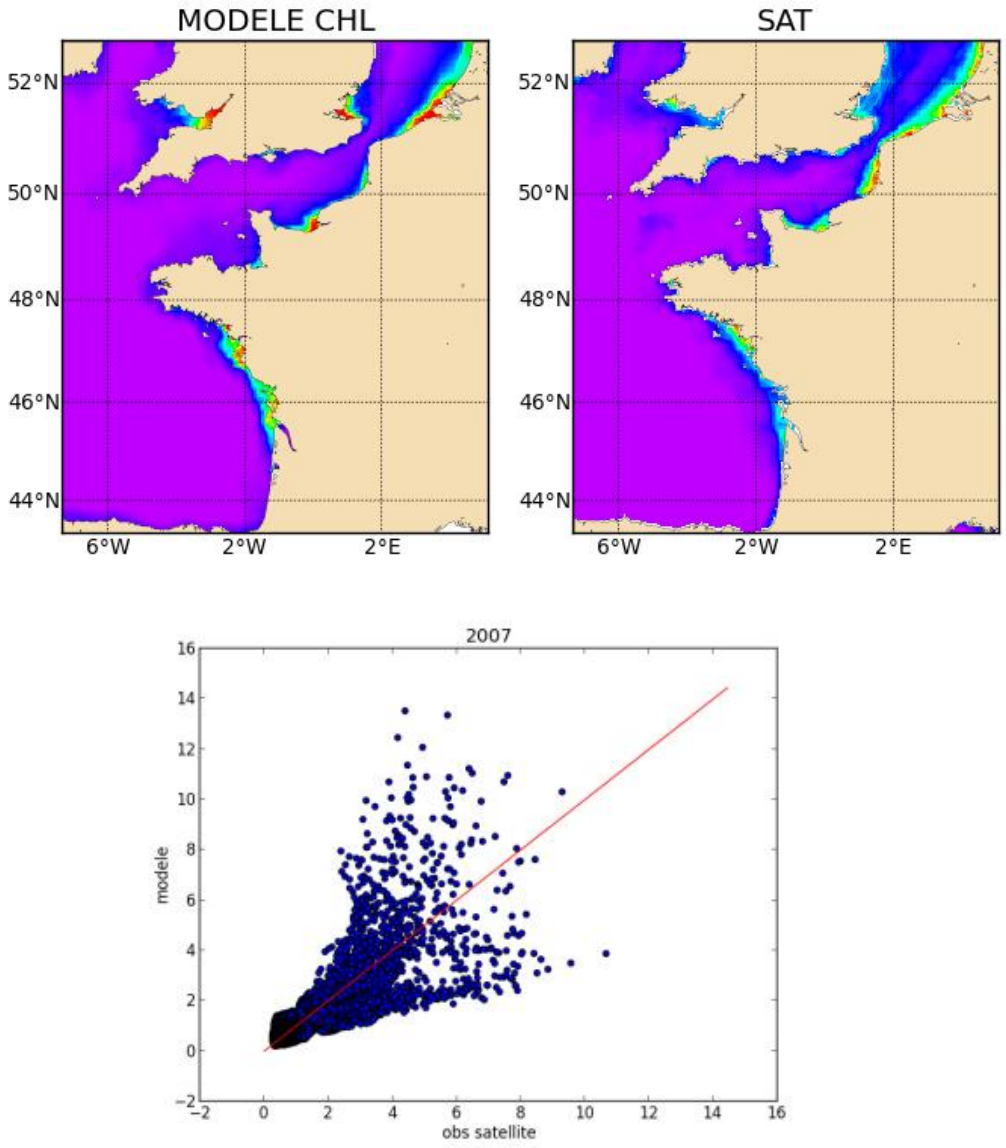

Figure 37: Mean annual surface chlorophyll for the year 2007 (left: model, right: MODIS satellite) and the scatterplot of simulated values (Y axis) against measured values (X axis).

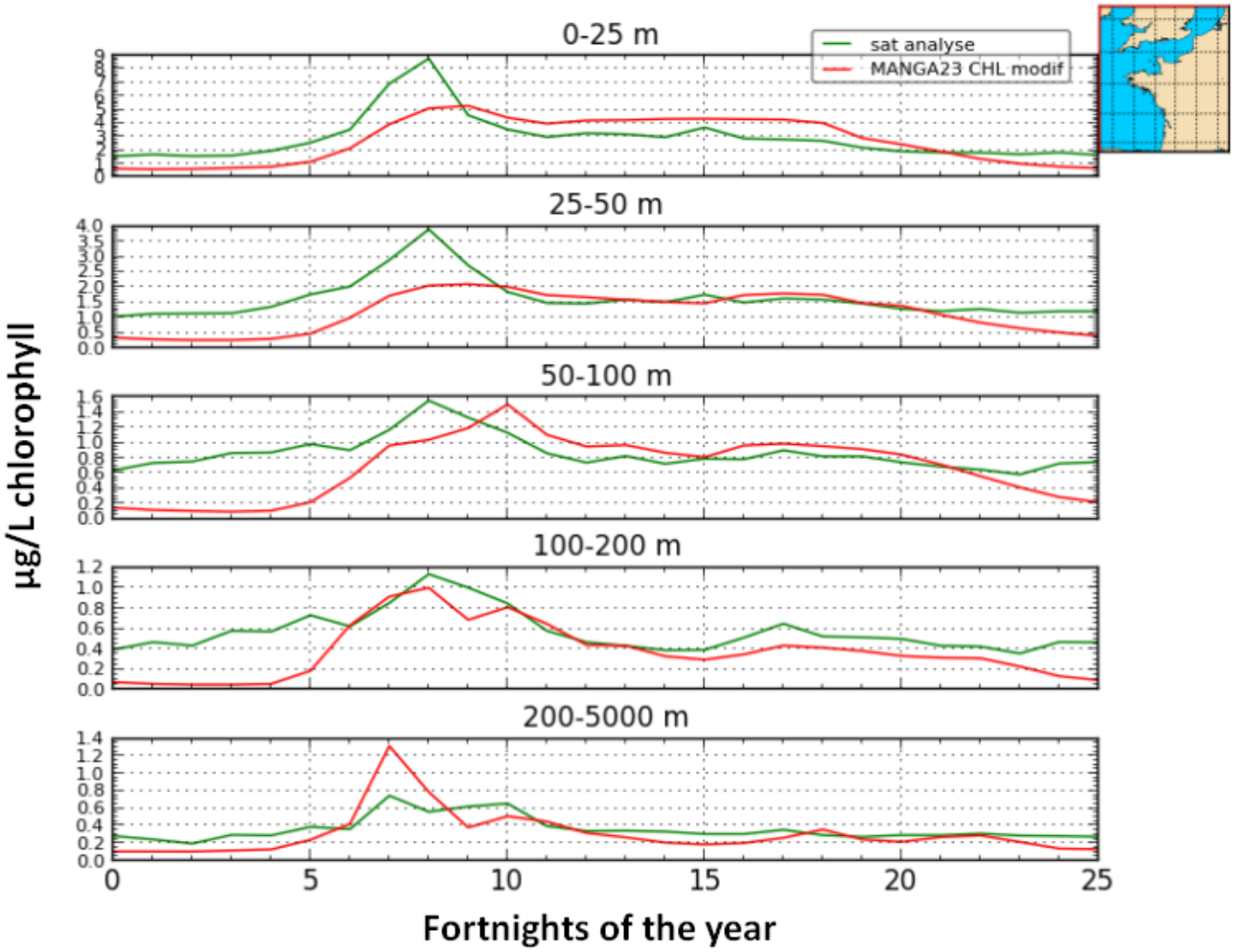

Figure 38: Time-course of the satellite-derived (green) and simulated (red) daily means of the chlorophyll, computed on 5 different bathymetric strata of the whole "small" MANGA domain.

The atmospheric depositions have then been added to the whole "small" MANGA domain. The effects on global chlorophyll levels are very weak, in spite of the locally non-negligible part of nitrogen diet of phytoplankton coming from atmospheric deposits (see section 3.4.2).

2.2.4 MIRO&CO

A validation analysis has been carried out on MIRO&CO simulation results. The simulation setup is the same as the Reference situation one described in Section 2.1.4, except that in-situ measurements of river nutrient loads and flows (see in Lacroix et al. 2007) have been used to force the model. Time series are used to validate the seasonal dynamics of dissolved inorganic nitrogen (DIN), phosphate (PO_4), dissolved silica (DSi), chlorophyll (CHL), sea surface salinity (SSS) and sea surface temperature (SST). Model results from MIRO&CO are compared against in situ observations at the reference station 330 (51°26.00'N, 2°48.50'E) situated in the center of the Belgian waters (Figure 39). Despite the few number of in situ observations, MIRO&CO captures the seasonal cycle and amplitude range of all variables quite well. Note, however, that the model underestimates the magnitude of spring bloom chlorophyll *a* concentration.

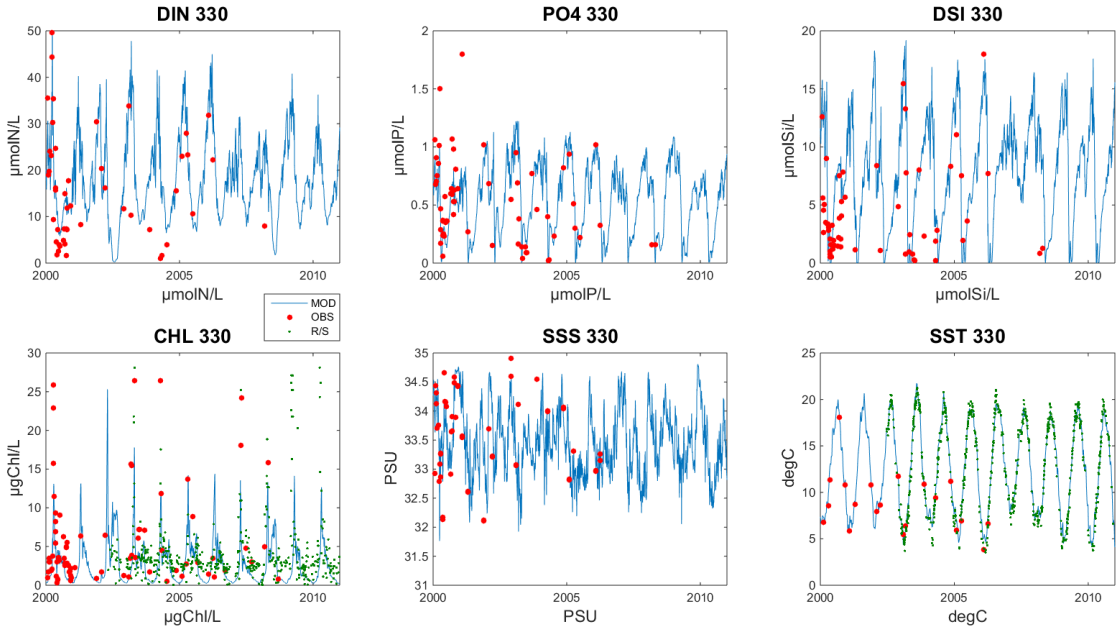

Figure 39: Time Series of dissolved inorganic nitrogen (DIN), phosphate (PO_4), dissolved silica (DSi), chlorophyll (CHL), sea surface salinity (SSS) and temperature (SST) at station 330 (51°26.00'N, 2°48.50'E). Miro&co results (blue), in situ observations (Belgian Marine Data Center, http://www.mumm.ac.be/datacentre/, red dots) and MERIS Chl or MODIS SST (green dots).

The validation is also performed at station 330 with statistics (median, P10 and P90) over the period 2000-2010 for chlorophyll *a* and nutrient concentrations (Figure 40) and for phytoplankton species (Figure 41). These figures illustrate how MIRO&CO reproduces the mean seasonal variations in the central part of the Belgian EEZ. Chl is well estimated on average though, some years, extreme blooms are not well represented in the model. This is due to the fact that MIRO&CO does not capture the magnitude reached by the *Phaeocystis* spring bloom, though the timing is generally very well reproduced. The model tends to overestimate the duration of the *Phaeocystis* bloom in summer. Regarding diatoms, the model reproduces well their dynamics, including the summer bloom showing very large variability in both the model and the data.

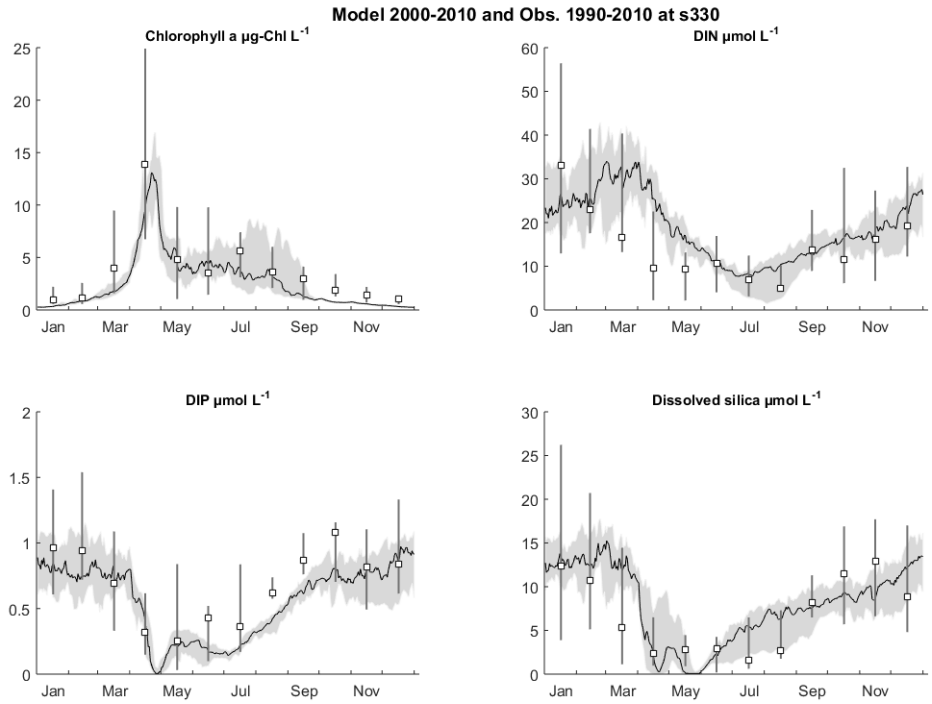

Figure 40: Timeseries of Chl and nutrient concentrations statistics (median, P10, P90 over decades, see title) at station 330 (51°26.00'N, 2°48.50'E). The black curve and the grey area respectively represent the model median and the P10-P90 range. The white dots and the vertical lines respectively illustrate the observations median values and P10-P90 range.

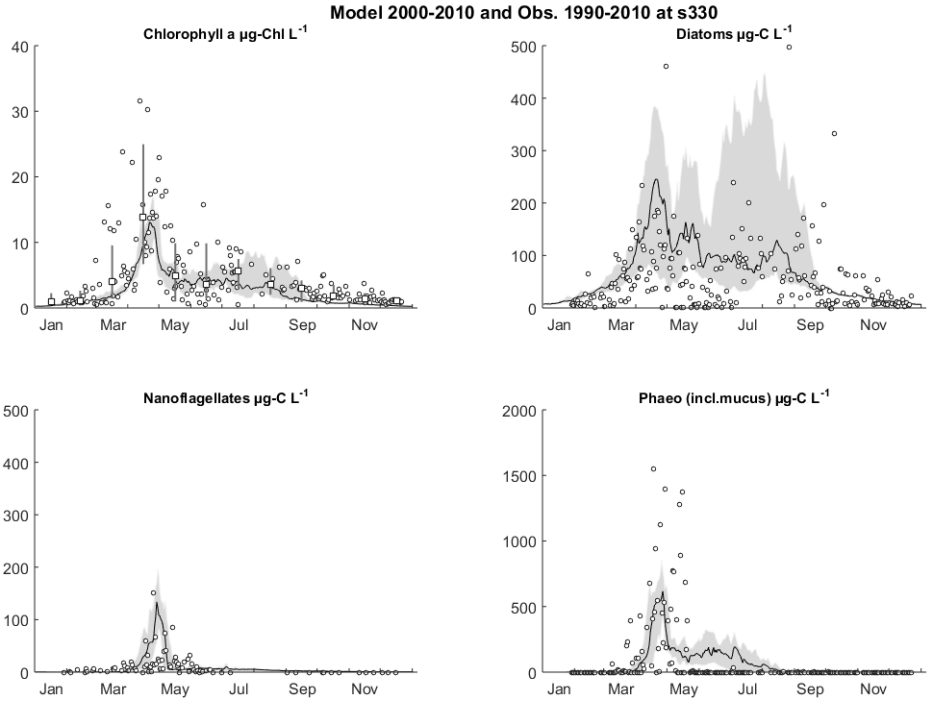

Figure 41: Time series of Chl and phytoplankton species concentrations at station 330 (see title for periods). The black curve and the grey area respectively represent the model median and the P10-P90 range. The species concentrations are not summarized by statistics but are shown altogether in the same year.

Model results and in-situ observations are also compared over the whole domain to assess the model accuracy to represent spatial distribution of the variables. The model results and data are averaged over different periods (SSS over the whole year; nutrients over winter (Dec-Feb) and chlorophyll over the productive season (Mar-Oct)). Model results and in situ observations[4] are averaged over the 2000-2010 period. For in situ observations, stations are kept only if there are more than 20 data over the whole period (for SSS) or more than 10 data over the season considered (for nutrients and chlorophyll *a*) and if there are data for at least 4 different years within the period 2000-2010 (Figure 42).

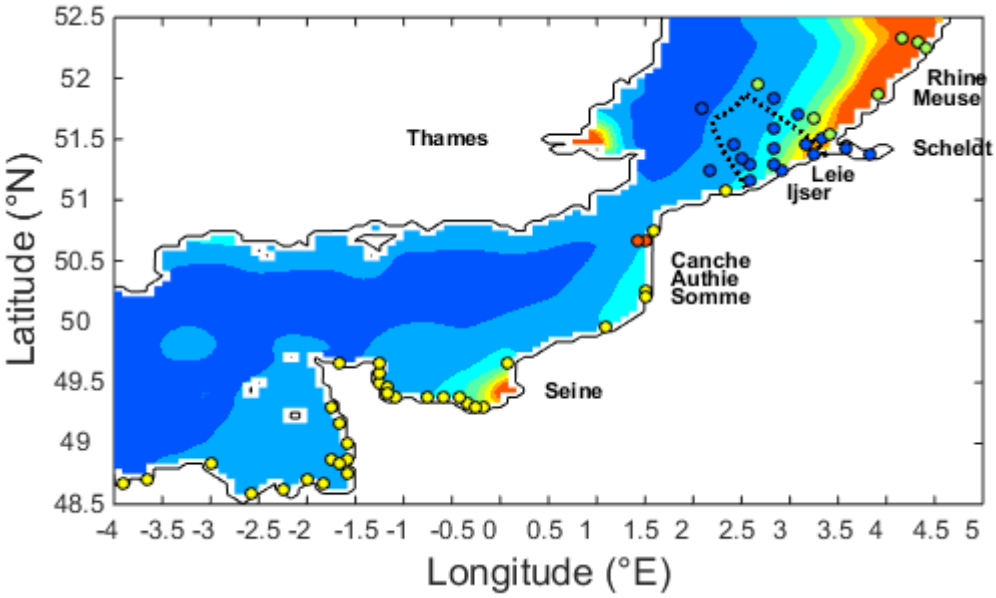

Figure 42 : Position of the stations used for model validation of chlorophyll concentration. Dots represent the stations where the number of observations is > 10 over the 2000-2010 period (Mar-Oct) and for which there are observations for at least 4 different years. BMDC stations (blue), RIKZ stations (green), REPHY stations (yellow) and SOMLIT stations (red).

The model accuracy is assessed by computing objective metrics (e.g. Allen et al. 2007) between model results and observations (2000-2010). The number of stations used for validation is given in Table 6.

[4] BMDC-BE: Belgian Marine Data Center (http://www.mumm.ac.be/datacentre/), RIKZ-NL: Rijkswaterstaat database (live.waterbase.nl), REPHY-FR: Réseau de Surveillance du Phytoplancton et des Phycotoxines (http://wwz.ifremer.fr/lerpc/Activites-et-Missions/Surveillance/REPHY), SOMLIT-FR: Service d'Observation en Milieu Littoral (http://somlit.epoc.u-bordeaux1.fr/fr/).

Table 6. Number of stations where the number of observations is > 20 (SSS) and > 10 (nutrients and chlorophyll) over the 2000-2010 period (whole year for SSS, Jan-Feb for nutrients, Mar-Oct for chlorophyll) and for which there are observations for at least 4 different years.

	SSS	CHL	NO_3	PO_4	DSi
BMDC-BE	4	25	5	5	5
RIKZ-NL	9	8	9	9	9
REPHY-FR	48	47	13	17	17
SOMLIT-FR	2	2	2	2	2
Total	63	82	29	31	31

The Taylor diagram computed using all stations shows good model skills for salinity and nutrients (NO_3, PO_4, DSi) and moderate skills for Chl (Figure 43, left). When only the stations situated in the Belgian and adjacent waters are considered (BMDC stations, shown in Figure 42), the Taylor diagram shows better correlation coefficients and lower standard deviations for all variables (Figure 43, right).

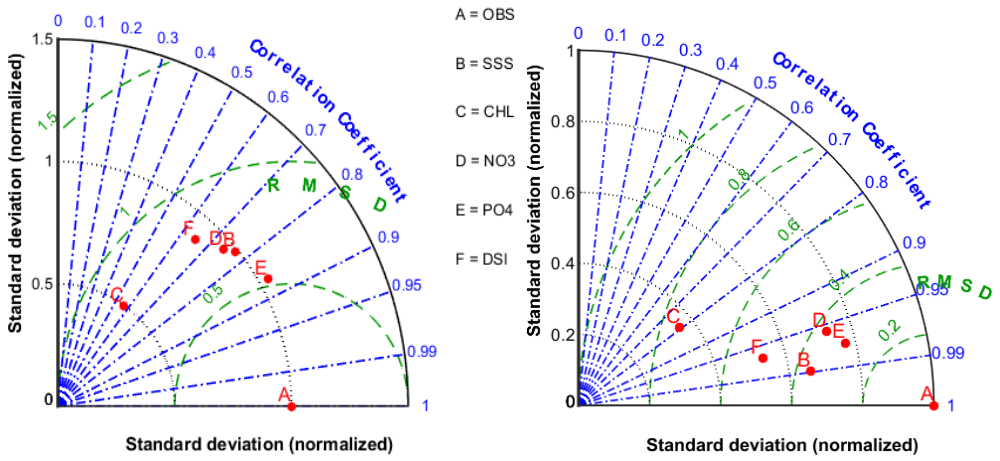

Figure 43 : Taylor diagram presenting MIRO&CO skills for sea surface salinity (B), chlorophyll (C), nitrate (D), phosphate (E) and dissolved silicate (F). Left: the whole MIRO&CO domain. Right: Belgian and adjacent waters only (BMDC stations).

2.3 Transboundary nutrient transport (TBNT)

2.3.1 TBNT with the Lagrangian tracers (BIOPCOMS)

The impact of the rivers along the Portuguese Coast was calculated by using a Lagrangian transport model coupled to the BIOPCOMS Hydrodynamic model. The Lagrangian model uses the concept of tracer: each tracer has an origin point and is defined by its position, volume and a list of properties and its movement can be influenced by the velocity field, surface wind and by random velocity.

The exchanges of water masses and nutrients along the Portuguese Coast were calculated across eight horizontal boxes, corresponding to the location of the main Portuguese riverine systems (Figure 44). The tracer origin, or the emitting tracer point, was defined as the mouth of the rivers Tagus (box4), Mondego (box5) and Douro (box6). Tracers were emitted at every 30 minutes, which means that each tracer has the equivalent volume of the river flow integrated over 30 minutes. The river discharges contain water, nutrients, and cohesive sediments concentrations provided by the PyNuts-Riverstrahler model. The surface box (first 9 meters) was used to monitor the movement of the emitted tracers and to assess the percentage of tracers coming from each origin into each box.

For each year of simulation, the ratio between the instantaneous volume coming from each river and the instantaneous water volume in each box was calculated. The time series of this ratio provided the river contribution to the water of each box.

This concept of boxes was also used to calculate fluxes of water and nutrients across the boxes, enabling to assess the exchanges of water masses, nutrients and phytoplankton along the Portuguese Coast. To this end each box was discretized into five vertical layers, covering the first 420 meters depth. This permitted not to just evaluate the flux at surface but also in the vertical.

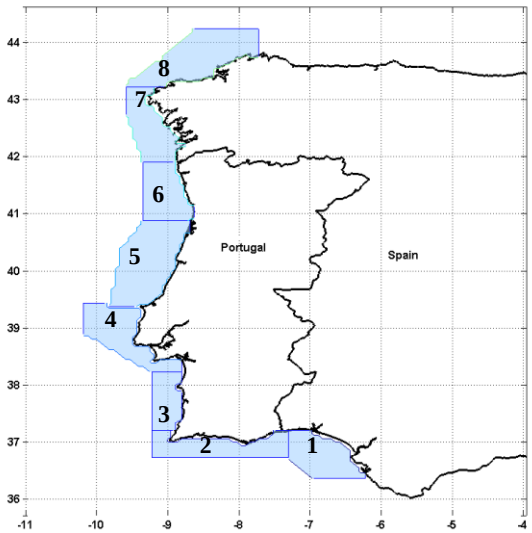

Figure 44: Boxes division along the Portuguese Coast. The numbers are used to identify the boxes located at the surface.

2.3.2 TBNT with the tagging technique

The pathways followed by a constituent in trophic web models can be investigated thanks to numerical tags fixed to the state variables containing this constituent. If the trophic model is coupled to a spatially resolved model of a region of interest, the tagging technique will provide the quantitative pathways followed by the constituent in the whole distributed trophic network. This technique has been used by IFREMER to track the various nitrogen sources leading to green algae (Ulva) mass accumulations (Ménesguen et al. 2005, Perrot et al. 2014), but also for assessing the mean age and geographic origin of diatoms (Ménesguen et al. 1997). The tagging of the origin requires doubling all the differential equations of the model which involve the constituent under study, as detailed in the insert below:

For the biogeochemical state variable B_i, having the signature $S(B_i)$:

- the current mass evolution equation is:

$dB_i/dt = sources(B_1,B_2,..B_n,t) - sinks(B_1,B_2,..B_n,t)$

- the new « signed mass » evolution equation is:

$dBs_i/dt = sources(B_1,B_2,..B_n,t) \times S(B_{1source},B_{2source},..B_{nsource}) - sinks(B_1,B_2,..B_n,t) \times S(B_i)$

- the signature $S(B_i)$ is:

$S(B_i) = Bs_i / B_i$

2.3.2.1 ECO-MARS3D

In order to perform the so-called "transboundary approach" (TBNT tracers), the tagging technique which was only applied to nitrogen in ECO-MARS3D has also been applied to phosphorus in the frame of the EMoSEM project. Since 2014, ECO-MARS3D is able to track simultaneously along the whole trophic web and over the whole domain, the nitrogen or the phosphorus coming from 3 different *ad libitum* sources. In the EMoSEM project, the different sources under consideration are the ocean (from the northern or western open boundaries), the atmosphere (only for nitrogen) and the rivers. The rivers have been gathered into 4 groups (Figure 45 and Table 7): the so-called *West-French* rivers (i.e. the Loire and the small rivers in Brittany), the *East-French* rivers (i.e. the Seine and the small rivers in eastern Channel), the *Belgian-Dutch* rivers (i.e. the Scheldt, the Rhine and Meuse) and the *English* rivers (i.e. the Thames and small rivers in southern England).

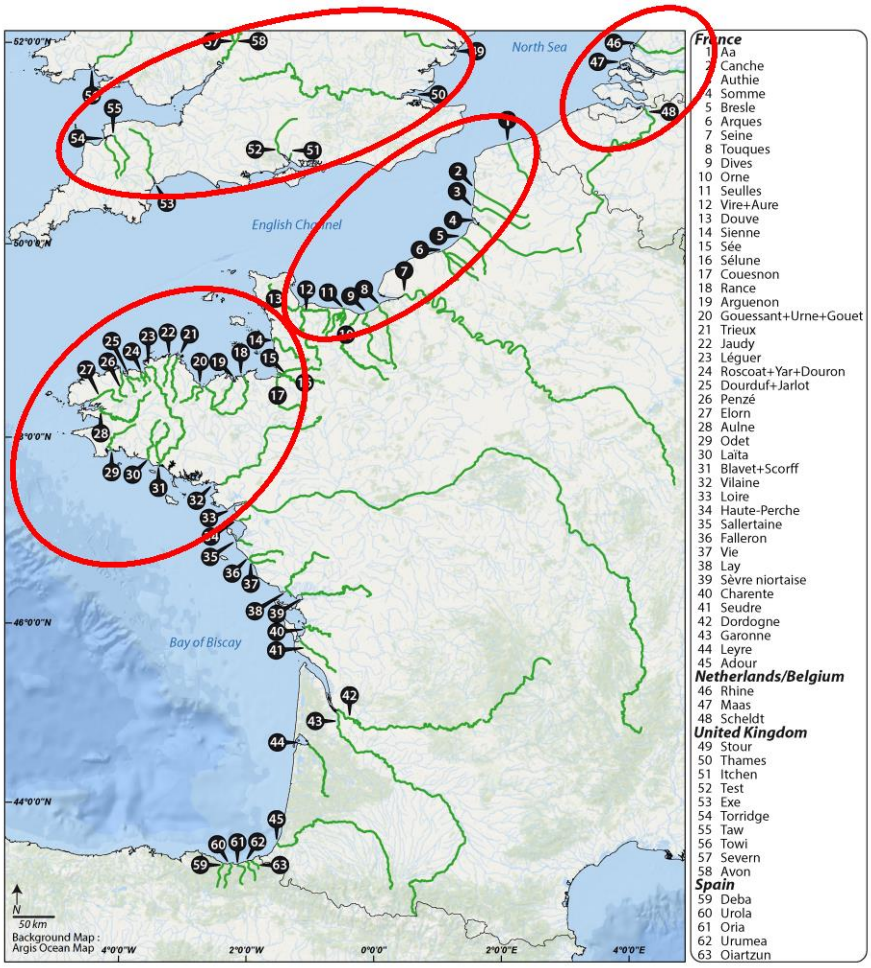

Figure 45: The ECO-MARS3D model domain covering the southern North Sea, the English Channel and the Bay of Biscay. Numbers indicate the rivers taken into account. Red ellipses represent the 4 groups of terrestrial nitrogen sources that are tracked with the TBNT method, in addition to the oceanic source and, for nitrogen, the atmospheric source.

2.3.2.2 MIRO&CO

The tagging approach from Ménesguen et al. (2006) strongly depends on the model equations and structure. In the framework of EMoSEM, this technique has been adapted to MIRO&CO and implemented in the model. Several preliminary tests have been conducted to validate the technique and its implementation in MIRO&CO. Eight sources have been tagged (see Figure 46 and Table 7). These include 4 groups of rivers hereafter called the *Seine and small French rivers*, the *Scheldt and small Belgian rivers,* the *Rhine and Meuse* and the *Thames*, plus the northern and the western ocean boundaries, the atmospheric deposition and the initial conditions. The corresponding river groups used in ECO-MARS3D may be found in Table 7. MIRO&CO simulations were performed over the 2000-2010 period with a 6-year spin up.

Table 7: Tagged sources in MIRO&CO and ECO-MARS3D by category. Complementary information can be found in Figure 45 and Figure 46.

MIRO&CO	ECOMARS
Atmospheric	
Atmospheric depositions	Atmospheric depositions
Oceanic	
Northern boundary at 52.5°N	Northern boundary at 52.74°N
Western boundary at 4°W	Western boundary at 8.13°W
Riverine	
Thames *Thames*	English rivers *Thames and small rivers in sourthern England*
Seine and small French rivers *Seine , Somme, Authie, Canche, Liane, Wimereux, Slack and Aa*	East-French rivers *Seine and small French rivers*
Rhine and Meuse *Rhine and Meuse*	
Scheldt and small Belgian rivers *Scheldt, Ijzer and the Gent-Ostend and Gent-Terneuzen Canals*	Belgian and Dutch rivers *Rhine, Meuse and Scheldt*
	West-French rivers *Loire and small French rivers*
Others	
Initial conditions	

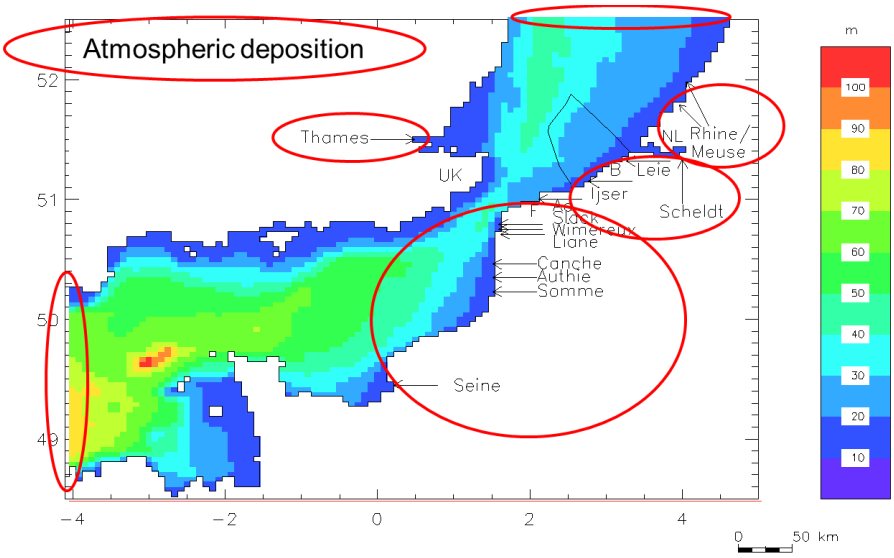

Figure 46: The MIRO&CO model domain covering the southern North Sea and the English Channel. Colors represent the bathymetry (Lacroix et al. 2004). Red circles represent the groups of nitrogen sources that are tracked with the tagging method.

2.4 Distance-To-Target (DTT)

The OSPAR concept of "distance to target" (DTT) (OSPAR Commission 2013[5], Los et al. 2014) is the nutrient reduction necessary in the rivers to reach the eutrophication GEnS in a marine region. This is based on the hypothesis that the high phytoplanktonic biomasses leading to eutrophication crisis are to be found where nutrient concentrations are highly elevated: outside natural upwelling, only plumes of enriched riversand, to a lesser but lore widespread extent atmospheric nitrogen depositions are able to do that. The extent of the atmospheric depositions of N in the sea makes it a non-negligible source of nitrogen in offshore areas, as previously shown by Troost et al. (2013). Nevertheless, only river loads are considered as controllable inputs to the sea in the present study.

As the river plumes may overlap, and lead to a cumulative effect in some regions, the question arises in the coastal zone about the exact contribution of remote, strong sources relatively to weak, but local sources to the eutrophication of a specific area. If we can formulate in a linear fashion the problem of estimating the best cost-effective nutrient reduction to impose specifically to each river, in order to reach the target everywhere, the linear optimisation technique called the Simplex method can answer that question (Dantzig 1963, Los et al. 2014). The technique consists in choosing a linear criterion to be minimized (e.g. the sum of the reductions of nutrient concentrations imposed to the different rivers) while obeying to fixed constraints (e.g. the marine nutrient concentration must stay under a predefined threshold, river nutrients cannot be reduced under a natural, pristine-like concentration, or a more elevated value imposed by economic feasibility).

As the TBNT simulations give the present proportions of nitrogen or phosphorus from different sources in the total marine concentration of a nitrogenous or phosphorous compartment, and because these proportions will change in the course of optimisation, the DTT approach first requires to convert the results of the TBNT into a non-changing map of relative influence of the various sources, i.e. the percentages of water coming from the various sources. This can be done as follows:

5 http://www.ospar.org/documents/dbase/publications/p00599/p00599_distance%20to%20target%20modelling%20assessment.pdf

If $C_{i,j}$ is the marine surface concentration of a biogeochemical compartment in the mesh (i,j) of the model grid, f_k the fraction of the water coming from the k^{th} river in this mesh, Cr_k the concentration of the nutrient under concern in the k^{th} river and Co its oceanic concentration:

the linear decomposition of the total concentration in mesh (i,j) is:

$C_{i,j} = \sum(f_k \, . \, Cr_k) + [1-\sum(f_k)] \, . \, Co$

the TNBT computation has delivered the parts coming from the various sources:

$C_{i,j} = \sum(C_k) + C_o$

so, the part of water in mesh (i,j) coming from the k^{th} river is:

$f_k = C_k / Cr_k$

Then, the DTT can be estimated for different criteria (DIN and DIP separately or together, i.e. taking into account their ratio in the living matter, 90^{th} percentile of chlorophyll *a* expressed in N or P currency, etc.). When DIN and DIP are optimised together (i.e., N/P constrained), the global function to be minimized is the sum of imposed concentration decrease in rivers for DIN and for DIP, but weighted by the N/P ratio, in order to equalize the weights of the two chemical elements N and P.

The DTT can also be estimated in reference to target-areas of different sizes (from WFD water masses up to MSFD sub-regions). Because the nutrients of the big rivers may be transported far away before complete dilution, not only coastal zones, but also remote offshore areas are sometimes subjected to undesirable eutrophication. This explains why the size of the target-area can considerably modify the optimal nutrient reductions required.

3 RESULTS

3.1 Past, present and future status of eutrophication

3.1.1 Description of scenarios and their effect on river water quality

3.1.1.1 Current conditions (called Reference)

The Reference situation has been built using the most recent level of pressures reported by national and European databases and was thus considered as a starting point for scenario building. It basically mixes information recently published and describing both natural and anthropogenic contributions over the timeframe 2000-2010 (Table 8).

Table 8: Information required by the PyNuts-Riverstrahler model and corresponding databases for NEA domain.

Natural and anthropogenic constraints	Databases	References
River catchment characteristics	CCM2	Vogt et al. 2007
Morphology and Reservoirs	Global Reservoir and Dam (GRanD) database	Global Water System Project 2014 (Lehneret al. 2008)
Urban point sources	Waterbase UWWTD	European Environment Agency
Diffuse sources	Corine Land Cover	European Environment Agency
	Eurostat	-
	Pesera	Kirkby et al. 2004
	Top soil organic content	Jones et al. 2005

Like all EMoSEM scenarios, this “current” reference scenario has been run using the wide range of hydrological conditions observed over the period 2000-2010, in order to integrate the variability of climatic conditions (see Figures 18-23). The mean level of nitrate and phosphate concentration calculated for the current reference scenario in the drainage network of NEA watershed is shown in Figure 47 and Figure 48 respectively.

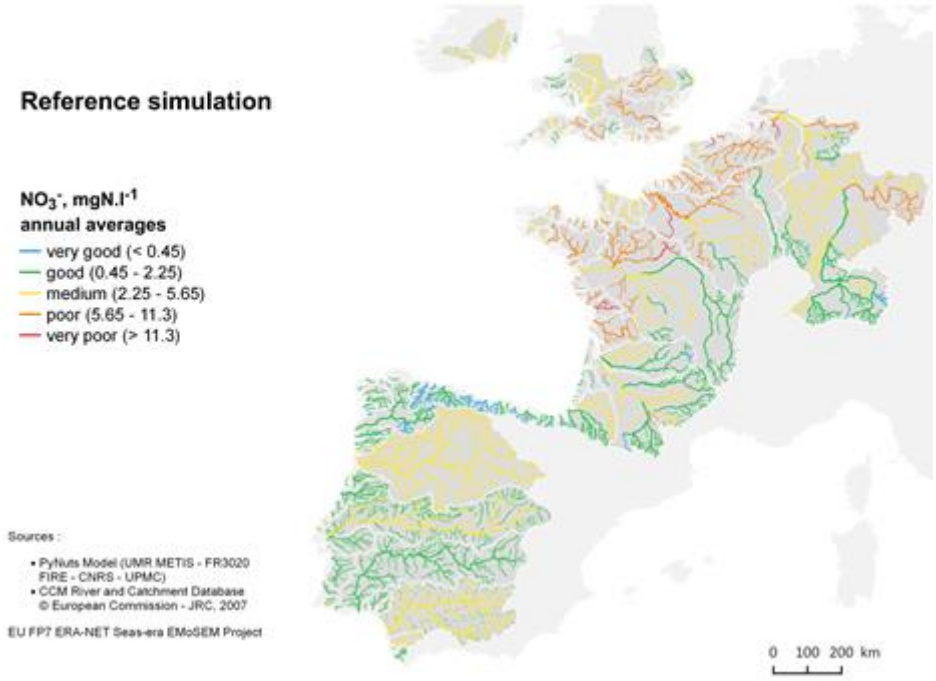

Figure 47: Annual mean concentrations of NO_3 in the NEA domain simulated for the Reference scenario.

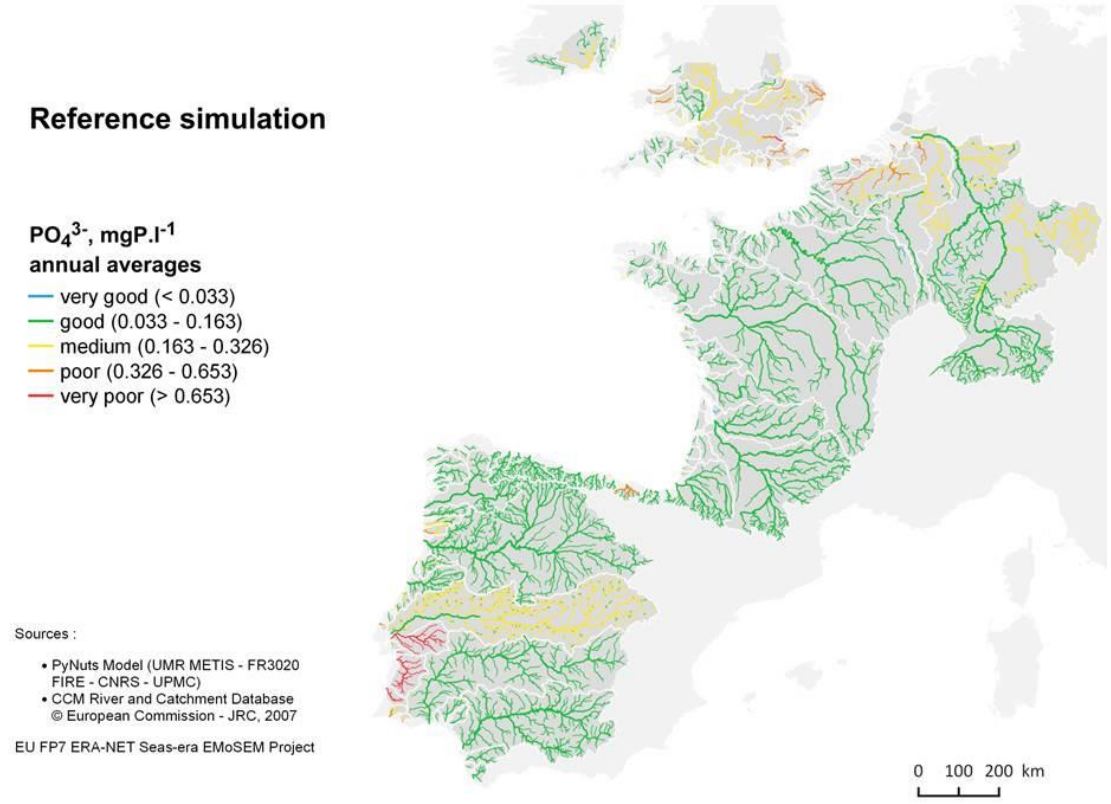

Figure 48: Annual mean concentrations of PO_4 in the NEA domain simulated for the Reference scenario.

3.1.1.2 Pristine situation (hereafter Pristine)

For the purpose of defining the "natural" levels of nutrients and to estimate what could be the functioning of coastal marine systems in the absence of any anthropogenic nutrient inputs, one major task of the EMoSEM project was to reconstruct through modelling computation pristine nutrient loadings from all rivers in the North-East Atlantic watershed.

Pristine loadings refer to the river inputs to the estuarine and coastal zone in the absence of direct human perturbation, *i.e.* under conditions of natural land cover and without hydrological management, but under current climate conditions.

Operationally, we have considered that the inputs to the drainage systems are those resulting from soil leaching and litter fall from the dominant climax vegetal formations in the different climatic and lithological zones of the NEA watershed. The unperturbed hydrological conditions have been inferred from the data available for the first half of the 20th century, when disturbance by damming and irrigation was still minimal.

The calculated pristine loadings are consistent with the few previous estimates mentioned in the literature and gathered in Table 9. These involve other modelling approaches, as well as a few observational data from Nordic rivers which can be considered as pristine in view of their minimal level of anthropogenic perturbation (Figure 49).

Table 9: short review of N, P and Si specific fluxes delivered to European seas.

		kgN/km²/y	kgP/km²/yr	kgSi/km²/yr
Europe (NANI, y intercept)	←	160		
Phison (Billen et Garnier, 1997)	▲	29	1	1230
3S (Thieu et al, 2010)	■	50 - 250	8 - 30	350 - 1500
Seine (Cugier et al., 2005)	▲	27 - 53	2 - 3	590 - 1120
Seine (Billen et al, 2007)	◆	30 - 100	2 - 5	500 - 1300
Swedish rivers (Humborg et al, 2003)	○	120 - 160	5 - 9	450 - 1100

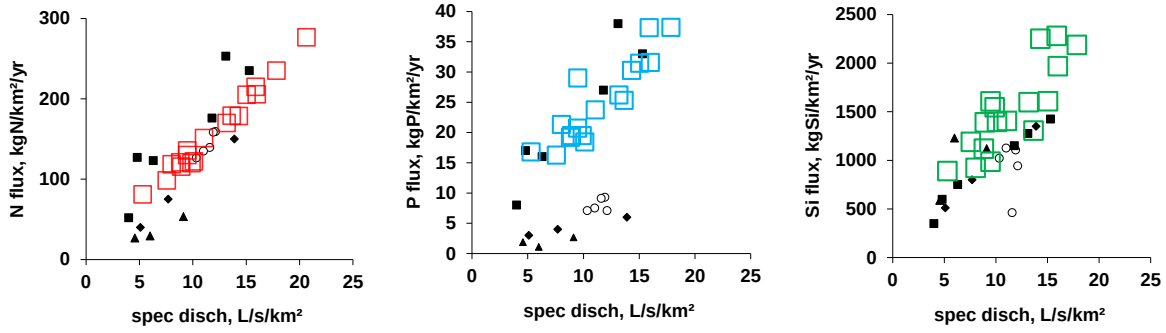

Figure 49: Pristine fluxes estimated from literature review (black and white symbol) compared to EMoSEM Pristine-like situation (calculated for 17 majors NEA river basins, red, blue and green squares).

The calculated mean levels of nitrate concentrations within the drainage network of the NEA coast under pristine conditions are shown in Figure 50. Values remain everywhere below 0.5 mgN L^{-1}.

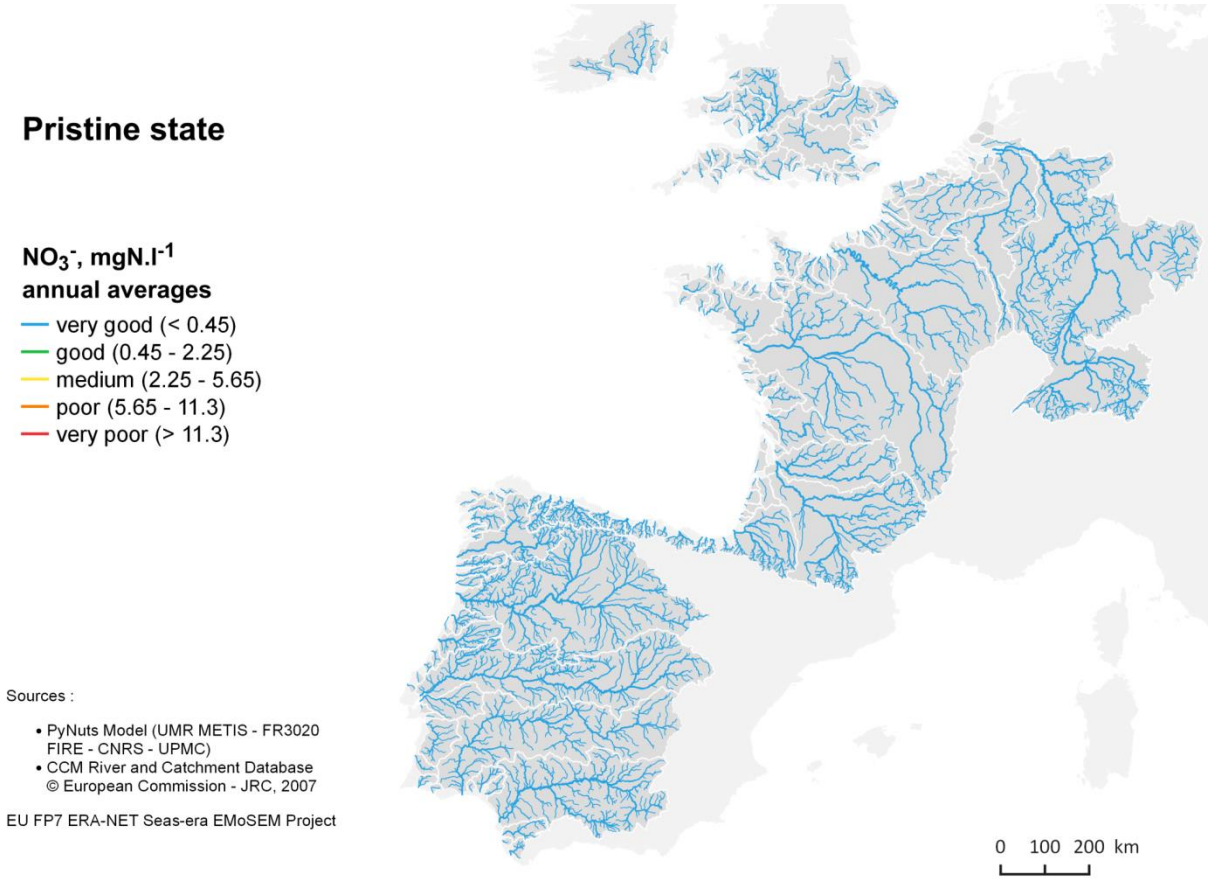

Figure 50: annual mean concentration of NO_3 in the NEA domain simulated for the Pristine situation.

3.1.1.3 Three future "realistic" scenarios (called UWTD, GAP and LocOrgDem)

The EMoSEM project aimed at defining "realistic"scenarios of changes in river nutrient inputs to the sea and exploring their effect on the marine ecosystem. "Realistic" means that these changes cannot be defined *a priori*, for instance as an arbitrary fraction of current inputs, but should be derived from changing the structure of the agro-food system in the watershed territory.

Three levers can thus be moved for defining possible scenarios: (1) The first one is related to the point sources of nutrient through urban wastewater (hereafter UWTD); (2) in addition to UWTD the second involves improving farming practices in the scope of the current agricultural systems (hereafter GAP, for Good Agricultural Practices); (3) in addition to UWTD the third one implies a radical reshaping of the structure of the agro-food system (hereafter LocOrgDem, for Local, Organic and Demitarian). These three levers are ordered following their degree of realism: the first mimicking the ongoing European legislation on point sources supported by the Urban Wastewater Treatment Directive (UWTD), the second corresponding to the more recent definition of Good Agricultural Practices (GAP), and finally the third one implying, in depth, changes in agricultural landscape, trade exchanges and human diet.

Improvement of wastewater treatment (UWTD scenario)

Mitigation of point sources could be an efficient way to reduce the amount of nutrients transferred to the aquatic system, especially for phosphorus. And despite their recent improvement, wastewater treatment plants of the NEA domain do not still fully comply with European requirements.

Consequently, this scenario involves a spatially explicit implementation of the Urban Wastewater Treatment Directive (Directive 91/271/EEC), implying:

•The Collection and treatment of waste water in all agglomerations of >2000 inhequ;

•Upgrading of wastewater treatment plant for non-compliant agglomerations, taking into account the sensitivity of receiving areas (Figure 51).

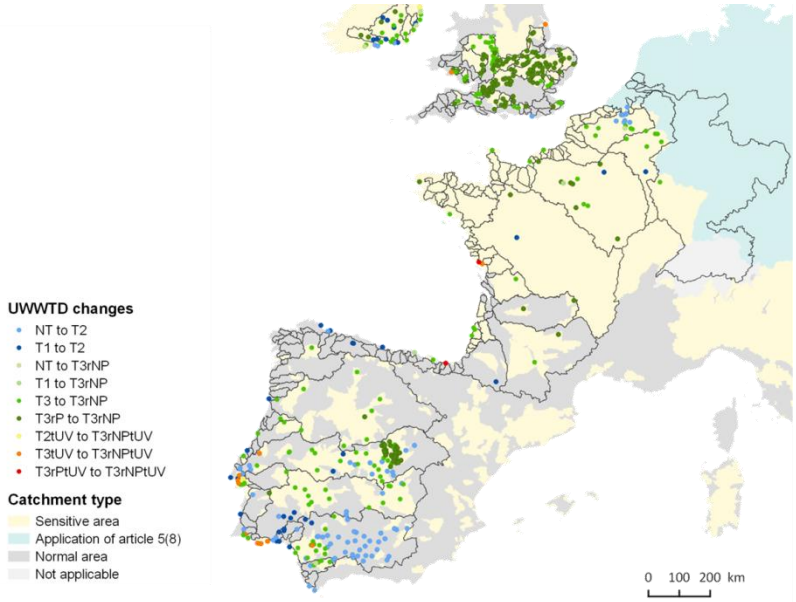

Figure 51: Upgrading of existing wastewater treatment plant and sensitivity of receiving area following the Urban Wastewater legislation, Directive 91/271/EEC.

This scenario also includes an additional reduction of the per capita human emissions of P, considering a complete ban of phosphorous in both laundry powders and dishwasher detergents, based on the Regulation (EC) No 648/2004 concerning the use of phosphates and other phosphorus compounds in household laundry products.

The calculated mean level of nitrate concentration within the drainage network of the NEA coast under UWTD (Urban Wastewater Treatment Directive) scenario is shown in Figure 52. Water quality is slightly improved in specific part of the drainage network: Strahler stream-orders lower than 6 for the Tagus river basin, lower than 4 on the Guadiana and the eastern part of the Great Ouse river basin move for medium to good quality. The downstream part of the Seine River (between Paris and Poses) is also improved.

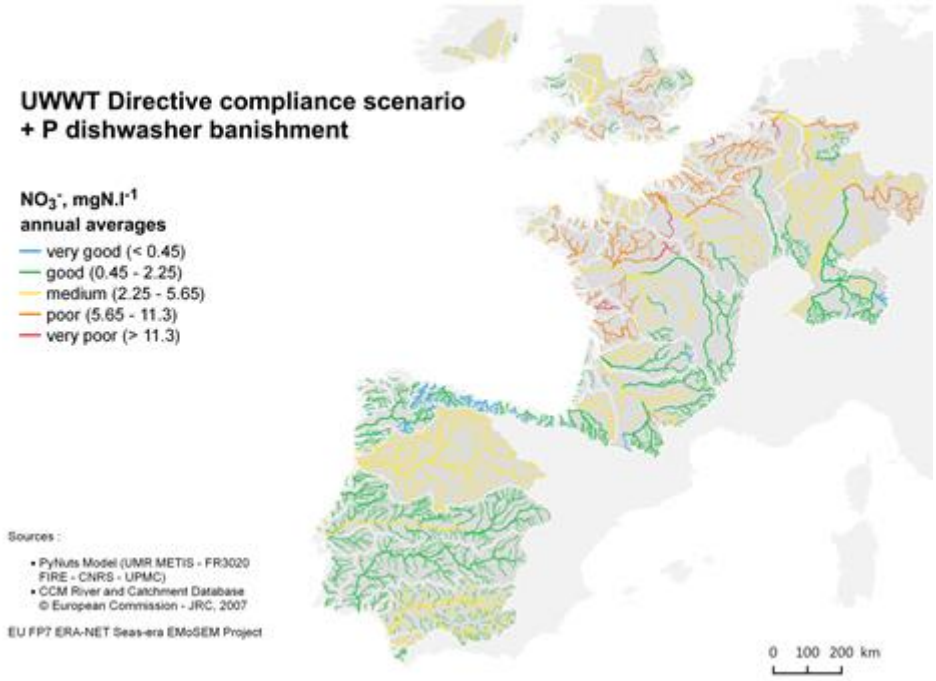

Figure 52: Annual mean concentrations of NO_3 in the NEA domain simulated for the UWTD scenario.

For phosphorous, the combined effect of improving wastewater treatment and reducing P emissions from laundry powders and dishwasher detergents leads to a significant reduction of P concentrations in northern river namely the Rhine, the Meuse, the Scheldt and all British Island rivers and also in the Tagus river (Figure 53).

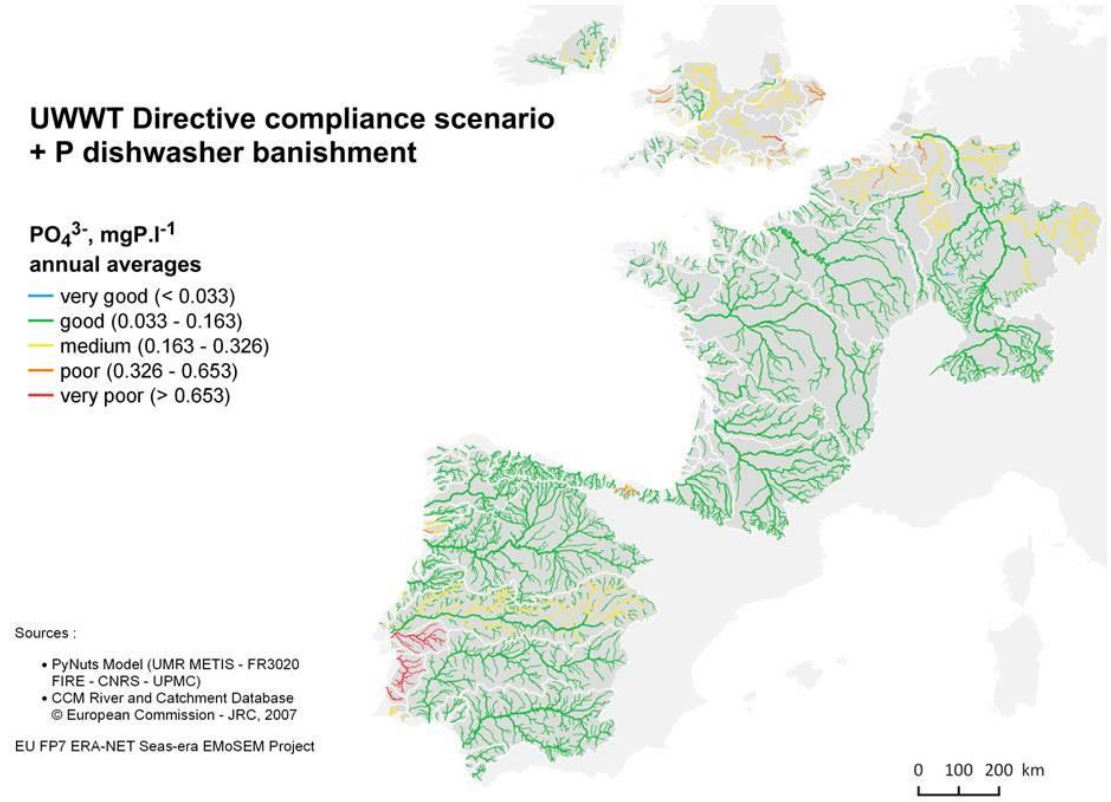

Figure 53: Annual mean concentrations of PO_4 in the NEA domain simulated for the UWTD scenario.

Reasoned agricultural practices (GAP scenario)

At least in most vulnerable areas, considerable efforts have been devoted since the last decades to adapt the level of fertilization to the needs of crop growth. The current situation described by the nitrogen soil balance of the different agricultural regions of NEA thus probably reflects the lower limit of the level of N surplus (defined as the difference between total N inputs to the soil and export of N with the harvest) which can be achieved without major change in the current cropping systems and yield objectives. The only lever that could lead to reduction of N leaching consists in the introduction of catch crops preventing bare soils during the autumn and winter period of intense drainage before spring crops. Such measure has indeed been demonstrated to significantly reduce the fraction of N surplus of arable lands being leached during the drainage period, provided its presence is taken into account for the adjustment of fertilization of the succeeding crop (Figure 54).

The efficiency limit of this measure is set by the frequency of spring crops in the cultural rotation cycle. For this reason, we found that, as a mean over all regions of the EMoSEM domain, only a 30% decrease of lixiviation can be expected from the generalization of catch crop implementation.

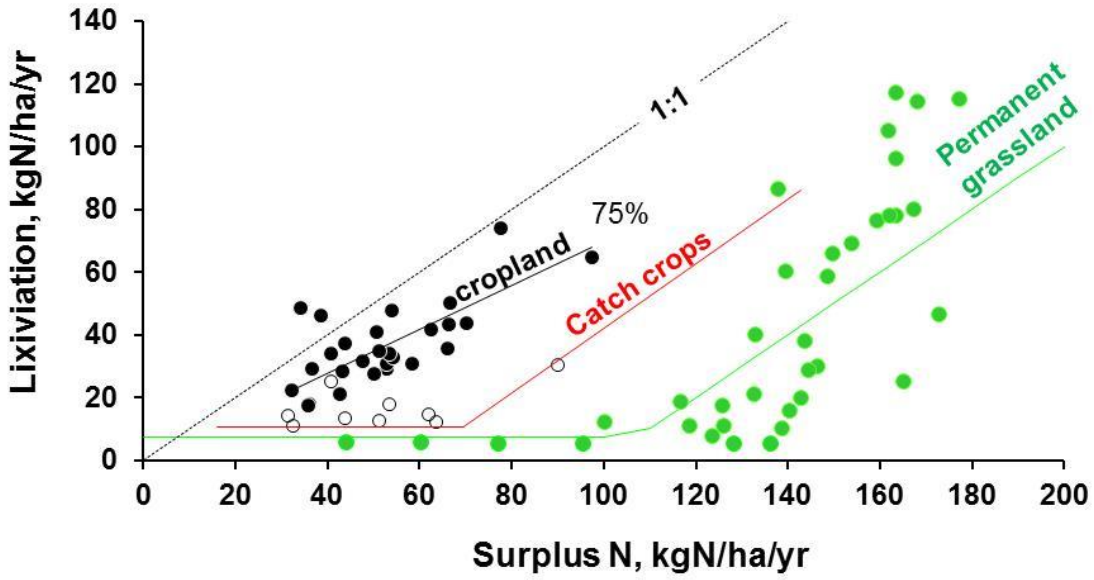

Figure 54: Relationship between leaching flux and N surplus to grassland, cropland and cropland with generalised implementation of catch crops (Anglade et al. 2015).

The GAP scenario simulates such a change to reasoned agricultural practices and results are significant when looking at mean nitrate concentrations calculated within the drainage network (Figure 55, to be compared with Figure 52).

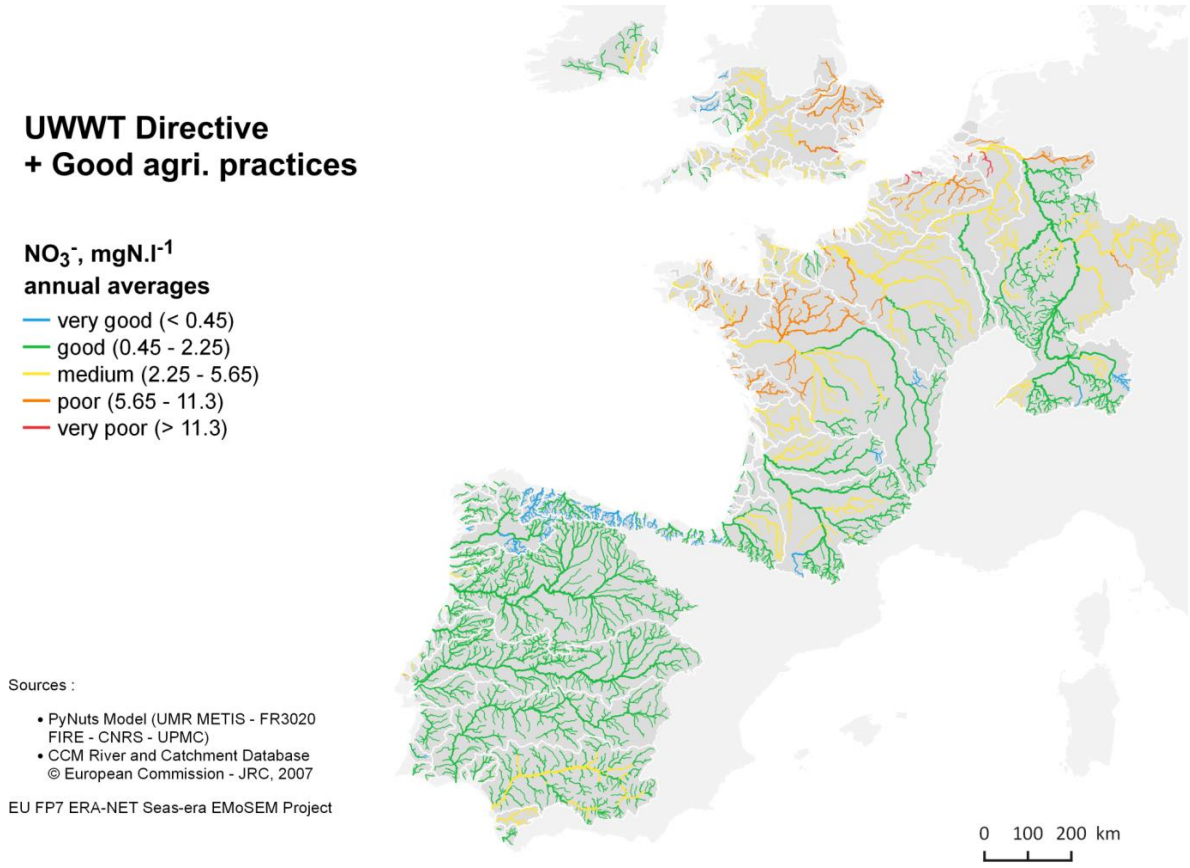

Figure 55: Annual mean concentration of NO_3 in the NEA domain simulated for the GAP scenario.

Radical change in the agro-food system (LocOrgDem scenario)

N losses to hydrosystems can be viewed as the direct consequence of the specialization and opening of territorial agro-food systems. Reshaping territorial N fluxes toward more connection between crop production and livestock farming, as well as between agriculture and local human food consumption is a radical option for reducing N contamination of water resources and fluxes to the sea.

The construction of this scenario for the EMoSEM domain involved the following steps:

(1) Revision of human diet, with a shift towards more vegetal and less animal protein ingestion (inverting the current 35% vegetal and 65% animal protein proportions) and a reduction of wastage.

(2) Adjustment of livestock numbers in each agricultural region to local human requirements of animal proteins, within a minimum of 0.1 and a maximum of 0.6 Livestosk Units (LU) per hectare of agricultural land (agland) and no reduction of livestock size by more than a factor of 3. Figure 56 shows the resulting livestock density over the whole EMoSEM domain.

(3) Organic cropping systems with long and diversified rotations involving legumes are established everywhere. N fertilisation is limited by the local availability of manure. The resulting yield is calculated assuming the same yield *vs.* fertilisation relationship as the one currently observed. The resulting changes in the structure of the agro-food system are illustrated in Figure 57 for 4-contrasted agricultural area of Spain and France.

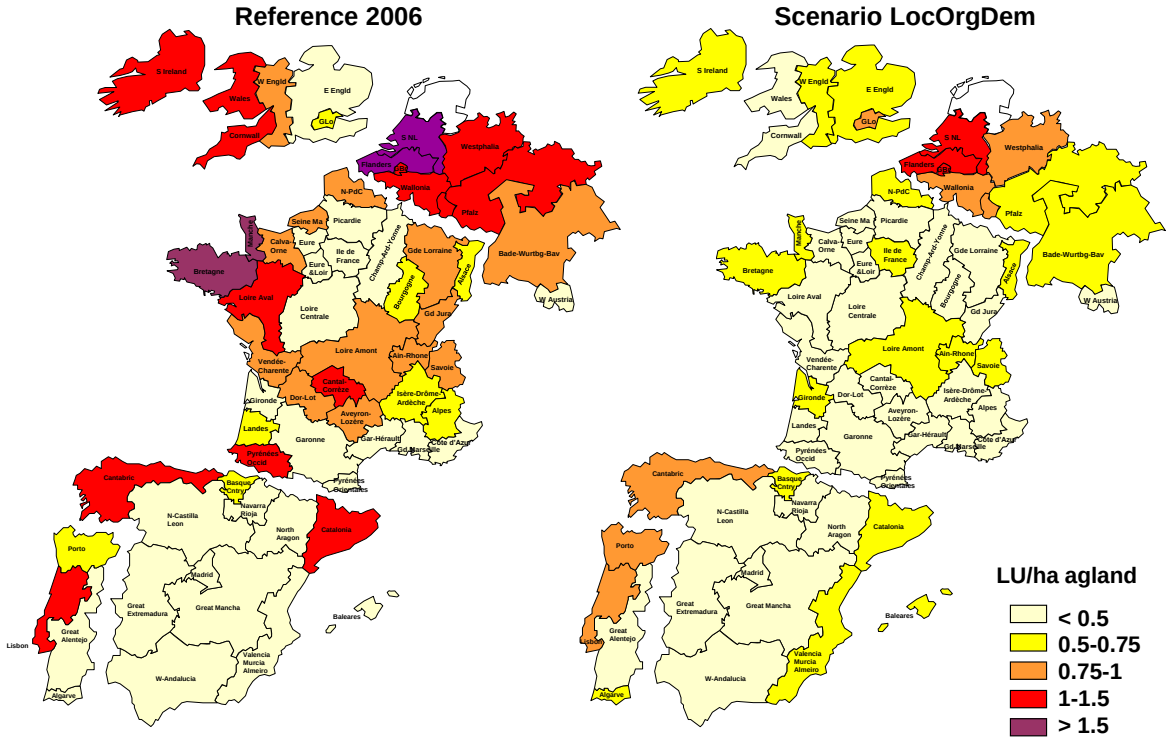

Figure 56: Distribution of livestock density in the reference and the LocOrgDem scenario.

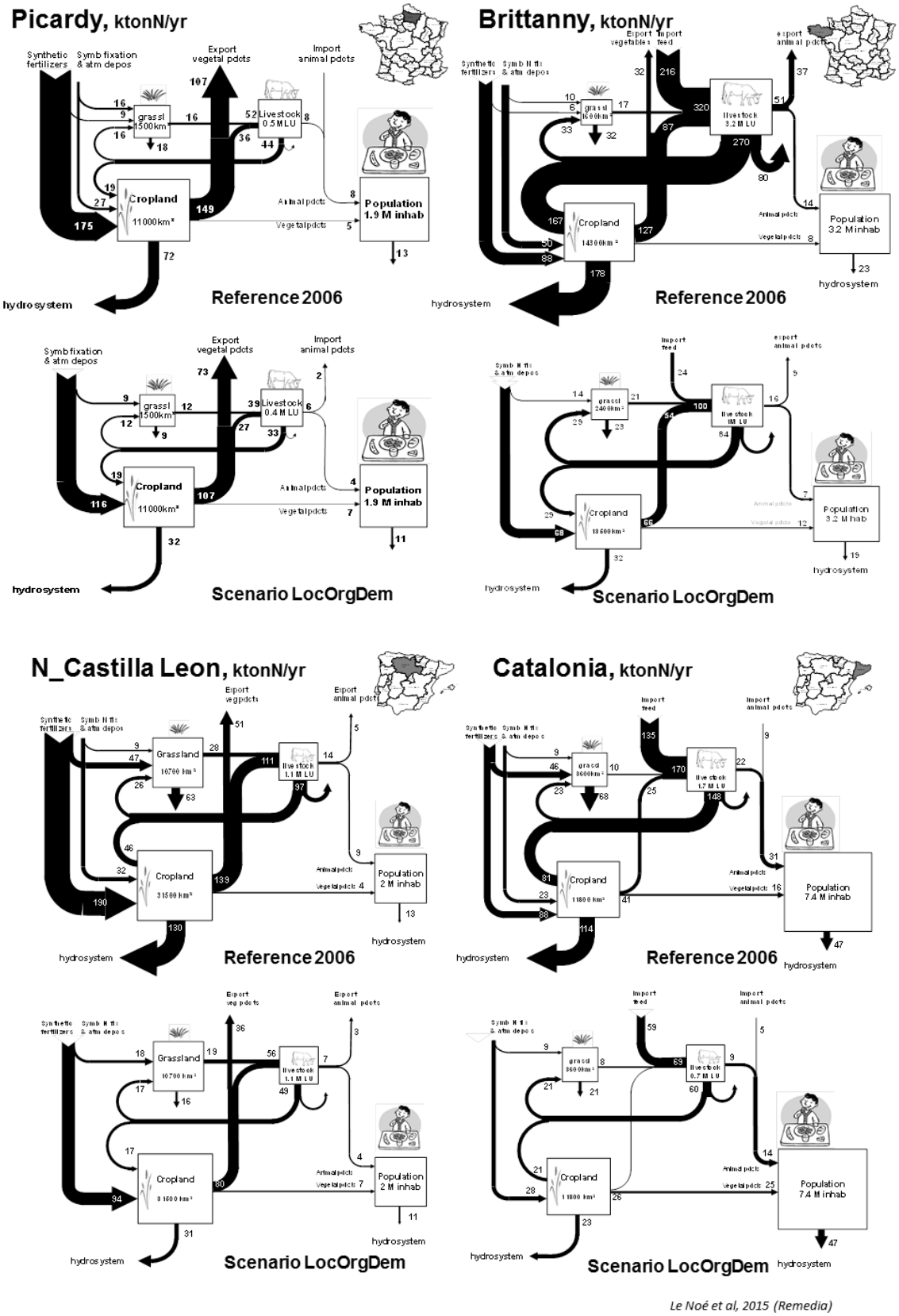

Le Noé et al, 2015 (Remedia)

Figure 57: Hypothetic scenario of reshaping the structure of the agro-food system of 4 regions of the EMoSEM domain, according to the principles of the LocOrgDem scenario. N fluxes to the hydrosystems are reduced by a factor of 2 to 5.

The effect of this scenario in terms of surplus reduction is considerable (Figure 58) and results in a significant improvement of water quality along the drainage networks (Figure 59) as well as in a strong reduction of N fluxes to the sea (Figure 60).

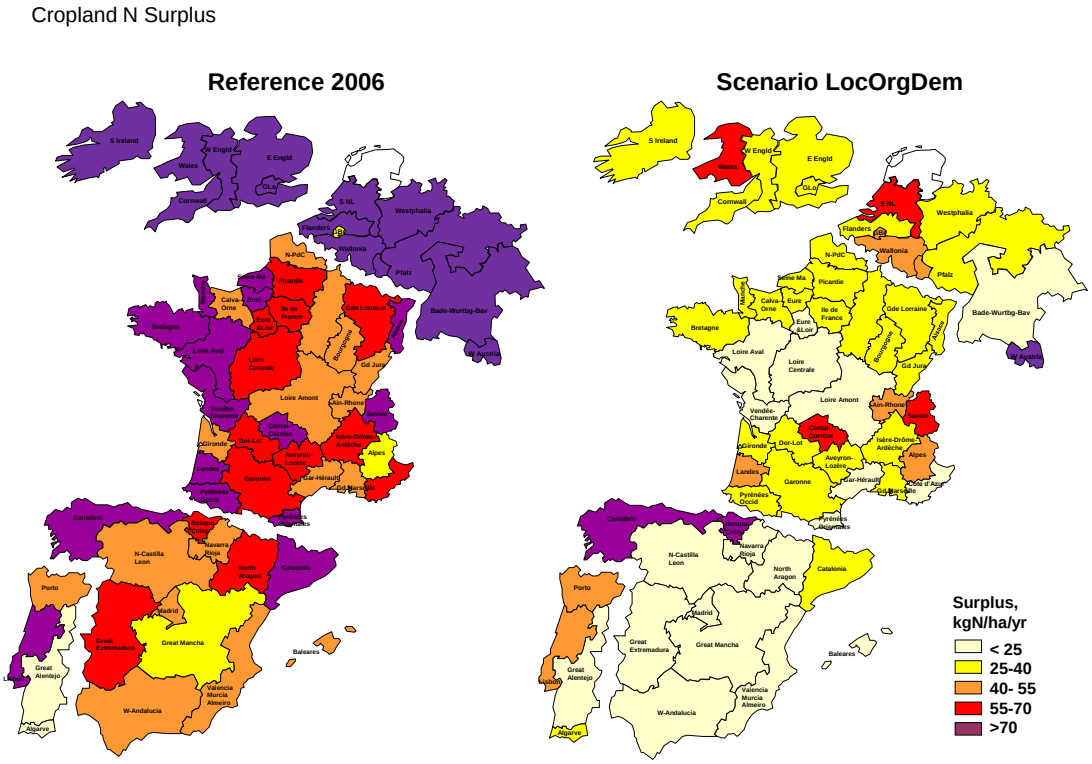

Figure 58: Distribution of the average N surplus on arable soils over the EMoSEM domain, in the current situation (left) and in the LocOrgDem scenario.

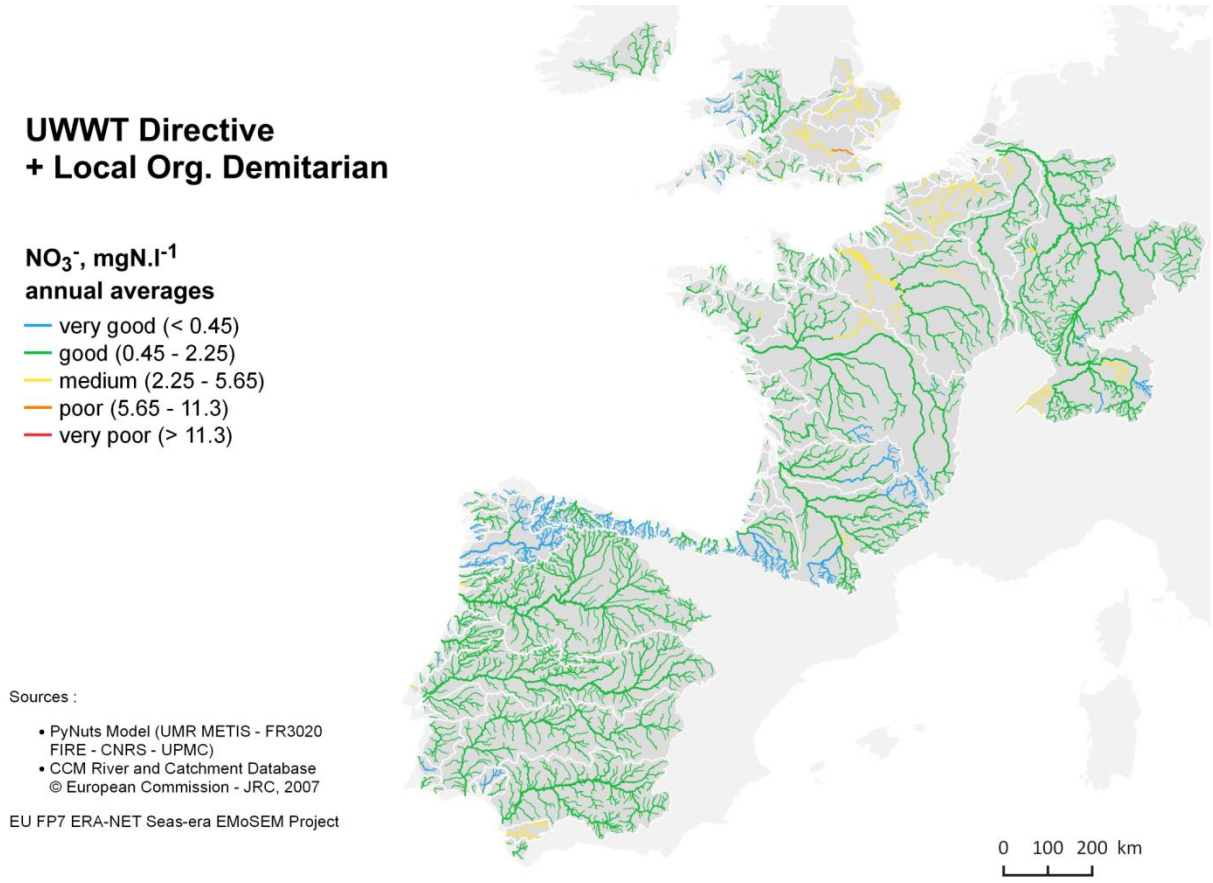

Figure 59: Annual mean concentration of NO_3 in the NEA domain simulated for the LocOrgDem scenario.

When calculating the specific fluxes of nitrogen delivered at the coastal zone by the main rivers, we can notice the importance of the contribution of largest ones (Seine, Scheldt, Meuse, Rhine, Thames, especially) (Figure 60). However, the sum of the specific fluxes of the small rivers (small watersheds) cannot be neglected. The results of the three scenarios are compared with the two references (Pristine and Reference situation) and shows that the LocOrgDem can only decrease significantly the riverine nitrogen fluxes to their coastal zones and that the Pristine scenario cannot be a target (Figure 60, top).
Regarding the direct point sources of nutrients, Figure 60 clearly shows that a reduction of nitrogen deliveries cannot be expected from wastewater treatments alone.
Regarding the N-ICEP indicator (excess N over Si with respect to the requirements of diatom growth, Billen and Garnier 2007) whereas the values are systematically negative for the Pristine scenario (i.e., Si in excess to N), N-ICEP remains positive for all scenarios, but the potential for eutrophication is well reduced, approaching zero, for the LocOrgDem scenario only (Figure 60, bottom).

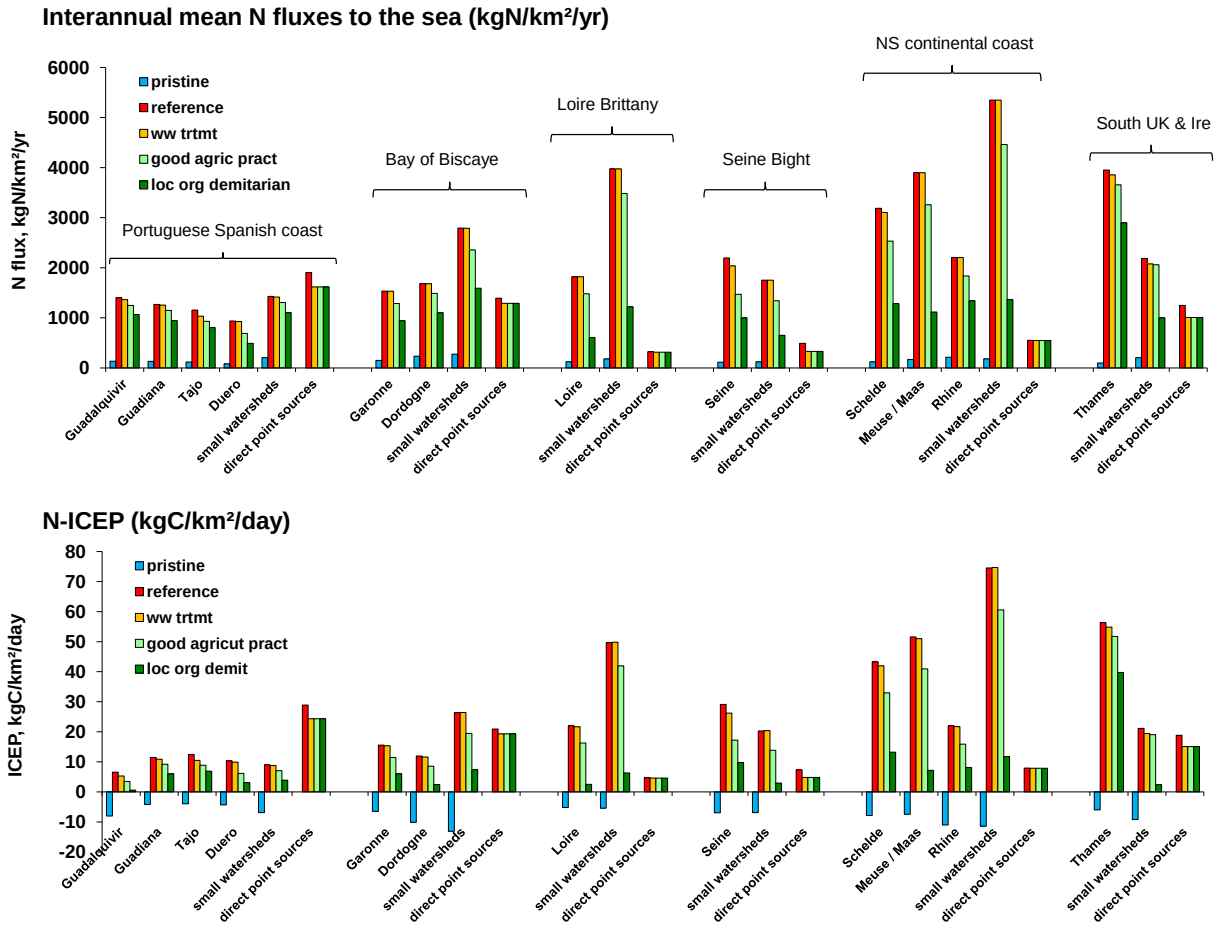

Figure 60: Summary of the fluxes of nitrogen delivered at the coastal zone by the main rivers and the direct point sources of nutrient for the three scenarios, compared with the two references (pristine and current situation). The N-ICEP indicator (excess N over Si with respect to the requirements of diatom growth, Billen and Garnier 2007) is also shown.

3.1.1.4 Implications of the Bio-Local-Demitarian scenario

In order to assess the implications of the Bio-Local-Demitarian scenario at the broad country scale, it has been applied to all French and Spanish agricultural regions. The results in terms of national food and feed production and consumption are summarized in Table 10.

Table 10: Summary of the results of the LocOrgDem scenario for the whole of France and Spain.

		France		Spain	
		2006	**LocOrgDem**	**2006**	**LocOrgDem**
population	Minhab	64	64	44	44
ag land area	M ha	26	26	26	26
% grassland	*%*	*31*	*33*	*34*	*35*
livestock	M LU	21	10	11	7
production meat & milk	ktN/yr	335	162	135	83
fraction used locally	*%*	*83*	*84*	*135*	*100*
available for export	ktN/yr	56	26	-48	0
grassland production	ktN/yr	769	517	268	196
fraction of livestock needs	*%*	*37*	*51*	*26*	*31*
crop production	ktN/yr	1708	1183	626	385
among which legumes	ktN/yr	545	941		122
cereals & non leg crops	ktN/yr	1163	241		263
fraction of human needs	*%*	*726*	*102*		*137*
available for exp or other use	ktN/yr	222	448	-236	-205
N surplus cropland	ktN/yr	1298	480	882	237

In France, as a result of the strong reduction of meat consumption, livestock and animal production are decreased by half. This reduction is not evenly distributed in the different regions, as one of the objectives of the scenario is to re-connect crop and animal farming in the over-specialized regions. The spatial distribution of livestock density is shown in Figure 61. Not all regions can reach self-sufficiency in terms of animal protein. Exchanges between regions are still required: the possible distribution of these exchanges is illustrated in Figure 61, and compared with the current exchanges of meat and milk revealed by the analysis of the Sitram data base (Le Noé et al. 2015). A number of constraints (maintaining a minimum livestock even in low population areas, avoiding too drastic reduction of livestock in regions currently specialized in animal farming) prevent the scenario to accurately adjusting the animal production to local needs. As a consequence, there is an excess animal production over human requirements, available for international export, of about 26 ktN/yr, less than half the current amount exported. Note that the total area of grassland has not changed a lot at the national scale (although it increases quite significantly in regions currently specialized in crop production). However, the part of grassland in animal feeding has increased quite significantly from the current value of 37% to 51%, in spite of a decrease of the absolute production of grass due to extensification.

Crop production slightly decreases in each French region with respect to the currently observed values. At the country scale, crop production decreases from 1700 to 1180 ktN/yr, i.e. by 30%, as a consequence of the lower total fertilization rate applied to cropland. Because of the introduction of legumes in crop rotations, the production of non-legumes, including

cereals, has reduced considerably, from currently 1160 ktN/yr to 240 ktN/yr in the scenario. However, the latter value matches exactly the human consumption of vegetable proteins.

Surprisingly, the amount of crop production in excess of national consumption by human and livestock is twice higher in the scenario than in the current situation: the excess production increases from 220 ktN/yr in 2006 to 450 ktN/yr in the scenario. This excess is however of a quite different nature: currently mostly cereals, and mostly forage (and grain) legumes in the LocOrgDem scenario. This material is available for export. It might also be suitable for non-food uses, such as energy production.

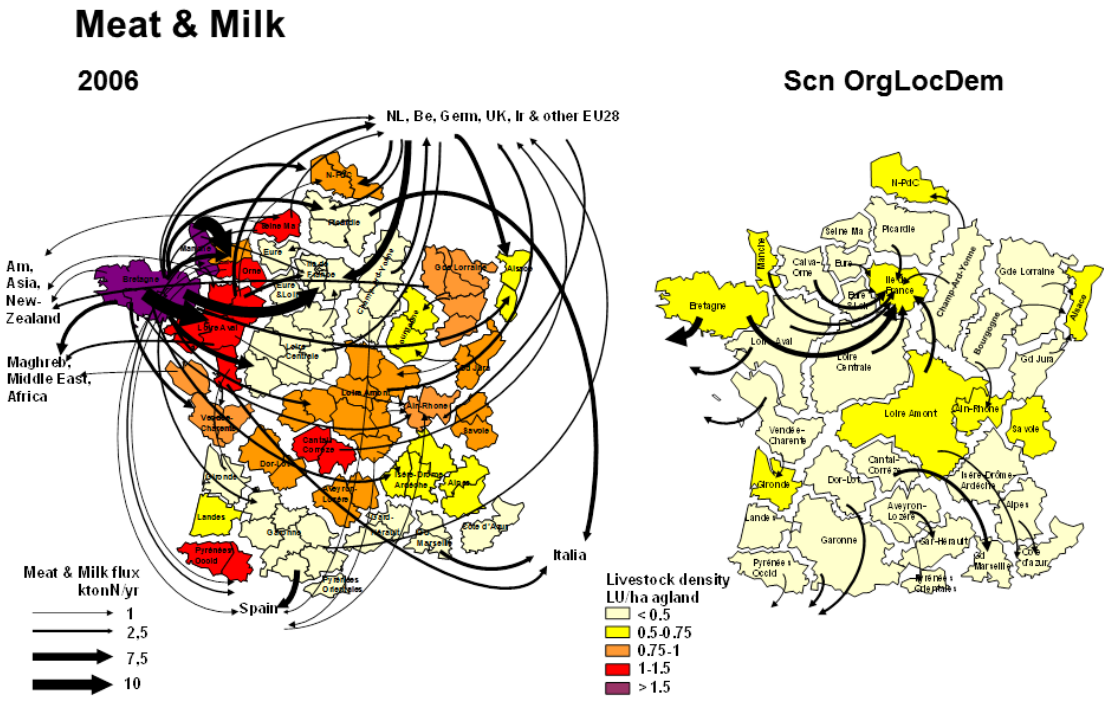

Figure 61: Distribution of livestock density and trade of animal products in the current situation (left) and in the LocOrgDem scenario (right).

In the current situation, Spain is not self-sufficient in terms of meat and milk production and imports about 48 ktN/yr of animal proteins. In the LocOrgDem scenario, owing to a strong reduction of the proportion of animal products in the diet, Spain as a whole becomes self-sufficient, even with a livestock size reduced by 40%. Regions like Madrid, Basque country, Baleares, Catalonia and Andalucia needs to import animal proteins from other such as Cantabric, North Aragon, Extremadura, Castilla Leon and Mancha which have the potential to produce excedents.

In the current situation, Spain is not self-sufficient for vegetal production and has a net balance of vegetal protein import of about 236 ktonN/yr. The imports mainly concern soybean from South America used for feeding livestock, but also cereals from France. In the LocOrgDem

scenario, this external dependence is not suppressed, but is reduced to a net importing balance of 205 ktonN/yr.

In both countries, the cropland N balance, a good indicator of environmental nitrogen contamination by agriculture, through leaching of nitrogen to the groundwater or emission to the atmosphere as NH_3 and N_2O, is reduced by a factor 3 to 4 in the scenario.

Note also that this scenario, which assumes the generalization of organic farming practices, implies a complete ban of pesticides application.

3.1.2 Marine eutrophication in the NEA: references and impact of scenarios

3.1.2.1 Integration of results

The five PyNuts-Riverstrahler simulations (Reference, Pristine, UWTD, GAP and LocOrgDem) have delivered nutrient loads at the river outlets along the coasts of the NEA domain. These nutrient river loads were used by the three marine ecological models to compute the resulting effects on the marine system and more specifically on the status of marine eutrophication. In the following, only the year presenting average meteorological conditions is represented for each model, i.e. 2007 for MIRO&CO (BE) and for ECO-MARS3D (FR), and 2010 for BIOPCOMS (PT). Since the GAP scenario leads to quite similar results as the scenario UWTD in the marine system, the scenario GAP is not shown here (see Appendix). The results of the three marine models have been combined (see Figure 62) to offer a global vision of the effects of scenarios across the NEA.

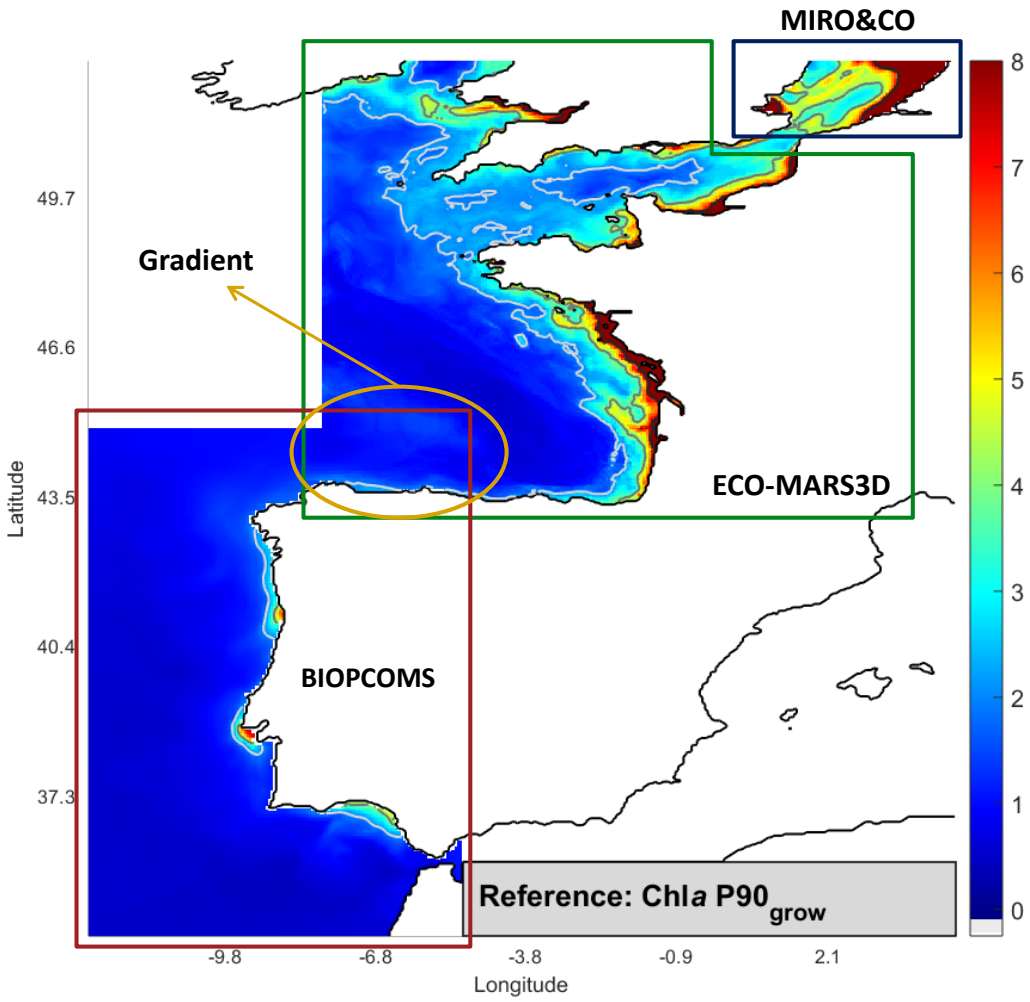

Figure 62: Map of model results for Chl P90 (µgChl L^{-1}) over the growing season (Mar-Oct) in 2007 (BE, FR) and 2010 (PT). The isolines indicate the values 2 (white), 4 (grey) and 8 (dotted black) µgChl L^{-1}.

In order to integrate the results of MIRO&CO (BE), ECO-MARS3D (FR) and BIOPCOMS (PT), a larger grid (matrix 516x335) was created along Latitude [52.77°N 34.23°N] and Longitude [-12.8°E 5.10°E] with constant mesh size equal to 0.036° of Latitude and 0.0536° of Longitude. Whenever an overlap between models is found, a gradient is calculated to smooth the transition. In some cases, the results show an abrupt transition in concentrations between the Southern Bight of the North Sea and the English Channel because of the transition from one model to the other (see Figure 62) and because the concentrations and gradients are generally high and highly variable in that area.

3.1.2.2 Chlorophyll a P90 (Mar-Oct)

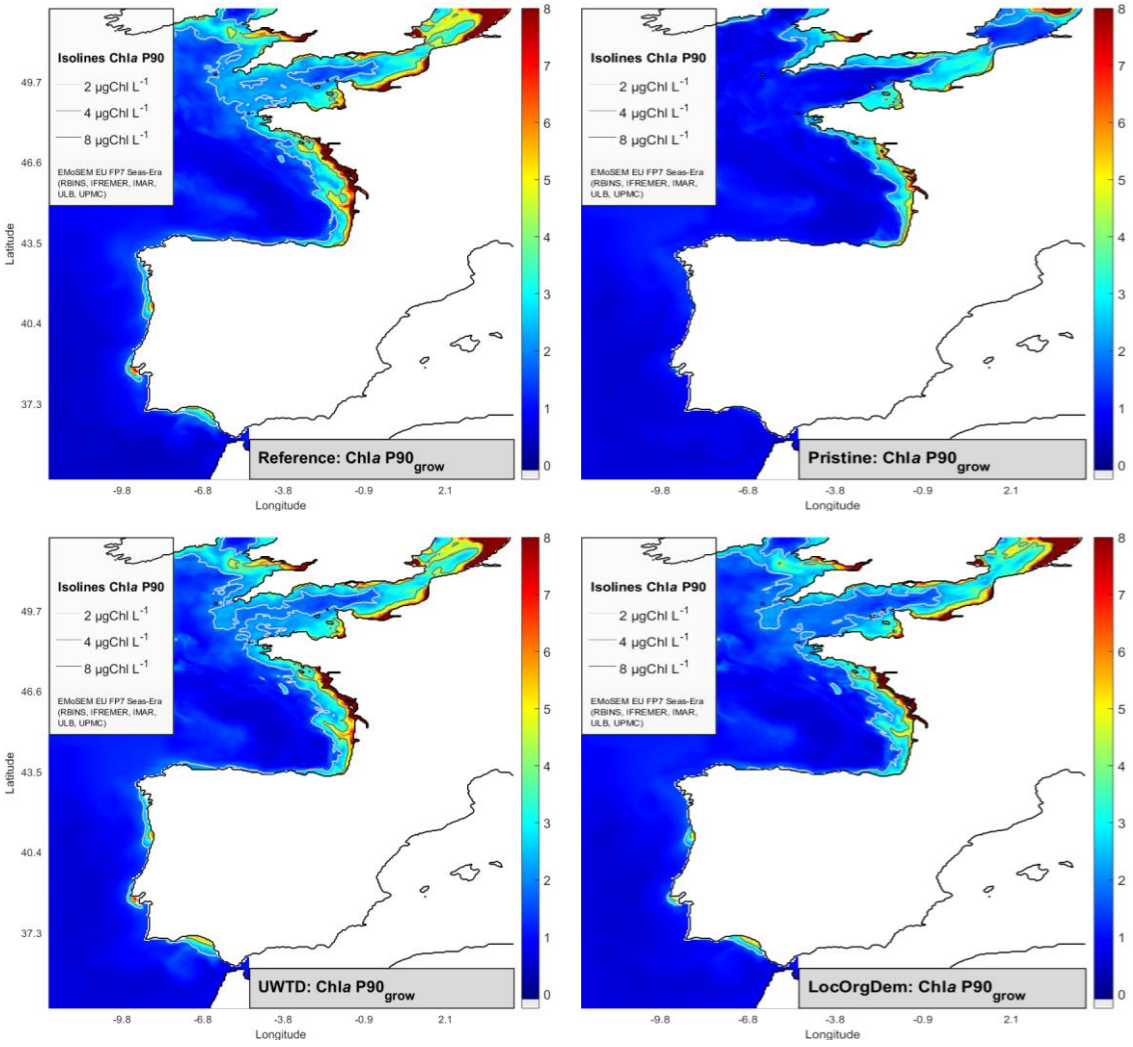

Figure 63: NEA-integrated contour maps of modelled chlorophyll a percentile 90 over the growing season (Mar-Oct) on a year with average meteorological conditions. Each graph represents a scenario: contemporary situation (Reference), pristine situation (Pristine) and two "future" scenarios (UWTD, LocOrgDem). Results from MIRO&CO, ECO-MARS3D and BIOPCOMS, with river inputs from PyNuts-Riverstrahler.

A first important result regarding Chl P90 distribution is that Chl P90 values are high along the coastal areas of the NEA for all scenarios, including current and pristine situation (Figure 63). The pristine situation reflects the natural enrichment of the marine domain characterized by the lowest Chl P90, except in the Bay of Biscay. In order to further compare the different scenarios, some difference maps are shown in Figure 64.

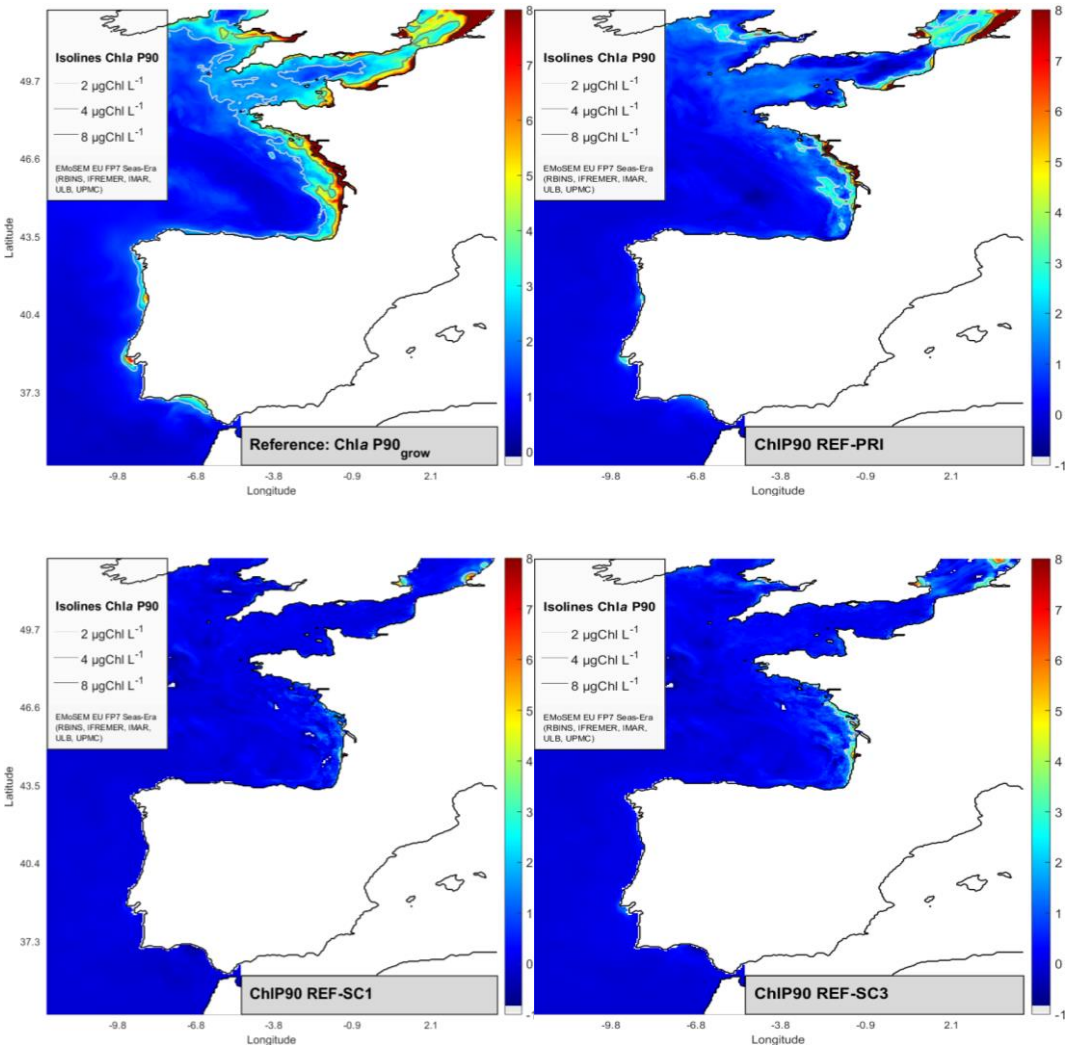

Figure 64: Model results of Chl P90 on a year with average meteorological conditions for Reference situation (top-left). Difference maps between Reference and Pristine (top-right), between Reference and UWTD (bottom-left) and between Reference and LocOrgDem (bottom-right).

The difference between Reference and Pristine points the zones of current anthropogenic eutrophication in the NEA. High anthropogenic eutrophication is found in the Belgian and Dutch coastal zones, in the Seine Plume and along the French coast of the Bay of Biscay. Less intense eutrophication is found offshore in the SBNS and along the coasts of Portugal. The Chl P90 does not change much in other scenarios except in the LocOrgDem close to the French coast of the Bay of Biscay, in some parts of the SBNS and at the mouth of the Scheldt estuary.

3.1.2.3 Winter DIN (Jan-Feb)

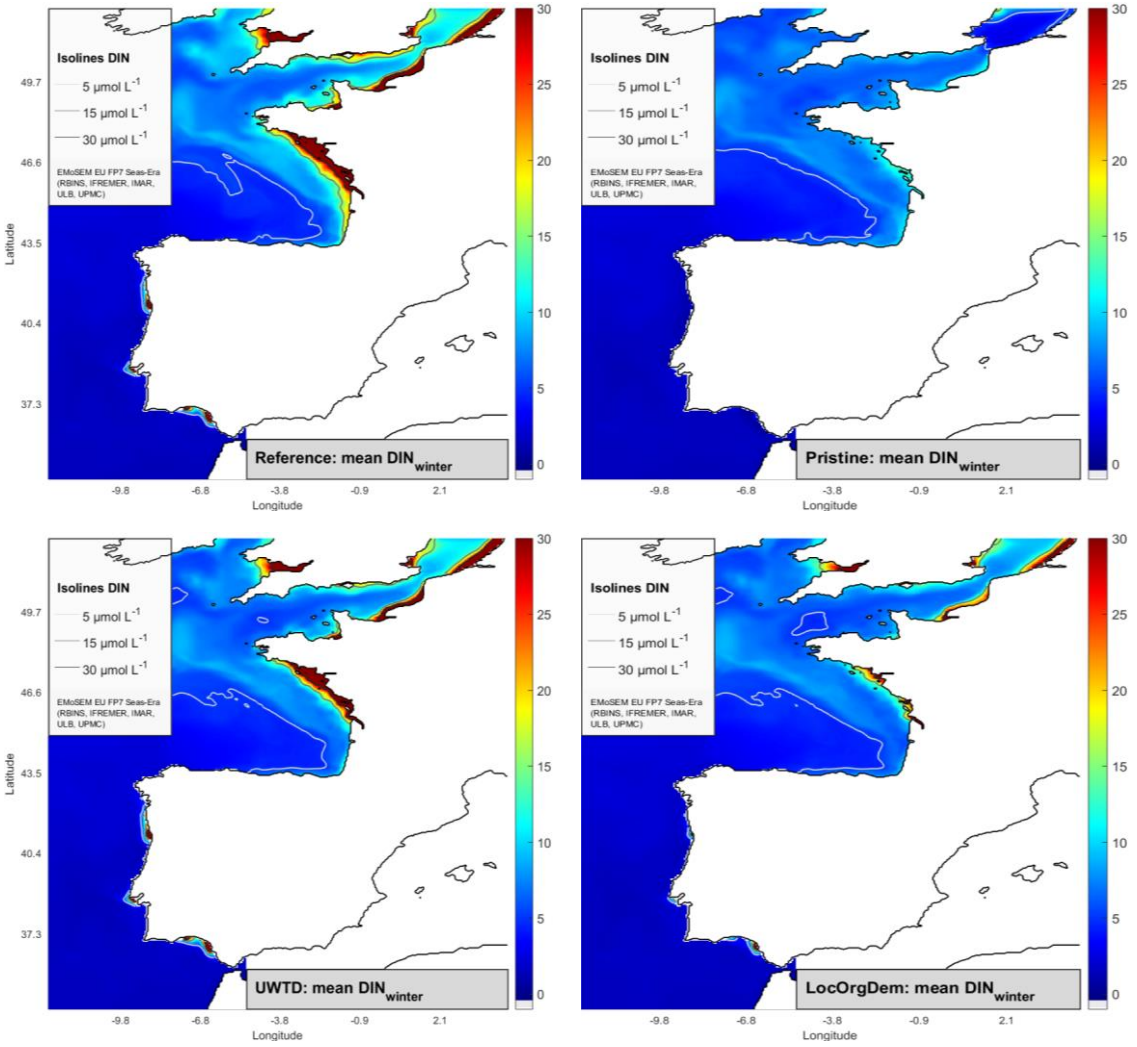

Figure 65: NEA-integrated contour maps of modelled winter DIN (Jan-Feb) on a year with average meteorological conditions. Each graph represents a scenario: contemporary situation (Reference), pristine situation (Pristine) and two "future" scenarios (UWTD, LocOrgDem). Results from MIRO&CO, ECO-MARS3D and BIOPCOMS, with river inputs from PyNuts-Riverstrahler.

The DIN concentrations are very high along the NEA coastal zones in the Reference situation (Figure 65, top-left) with a mean coastal value across the NEA[6] of 35.1 µmol L^{-1}, which can be compared to the Pristine situation (Figure 65, top-right) showing a mean coastal concentration of 6.6 µmol L^{-1}. Some reduction in coastal concentrations of winter DIN is achieved in the UWTD (Figure 65, bottom-left) and the GAP (not shown) scenarios, where the mean coastal values are respectively 29.5 and 24.8 µmol L^{-1}. A marked decrease in coastal concentrations is obtained with the LocOrgDem scenario (Figure 65, bottom-right), where the mean coastal value drops down to 18.3 µmol L^{-1}, which is almost half the Reference mean coastal concentration but is still a factor 3 higher than the natural "pristine" level. The decrease in

6 The mean coastal and offshore values are derived from the probability distribution functions that are presented and further discussed later in the report. Some values are used here to quantify better the changes observed between scenarios.

concentrations along the coasts between the Reference situation and the LocOrgDem scenario is accompanied by a decrease in offshore concentrations, especially in the English Channel and the SBNS where mean concentrations decrease from 11.2 to 6.8 µmol L^{-1}.

3.1.2.4 Winter DIP (Jan-Feb)

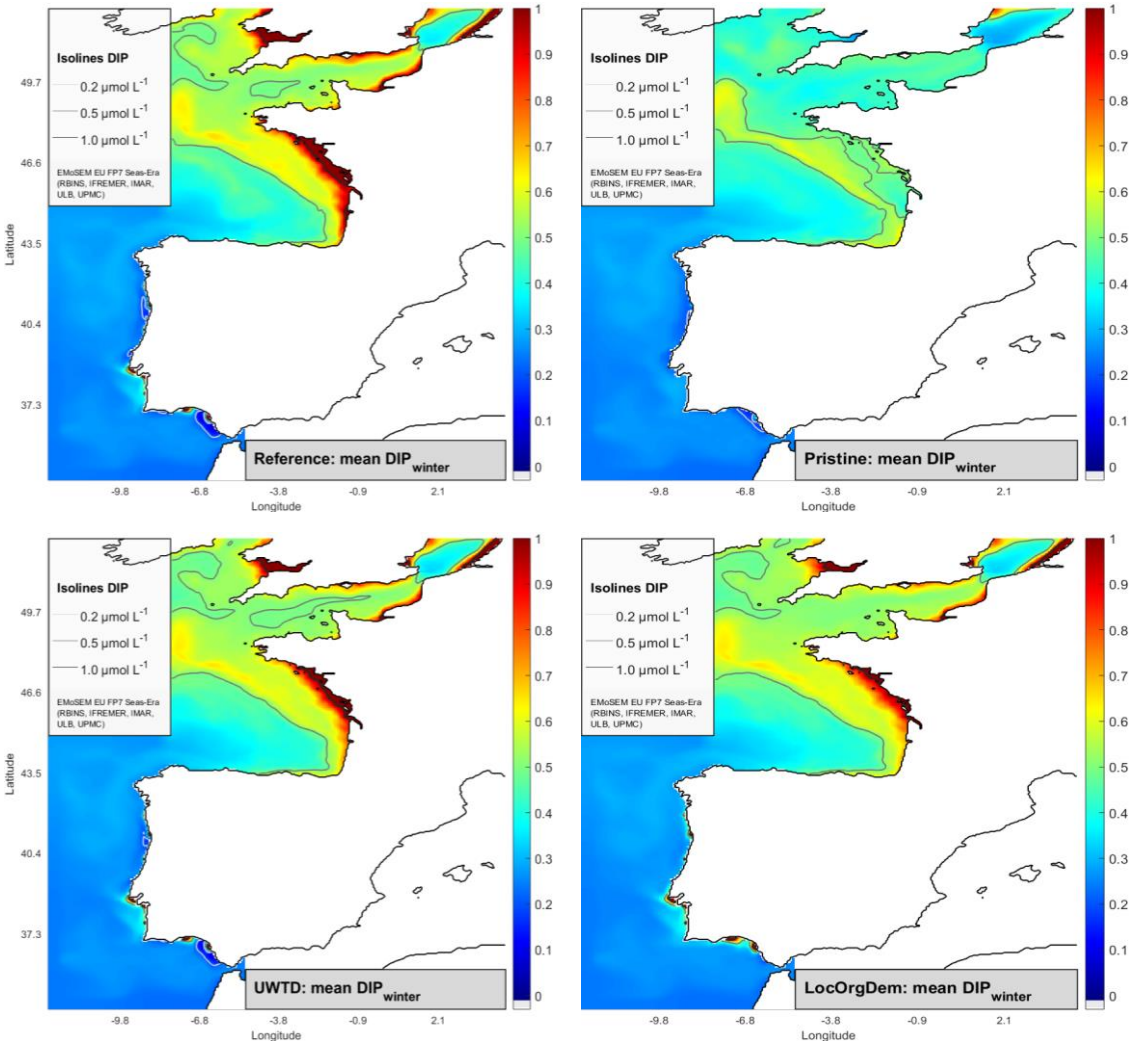

Figure 66: NEA-integrated contour maps of modelled winter DIP (Jan-Feb) on a year with average meteorological conditions. Each graph represents a scenario: contemporary situation (Reference), pristine situation (Pristine) and two "future" scenarios (UWTD, LocOrgDem). Results from MIRO&CO, ECO-MARS3D and BIOPCOMS, with river inputs from PyNuts-Riverstrahler.

The Pristine situation shows that, in the absence of human activities, the oceanic margin becomes one of the main sources of DIP (Figure 66, top-right). The differences in winter DIP between the Reference situation and UWTD or LocOrgDem scenarios (Figure 66, bottom-left and right) are not very significant along the coasts (mean coastal values are respectively 0.9, 0.8 and 0.8 µmol L^{-1}). The weakness of the improvement is due to the fact that most directives regarding P-reductions are already implemented. Still, the area where the DIP concentration is higher than the threshold 0.8 µmol L^{-1} experiences a slight decrease between the Reference situation and LocOrgDem scenario along the coastal zones of the NEA (from 71% to 60%). This

is visible in the French coastal zone of the Bay of Biscay. Only the Pristine situation, where a dual reduction in both riverine DIP and DIN is achieved, shows a significant decrease in the amplitude of the spring chlorophyll *a* blooms in the coastal areas (see Figure 63 and section 3.1.2.2). This suggests that the decrease in the chlorophyll *a* maximum requires a further decrease in winter DIP in the coastal zones, even if it is largely accepted that the N-reduction should be prioritized to limit the dominance of phytoplankton nuisance species (Lancelot et al. 2005, Gypens et al. 2007).

3.1.2.5 Winter DSi (Jan-Feb)

The change in DSi marine concentrations is indirectly linked to nutrient reduction policies applied on the watershed. Reduction in DIN and DIP loads to the river system will reduce the diatom production and hence the consumption of DSi in the river, making more DSi available to coastal diatoms. This increase in DSi delivery due to reduction in P loads has already been observed in the Rhine (Hartmann et al. 2011) and in the Dutch rivers and the Dutch Continental Shelf (Prins et al. 2012). It has also been modelled in the southern North Sea (Lancelot et al. 2013). The UWTD and LocOrgDem show lesser DSi concentrations in the coastal zones compared to the Reference (Figure 67), but they both show a slight increase of DSi concentration offshore. Besides, that increase of DSi concentrations offshore is quite comparable to the Pristine situation, though there seems to be even more DSi along the Bay of Seine in the Pristine situation.

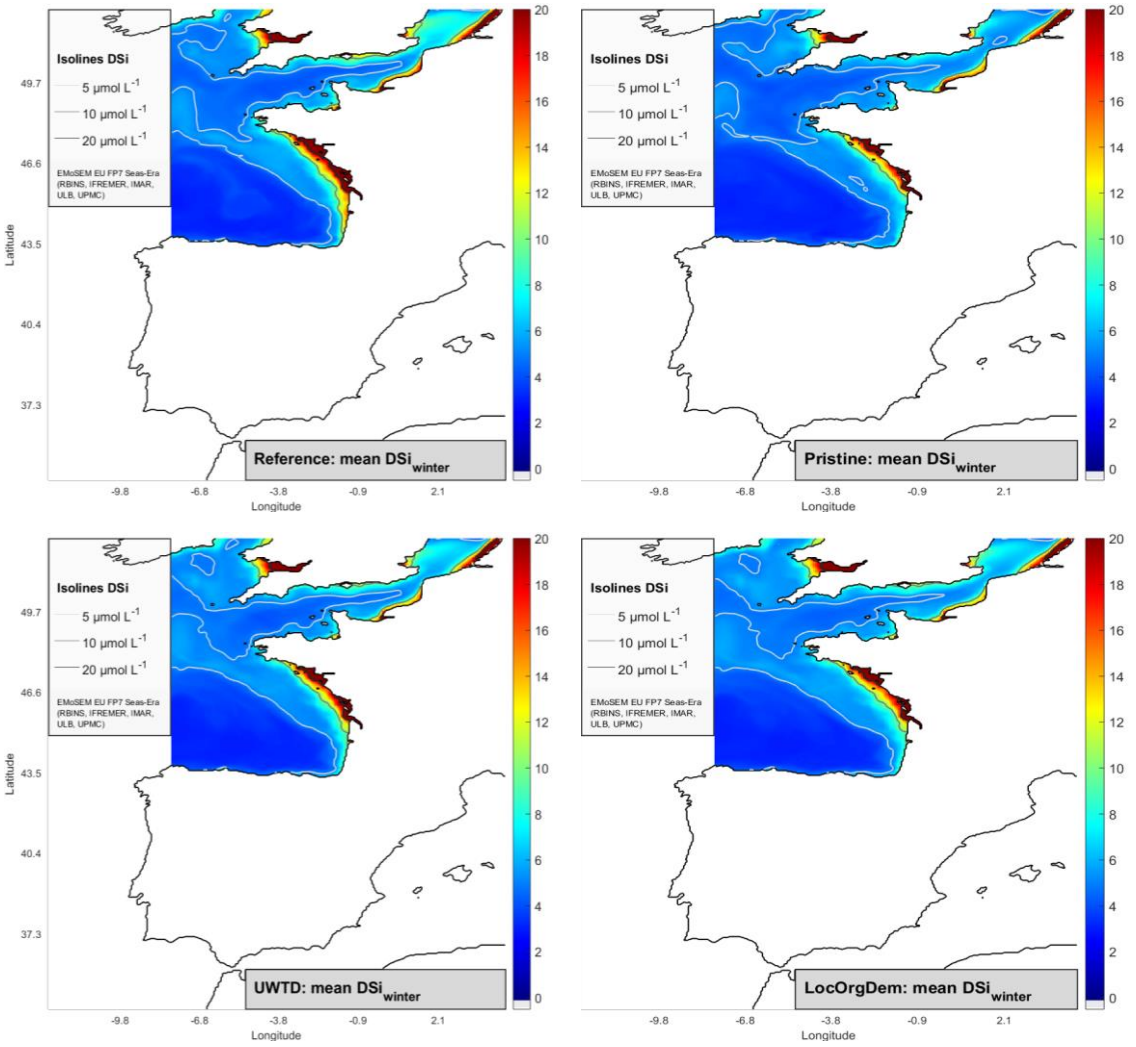

Figure 67: NEA-integrated contour maps of modelled winter DSi (Jan-Feb) on a year with average meteorological conditions. Each graph represents a scenario: contemporary situation (Reference), pristine situation (Pristine) and two "future" scenarios (UWTD, LocOrgDem). Results from MIRO&CO, ECO-MARS3D and BIOPCOMS, with river inputs from PyNuts-Riverstrahler.

3.1.2.6 Winter DIN:DIP (Jan-Feb)

The winter DIN:DIP is particularly high in the current situation (Reference), reaching values well above 40 molN $molP^{-1}$ in most sensitive areas across the NEA (Figure 68). The DIN:DIP ratio is considered an important indicator because an imbalanced ratio may often favour phytoplankton nuisance species. It is long known that on global average phytoplankton internal N:P ratio is 16 molN $molP^{-1}$ and caused in time the large-scale oceanic NO_3^-:PO_4^{3-} ratio to reach that value as well (Redfield et al. 1963, Falkowski and Davis 2004). This does not mean, however, that DIN:DIP ratios in coastal waters should always be expected to reach 16 molN $molP^{-1}$ exactly in order to conclude to a "good status". In fact, at smaller scales than the ocean basin, the phytoplankton internal N:P ratio may vary from 6:1 to 60:1 depending on the species and the growth conditions (Falkowski and Davis 2004). Desmit et al. (2015) concluded that, to mitigate *Phaeocystis* nuisances in the SBNS, the winter nutrients should preferably be reduced while keeping the DIN:DIP ratio below 34.4 molN $molP^{-1}$ in Belgian waters and 28.6 molN $molP^{-1}$ in Dutch waters.

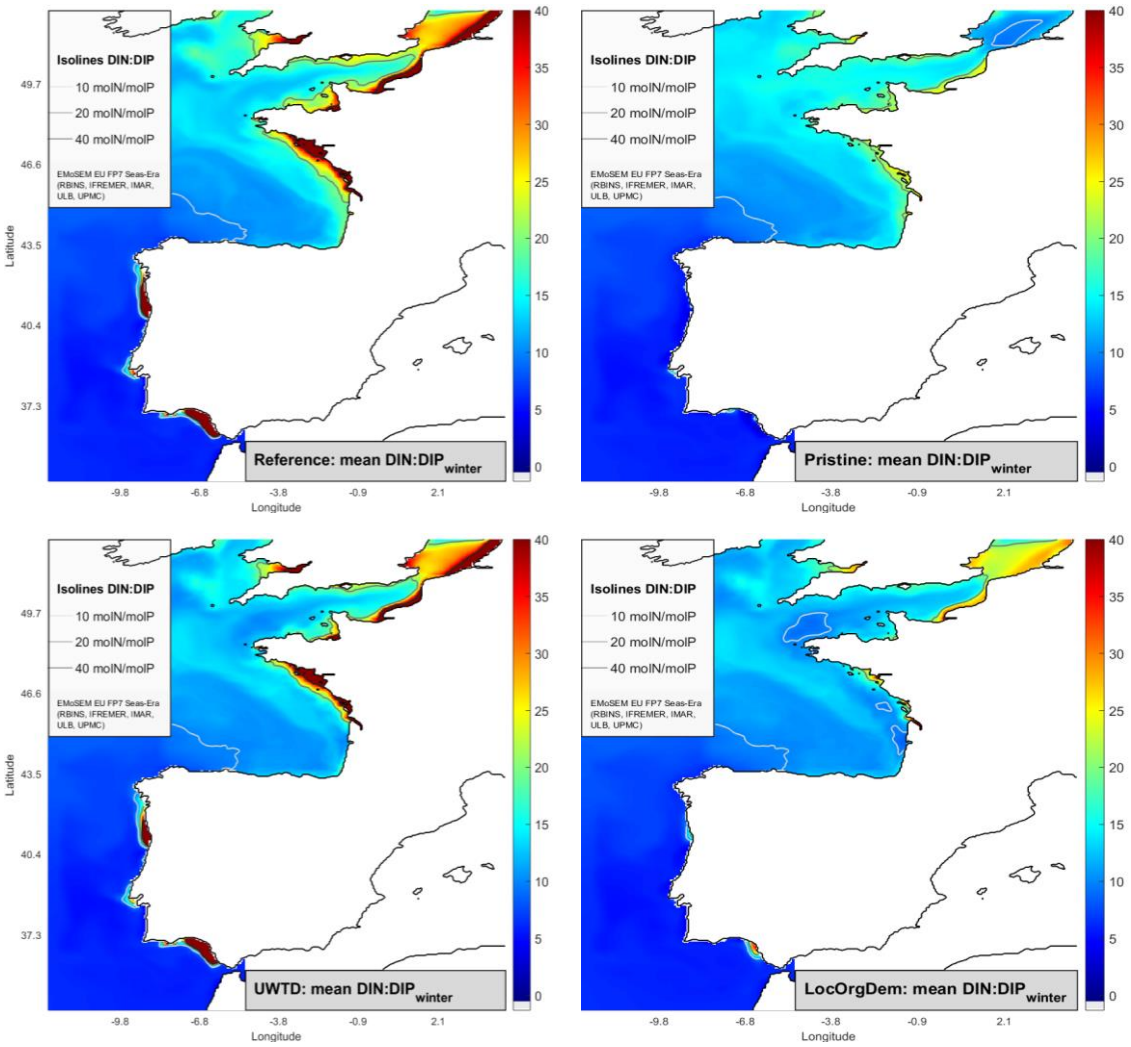

Figure 68: NEA-integrated contour maps of modelled winter DIN:DIP ratio (Jan-Feb) on a year with average meteorological conditions. Each graph represents a scenario: contemporary situation (Reference), pristine situation (Pristine) and two "future" scenarios (UWTD, LocOrgDem). Results from MIRO&CO, ECO-MARS3D and BIOPCOMS, with river inputs from PyNuts-Riverstrahler.

In the different scenarios proposed here, the DIN:DIP winter ratio changes mainly due to the N-reduction in the rivers as the P-reduction is quite limited, except in the Pristine situation. The Pristine conditions show the lowest DIN:DIP ratios amongst all scenarios, and still high values are found in French coastal zones (~25 molN $molP^{-1}$). This shows that the theoretical pristine conditions in coastal zones are not always identical to ocean conditions because of the N- and P-inputs from the lands. The UWTD scenario does not show significant changes compared to Reference, except in some parts of the French coast around the Cotentin peninsula and close to the Gironde, and in some parts of the Iberian coast in the Bay of Vigo and close to the river Tagus. The LocOrgDem scenario considerably reduces the DIN:DIP ratio across the NEA and almost reaches pristine levels everywhere, except in Southern Bight of the North Sea, the south of Spain at the mouth of the Rio Guadalquivir. It is remarkable that in the Bay of Mont Saint-Michel and close to the Gironde outlet, the winter DIN:DIP ratio reaches lower values in LocOrgDem than in Pristine.

3.1.2.7 Phytoplankton Functional Types (PFT)

Only the results of the model MIRO&CO are used to analyse the effect of scenarios on the marine phytoplankton species composition. The other models (ECO-MARS3D and BIOPCOMS) are also routinely calculating the phytoplankton species composition but a series of technical issues prevented the delivery of the results before the end of the project. Globally, MIRO&CO reproduces well the dynamics of diatoms and of *Phaeocystis globosa* in the SBNS (see validation, section 2.2.4, Figure 41). However, the model does not reproduce accurately the species composition in the English Channel as the diatoms observed there are not well simulated by MIRO&CO (Figure 69). In the Seine plume and in the region of the Channel Islands, MIRO&CO overestimates the *Phaeocystis* bloom (Figure 70) in comparison to what is observed and conversely underestimates the dominance of diatoms. For that reason, in this section, the species composition produced by the model is analysed in the Southern Bight of the North Sea, and only some aspects of the change in species composition in the Seine Plume are mentioned.

In the Reference situation, the mean values (Mar-Oct) of diatoms (Figure 69) and *Phaeocystis* colonies carbon biomass (Figure 70) are above 100 µgC L^{-1} in most coastal zones with the highest values found in the Belgian and Dutch coastal zones. Problematic areas where *Phaeocystis* biomass accumulates can be identified from the Reference situation. Along the Belgian and Dutch coasts, the P90 of *Phaeocystis* abundance (Figure 71) is higher than $15x10^6$ cells L^{-1}, which indicates a decrease in the trophic efficiency during the spring when *Phaeocystis* colonies dominate the bloom while being inedible to zooplankton and their biomass being directly transferred to the microbial food chains (Rousseau et al. 2000, Lancelot et al. 2009). In addition, the number of days during which *Phaeocystis* abundance remains above the reference level of $4x10^6$ cells L^{-1} is larger than 100 days (Figure 72). That means that more biomass builds up in time, which eventually decays and may cause oxygen depletion in shallow areas.

The Pristine simulation shows a situation where the diatoms are blooming mainly in the coastal zones with values lesser than 100 µgC L^{-1} and where *Phaeocystis* colonies, while present, never reach undesirable abundances (> $4x10^6$ cells L^{-1}).

The UWTD scenario does not induce significant change in the phytoplankton functional types composition. As the wastewater treatment plants requested by the EU Directive UWWTD are almost all implemented, the UWTD scenario is very close to the Reference situation regarding the nutrient inputs from the watersheds to the sea (see above).

Therefore the marine phytoplankton composition and dynamics remain quite similar. An identical conclusion may be drawn for the GAP scenario (not shown) where the implementation of good agricultural practices decreases the winter DIN concentrations in the coastal zones (from 35 to 25 µmol L^{-1} on average, see section 3.1.2.3) without any concomitant decrease in DIP concentrations, which results in no significant change in the marine PFT composition in spite of positive effects in the rivers.

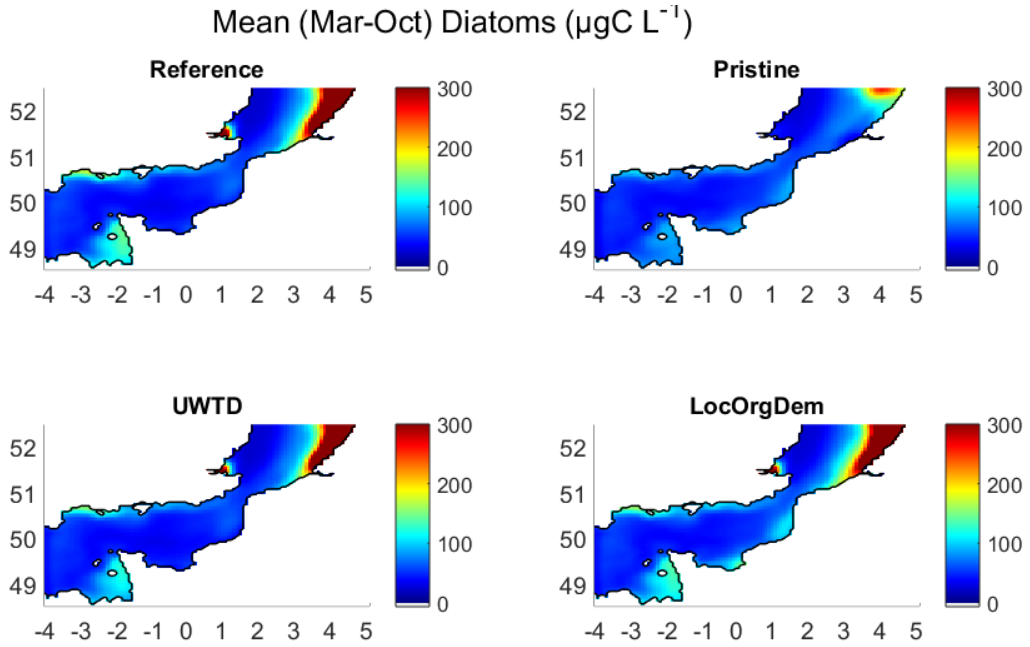

Figure 69: Multiyear average MIRO&CO model results (2000-2010). Mean values (Mar-Oct) of diatom carbon biomass in the English Channel and the Southern Bight of the North Sea for the Reference and Pristine situations and UWTD and LocOrgDem scenarios. Units are expressed in µgC L^{-1}.

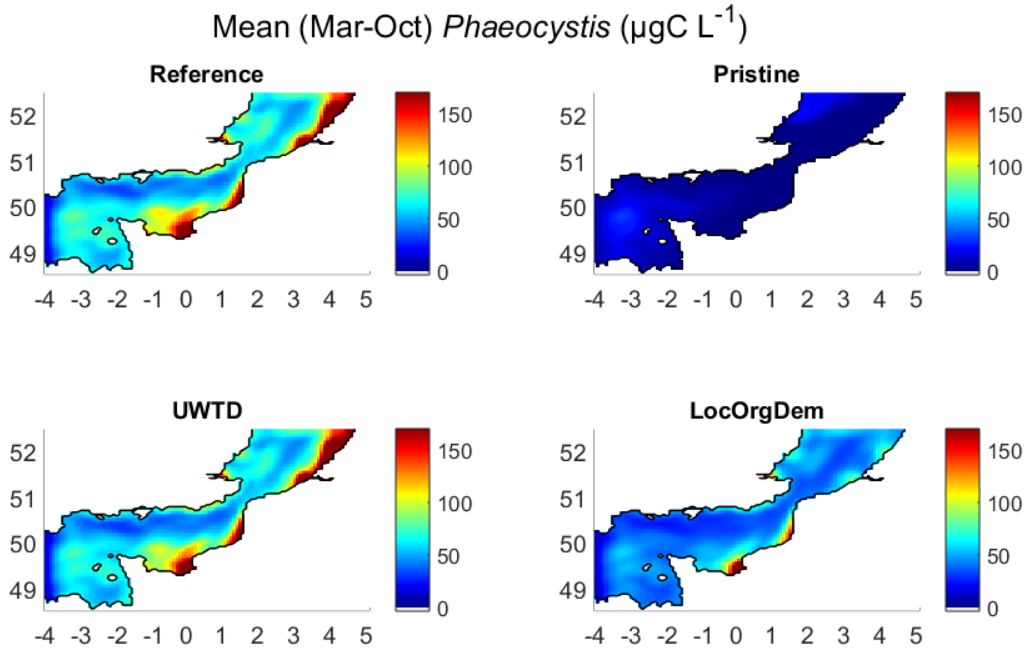

Figure 70: Multiyear average MIRO&CO model results (2000-2010). Mean values (Mar-Oct) of *Phaeocystis* colonies carbon biomass in the English Channel and the Southern Bight of the North Sea for the Reference and Pristine situations and UWTD and LocOrgDem scenarios. Units are expressed in µgC L^{-1}.

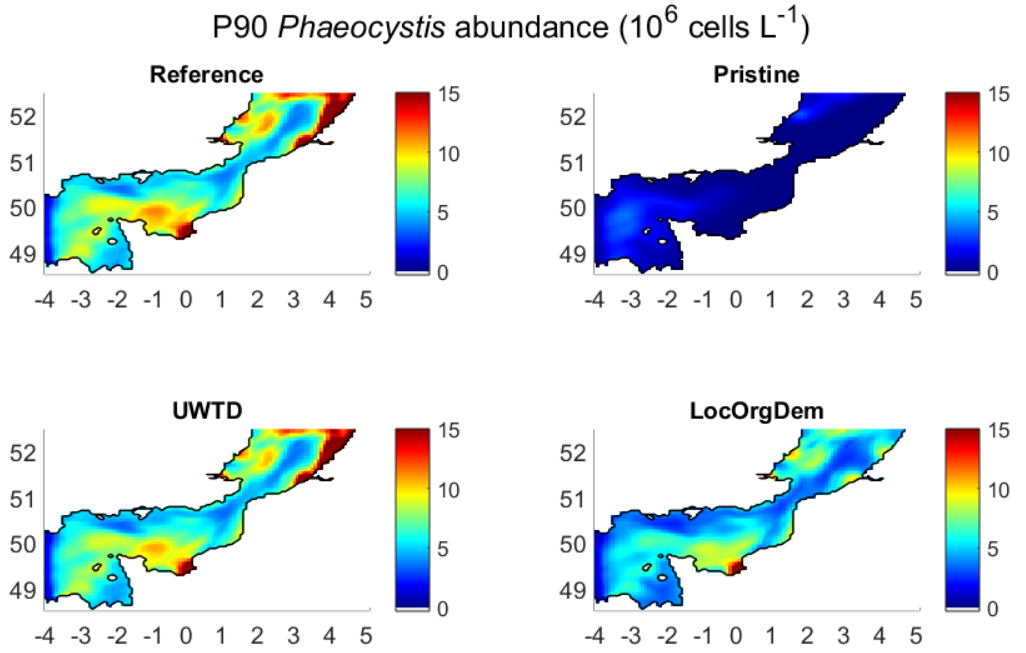

Figure 71: Multiyear average MIRO&CO model results (2000-2010). Percentile 90 of *Phaeocystis* abundances in the English Channel and the Southern Bight of the North Sea for the Reference and Pristine situations and UWTD and LocOrgDem scenarios. Units are expressed in 10^6 cells L^{-1}.

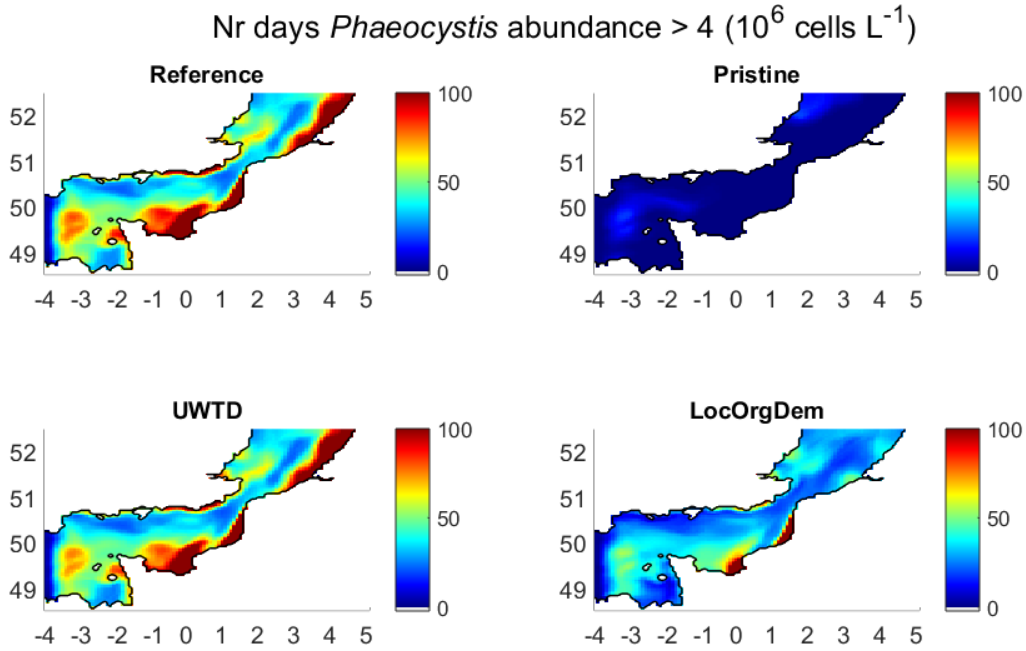

Figure 72: Multiyear average MIRO&CO model results (2000-2010). Number of days during which *Phaeocystis* abundance exceeds the reference level $4x10^6$ cells L^{-1} in the English Channel and the Southern Bight of the North Sea for the Reference and Pristine situations and UWTD and LocOrgDem scenarios. Units are expressed in days.

The scenario LocOrgDem brings considerable changes in the composition of marine phytoplankton by comparison with the Reference situation. The significant reduction in

riverine nitrogen brings improvements regarding the phytoplankton functional types composition:

1/ While the mean value (Mar-Oct) of diatom concentration is preserved in scenario LocOrgDem compared to the Reference situation, the mean value (Mar-Oct) of *Phaeocystis* colonies concentration over the period considerably decreases from values above 150 µgC L^{-1} to values below 100 µgC L^{-1} in the Belgian and Dutch waters. In the Bay of Seine, the extension of *Phaeocystis* also decreases in LocOrgDem scenario.

2/ The difference in *Phaeocystis* P90 abundance between the Reference situation and the LocOrgDem scenario is significant as it brings the P90 of *Phaeocystis* abundance to $5x10^6$ cells L^{-1} in most parts of the Belgian and Dutch coastal zones, except close to the river outlets (Figure 71). With the LocOrgDem scenario, the P90 of *Phaeocystis* abundance is reduced by an amount equal to $5x10^6$ up to $10x10^6$ cells L^{-1} in the Belgian coastal zone and by more than $15x10^6$ cells L^{-1} in the Dutch coastal zone. A decrease of such amplitude was not obtained with scenario UWTD or GAP. It is necessary to point out here that the P90 of *Phaeocystis* abundance does not decrease so much due to a decrease in the spring maximum, but due to the elimination of the summer bloom of *Phaeocystis* colonies in the model. A significant N reduction without a concomitant P reduction eliminates the summer bloom and reduces the duration of the *Phaeocystis* bloom (see point 3 below). The spring maximum of colonial *Phaeocystis* abundance does not change much between the Reference situation and the LocOrgDem scenario (spring maximum value in the Belgian coastal zone decreases from $27x10^6$ to $22x10^6$ cells L^{-1}), suggesting that a P reduction is still necessary to further reduce the spring peak in the coastal zone.

3/ The scenario LocOrgDem causes a significant decrease in the period during which *Phaeocystis* abundance exceeds its reference level (i.e. $4x10^6$ cells L^{-1}). That reference level indicates the abundance above which *Phaeocystis* forms large-size colonies that are inedible to zooplankton copepods (Rousseau et al. 2000, Daro et al. 2006, Lancelot et al. 2009). A decrease in the period of high *Phaeocystis* abundance indicates a decrease in the biomass accumulation and hence a lesser microbial activity, which in turn results in a lower risk of oxygen depletion. The scenario LocOrgDem, with 50 days maximum of excessive abundance (>$4x10^6$ cells L^{-1}) in the Belgian and Dutch coastal zones, reaches the "Good Ecological Status" (GES) according to the WFD criteria (i.e. less than 2 months).

The scenario LocOrgDem, decreases the duration of the *Phaeocystis* colonial bloom by suppressing the summer bloom, while the diatom biomass remains relatively stable. The Chl P90 also remains quite stable as the spring maximum of colonial *Phaeocystis* remains. This numerical study shows that the LocOrgDem scenario is the only one able to achieve significant improvements regarding colonial *Phaeocystis* presence. This indicates that the status of eutrophication might be significantly improved if a scenario like LocOrgDem was implemented in reality.

3.1.2.8 Conclusions

- The different realistic scenarios simulate a reduction in riverine nutrient (N and P) loads, which affects the phytoplankton production in the river network and therefore also the Si loads.
- Most scenarios, except Pristine, do not significantly reduce P loads because the implementation of EU Directive UWWTD has already taken place in most regions of Western Europe.
- Most scenarios do, however, reduce N concentrations in the rivers and in the coastal zones, with scenario LocOrgDem showing the largest reduction (i.e. closest to the pristine situation).
- The Chl P90 does not vary much between scenarios, which suggests that the amplitude of the Chl maximum is generally limited by P availability, even in coastal zones.
- As a result of the decrease in the winter DIN:DIP ratio, the phytoplankton composition changes from one scenario to the other, with an increase in the relative presence of diatoms when DIN:DIP is lower.
- The LocOrgDem scenario is the scenario that gives the best results in terms of eutrophication mitigation.

More generally, it is also concluded that Chl P90 can obviously not be the only indicator used in the assessment of GEnS regarding undesirable eutrophication, and that the phytoplankton composition must be taken into consideration. Therefore, in what follows, it is suggested to focus also on the non-diatom chlorophyll *a* (or NDAChl) as it is a useful indicator of the potential phytoplankton nuisance in the NEA waters.

3.2 Scaling Reference vs. Pristine & LocOrgDem

3.2.1 Ecozones

The focus of the present study on the whole NEA and the transboundary approach in EMoSEM both suggest that coastal and offshore budgets of nutrients could be estimated across the NEA in sub-areas that present an ecological meaning (Ecozones) instead of in sub-areas constrained only by political boundaries. These Ecozones allow us to measure the effects of nutrient reduction across the NEA from the Iberian shelf to the North Sea in similar area types (e.g. highly eutrophic vs. oligotrophic).

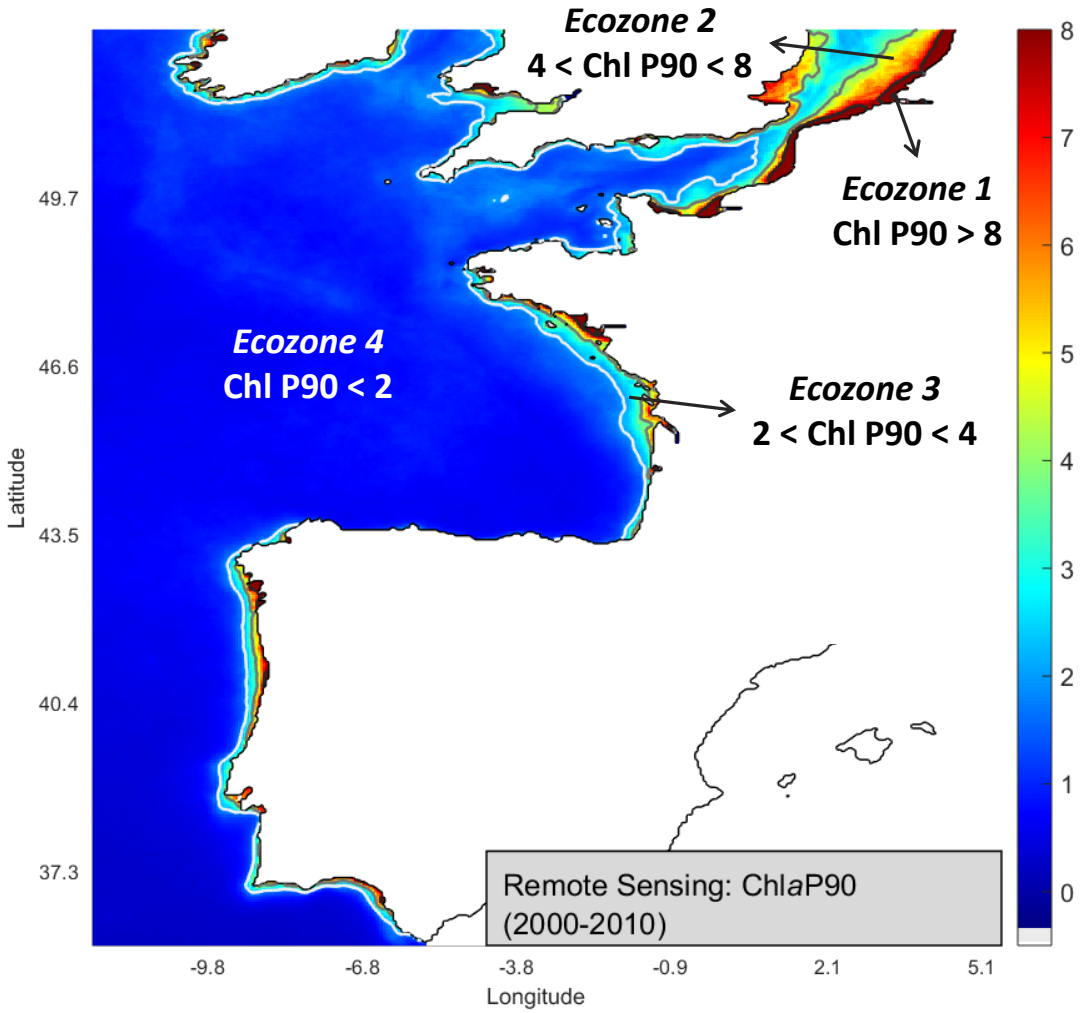

Figure 73: Multiyear average RS Chl P90 over the growing season in the NEA (SeaWIFS 2000-2010) illustrating the four Ecozones. Isolines 2 (white), 4 (grey) and 8 (black) µgChl L^{-1} are shown (from SeaWiFs and MODIS data treated by F.Gohin/IFREMER).

Discussions have taken place to define the criteria determining the Ecozones. Attempts have been made to define them on the basis of a combination of physical parameters influencing the phytoplankton production such as euphotic and mixing depths, salinity, etc. There is no combination of parameters that may be universally applied across the NEA, and there is always

a need for more complexity and for introducing new parameters (e.g. residence time, stratification). In addition, most of these parameters are not known and may only be derived from models. After many attempts and discussions, the partners of EMoSEM estimated that a rational criterion to define the boundaries of the Ecozones could be the satellite-borne long-term averaged Chl P90 (Figure 73). The long-term averaged Chl P90 gives a good vision of the eutrophied areas where potential phytoplankton nuisances might occur, whatever the biogeochemical conditions prevailing. The satellite-borne Chl P90 presents the advantages to be simple, easily accessible and measured in many other areas than the sole NEA, which allows a possible extension of the method, if deemed appropriate.

A distribution of the multiyear mean of Remote-sensing (RS) Chl P90 (2000-2010) is used to design the limits of the Ecozones. The global Chl P90 histogram has been empirically decomposed into a sum of 4 gamma distributions (Figure 74). The boundaries of the different Ecozones, i.e. 2 µgChl L^{-1}, 4 µgChl L^{-1} and 8 µgChl L^{-1}, have then been arbitrarily set at the points where the relative heights of two successive gamma distributions become equal, which are also the inflexion points of a cumulative sum curve of the distribution (not shown). These are not threshold values or reference values. These are only the boundaries of the four Ecozones used in this report.

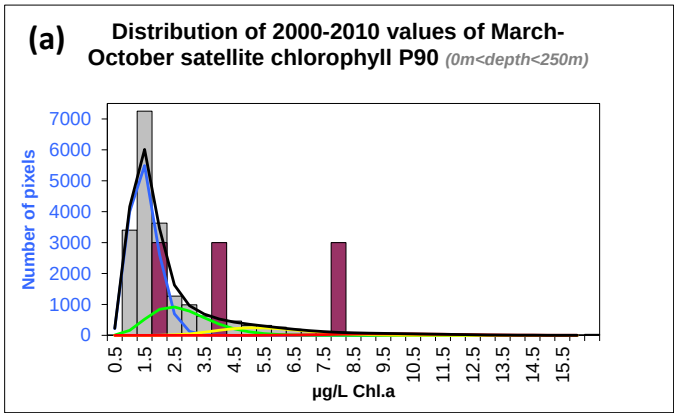

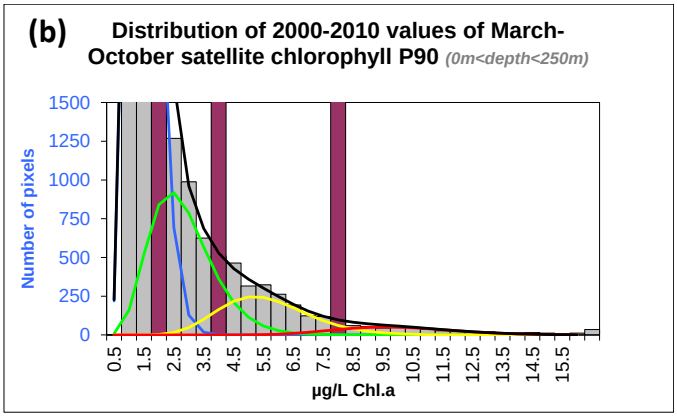

Ecologically-based subareas limits: [2, 4, 8] µg Chla L^{-1}

Subarea 1 (Eutrophic):
Chl P90 > 8 µg Chla L^{-1}

Subarea 2:
4 < Chl P90 < 8 µg Chla L^{-1}

Subarea 3:
2 < Chl P90 < 4 µg Chla L^{-1}

Subarea 4 (Oligotrophic):
Chl P90 < 2 µg Chla L^{-1}

Figure 74: (a) Probability distribution function (PDF) of chlorophyll a percentile 90 (Chl P90) across the French domain of the NEA in 2000-2010 (data from remote sensing, RS, and its decomposition into four gamma PDFs; purple bars indicate the 2, 4 and 8 µgChl L^{-1} thresholds.(b) Zoom on figure (a).

3.2.2 PDFs and reference values for indicators

3.2.2.1 Projection of indicators into Ecozones

The Probability Distribution Functions (PDFs) are calculated for several modelled indicators (Chl P90, winter DIN, DIP and DIN:DIP ratio, and NDAChl) in the four Ecozones drawn by RS Chl P90 isolines 2, 4 and 8 µgChl L^{-1} (Figure 75, top left). The projection of RS Chl P90 isolines on the map of modelled Chl P90 shows how modeled results distribute into the different Ecozones (Figure 75, top right).

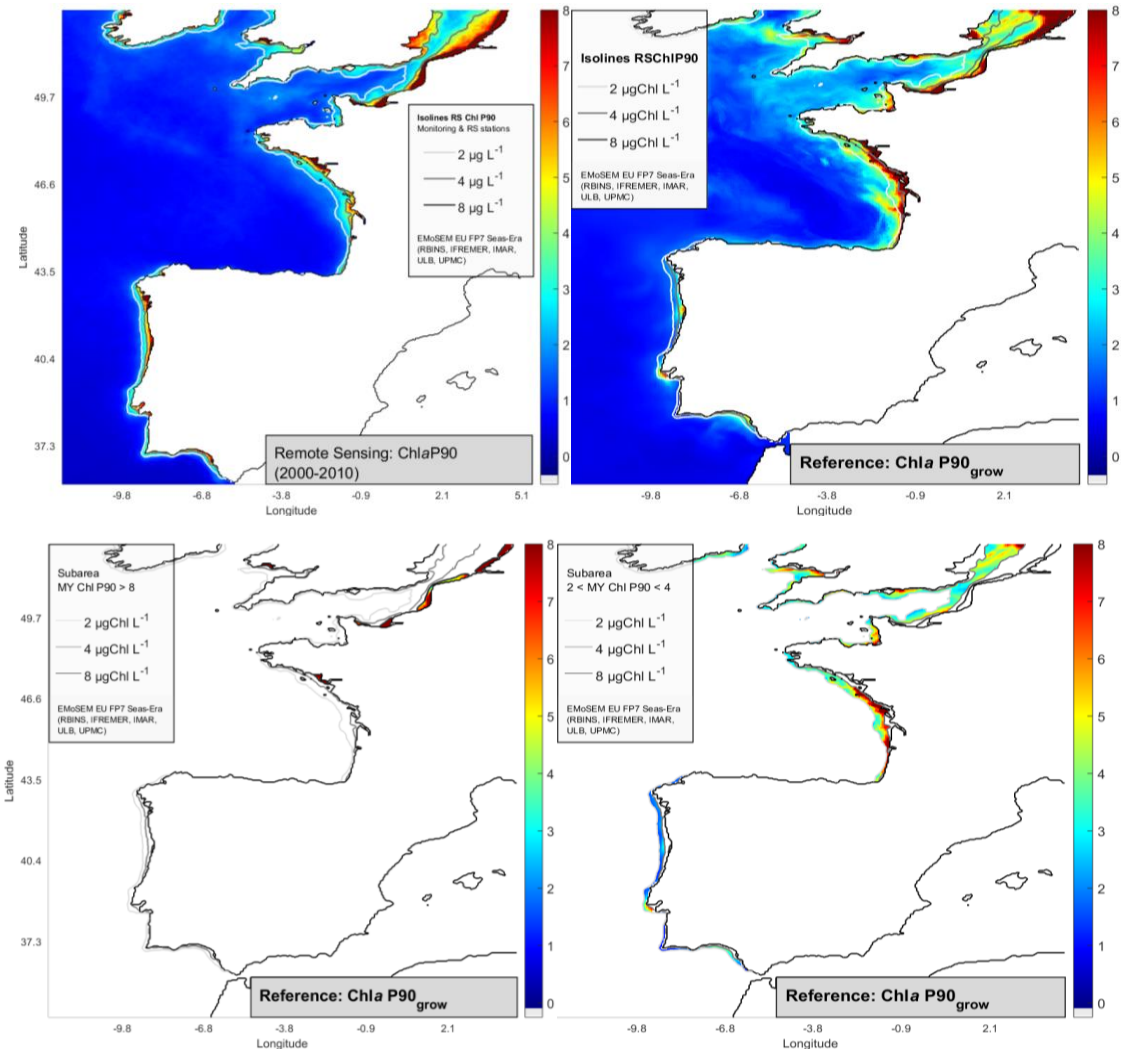

Figure 75: Top left – Multiyear average of remote sensing Chl P90 (SeaWIFS 2000-2010) with isolines at 2, 4 and 8 µgChl L^{-1}. Top right – Integrated map across the NEA of model results of Chl P90 with the isolines 2, 4 and 8 µgChl L^{-1} derived from remote sensing Chl P90 (i.e. from top left graph). Bottom – Examples of Ecozones applied on modelled Chl P90. Bottom left – Modelled Chl P90 in Ecozone 1 (i.e. RS Chl P90 > 8 µgChl L^{-1}). Bottom right – Modelled Chl P90 in Ecozone 3 (i.e. 2< RS Chl P90 < 4 µgChl L^{-1}).

The modelled Chl P90 is very well comparable to the RS one, except in some parts of the Bay of Biscay and the SBNS where the coastal-offshore gradient differs: in the model, the high Chl P90 extends further offshore than in the RS data. In the SBNS, the high modelled Chl P90 is

concentrated along the coasts and along the south-west to north-east axis while the RS Chl P90 shows a more continuous coastal-offshore gradient. In the SBNS, the differences between RS and modelled Chl p90 are due to at least two reasons: first there is a technical issue with the northern boundary of MIRO&CO that creates some accumulation in the domain, and secondly the model Chl P90 results shown in these integrated maps are those of the growing season of 2007 while the RS Chl P90 is the long-term average in 2000-2010 (multiyear mean of yearly Chl P90 values).

Any indicator can be projected into the Ecozones. As an example, modelled Chl P90 is projected into two Ecozones in Figure 75 (bottom panels). This figure shows that the "high chlorophyll" Ecozone (i.e. RS Chl P90 > 8 µgChl L^{-1}) does not include Portuguese results of Chl P90 but only French and Belgian results, and that the third Ecozone (i.e. 2 < RS Chl P90 < 4 µgChl L^{-1}) may still include a large range of modelled Chl P90 values, including values above 8 µgChl L^{-1}.

3.2.2.2 PDFs of indicators, including NDAChl

By plotting the frequency distribution of indicators values in each Ecozone, both the extreme and the most frequent values clearly appear, which allows comparing different scenarios. Also, when matching the frequency distributions of an indicator in a given Ecozone with its reference level, one can calculate the relative geographical area where the parameter shows higher values than the reference level. It was chosen to compare Reference with Pristine situation to estimate the change in frequency distributions between the current situation and the "natural" pristine situation. It is proposed to derive a background value from the maximum value found in the pristine situation. The most promising future "realistic" scenario, the LocOrgDem scenario, is also illustrated to scale the possible mitigation of eutrophication.

The indicators in this analysis are the Chl P90 (Figure 76), the winter DIN (Figure 77), the winter DIP (Figure 78), the winter DIN:DIP ratio (Figure 79) and the non-diatom chlorophyll *a* (NDAChl) (Figure 80).

The NDAChl indicator was chosen after many discussions. Initially, the idea was to find an indicator that reflects the proportion of undesirable algae, to measure the "risk" of nuisance. Considering that most undesirable algae are non-diatom, the ratio "non-diatom/total phytoplankton" (NDA/Phy) was chosen. However, the NDA/Phy ratio turns out to be a poor indicator of eutrophication nuisances as it may show high values in low-chlorophyll *a* areas, and vice versa. Hence, it was useful to weight it with the chlorophyll *a* concentration, i.e. the indicator became Chl*NDA/Phy. With the simple hypothesis that the internal "carbon-to-chlorophyll *a*" ratio of phytoplankton (C:Chl) remains constant in time, in space and between species, the total phytoplankton concentration becomes equal to the chlorophyll *a* concentration times the C:Chl ratio, i.e. Phy = Chl*C:Chl. Thus, with that simple hypothesis, the weighted indicator Chl*NDA/Phy is actually equal to the non-diatom chlorophyll *a*, i.e. NDAChl.

The reference levels associated to these indicators in the present approach have been determined in different ways:

- Regarding the winter DIN concentration, the reference value is the one recommended by OSPAR and chosen by the MSFD for Belgian coastal waters (15 µmol L^{-1}).

- Regarding the winter DIP concentration, the reference value is the one recommended by OSPAR and chosen by the MSFD for Belgian waters (0.8 µmol L^{-1}).
- Regarding the winter DIN:DIP ratio, the reference value was chosen to fit the mean oceanic elemental composition of phytoplankton, i.e. 16 molN $molP^{-1}$ (Redfield et al. 1963), even if higher values for this ratio may be tolerated in some coastal areas. Desmit et al. (2015) showed that spring phytoplankton blooms in Belgian and Dutch coastal zones grow based on a ratio closer to 30 molN $molP^{-1}$ on average in the period 2000-2010 (see also further discussion in section 4.2.2 about winter DIN, DIP and DIN:DIP).
- Regarding the Chl P90, we compare the results with the limit value determining the first Ecozone containing the highest values of RS Chl P90. This limit was defined at 8 µgChl L^{-1}, which is quite lower than the thresholds chosen by the WFD and MSFD for coastal waters (e.g. in Belgium coastal zone and in France, 15 µgChl L^{-1}). In the present exercise, as the Chl P90 value of 8 µgChl L^{-1} is also the upper limit of coastal values in the pristine situation, we suggest that this value constitutes a background value reflecting a status of eutrophication close to the "pritine-like" status. It should be noted that the real background value might well be slightly higher than 8 µgChl L^{-1}, as our models tend to underestimate the spring maximum of chlorophyll *a*. This tends to support the choice of 10 µgChl L^{-1} for the current background value of coastal Chl P90 discussed in the frame of the WFD.
- Regarding the NDAChl, the frequency distributions were only performed with MIRO&CO results (see section 3.1.2.7). Therefore the reference level of non-diatoms could be computed on the basis of the known reference level for *Phaeocystis globosa* abundance, i.e. $4x10^6$ cells L^{-1} (Rousseau et al. 2000, Daro et al. 2006, Lancelot et al. 2009). The conversion of this abundance into chlorophyll *a* gives a reference level for NDAChl equal to 2 µgChl L^{-1} (only valid for *Phaeocystis*). It is important to point out that other species than the colonial *Phaeocystis globosa* may require other reference levels, and that toxic species are sometimes found in low concentrations.

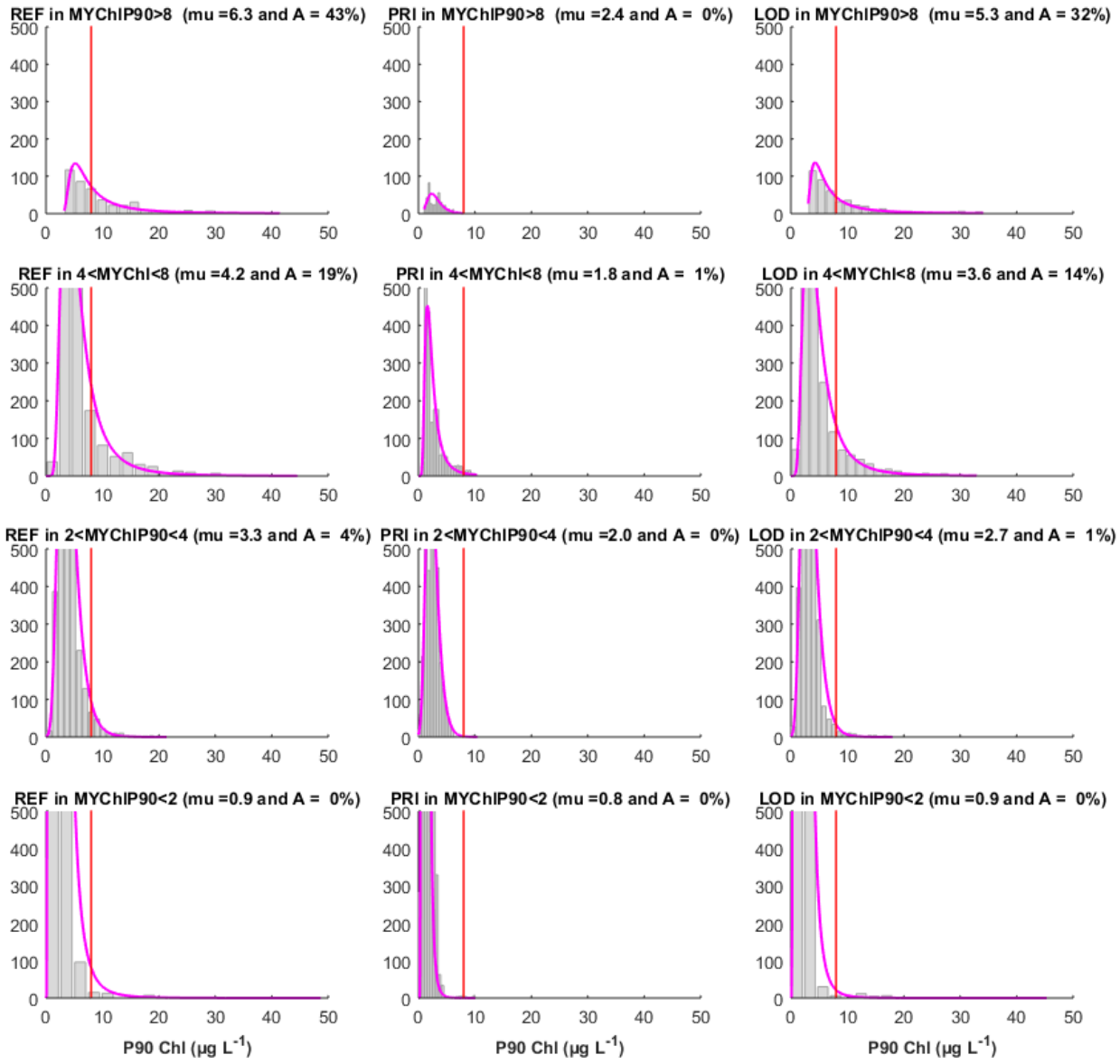

Figure 76: Probability distribution functions (pink curve) of Chl P90 in the four Ecozones across the NEA for the Reference situation (left column), the Pristine situation (middle column) and the LocOrgDem scenario (right column). The vertical red line indicates the background level (8 µgChl L^{-1}) chosen as the superior limit of the Pristine coastal PDFs. The title of each graph indicates the central tendency of the PDF (mu) and the percentage of the Ecozone area (A) where the Chl P90 exceeds the background level.

As previously observed, the Pristine situation is the only one showing Chl P90 < 8 µgChl L^{-1} in all Ecozones (Figure 76), with an average value in the first Ecozone (coastal) equal to 2.4 µgChl L^{-1} across the NEA. By comparison, the LocOrgDem scenario presents 32% of coastal areas above the background values of 8 µgChl L^{-1}, and an average coastal value of 5.3 µgChl L^{-1} across the NEA. When compared to the Reference situation, the LocOrgDem scenario induces a decrease of 16% in the mean coastal Chl P90 value, and a reduction of the "high chlorophyll *a*" area from 43% to 32% of the first Ecozone across the NEA.

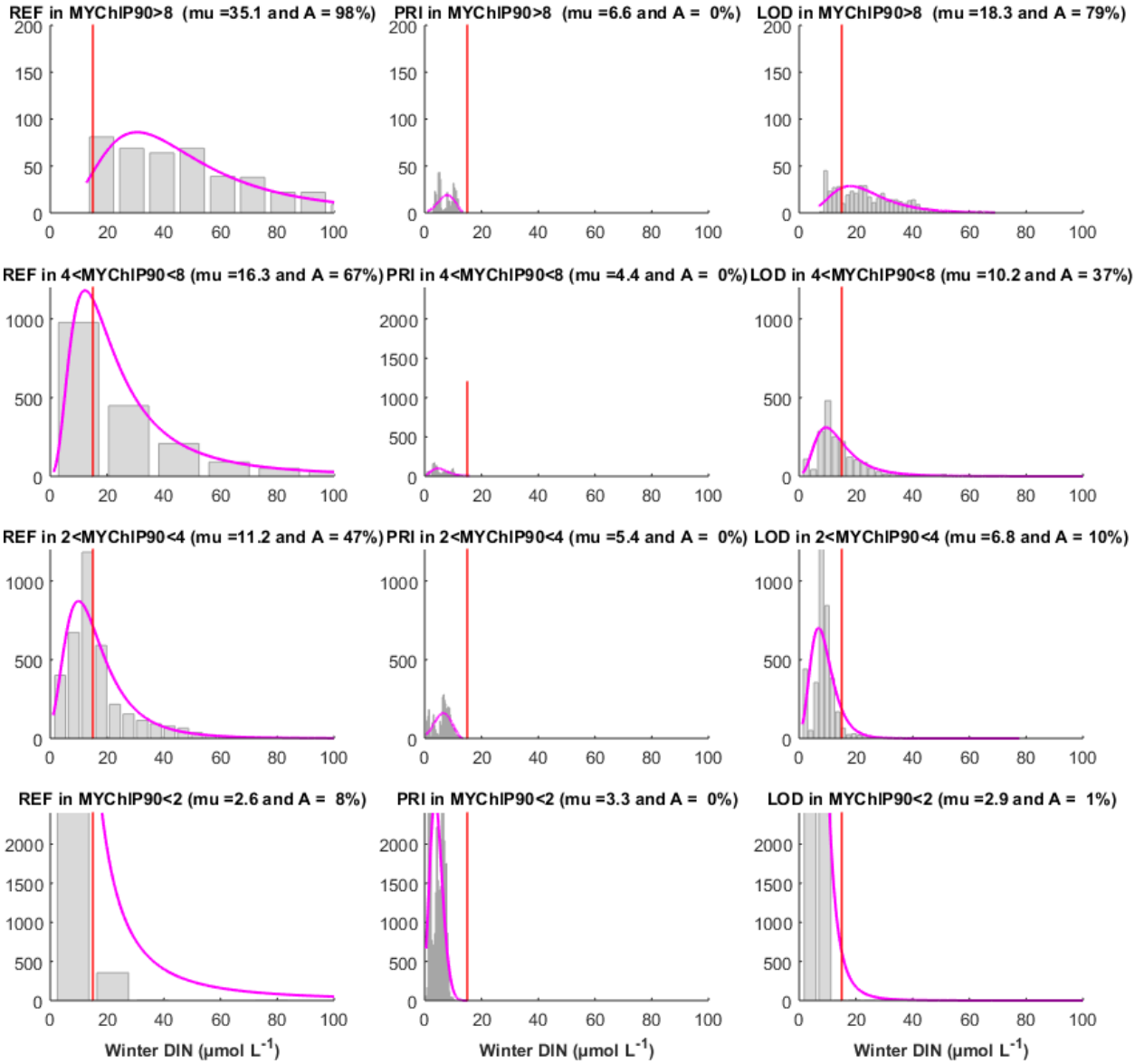

Figure 77: Probability distribution functions (pink curve) of winter DIN in the four Ecozones across the NEA for the Reference situation (left column), the Pristine situation (middle column) and the LocOrgDem scenario (right column). The vertical red line indicates the WFD/MSFD threshold value for coastal zones (15 µmol L^{-1}). The title of each graph indicates the central tendency of the PDF (mu) and the percentage of the Ecozone area (A) where the winter DIN exceeds the threshold value.

In the Reference situation the winter DIN (Figure 77) in the coastal zone remains largely above the WFD/MSFD threshold value (98% of the area is above 15 µmol L^{-1}). In contrast, the winter DIN is always lower than the threshold in the pristine situation. Remarkably, the highest winter DIN value observed in the pristine situation, which could be seen as a "background value", is identical to the threshold used by WFD/MSFD, i.e. 15 µmol L^{-1}. In the LocOrgDem scenario, the coastal winter DIN is considerably reduced compared to the Reference situation (mean coastal values are resp. 18.3 compared to 35.1 µmol L^{-1}), but 79% of the coastal area across the NEA still shows higher values than the threshold.

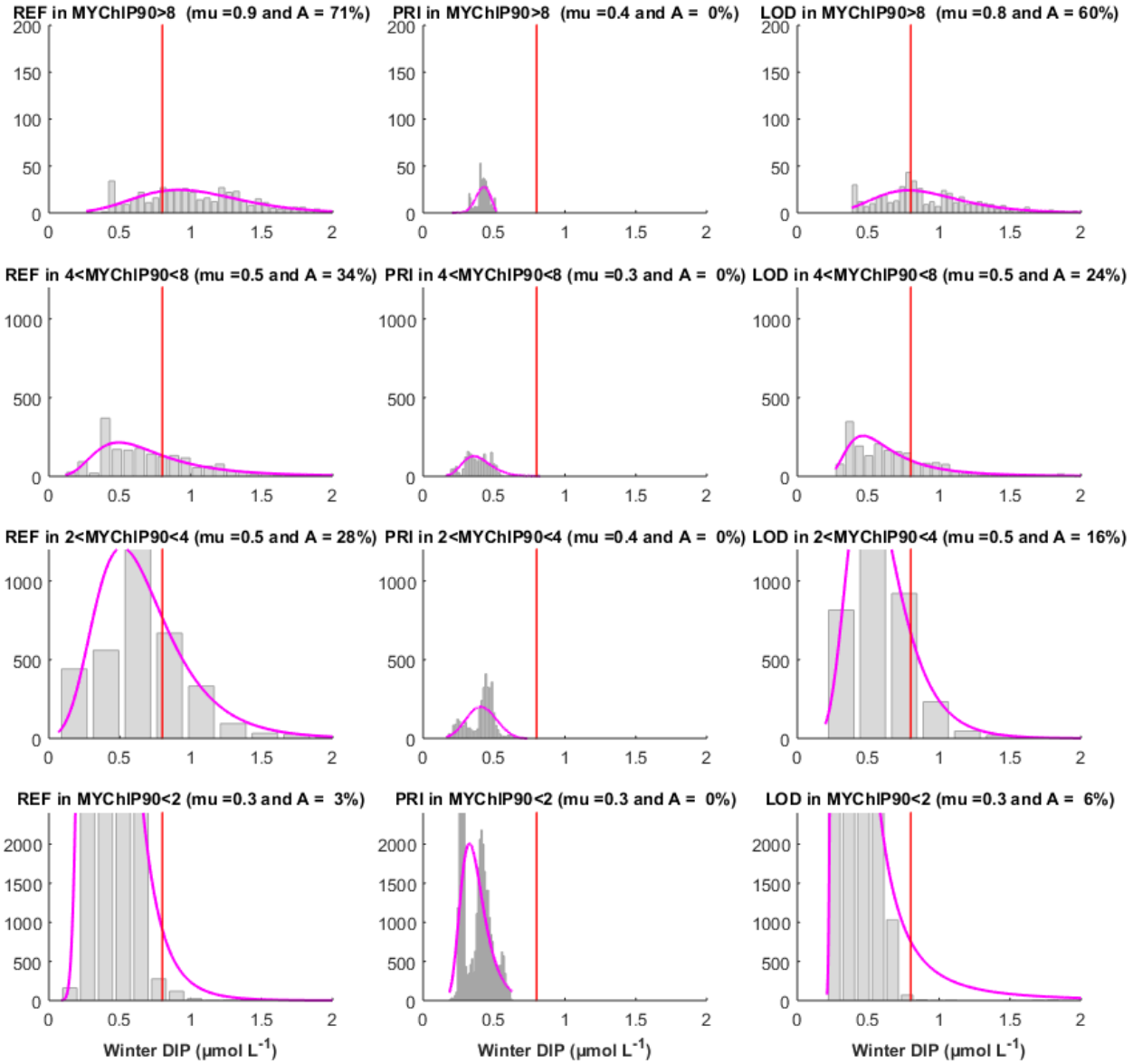

Figure 78: Probability distribution functions (pink curve) of winter DIP in the four Ecozones across the NEA for the Reference situation (left column), the Pristine situation (middle column) and the LocOrgDem scenario (right column). The vertical red line indicates the WFD/MSFD threshold value for coastal zones (0.8 µmol L^{-1}). The title of each graph indicates the central tendency of the PDF (mu) and the percentage of the Ecozone area (A) where the winter DIP exceeds the threshold value.

In the Reference situation, the winter DIP (Figure 78) in the coastal zone remains above the WFD/MSFD threshold value (71% of the area is above 0.8 µmol L^{-1}). The winter DIP is always lower than the threshold in the pristine situation. The highest winter DIP value observed in the coastal zone in the pristine situation (i.e. 0.5-0.6 µmol L^{-1}), which could be seen as a "background value", is smaller than the threshold used by WFD/MSFD, i.e. 0.8 µmol L^{-1}. In the LocOrgDem scenario, the coastal winter DIP is not reduced significantly compared to the Reference situation (mean coastal values are resp. 0.8 and 0.9 µmol L^{-1}), and 60% of the coastal area across the NEA still shows higher values than the threshold.

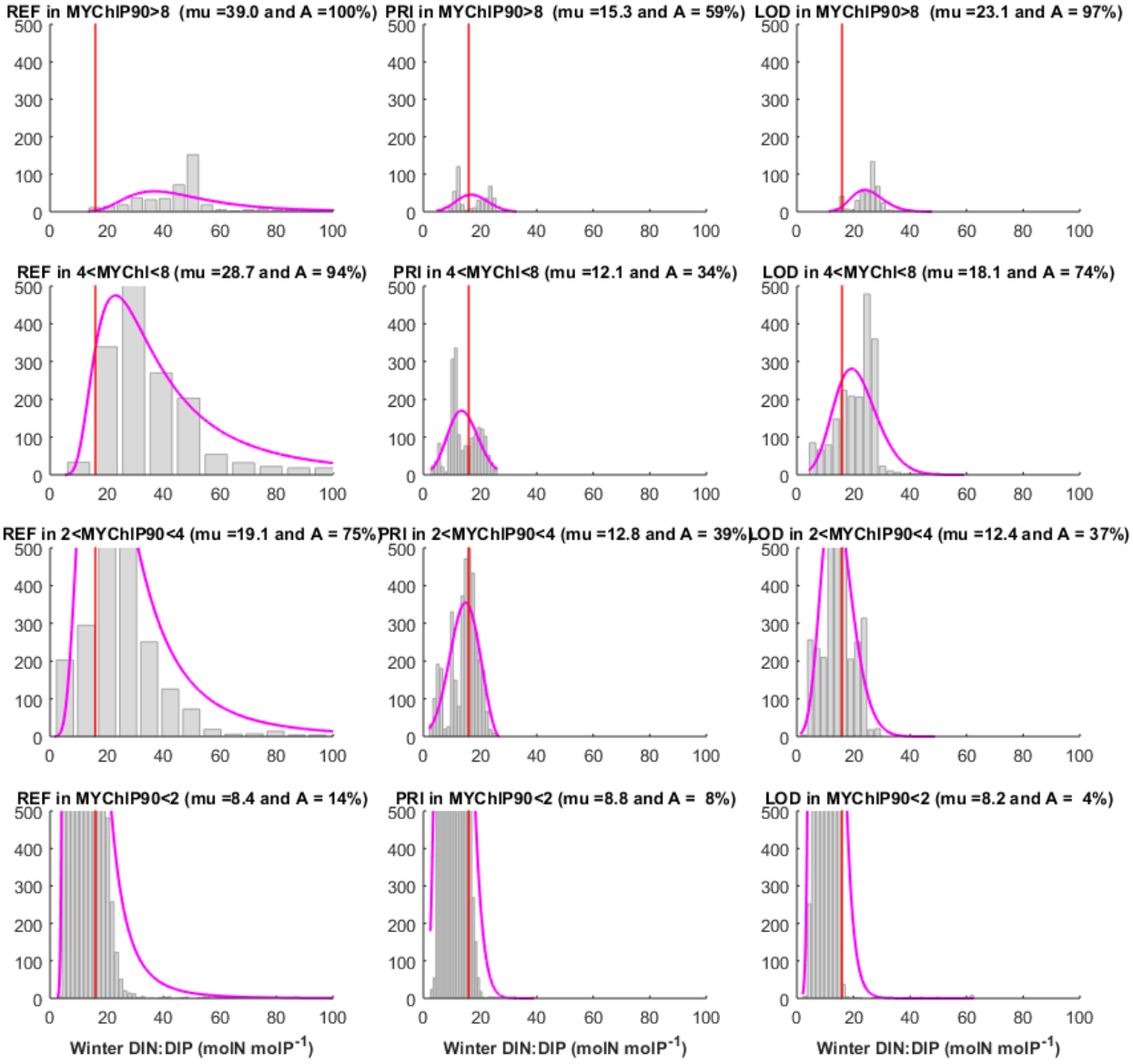

Figure 79: Probability distribution functions (pink curve) of winter DIN:DIP ratio in the four Ecozones across the NEA for the Reference situation (left column), the Pristine situation (middle column) and the LocOrgDem scenario (right column). The vertical red line indicates the oceanic reference level (16 molN $molP^{-1}$). The title of each graph indicates the central tendency of the PDF (mu) and the percentage of the Ecozone area (A) where the winter DIN:DIP ratio exceeds the reference value.

The projection of the winter DIN:DIP ratio into the Ecozones results in a high disparity of values (Figure 79). Some high values of the winter DIN:DIP ratio are found in offshore Ecozones and vice versa, and there is occurrence of bimodal distributions. This shows that the DIN:DIP ratio is highly variable in space and is not always consistent with the proposed Ecozones even when coastal-offshore gradients seem obvious. In the Reference situation, the winter DIN:DIP ratio shows an average coastal value of 39 molN $molP^{-1}$ and 100% of the coastal areas in the NEA are above the oceanic threshold. That mean value tends to decrease along the coastal-offshore axis with a very low value in Ecozone 4, i.e. 8.4 molN $molP^{-1}$, as the oceanic waters become predominant. The low winter DIN:DIP ratio in Ecozone 4 is due to the fact that the Portuguese model predicts a phytoplankton production in winter already in the oceanic areas, that rapidly

consumes DIN and causes a significant decrease in the ratio. The pristine situation shows an average value of 15.3 molN $molP^{-1}$, which is close to the Redfield ratio. Still, the maximum coastal value in the pristine situation, which may be seen as a background value, is 32 molN $molP^{-1}$, and that value shows that even under pristine conditions the natural system produces quite high winter DIN:DIP ratios in some coastal zones (e.g. French coast of Bay of Biscay, Bay of Seine and Somme). It should be pointed out that it is very probable that the winter DIN:DIP ratio in Belgian and Dutch coastal zones shown in Figure 68 is underestimated as the DIN:DIP ratio output in Rhine/Meuse waters is underestimated by almost a factor 2 (see validation PyNuts/Riverstrahler in section 2.2.1, Figure 18 and Figure 20). Therefore, the Belgian and Dutch coastal waters would probably exhibit winter DIN:DIP ratios comparable to those found in French coastal waters, including under pristine conditions (i.e. close to 30 molN $molP^{-1}$).

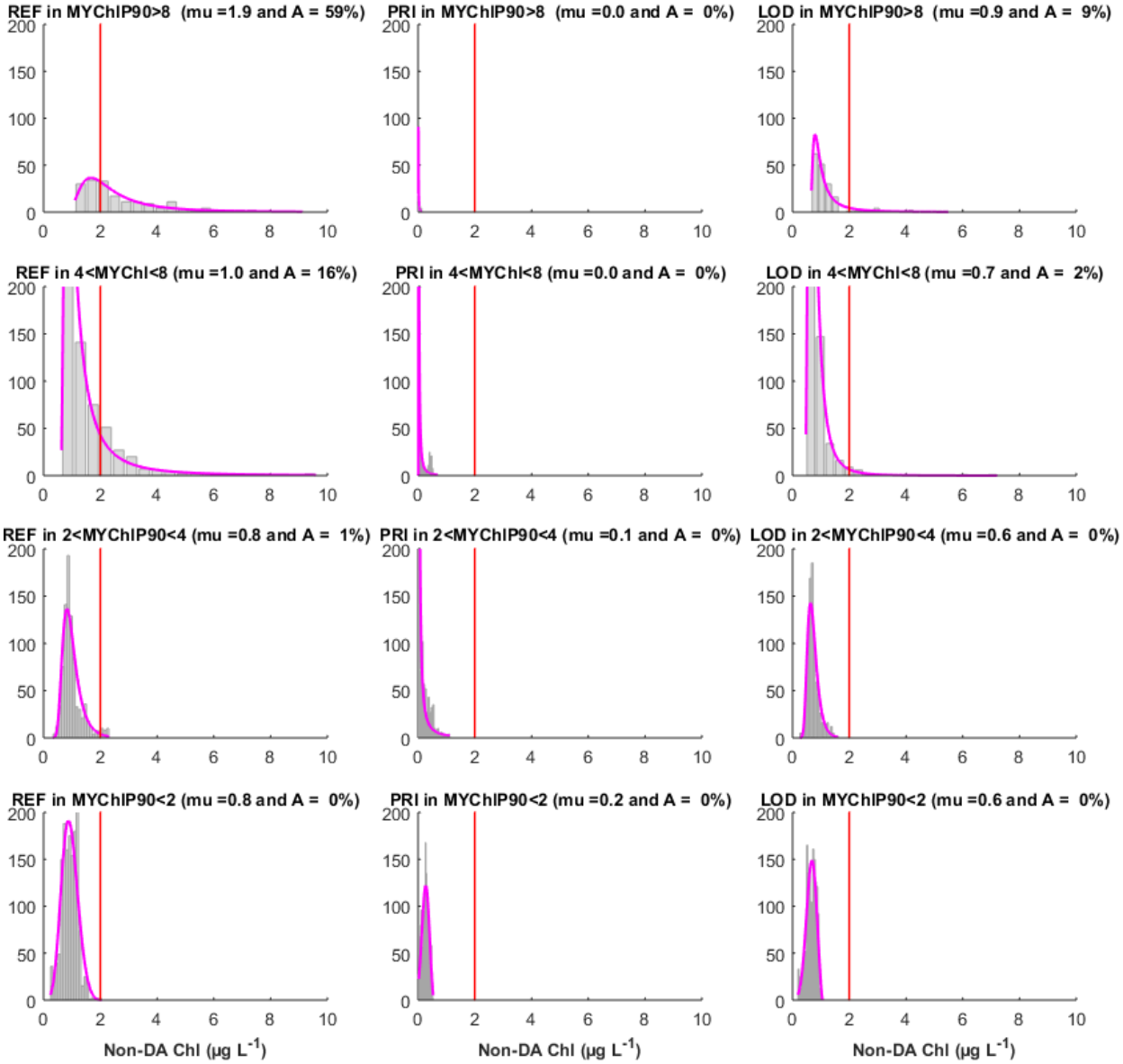

Figure 80: Probability distribution functions (pink curve) of mean NDAChl (Mar-Oct) in the four Ecozones across the SBNS and the English Channel (MIRO&CO domain) for the Reference situation (left column), the Pristine situation (middle column) and the LocOrgDem scenario (right column). The vertical red line indicates the reference level (2 µgChl L^{-1}), which corresponds to the reference value for colonial *Phaeocystis* chlorophyll a in the North Sea (i.e. it corresponds to an abundance of $4x10^6$ cells L^{-1}). The title of each graph indicates the central tendency of the PDF (mu) and the percentage of the Ecozone area (A) where the mean NDAChl (Mar-Oct) exceeds the reference value.

The indicator NDAChl is very instructive as it follows well the changes in nutrients imposed by the different scenarios (Figure 80). The reference value for this indicator, that was chosen on the basis of previous studies (see section 3.2.2.2), seems confirmed by the present study. The mean NDAChl (Mar-Oct) exceeds the reference level of 2 µgChl L^{-1} in 59% of the coastal areas (MIRO&CO domain) in the Reference situation while that area is reduced to 9% in the LocOrgDem scenario, and to 0% in the Pristine situation. The reduction of mean NDAChl in the SBNS is especially due to the suppression of colonial *Phaeocsytis* summer bloom and to the reduction in the duration of the bloom (see 3.1.2.7).

3.3 Suggestion for a novel indicator of eutrophication

On the basis of the results obtained above (PDFs), a tentative indicator is proposed for assessing the GEnS regarding chlorophyll *a* and potential nuisance phytoplankton species (e.g. haptophyte *Phaeocystis globosa* in NE-French, Belgian, Dutch and German coatal waters, and dinoflagellate *Karenia* along the Ushant front at the Channel entrance). The areas where Chl P90 exceeds the background value 8 µgChl L^{-1} (Figure 76) may be considered "potential" problem areas (PAs). In any such potential PA, the areas where NDAChl exceeds a reference value to be determined depending on the species (e.g. 2 µgChl L^{-1} for *Phaeocystis* colonies in the SBNS) may be considered as PA, with potential nuisance and/or toxicity depending on the species. The proposed assessment is summarized in Figure 81. The relevance of this indicator was tested on the SBNS and the English Channel with the results of MIRO&CO computed for the Reference and Pristine situations, and the UWTD and LocOrgDem scenarios (Figure 82).

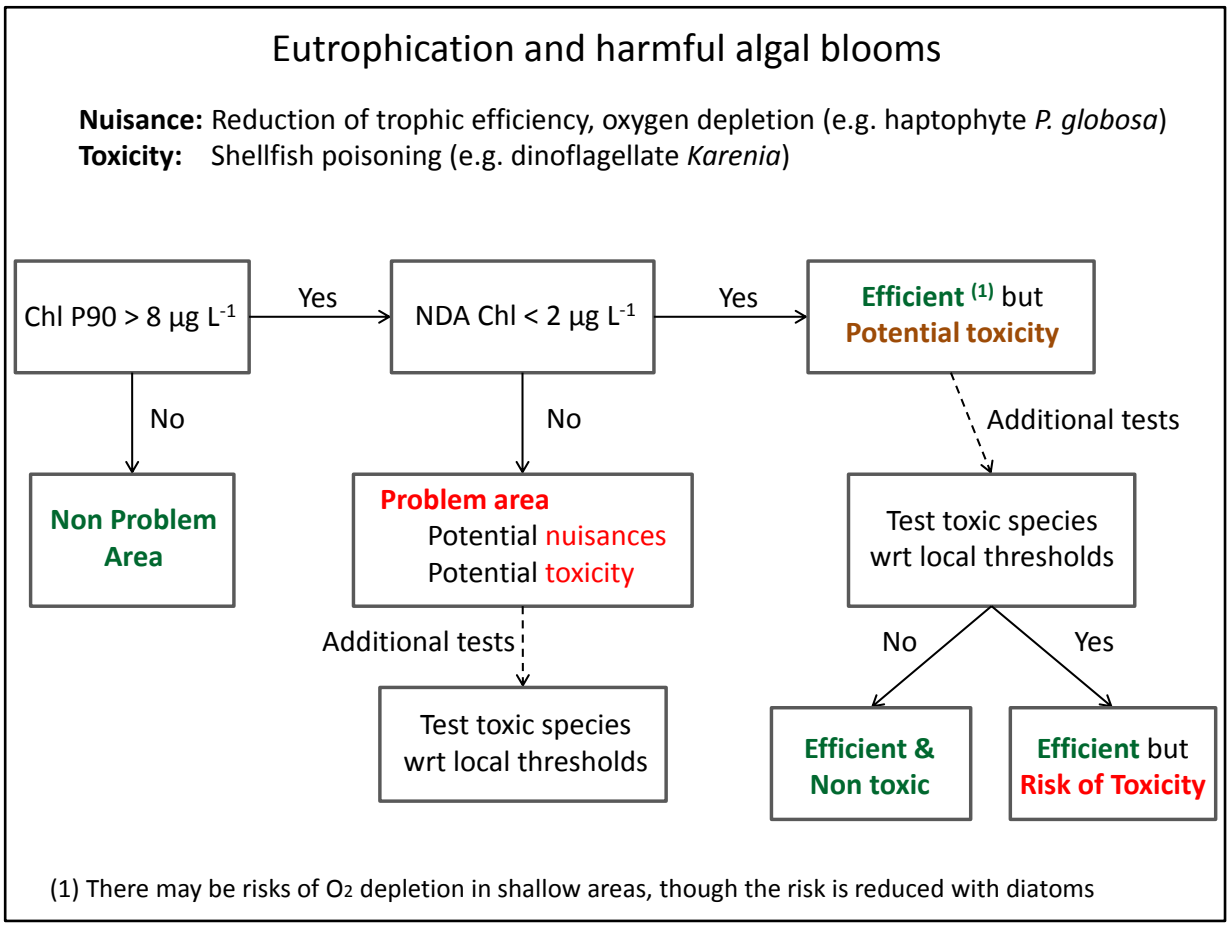

Figure 81: Summary of the undesirable-eutrophication assessment method proposed to estimate the PAs and non-PAs regarding phytoplankton species in the NEA waters. The NDAChl reference level of 2 µgChl L^{-1} is derived from previous studies on *Phaeocystis* colonies only (Rousseau et al. 2000, Daro et al. 2006, Lancelot et al. 2009). Other reference levels should be defined for the other undesirable species.

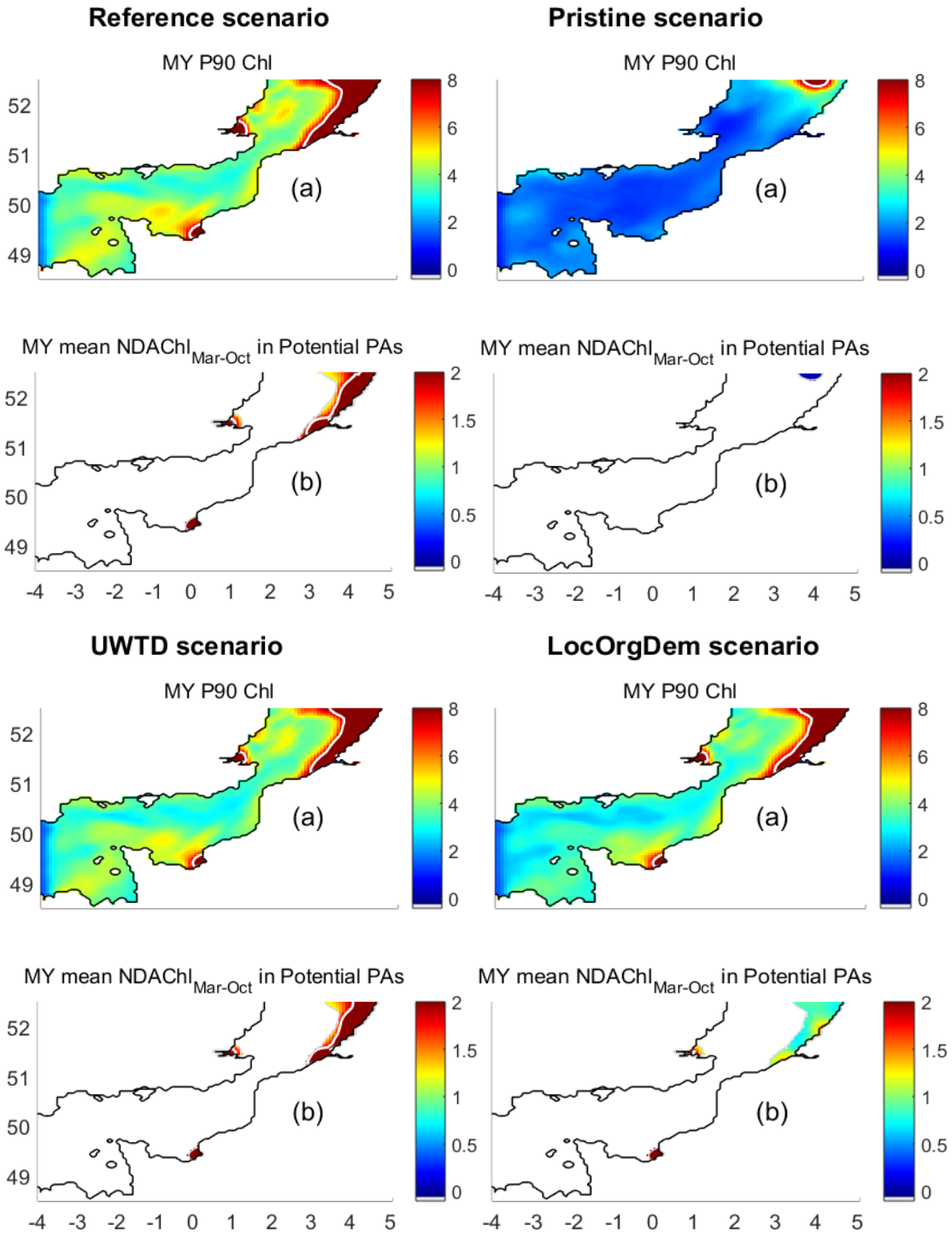

Figure 82: The multiyear (MY) average P90 of chlorophyll a (a) is shown with an isoline at reference value 8 µgChl L^{-1} for four scenarios. The area where chlorophyll a P90 exceeds this reference value may be considered as potential PA. In the potential PA, the Non-diatom chlorophyll a mean concentration (b) is shown with an isoline at reference value 2 µgChl L^{-1}, above which *Phaeocystis* colonies are considered undesirable.

Figure 82 shows that the Reference situation results in high Chl P90 and high NDAChl values, both well above their reference values in some coastal zones where nuisances are found. Therefore, these coastal zones may be seen as PAs. The Pristine situation exhibits no PA at all according to the criteria proposed above. The UWTD scenario shows similar results as the Reference situation, with some coastal zones having Chl P90 > 8 µgChl L^{-1} and the mean NDAChl (Mar-Oct) remaining the same as in the Reference situation. In the GAP scenario the area of Chl P90 > 8 µgChl L^{-1} remains as in Reference and UWTD scenarios, and the NDAChl decreases slightly (not shown). In the LocOrgDem scenario the area of Chl P90 > 8 µgChl L^{-1} remains similar as in the Reference situation but the mean NDAChl (Mar-Oct) decreases considerably. The P90 of NDAChl (not shown) does not decrease so much, however, in the LocOrgDem scenario compared to the Reference situation (mean coastal values of resp. 8.4 compared to 10 µgChl L^{-1}), whereas it is close to zero in the pristine situation. The weak decrease in NDAChl P90 between Reference and LocOrgDem is due to the fact that the proposed nutrient reductions do not reduce the spring maximum of *Phaeocystis* colonies (see section 3.1.2.7), but they suppress the summer bloom of *Phaeocystis* colonies and hence the duration of the bloom, which is reflected into the mean NDAChl.

3.4 Transboundary nutrients transport (TBNT) results

3.4.1 BIOPCOMS TBNT results

3.4.1.1 Lagrangian approach

MOHID Lagrangian approach was applied to study river discharges and their input contribution in Portuguese coastal waters. The Lagrangian simulations were carried out for the years 2010 (wet year) and 2011 (dry year). For each year, the ratio between the instantaneous volume coming from each river and the instantaneous coastal water volume in each box was calculated. This was used to analyze the influence of each river in the different coastal areas of the Portuguese coast. In this study, only the results of the boxes corresponding to the main west coast river discharges were analyzed: box 4 (Tagus river discharge); box 5 (Mondego river discharge); box 6 (Douro river discharge). The results of the Lagrangian simulations for 2010 and 2011 are presented in Figure 83 and Figure 84, respectively.

The results are analyzed in terms of water volume, providing information on the extension of each river plume along the coast. Regarding the river discharges, the Tagus is the most important river that flows into the west Portuguese coast, followed by the Douro and the Mondego. This appears clearly when observing the results in the boxes at the outlet of the rivers, both in wet and dry meteorological conditions. The major difference between years is the percentage of river water volume in each box. Notice that the scale for the year 2010 goes up to 40% (Figure 83) while in 2011 it is close to 15% (Figure 84).

As the Tagus River discharges in box 4, Mondego in box 5 and Douro in box 6, the volume of water from these rivers in their associated boxes is higher, a fact that is confirmed when higher river flows are registered. Although this is clear in both years the impact of each river flow along the Portuguese west coast is more evident during wet year (Figure 87 and Figure 88).

Coastal currents in the Portuguese west coast are highly dependent on the wind regime. Winds from the southern quarters are frequent during autumn, winter and sometimes beginning of spring and most of the times related to storms and raining periods. Spring, summer and sometimes beginning of autumn are dominated by northern winds. This wind regime induces a northward coastal current during winter on the Portuguese west coast and a southward current during the summer.

During the winter regime, river plumes are transported – due to the prevailing winds – northward (Figure 85). Figure 83 shows this effect, where northward winds pushes the Tagus water to Box 6 (near the Douro river) and its water represents up to 20 % of the water in that box. In summary, in winter, the water discharged by the southern rivers is transported north and the inverse occurs during summer (Figure 86) were northern waters can reach the southern part of the west coast of Portugal.

With regard to the nitrate concentration, each river has a different area of influence, but over time the influence of the rivers on marine nitrate concentrations is diminished due to the mixture with ocean waters, clearly seen in the nitrate concentration results in Figure 85 and Figure 86 where the blue dots represent ocean nitrate concentrations.

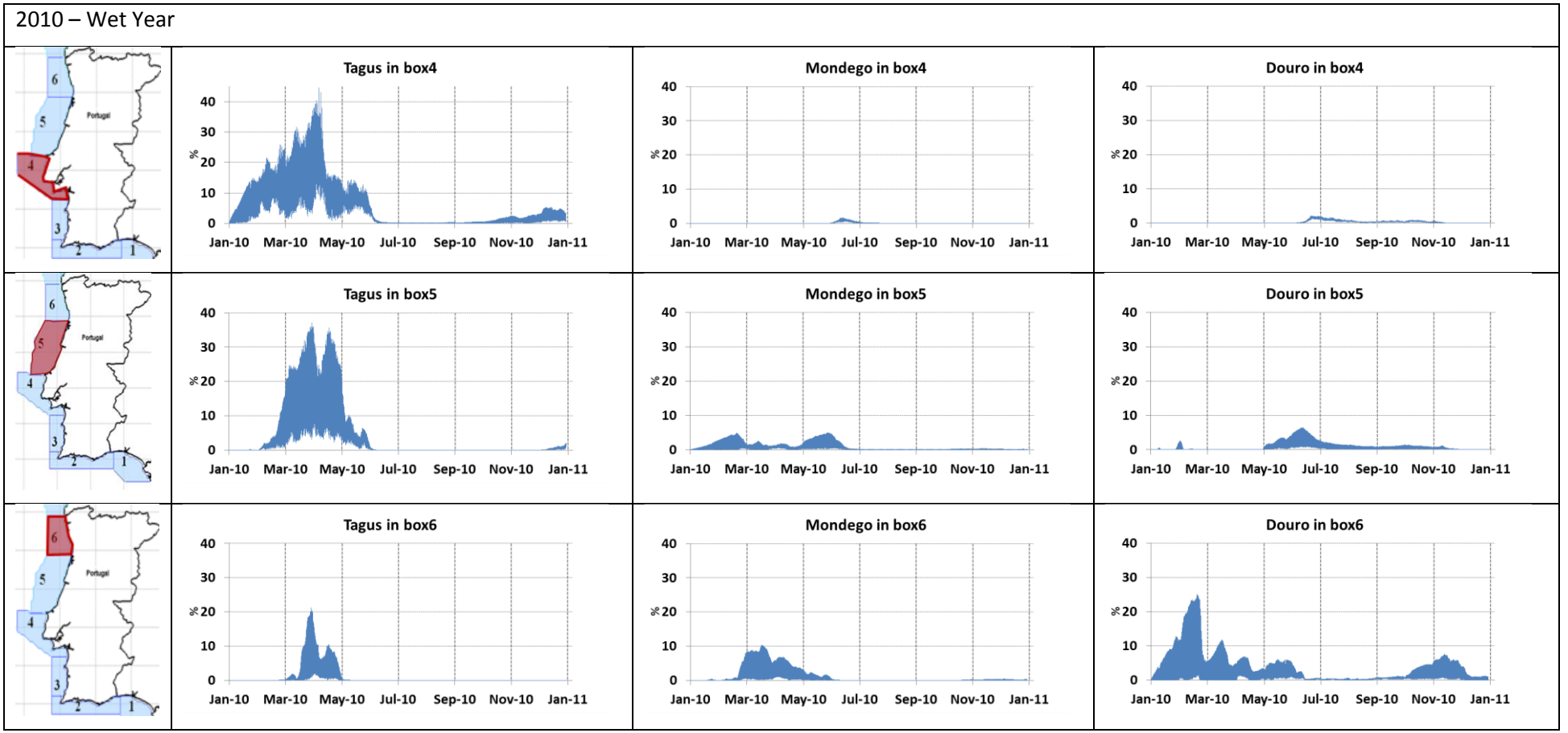

Figure 83 - Ratio between the instantaneous volume coming from each river and the instantaneous water volume in each box for the wet year (2010).

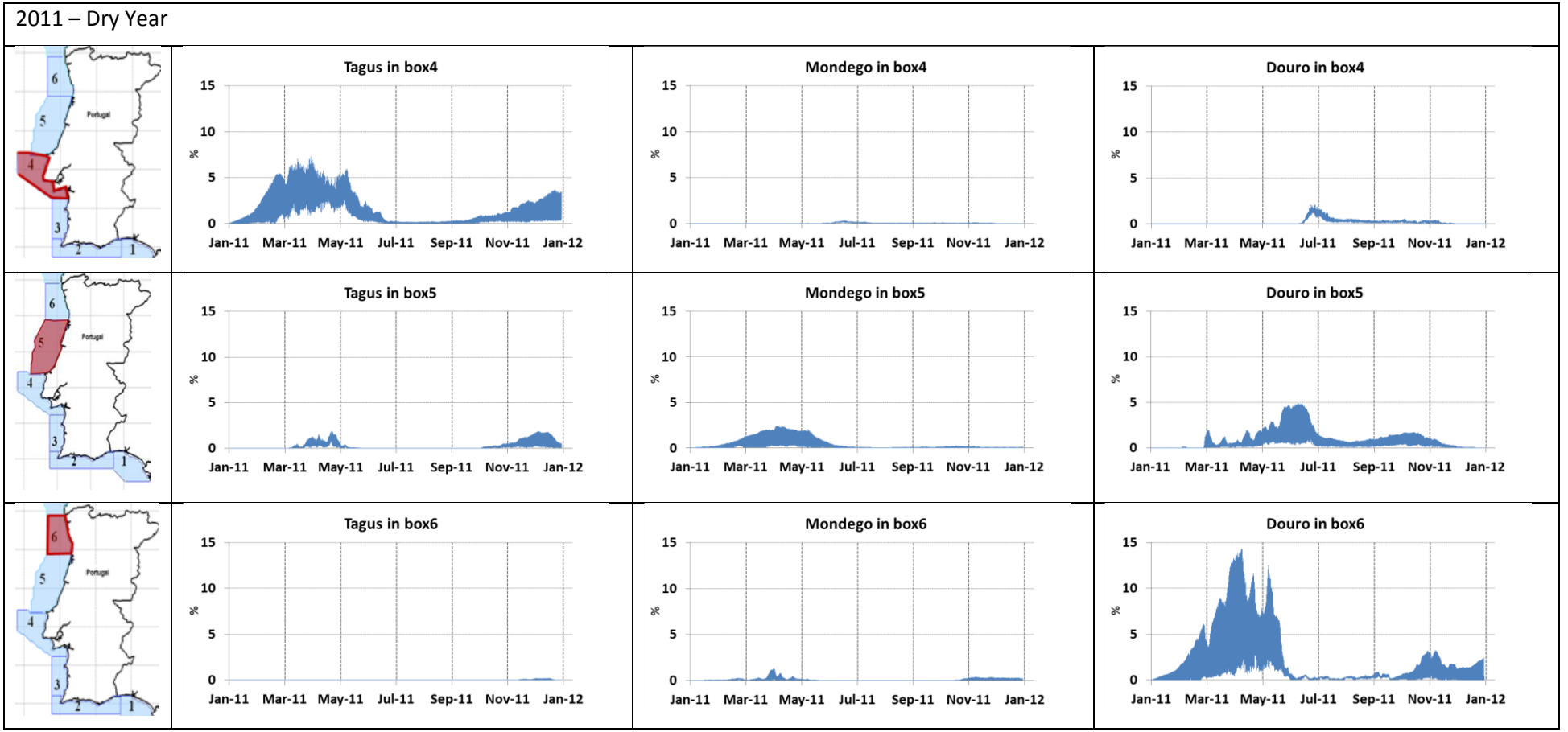

Figure 84- Ratio between the instantaneous volume coming from each river and the instantaneous water volume in each box for the dry year (2011).

30 March 2010 – Wet Year

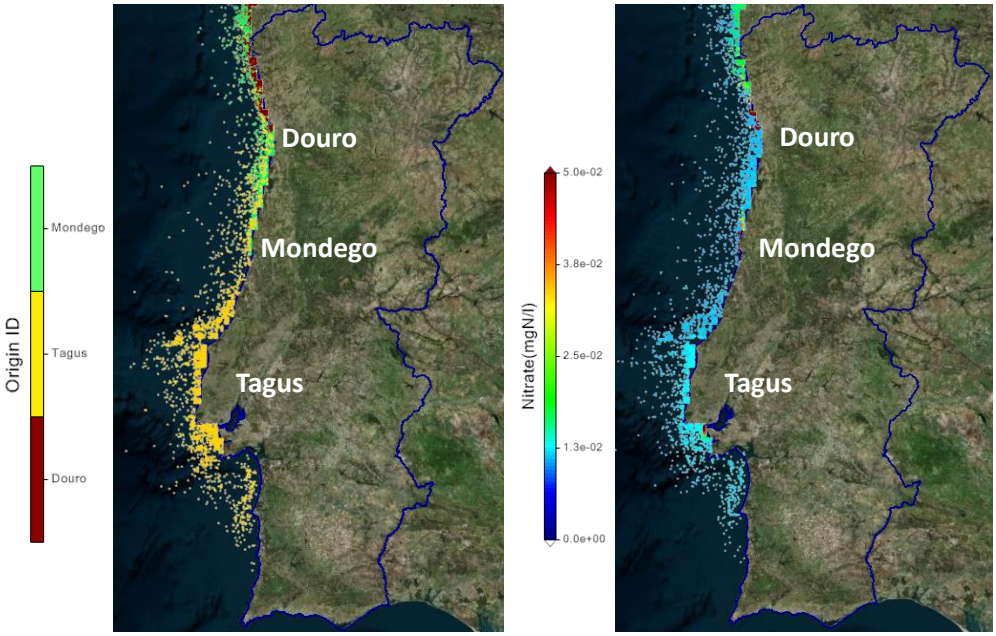

Figure 85: Image from the left shows the dispersion of Tagus (yellow), Mondego (green) and Douro (brown) rivers along the Portuguese Coast on March 30 (winter regime) on a wet year. On the right, the riverine nitrate concentration.

1 July 2010 – Wet Year

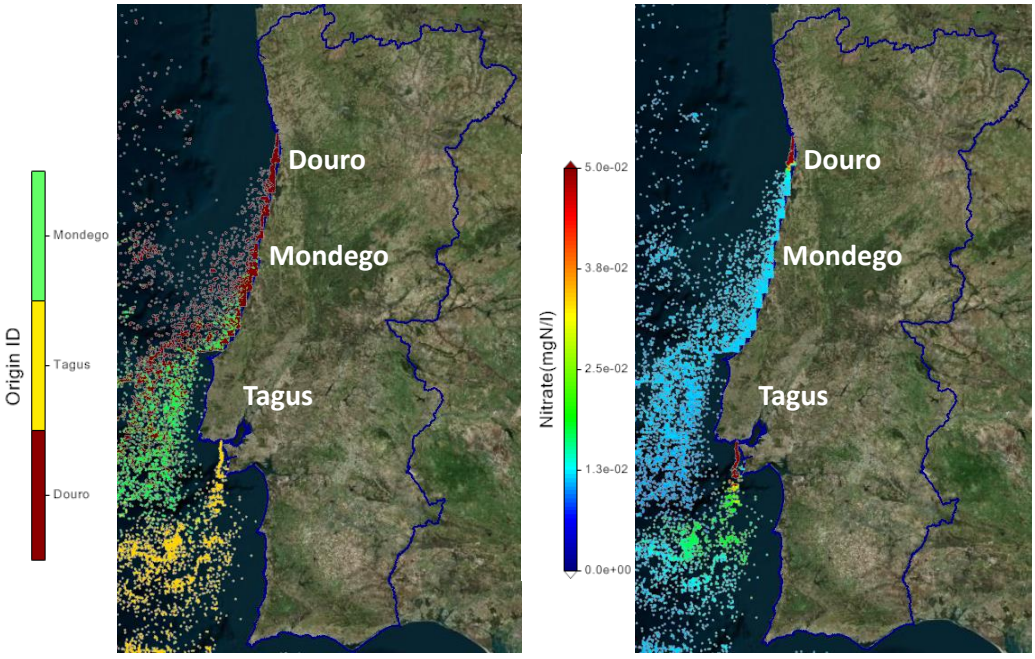

Figure 86: Image from the left shows the dispersion of Tagus (yellow), Mondego (green) and Douro (brown) rivers along the Portuguese Coast on the 1st of July (summer regime) on a wet year. On the right, the riverine nitrate concentration.

3.4.1.2 BIOPCOMS – Fluxes of nutrients and phytoplankton

Reference situation for the period of Jan-Feb – Wet Year	
Surface horizontal fluxes	Vertical fluxes
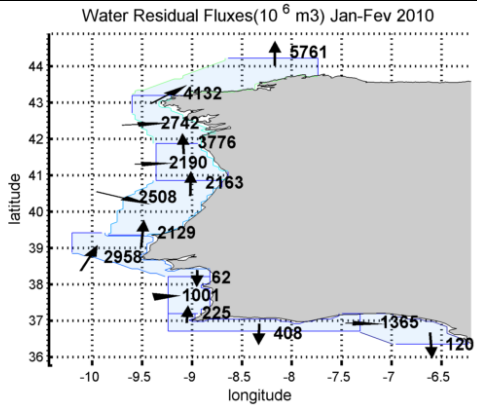	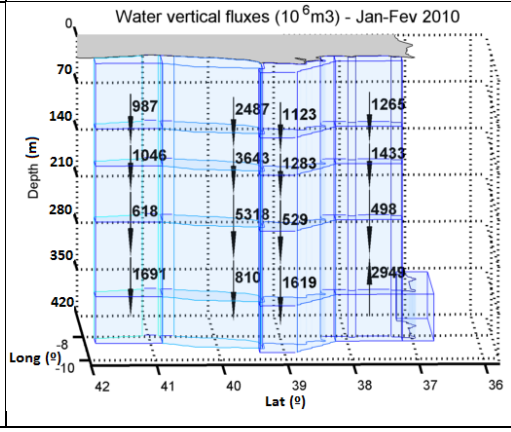
Jan-Feb – Dry Year	
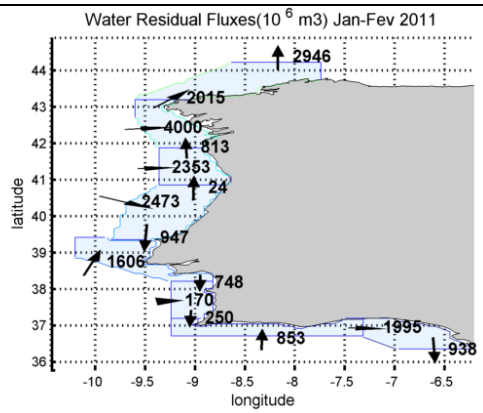	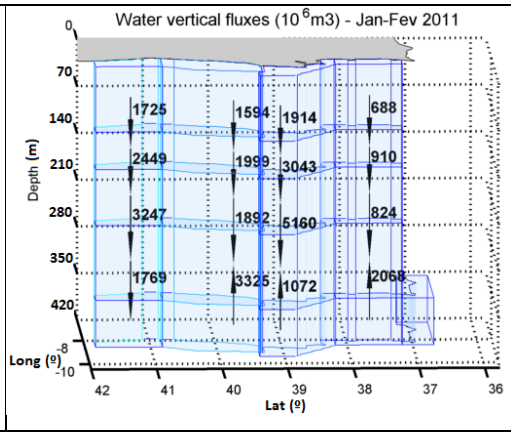
Mar-Oct – Wet Year	
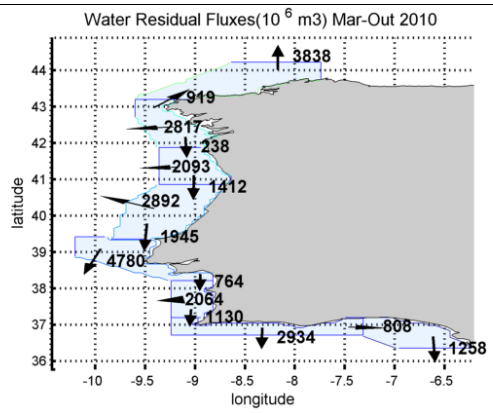	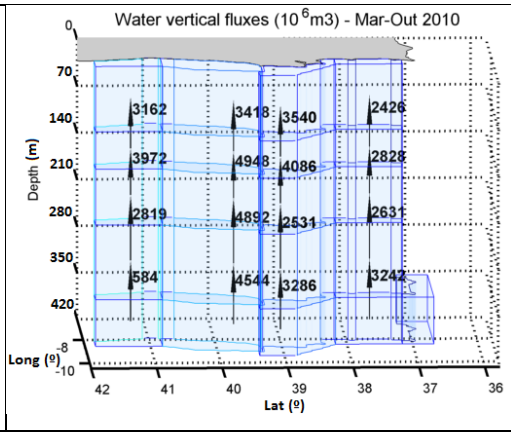

Mar-Oct – Dry Year

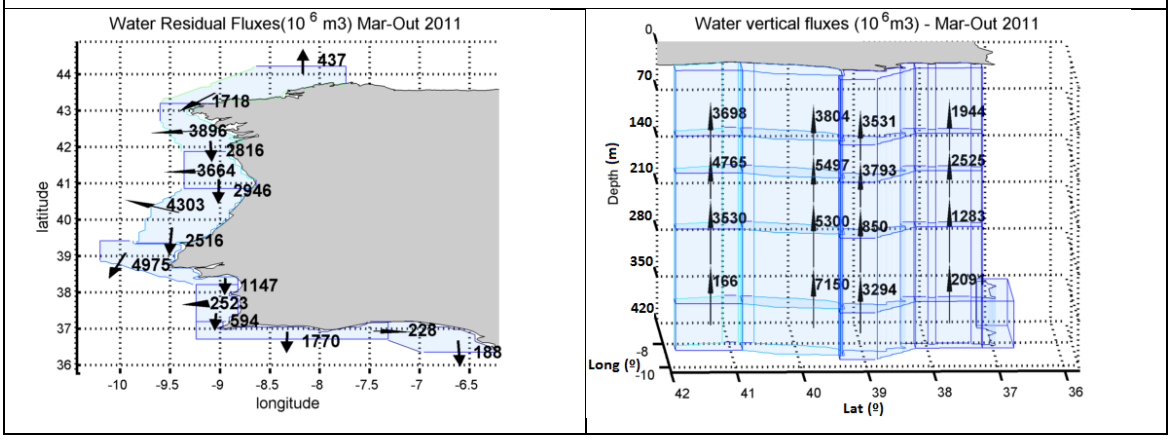

Figure 87: Horizontal water fluxes at the surface (9m), and vertical water fluxes, for the periods of Jan-Feb and Mar-Oct 2010 and 2011.

Horizontal fluxes along the Portuguese coast are often associated with the prevailing wind conditions along the year. Figure 87 shows the fluxes results for the 8 surface boxes and the vertical boxes corresponding to surface Boxes 3 to 6 where the influence from the main west coast Portuguese rivers can be observed.

During the January-February period of both years the surface and vertical water fluxes indicate downwelling which is typical for this time of the year, when south eastern and western wind prevail and are responsible for storms and rain events. This northward winds together with the Coriolis force turn the water towards land where it sinks, leading to downwelling conditions.

During the period March-October, the west Portuguese coast is characterized by prevailing southward winds inducing upwelling events, which results from the upward transport of bottom waters that are cold and rich in nutrient. Between the wet year and the dry year, the main observed difference is the higher intensity of the southward fluxes during the dry year, corresponding probably to more persistent and intense southward winds.

Nitrate fluxes integrated over the period of Jan-Feb – Wet Year	
Pristine situation	
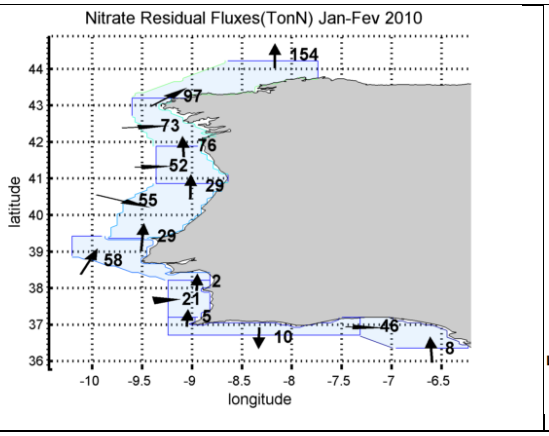	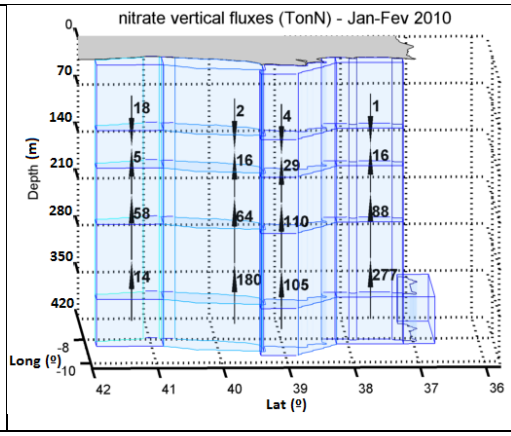
Reference situation	
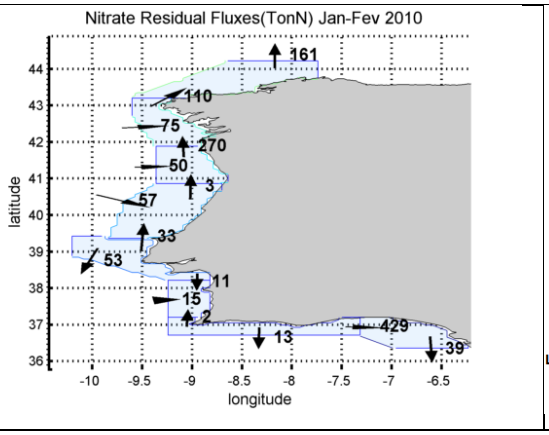	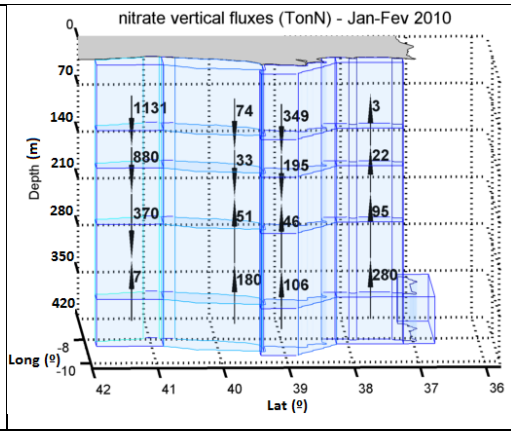
UWTD Scenario	
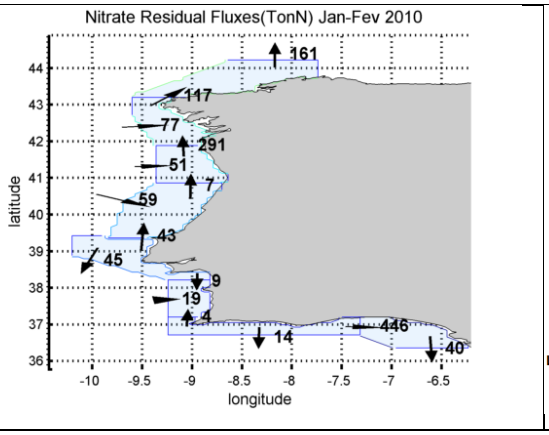	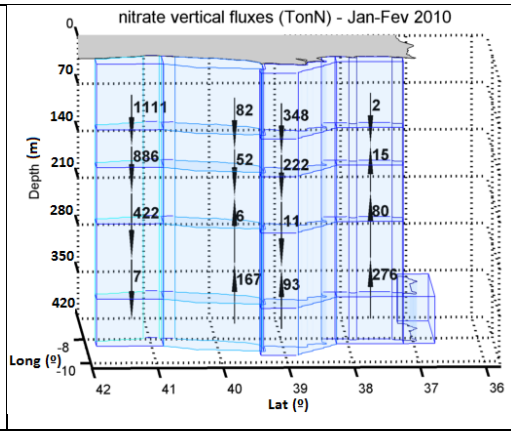

LocOrgDem Scenario

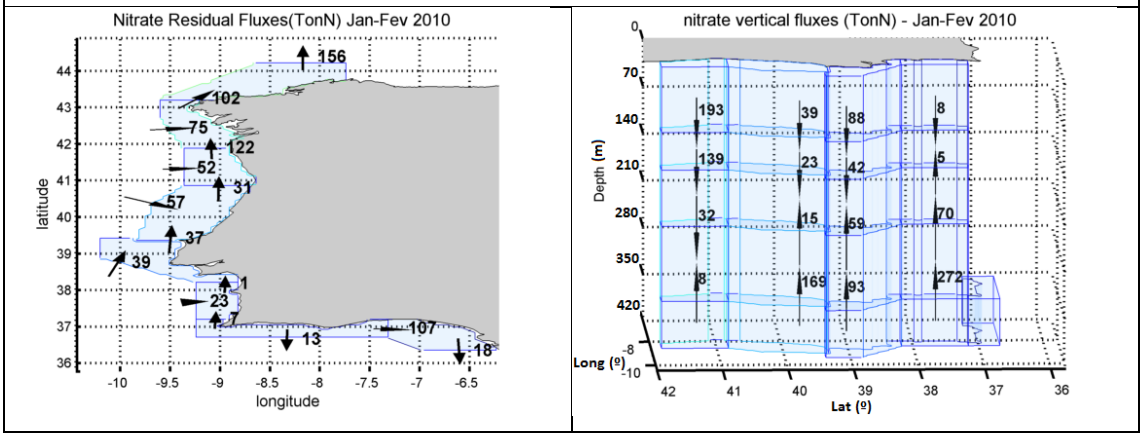

Figure 88: Surface horizontal nitrate fluxes and nitrate vertical fluxes integrated over the êriod fromJanuary to February of the Wet Year (2010).

Phosphate fluxes integrated over the period of Jan-Feb – Wet Year

Pristine situation

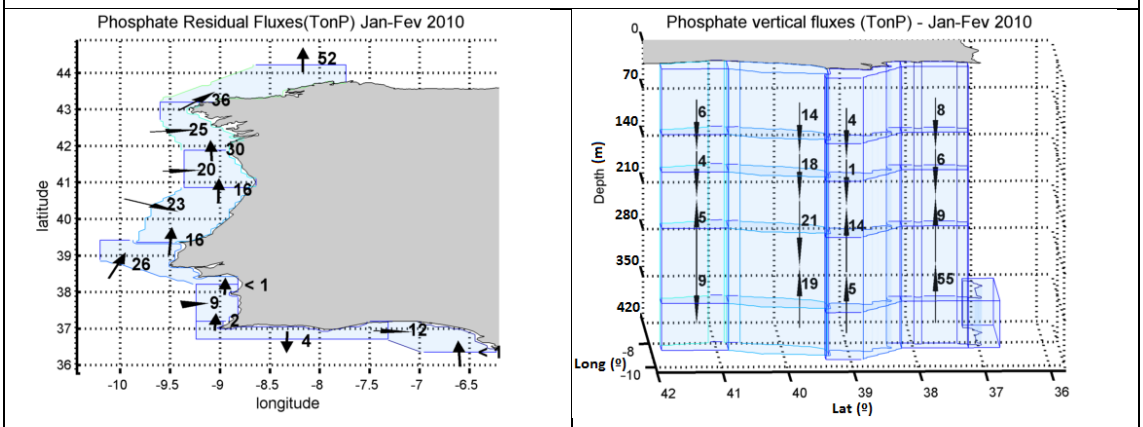

Reference situation

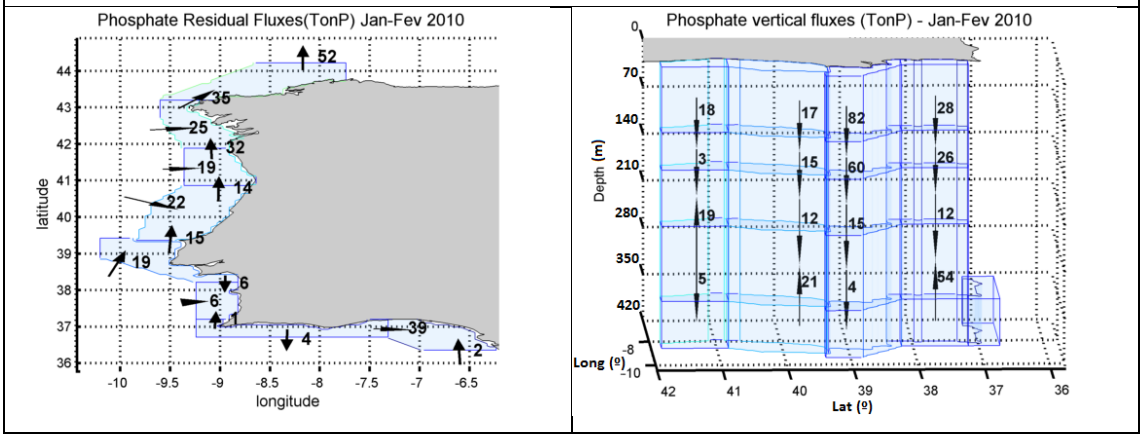

UWTD Scenario

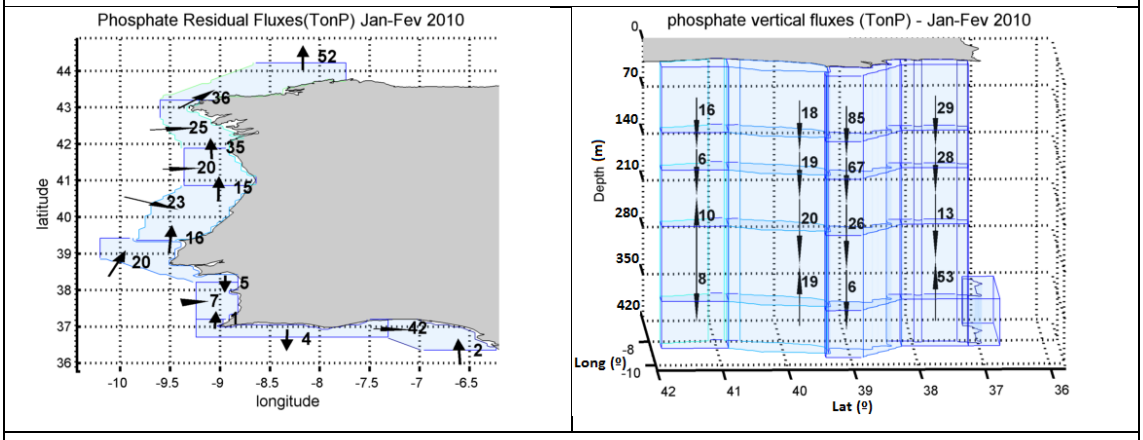

LocOrgDem Scenario

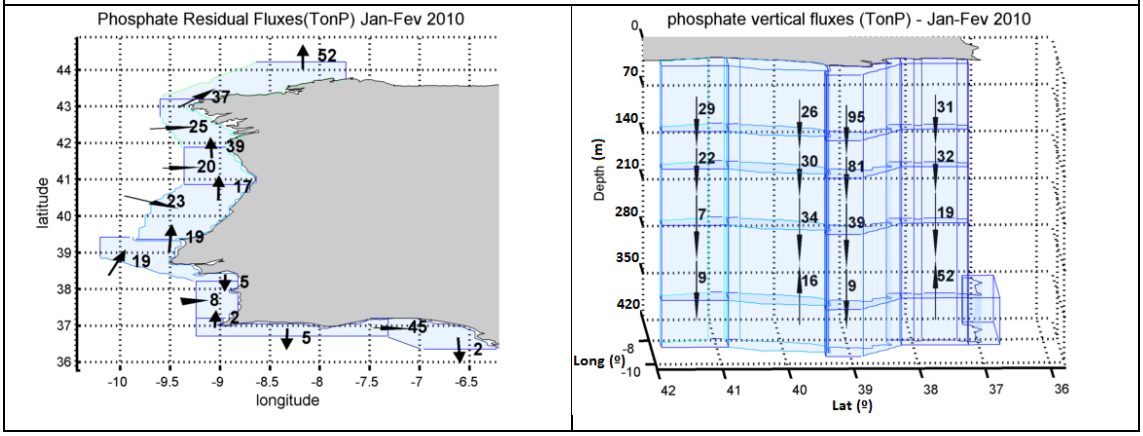

Figure 89: Surface horizontal phosphate fluxes and phosphate vertical fluxes integrated over the êriod fromJanuary to February of the Wet Year (2010).

Nutrient fluxes along the Portuguese coast are influenced by wind inducing downwelling or upwelling and river discharges. Therefore, during the periods of higher river flows (autumn and winter) the nutrient fluxes are expected to increase northward, following the coastal surface currents, due to prevailing northward winds. This effect is shown in both Figure 88 and Figure 89, for nitrate and phosphate fluxes respectively.

The results show a strong difference between the Pristine and the Reference situations for both nutrients especially for nitrate. Considering the two first box layers where the Tagus and Douro discharged, this discrepancy is maximum 4 to 349 tons N in the Tagus region and 18 to 1131 tons N in the Douro region. These winter nutrients are downwelled due to wind conditions and the reduced primary consumption in this time of the year.

For the nutrient reduction scenarios (UWTD and LocOrgDem), there are no visible differences when looking at surface fluxes. If we look at the the vertical profiles and in particular for the top layer, the major difference in nutrient concentrations are found for nitrate in the LocOrgDem scenario. The major

inland source for nitrates is agriculture, and these results indicate that only a profound change in agriculture practices is able to reduce the fluxes of nitrates into coastal waters.

In comparison to the wet year, the results for the dry year show that nitrate and phosphate fluxes along the coast and the vertical fluxes associated with the river discharges are significantly reduced – by one and in some cases two orders of magnitude (Figure 89 and Figure 90) – due to smaller river nutrient load.

With regard to the reduction scenarios and for both nutrients, the reduction of the nutrient load in the dry year had a smaller impact on nutrient fluxes compared to the wet year, as the total amount of nutrients being discharged to the ocean was considerably smaller.

Nitrate fluxes integrated over the period of Jan-Feb – Dry Year	
Pristine situation	
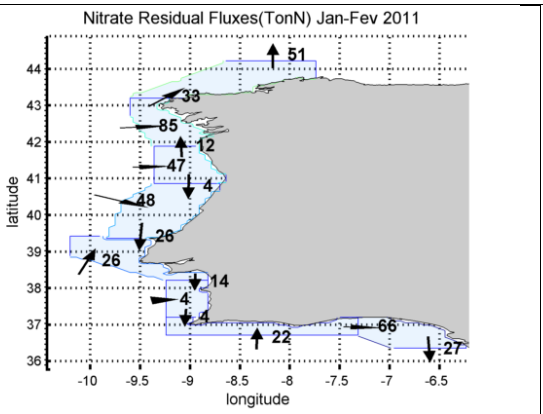	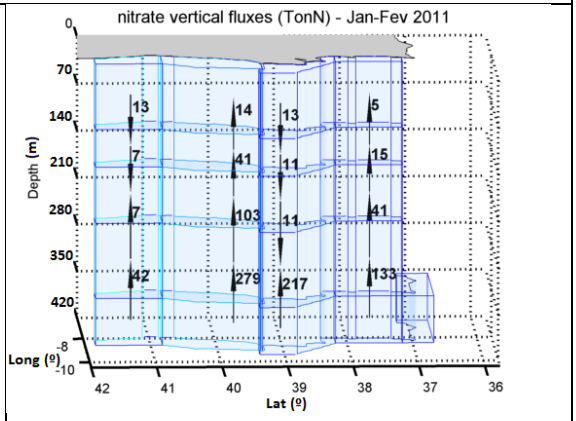
Reference situation	
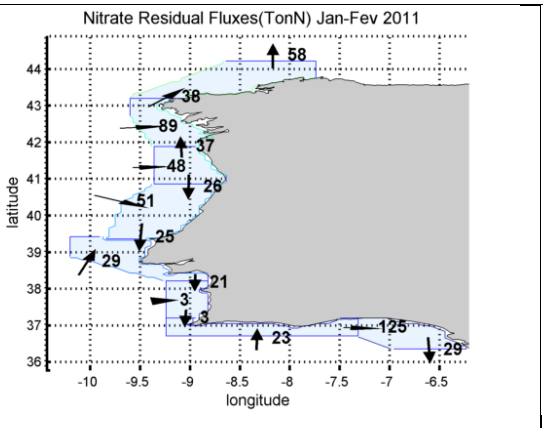	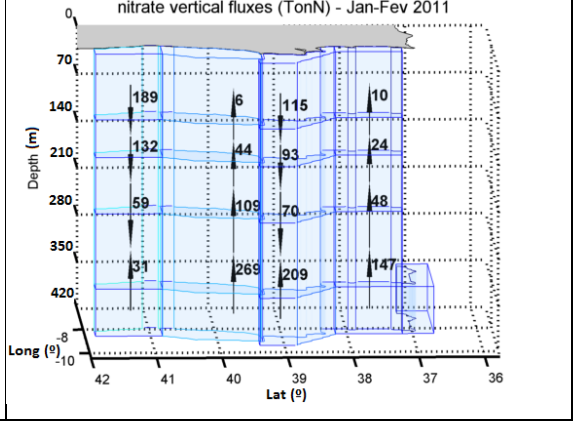

UWTD Scenario

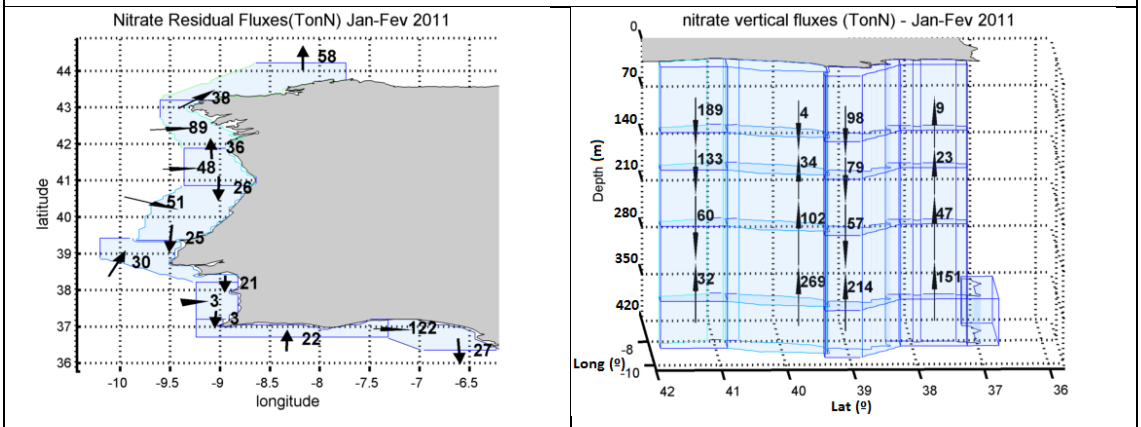

LoCorgDem Scenario

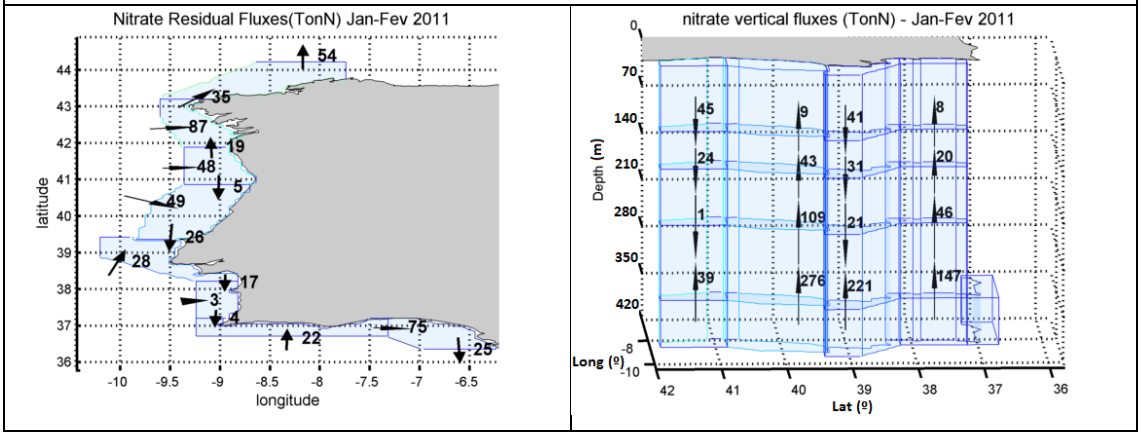

Figure 90: Surface horizontal nitrate fluxes and nitrate vertical fluxes integrated over the period from January to February of the Dry Year (2011).

Phosphate fluxes integrated over the period of Jan-Feb – Dry Year

Pristine situation

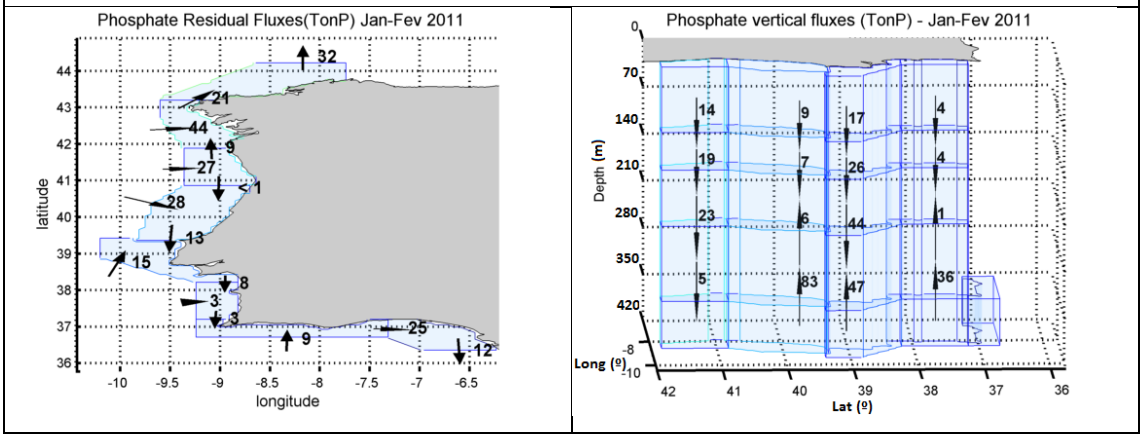

Reference situation

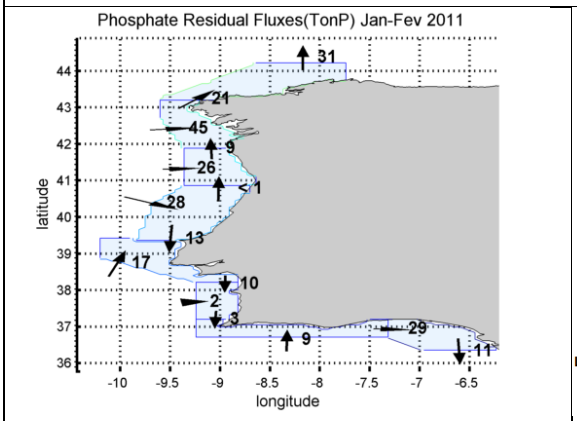

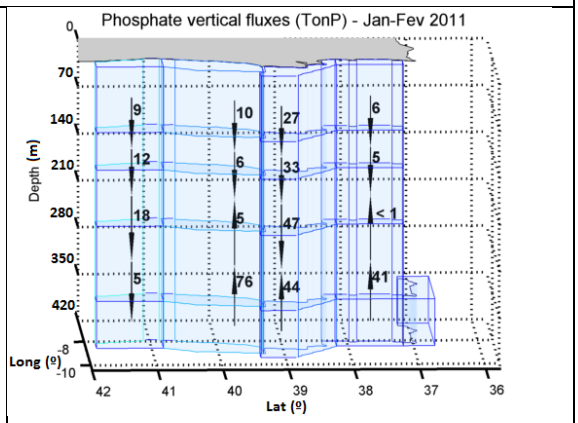

UWTD Scenario

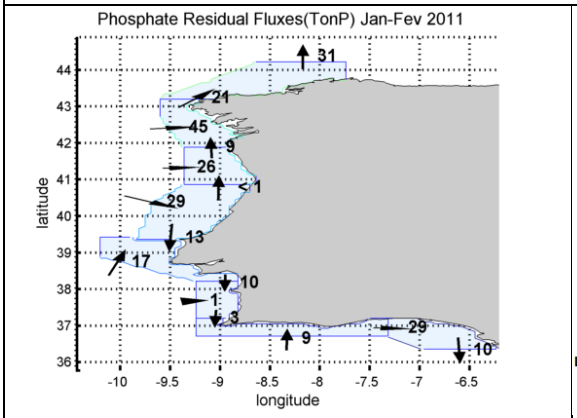

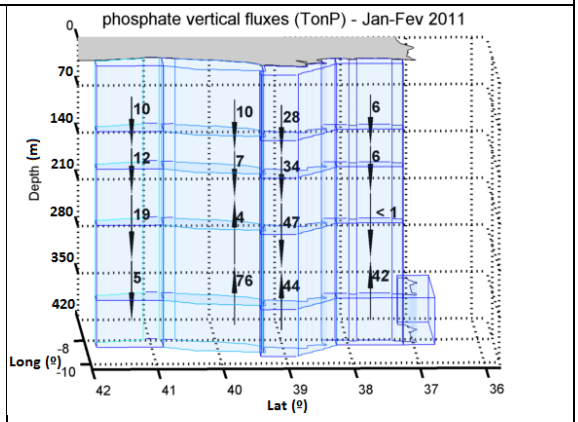

LocOrgDem Scenario

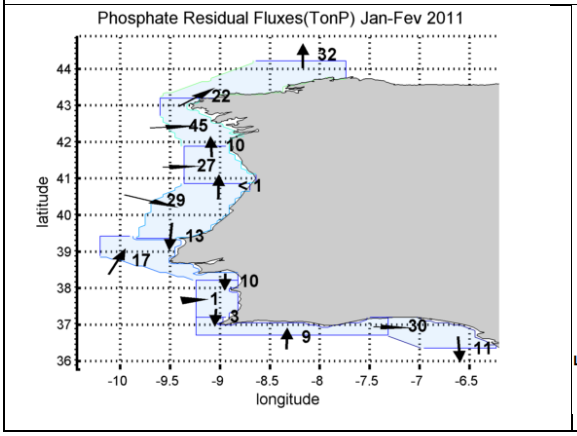

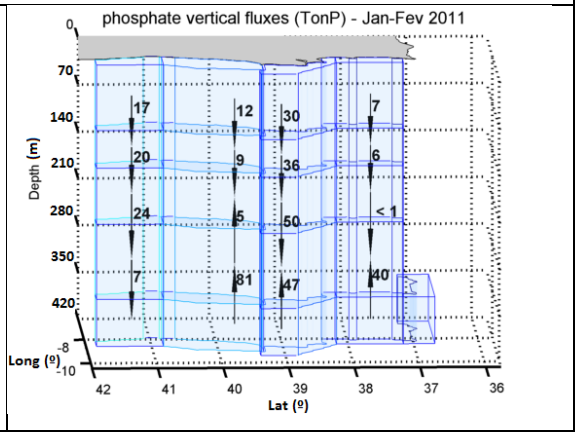

Figure 91: Surface horizontal phosphate fluxes and phosphate vertical fluxes integrated over the period from January to February of the Dry Year (2011).

Figure 92 and Figure 93 show the results for the four analyzed scenarios, for the wet and dry years, respectively, corresponding to phytoplankton fluxes integrated for the period March-October. As referred previously during spring and mostly during summer, the winds prevail from northward inducing a southward current that is overt in the surface maps where fluxes are southward near the coast.

For the Pristine situation and for the wet year, phytoplankton fluxes show a positive correlation with the vertical water fluxes presented in Figure 87. However, for other scenarios and years the phytoplankton vertical fluxes show a strong negative correlation in terms of flux direction. The water flows upward as expected for an upwelling event, but the phytoplankton is carried down into the bottom layers. This is related to the considerable increase of nutrient river loads (Figure 88, Figure 89) from the pristine to the reference situation and consequent phytoplankton production which is then transported down due to its settling velocity. The LocOrgDem scenario approaches the pristine conditions with an inversion of some of the vertical fluxes from downward in the reference and UWTD scenario to upward in this scenario.

Phytoplankton fluxes integrated over the period of Mar-Oct – Wet Year	
Pristine situation	
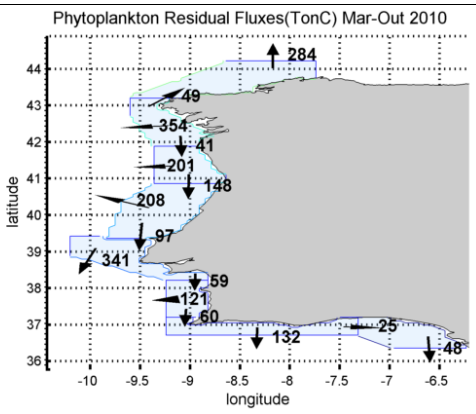	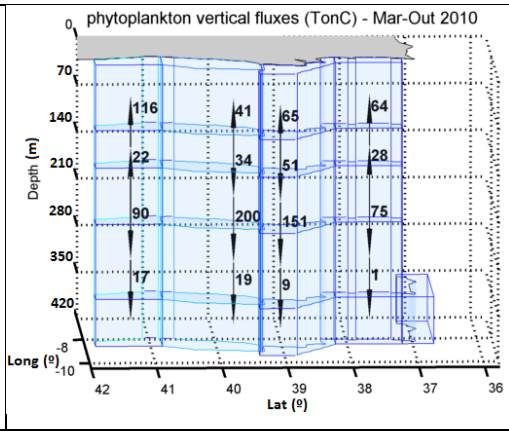
Reference situation	
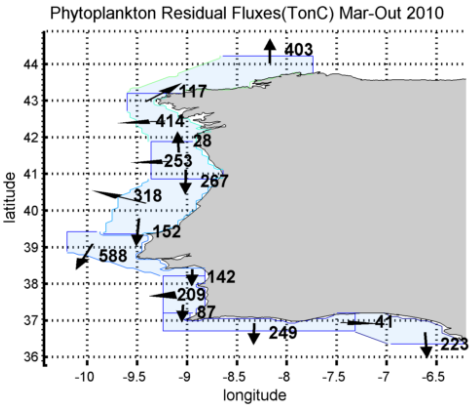	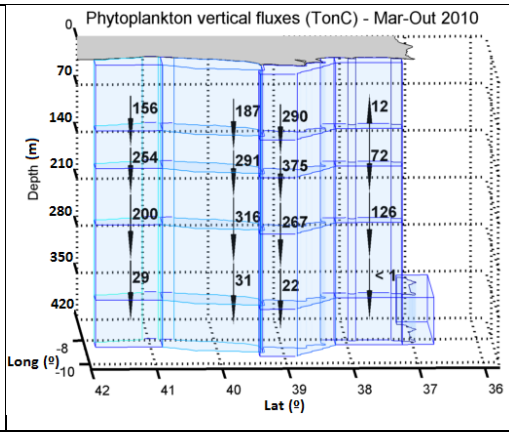

UWTD Scenario

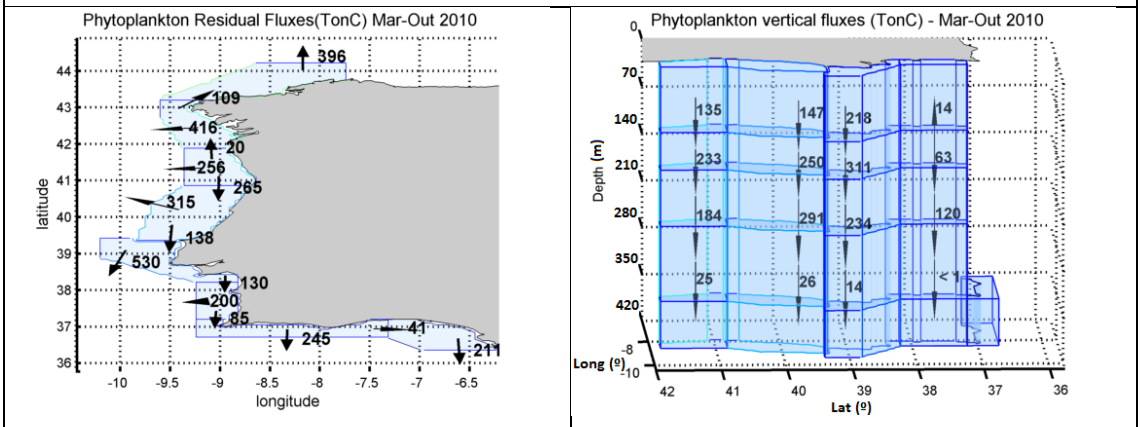

LocOrgDem Scenario

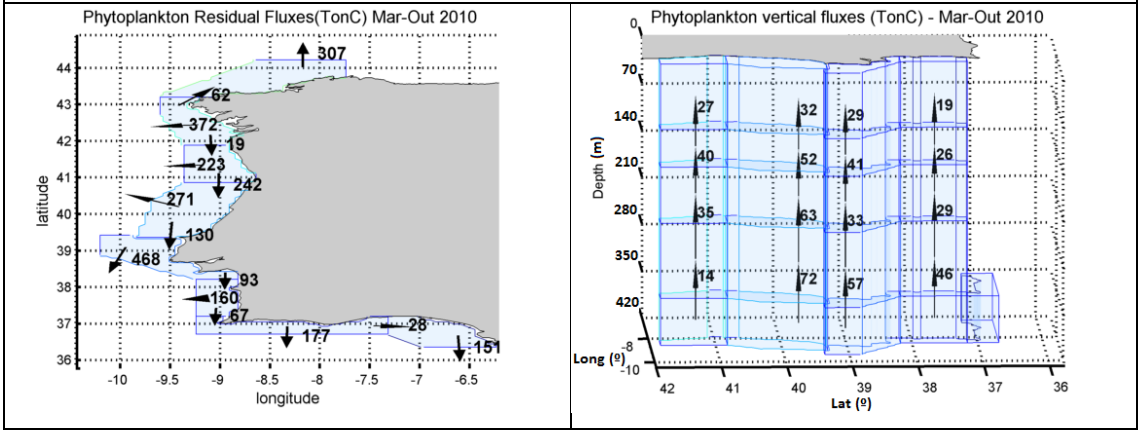

Figure 92: Surface horizontal phytoplankton fluxes and phytoplankton vertical fluxes integrated over the period from March to October of the Wet Year (2010).

Phytoplankton fluxes integrated over the period of Mar-Oct – Dry Year

Pristine situation

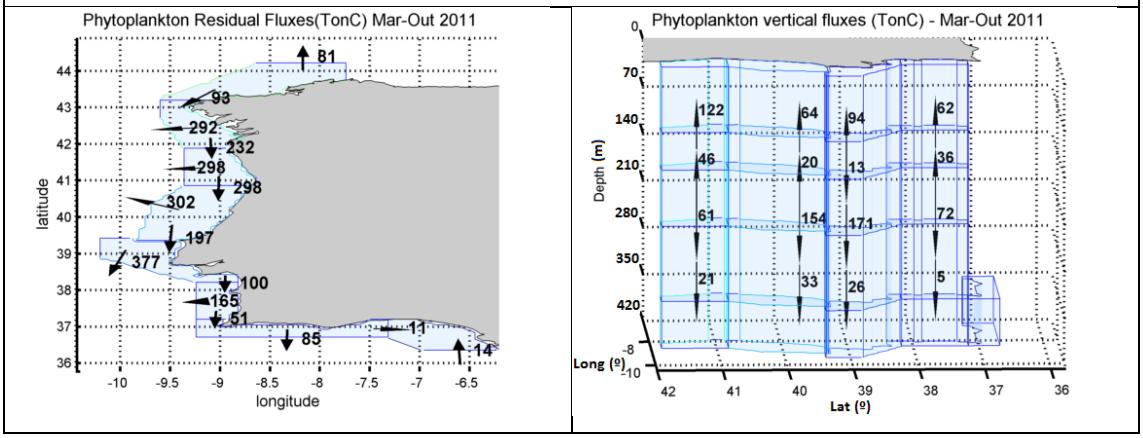

Reference situation

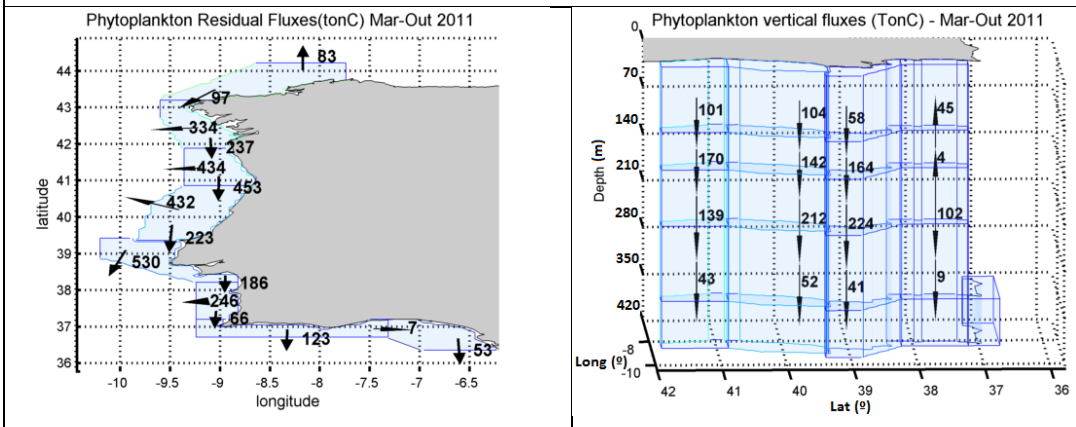

UWTD Scenario

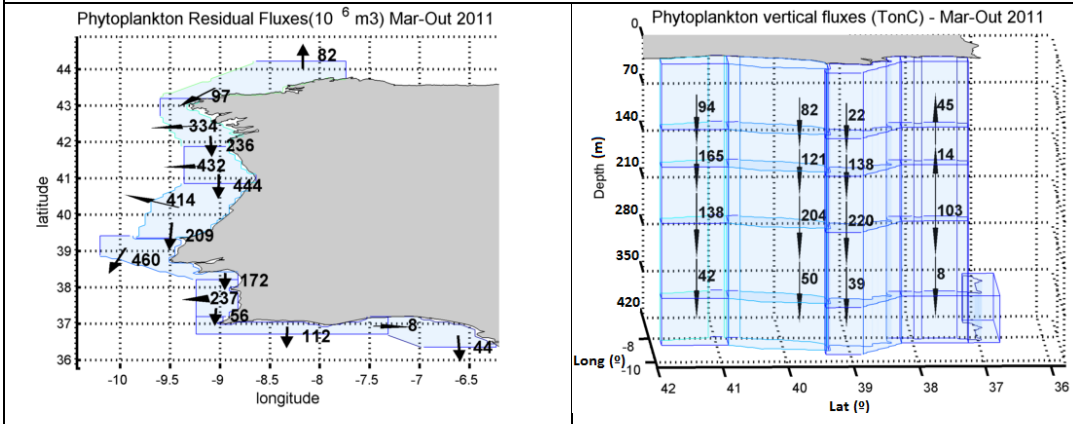

LocOrgDem Scenario

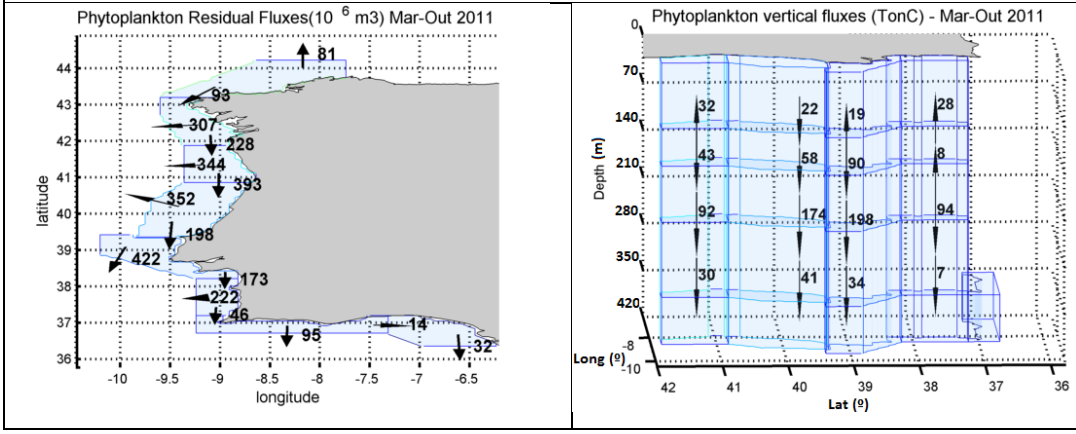

Figure 93: Surface horizontal phytoplankton fluxes and phytoplankton vertical fluxes integrated over the period from March to October of the Dry Year (2011).

3.4.2 ECO-MARS3D TBNT results

The ECO-MARS3D model gives the fraction of nitrogen (resp. phosphorus) in any biological nitrogenous (resp. phosphorous) compartment. As the total chlorophyll is a common metric for assessing the eutrophication level, we have pooled the results obtained on the four phytoplanktonic state variables of the model (diatoms, dinoflagellates, nanoflagellates and *Phaeocystis*), and we have computed the ratio of the 2000-2010 "growing season" mean of tagged phytoplankton over the 2000-2010 "growing season" mean of total phytoplankton. This produces a unique, global map of the decadal mean contribution of each source of nutrient in the marine phytoplankton biomass. The Figure 94 shows that the contribution of oceanic fluxes entering the boundaries remain dominant, except along the coast between the Seine and Rhine estuaries, where the big rivers Seine, Scheldt and Rhine maintain a strong river influence. But the atmospheric deposits seem to exert a 10 to 20% influence all over the continental shelf.

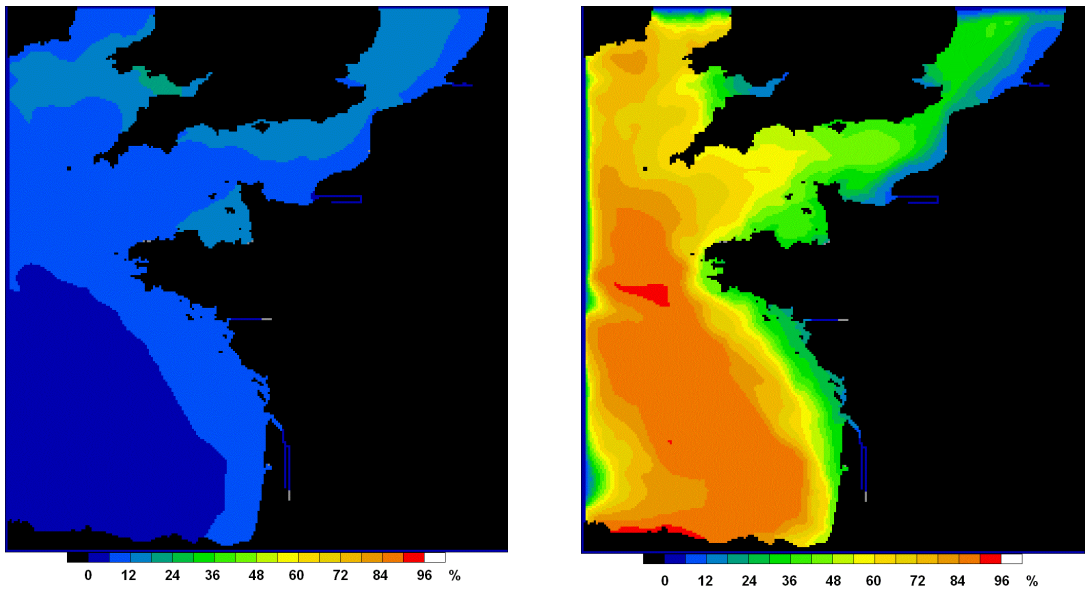

Figure 94: Relative contribution (%) of atmospheric nitrogen deposits (left) and oceanic DIN (right) to the nitrogen content of the surface marine phytoplankton, averaged on the 2000-2010 "growing season" period.

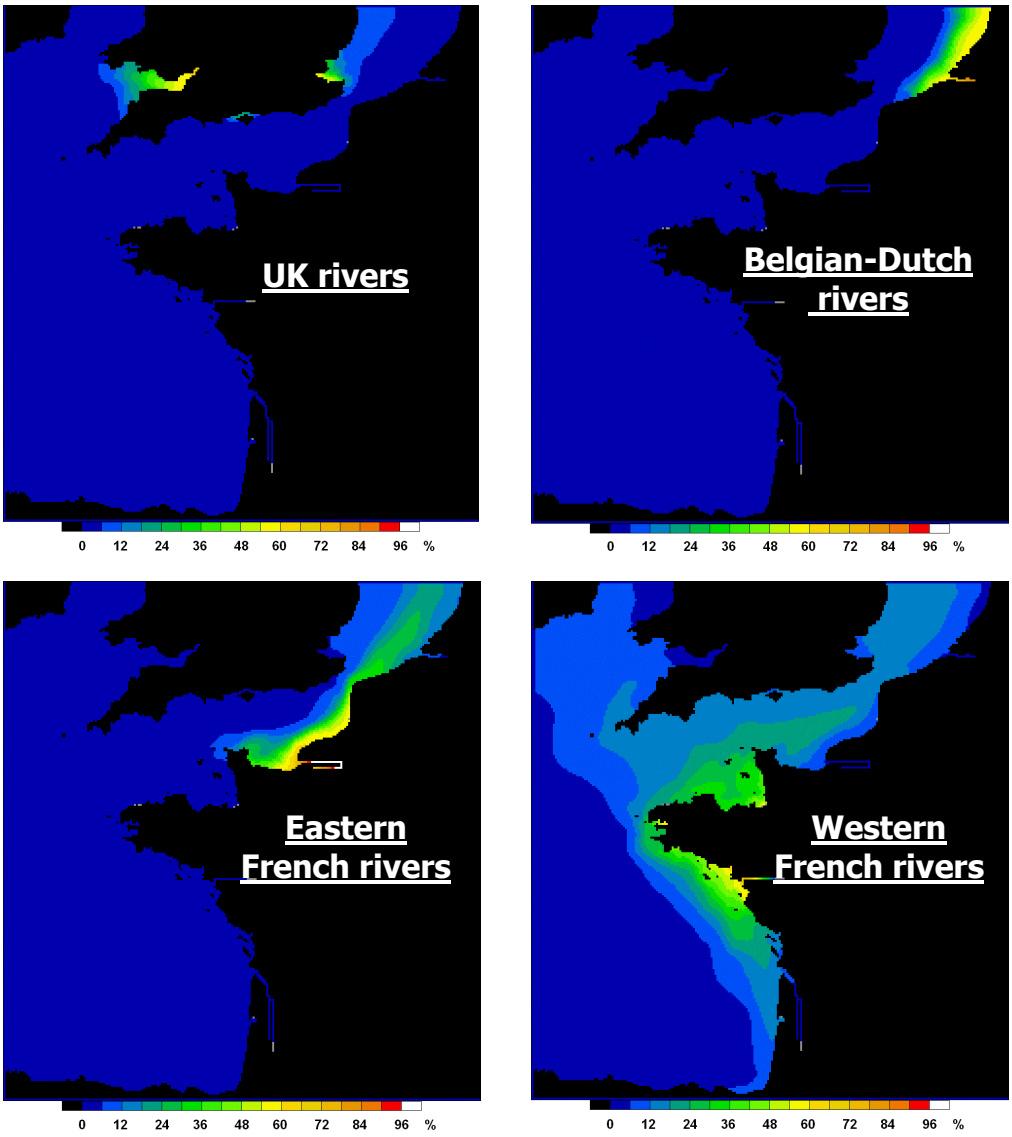

Figure 95: Relative contribution (%) of four groups of rivers to the nitrogen content of the surface marine phytoplankton, averaged on the 2000-2010 period. Upper-left: English rivers, upper right: Belgian-Dutch rivers, bottom-left: East-French rivers and bottom-right: West-French rivers.

The Figure 95 shows that the nitrogenous contributions of the UK, as well as the Belgian-Dutch rivers are confined in the northern part of the domain, *i.e.* the southern North Sea and the Bristol Channel; UK contribution appears to be particularly limited to a short range. The group of Eastern French rivers, mainly driven by the Seine river, provides a high proportion of the phytoplankton requirements in the southern half of the Eastern English Channel, and continues to account for 25% in the middle part of the Southern Bight of the North Sea. The group of Western French rivers, mainly driven by the Loire river, exerts a long range influence: it spreads over a large part of the continental shelf, enters deeply in the English Channel and contributes still more than 10% to the nitrogenous content of the phytoplankton entering the North Sea through the Straits of Dover.

The situation appears to be somewhat different for the phosphorus. The Figure 96 shows that the group of Western French rivers has a strongly reduced area of influence for the phytoplankton phosphorus in comparison to the nitrogen. The UK rivers on the contrary exert a longer range influence for phosphorus than for nitrogen.

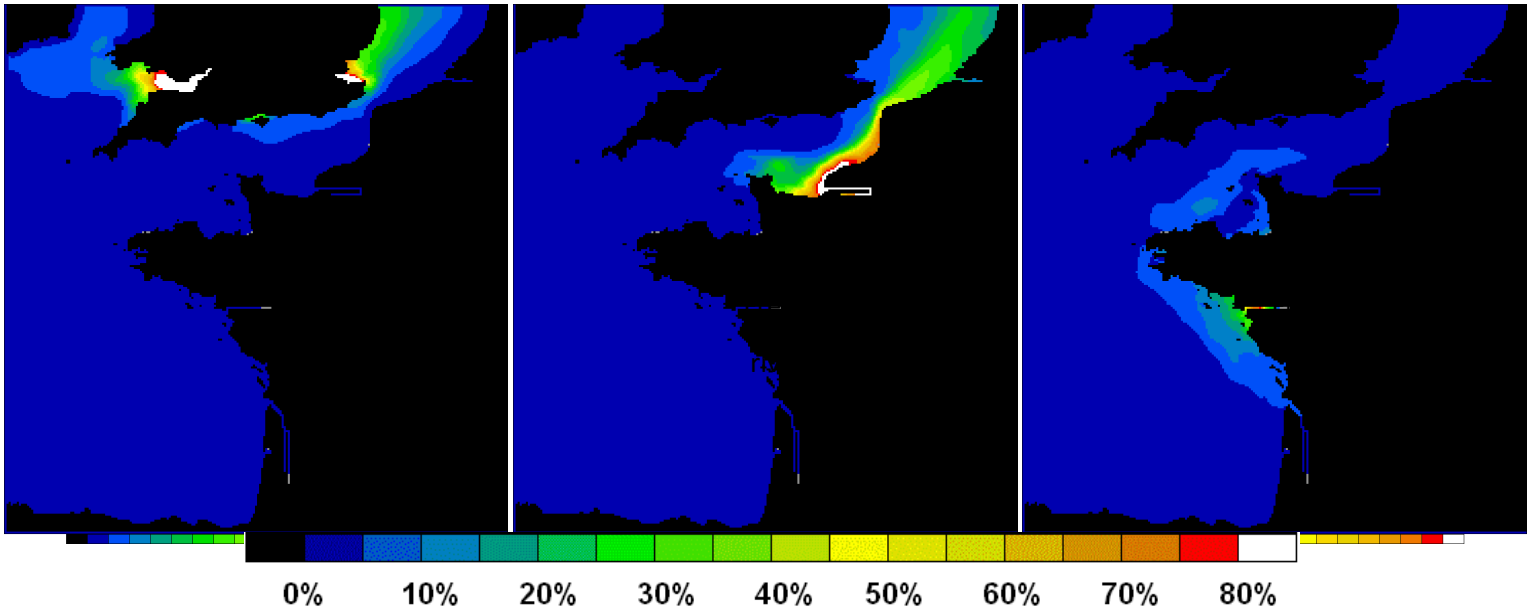

Figure 96: Relative contribution (%) of three groups of rivers to the phosphorus content of the surface marine phytoplankton, averaged on the 2000-2010 period. English rivers (left), East-French rivers (middle) and West-French rivers (right).

3.4.3 MIRO&CO TBNT results

3.4.3.1 Spatial distributions of contributions from N sources

The TBNT approach has been implemented in MIRO&CO to tag the original sources of nitrogen in all biological nitrogenous compartments of the model and simulations have been performed for each scenario (i.e. Reference, UWTD, GAP, LocOrgDem and Pristine). For clarity purpose, we will only present model results for the Reference, LocOrgDem and Pristine situation.

As shown in Figure 97, mean winter dissolved inorganic nitrogen (DIN) concentration is clearly reduced in the LogOrgDem scenario compared to the Reference one. For the Pristine situation, mean winter DIN concentrations are below 5 µmolN L^{-1} for most of the domain. Daily ratios between tagged and untagged DIN have been computed and averaged over 2000-2010 winter periods to provide the averaged relative contribution of each tagged source to the winter DIN concentration. Respective relative contributions from the tagged source groups to winter DIN are presented hereafter.

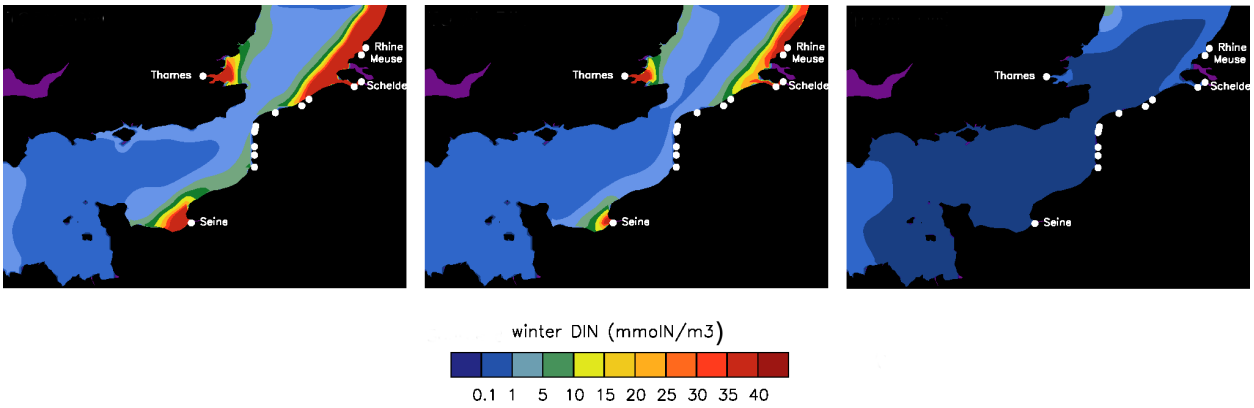

Figure 97: 2000-2010 averaged winter DIN estimated by MIRO&CO for the Reference situation (left) LocOrgDem scenario (middle) and the Pristine situation (right).

MIRO&CO results for the Reference situation (Figure 98) show that the western ocean boundary and atmospheric depositions significantly contribute to winter DIN over the whole MIRO&CO domain, except in coastal zones next to large estuaries such as the Scheldt, Rhine, Meuse, Seine and Thames where the influence of the rivers dominates. Northern marine boundary contribution to DIN remains in the northern part of the domain including the eastern coasts of UK. Nitrogen from the Rhine, Meuse, Scheldt and small Belgian rivers play a significant role along the Belgian-Dutch coast and, to a less significant extent, also to the DIN concentration in the SBNS. The Thames plays a significant role in the UK coastal waters and in the eastern North Sea only. The French rivers significantly contribute to the winter DIN concentration along the French coast and in the axis of the SBNS in front of Belgium.

For the LocOrgDem scenario, the zones of influence of the different river groups remain similar than for the Reference situation although the relative contributions from these rivers are significantly lowered (Figure 99). In opposition, the relative contributions from the western ocean boundary and the atmospheric depositions are larger than for the Reference situation. For the Pristine situation, the zones of influence of the different river groups are significantly narrower and the main nitrogen contributor to winter DIN over nearly the whole domain is the western ocean boundary (Figure 100).

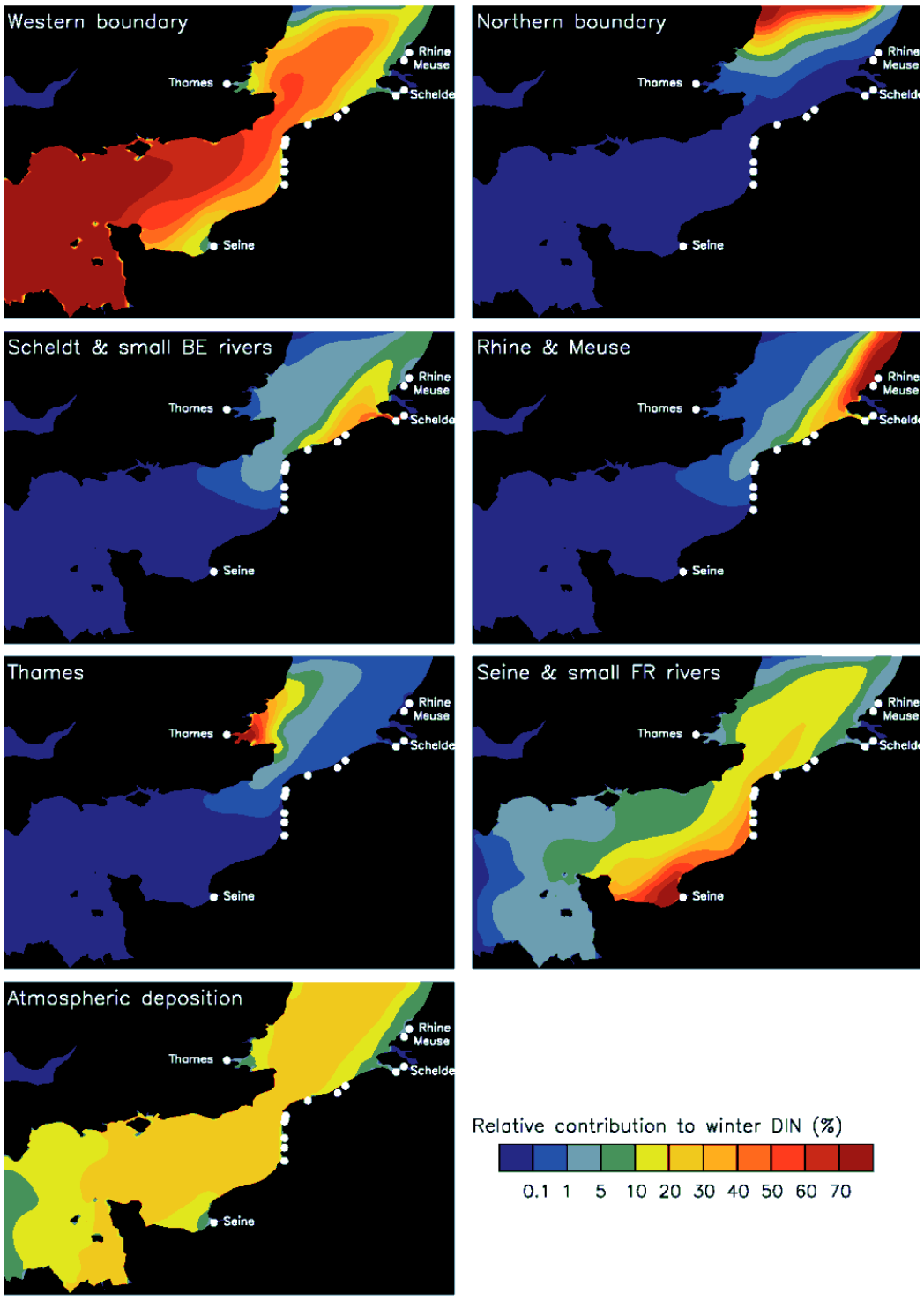

Figure 98: Spatial distributions of 2000-2010 averaged relative contribution (%) of each tagged source group to nitrogen content in winter DIN. Contributions are computed from MIRO&CO simulation results for the Reference situation (see Table 4).

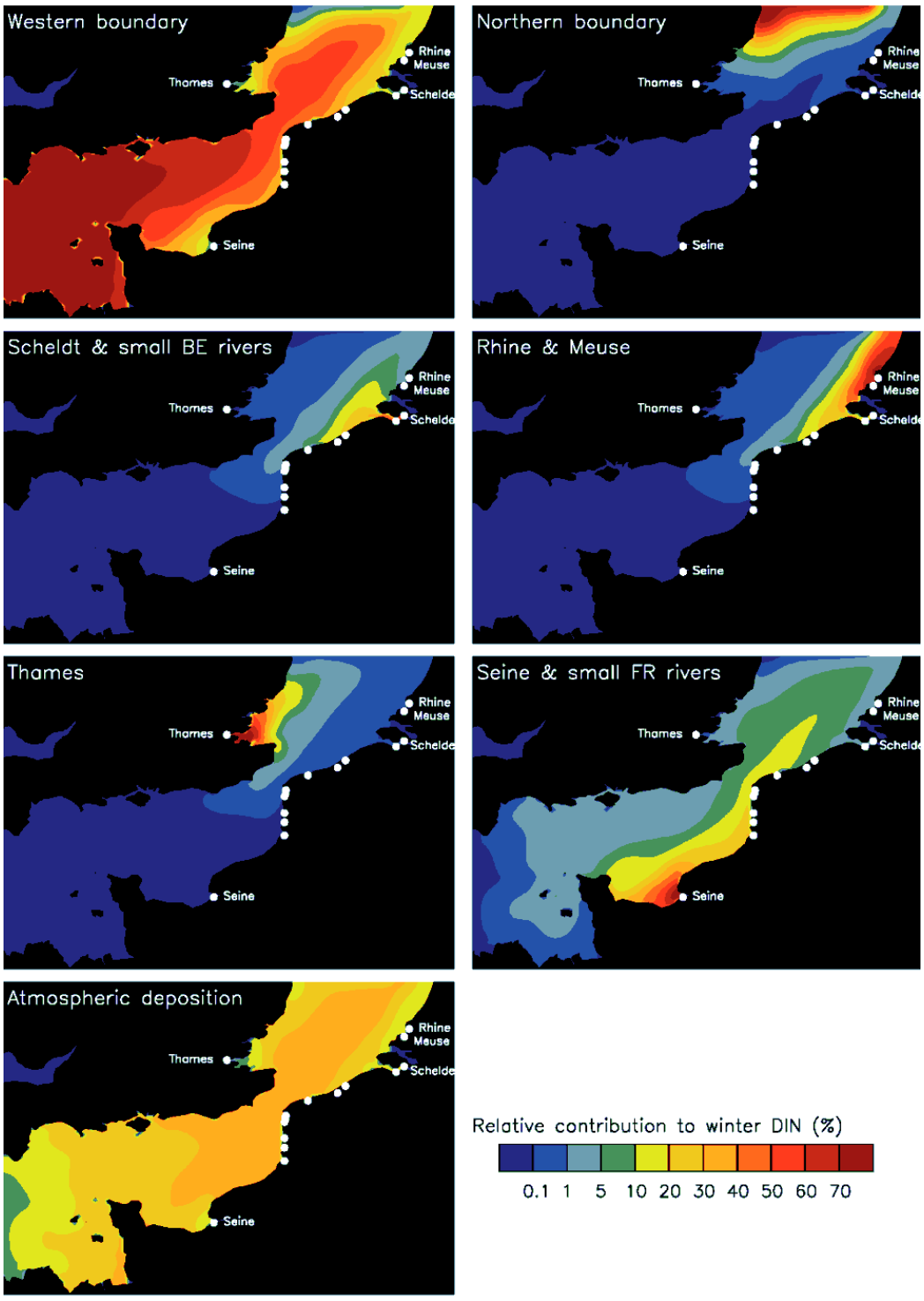

Figure 99: Spatial distributions of 2000-2010 averaged relative contribution (%) of each tagged source group to nitrogen content in winter DIN. Contributions are computed from MIRO&CO simulation results for the LocOrgDem scenario (see Table 4).

Figure 100: Spatial distributions of 11-year averaged relative contribution (%) of each tagged source group to nitrogen content in winter DIN. Contributions are computed from MIRO&CO simulation results for the Pristine situation (see Table 4).

3.4.3.2 Nitrogen source contributions in OSPAR zones

The mean relative contributions of the different tagged source groups to the winter DIN concentration are presented in Figure 101 for the Belgian coastal waters (BCW, 30 > salinity > 34.5 top panels) and the Belgian offshore waters (BOW, salinity > 34.5, bottom panels) and for the 3 considered scenarios. In the Reference situation, the main contributor is the Scheldt and small BE rivers group (32%) followed by the Rhine and Meuse (24%) and the western boundary conditions (20%). The atmospheric depositions account for 14% of the mean winter DIN and the Seine and small FR rivers for 10%. In the LogOrgDem scenario, the relative N contributions from the rivers decrease while the relative nitrogen contribution

from atmospheric depositions and western boundaries reach 26% and 31% respectively. In the Pristine situation, the relative nitrogen contributions from the rivers are even lower and as atmospheric depositions were assumed to be non-existent, the relative N contribution from the western boundaries to the winter DIN reaches 88%.

The Belgian offshore waters are less affected by the rivers from the eastern part of the Eastern Channel than the BCW. The three main nitrogen contributors are the western boundaries (46%), atmospheric depositions (26%) and the Seine and small FR rivers (19%). Like in the BCW, the nitrogen contributions from rivers decrease in the LocOrgDem scenario compared to the Reference situation and reach quasi-null values in the pristine situation. The main contributors are then the western boundaries (51%), atmospheric depositions (34%) and the Seine and small FR rivers (10%) for the LogOrgDem scenario, and the western boundaries only (96%) in the Pristine situation.

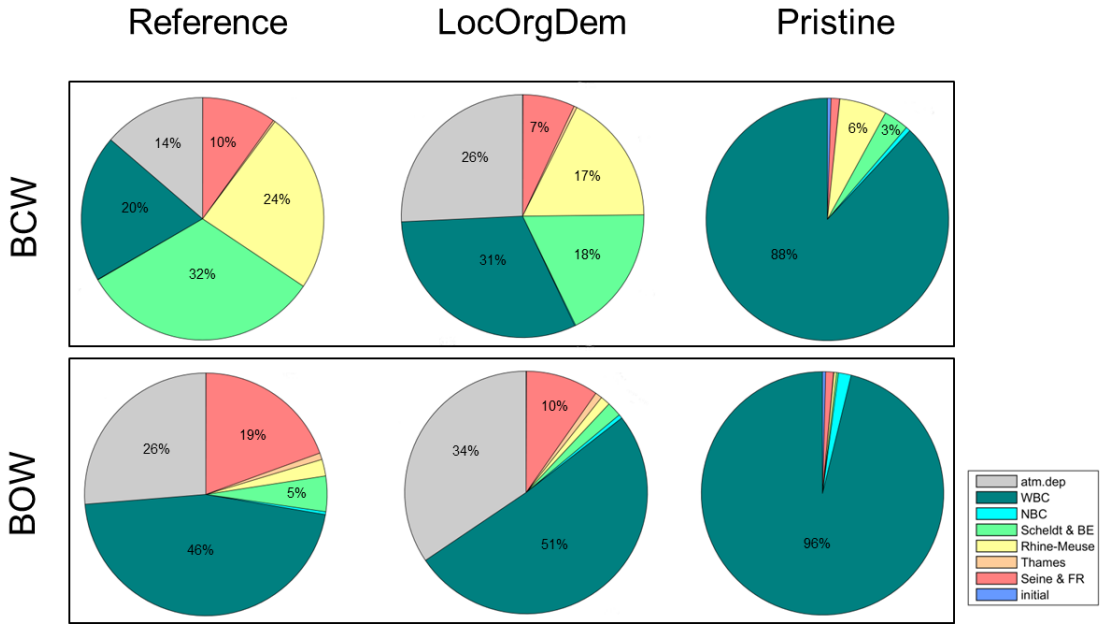

Figure 101: 11-year averaged relative contribution of different N sources to winter DIN in Belgian coastal waters (BCW, top row) and Belgian offshore water (BOW, bottom row) as estimated by MIRO&CO using river loads from PyNuts. Reference (left column), LocOrgDem (middle column) and Pristine (right column) scenarios.

3.4.3.3 N source contribution in Ecozones

The mean relative contributions of the different tagged source groups to the winter DIN concentration have been computed over the ecologically-based zones and are presented in Figure 102 for the Reference situation, LogOrgDem scenario and Pristine situation. N sources have been aggregated by source type: atmospheric, riverine or oceanic. For all scenarios, Ecozone 1 is more affected by the riverine nitrogen input (76%-55%-20% for the Reference situation, LogOrgDem scenario and Pristine situation) than Ecozone 2 (54%-35%-5%) and much more than Ecozone 3 (21%-11%-<1%) and Ecozone 4 (4%-3%-0%). The main contributor in Ecozones 3 and 4 is the ocean. The ocean is also the main contributor in all areas during the Pristine situation. Finally, atmospheric deposition relative contributions to winter DIN are 11-25% for Reference situation and 21-31% for LocOrgDem scenario with the highest relative contributions in Ecozone 3 and lowest in Ecozone 1.

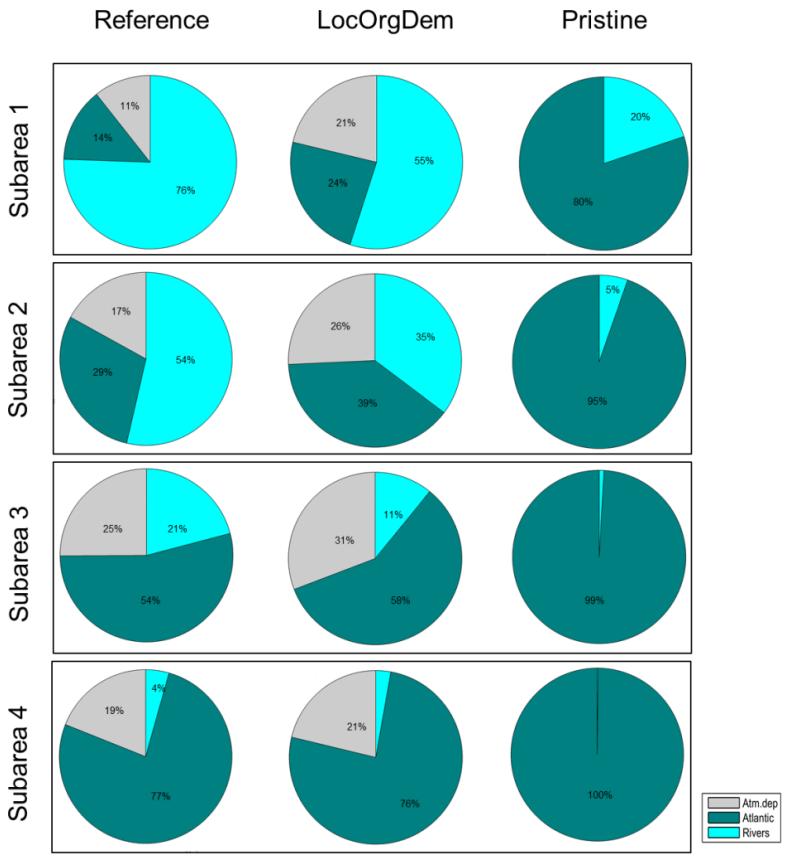

Figure 102: 11-year averaged relative contribution of different N source types to winter DIN in the four ecologically-based Ecozones as estimated by MIRO&CO using river loads from PyNuts for the Reference situation (left column), the LocOrgDem scenario (middle column) and the Pristine situation (right column).

3.4.3.4 Temporal variability in N contributions

In average over 2000-2010 and for the Reference situation, MIRO&CO estimates the daily DIN concentration in BCW between 10 µmol L^{-1} in summer and 40 µmol L^{-1} in winter, and a *Phaeocystis* concentration that reaches 150 µgC L^{-1} during the spring bloom (Figure 103). The respective mean contributions from the different sources to daily DIN and *Phaeocystis* (mucus not included) concentrations are also shown in Figure 103. All year round, the contributions from the Rhine, Meuse, Scheldt and small BE rivers are larger than the contributions from atmospheric depositions, western boundary and Seine and small FR rivers. Contributions from the Thames and the northern boundary are close to null.

In addition to the seasonal variability, there is a fairly large inter-annual variability in the daily DIN and *Phaeocystis* concentrations as shown by the gray lines in Figure 103 (top row). A large portion of this variability can be attributed to the variability in the nitrogen that originates from the Rhine, Meuse, Scheldt and small BE rivers, and that reaches the BCW (5^{th} and 6^{th} rows in Figure 103). Nitrogen contributions from atmospheric depositions, western boundaries, and Seine and small FR rivers to DIN and *Phaeocystis* concentrations in BCW are less variable in time than the contributions from above cited sources.

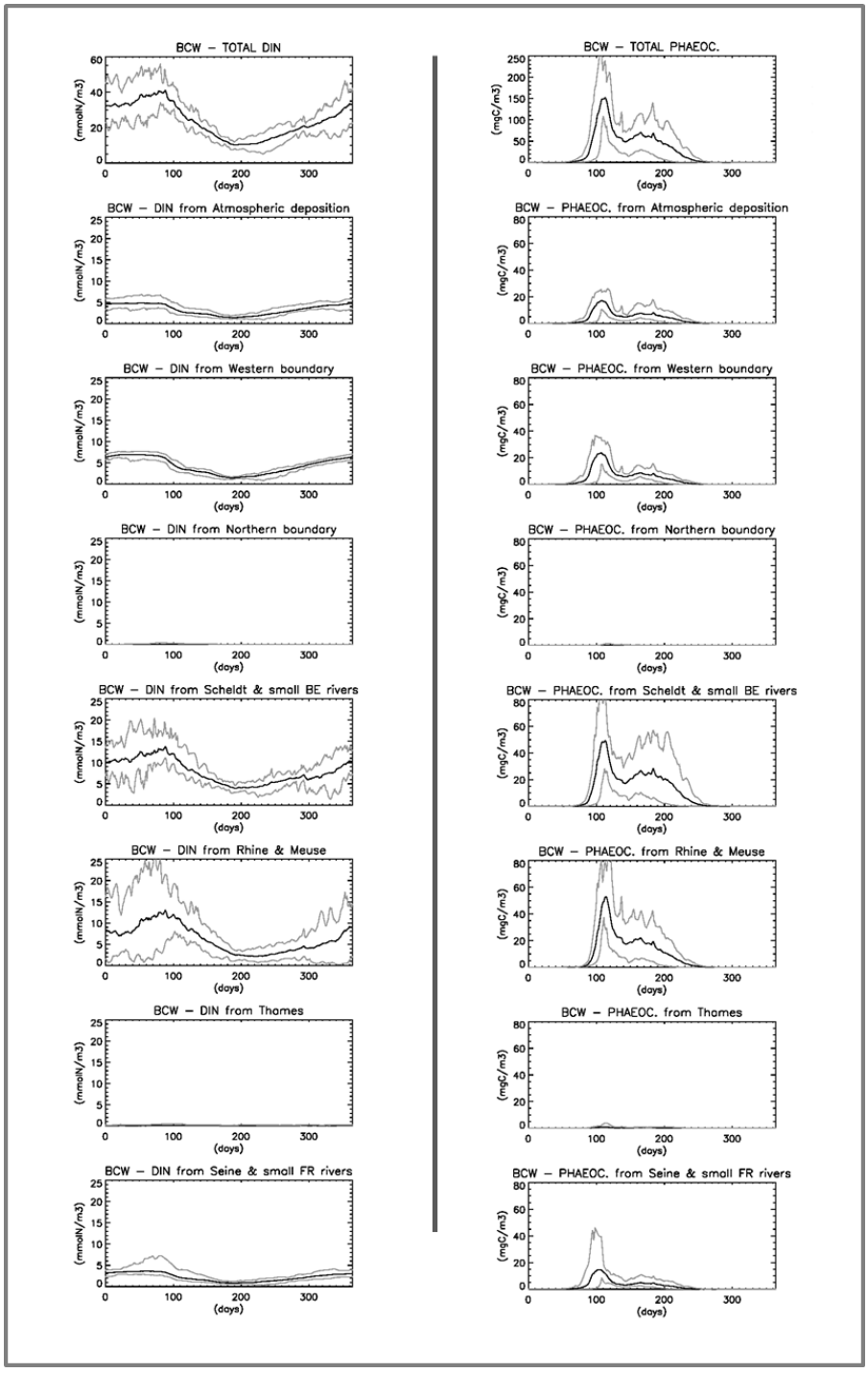

Figure 103: Top row : time series of mean daily DIN (left) and *Phaeocystis* (right) concentrations estimated by MIRO&CO for the Belgian coastal waters (BCW) and computed over the 2000-2010 time period. Next 7 rows : time series of mean daily DIN (left panels) and *Phaeocystis* (right panels) concentrations based on nitrogen coming from one of the 7 tagged sources and computed for the BCW over the 2000-2010 time period. Corresponding minimum and maximum daily values are represented by gray lines. Results are shown for the Reference situation.

3.5 Distance-to-target (DTT) results

Starting from the decadal means for DIN and DIP in all the rivers, a weighted mean of them has been computed for each of the 4 river groups (the weight of a river is its decadal mean flow rate). These means (Table 11) have then been used to map the mean theoretical dilution of water coming from the 4 sources, which produces the actual computed repartition of nitrogen in phytoplankton. The Figure 104 shows that the French and the Belgian models give comparable forms of dilution plumes of the main rivers, even if not totally quantitatively similar.The step further is to define what thresholds will be used to define the Good Ecological Status in the marine waters. In the previous OSPAR ICG-EMO workshops, only a simple approach has been adopted: because the control variables of the problem are DIN or DIP concentrations in rivers, the marine thresholds have been defined as unique and ubiquitous values for winter DIN and DIP taken independently. The two major drawbacks of this naive approach are: 1/ present DIN and DIP contents of the marine water are not totally available for the algae: because of the imposed Redfield stoichiometry of the living organic matter, the most limiting nutrient fixes the available part of the other nutrient; consequently, DIN and DIP should be treated together, in a distributed manner with respect to the local Redfield ratio. 2/ DIN and DIP alone are not harmful, only their derived products (chlorophyll, oxygen concentration) are able in some circumstances to cause eutrophication damages; the reduction of river nutrients should then be deduced directly from the values of a real eutrophication indicator, chlorophyll, or dissolved oxygen, or abundance of toxic phytoplanktonic species. In this project, we propose to start from the observed chlorophyll 90^{th} percentile (computed from satellite data over the 2000-2010 decade, as previously described in Figure 1), and to go back to locally available DIN and DIP by a simple relationship. The technique consists in replacing in every mesh of the marine model the crude computed DIN (or DIP) concentration by its "fully bioavailable" component. As algal accumulation is driven by 3 local factors (light availability, nutrient availability and residence time), a complete determination of the "fully bioavailable" component should multiply the crude computed nutrient by 3 limitation factors. Due to the ambiguous definition of residence time (what water volume should we take into account?), we have only defined the light and nutrient limiting factors, as follows:

If $P90_{i,j}$ is the observed 90th percentile of total surface chlorophyll in the mesh (i,j) of the model grid, $DIN_{i,j}$ and $DIP_{i,j}$ the crude simulated DIN and DIP concentrations of the water, $k_{i,j}$ the extinction coefficient due to inorganic matter and $H_{i,j}$ the mean mixed layer depth in this mesh:

the light limitation factor in mesh (i,j) is:

$$light\_lim_{i,j} = 1-e^{-ki,j*Hi,j} /(k_{i,j}*H_{i,j})$$

the nutrient limitation factors in mesh (i,j) are:

$$nutrient\_lim\_DIN_{i,j} = \min (DIN_{i,j}, 16* DIP_{i,j})/ DIN_{i,j}$$

$$nutrient\_lim\_DIP_{i,j} = \min (DIN_{i,j}/16, DIP_{i,j})/ DIP_{i,j}$$

so, the "fully available" nutrients in mesh (i,j) are:

$$DIN\_avail_{i,j} = DIN_{i,j}* nutrient\_lim\_DIN_{i,j}* light\_lim_{i,j}$$

$$DIP\_avail_{i,j} = DIP_{i,j}* nutrient\_lim\_DIP_{i,j}* light\_lim_{i,j}$$

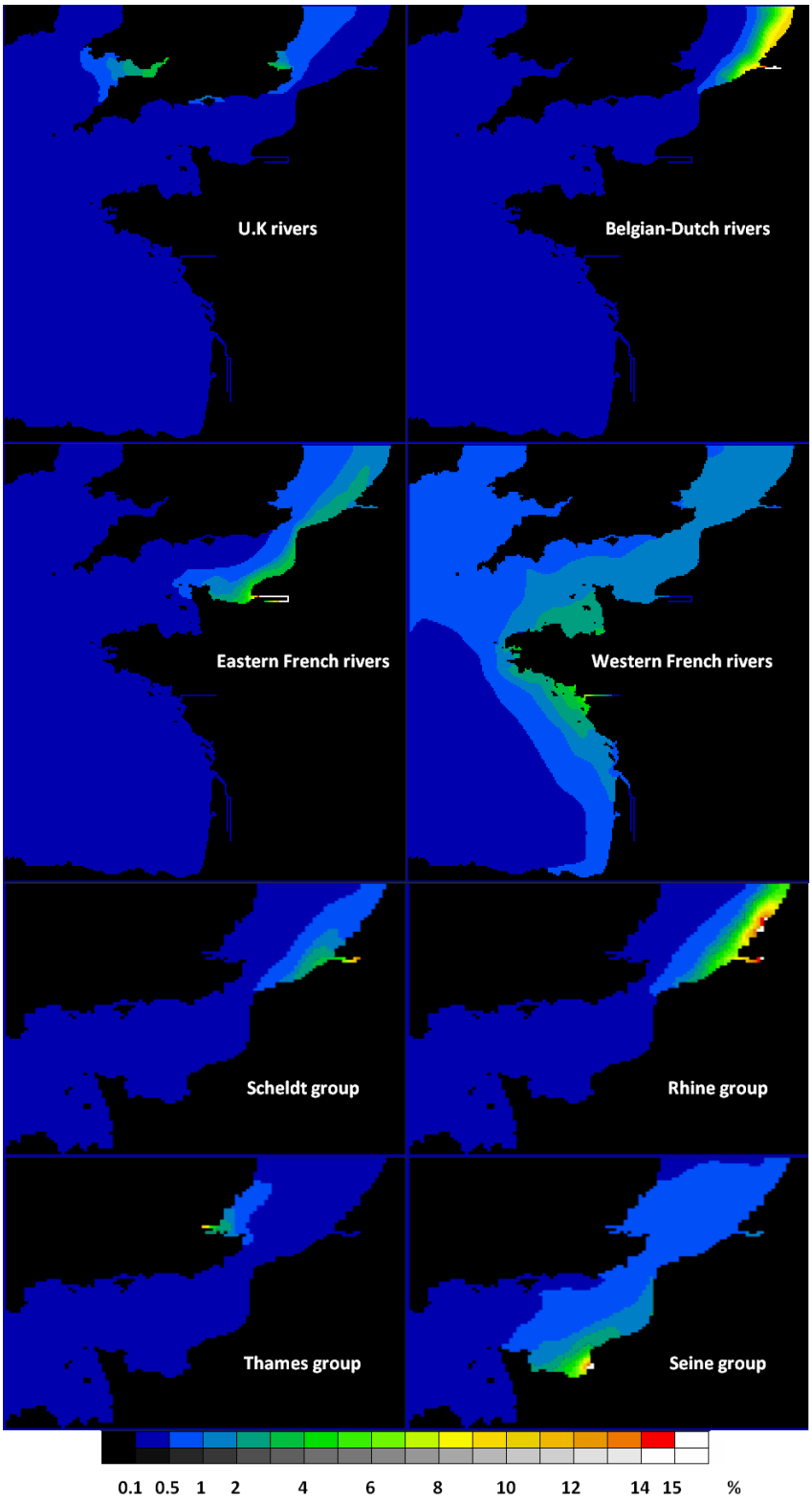

Figure 104: Maps giving the percentage of marine water coming from the 4 groups of rivers in ECO-MARS3D (top panels) and MIRO&CO (bottom panels).

As shown in the Figure 105, taking into account the light-limitation only does not linearize the cloud made by the (P90, nutrient) couples coming from all the marine meshes of the ECO-MARS3D model, whereas taking into account the joint nutrient- and light-limitations does it. A rather good exponential relationship comes out between the "fully available" DIN or DIP and the observed chlorophyll 90th percentile (r^2=0.7), with the two exponents in the imposed Redfield ratio (16 molN molP^{-1}).

Now, if we set 8 µgChl L^{-1} as the eutrophication GEnS threshold for P90 chlorophyll *a* (see 3.2.2), we can deduce two rigorous "fully bioavailable" DIN and DIP GEnS thresholds, as follows:

DIN threshold_rigorous = Ln(8/0.617)/0.284 ≈ 9.0 µmol L^{-1}

DIP threshold_rigorous = Ln(8/0.617)/4.546 ≈ 0.56 µmol L^{-1} (=DIN threshold_rigorous /16)

If we keep the official WFD/MSFD value 15 µgChl L^{-1} as the eutrophication GEnS threshold for P90 chlorophyll *a*, we obtain two other, lenient "fully bioavailable" DIN and DIP GEnS thresholds

DIN threshold_lenient = Ln(15/0.6814)/0.1579 ≈ 19.5 µmol L^{-1}

DIP threshold_lenient = Ln(15/0.6814)/4.737 ≈ 0.65 µmol L^{-1} (=DIN threshold_lenient /30)

These thresholds have been applied in the Simplex procedure, first to the crude DIN and DIP linearly deduced from the dilution of river loadings, and then to their "fully bioavailable" components. A last problem arises in the Simplex procedure: during the algorithm iterations, the coefficients of river concentrations in the linear constraints on the marine nutrients in each cell do not change, whereas in our case, they should be able to change due to changing nutrient-limitation in response to non-proportional reductions of the river DIN and DIP. This problem can be solved by iterating a few times the whole Simplex procedure, starting the (n+1)th run with the optimised river concentrations produced by the (n)th run: the convergence is quickly obtained.

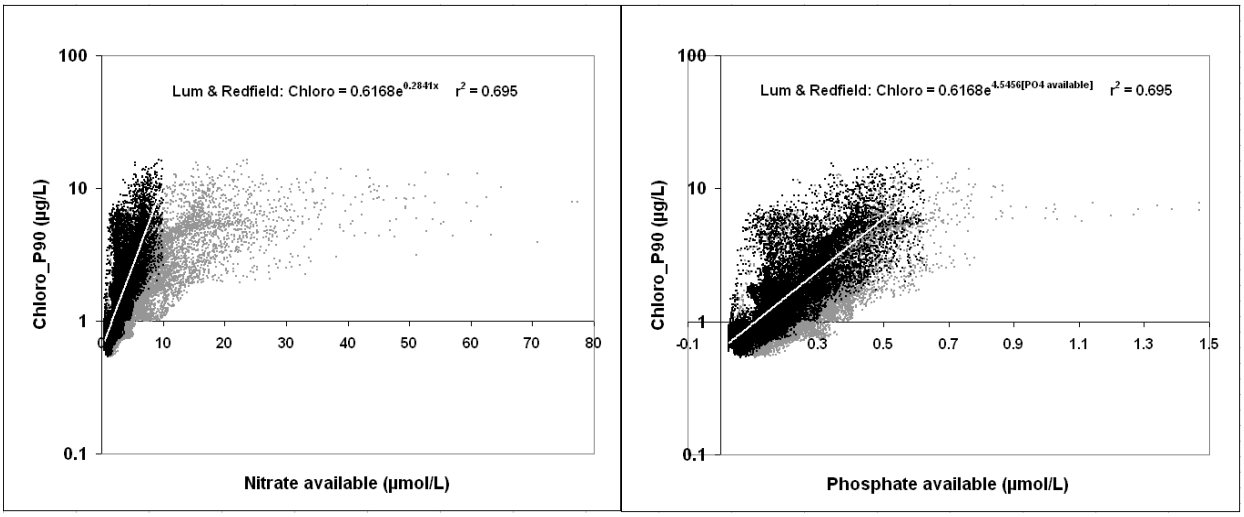

Figure 105: Relation between light-limited (grey dots) and light and nutrient-limited (black dots) "bioavailable" DIN and DIP and the satellite-derived 90th percentile of surface chlorophyll over the 2000-2010 period, when the phytoplankton N/P ratio=16. The white lines give the semi-log linear regression through the black clouds.

The three types of geographical targets used are displayed in Figure 106. The optimal sets of river DIN and DIP concentrations obtained by both models for three types of geographical targets are presented in Table 11.

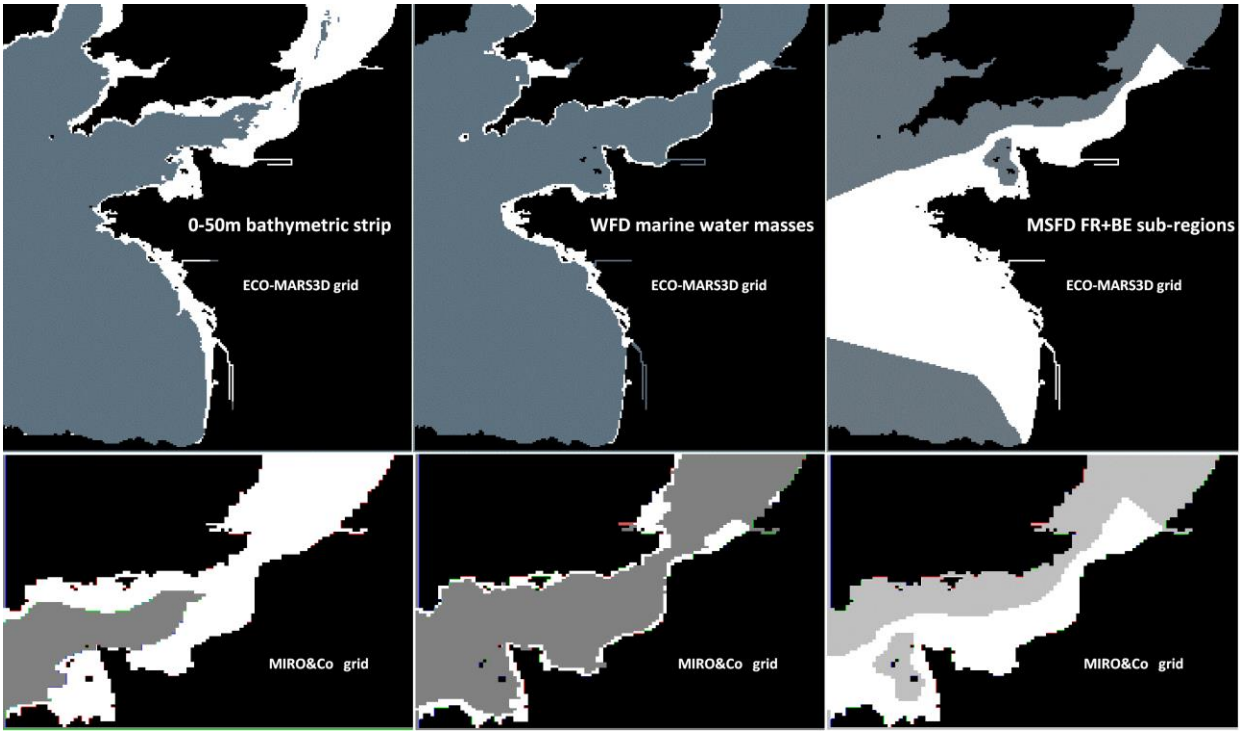

Figure 106: Meshes of ECO-MARS3D model (top panels) and MIRO&CO (bottom panels) retained (in white) in the 3 types of geographical targets where GEnS is to be obtained.

3.5.1.1 Conclusions

- Taking into account the light availability and the N/P ratio in the bioavailability of nutrients at sea reduces drastically the bioavailable nutrients and, hence, the number of marine meshes staying above the GEnS threshold in the current situation, which lowers considerably the nutrient reductions imposed to rivers.
- Taking lenient GEnS thresholds for marine DIN and DIP instead of rigorous ones reduces the number of marine meshes which are actually above these GEnS thresholds, and then relaxes the constraints over the river nutrients. But the groups of rivers concerned by nutrient reduction remain the same, except in the case of UK group which can be concerned for DIN in the rigorous procedure, and not in the lenient one.
- In the ECO-MARS3D model, which uses river measurements of DIN and DIP which are lower than the PyNuts simulated values used by the MIRO&CO model for 3 of the 4 river groups, only two groups of rivers need to be treated, for DIN as well as for DIP:

  The Holland-Belgium group: DIN -> 200 µmol L^{-1} down to 30 µmol L^{-1} (rigorous) or 100 µmol L^{-1} (lenient), DIP -> 8 µmol L^{-1} down to 3 µmol L^{-1} (rigorous) or 4 µmol L^{-1} (lenient).

The Eastern French group: DIN -> 430 µmol L^{-1} down to 70 µmol L^{-1} (rigorous) or 90 µmol L^{-1} (lenient),, DIP -> 3.2 µmol L^{-1} down to 0.6 µmol L^{-1} (rigorous as well as lenient).

- In the MIRO&CO model, due to its higher simulated DIN and DIP river loadings, 3 among the 4 groups of rivers need to be treated, for DIN as well as for DIP; the N/P constrained scenarios on targets including the Netherlands coast lead to:

  The Thames group: only concerned if the target includes the UK coastal zone; DIN -> 1200 µmol L^{-1} down to 400 µmol L^{-1} (rigorous) or 700 µmol L^{-1} (lenient), DIP-> 45 µmol L^{-1} down to 12 µmol L^{-1} (rigorous) or 16 µmol L^{-1} (lenient).

  The Rhine group: DIN -> 260 µmol L^{-1} down to 100 µmol L^{-1} (rigorous) or 200 µmol L^{-1} (lenient), DIP-> 6.4 µmol L^{-1} down to 3 µmol L^{-1} (rigorous) or 4 µmol L^{-1} (lenient).

  The Seine group: DIN -> 450 µmol L^{-1} down to 150 µmol L^{-1} (rigorous as well as lenient), DIP-> 4.7 µmol L^{-1} down to 2.0 µmol L^{-1} (rigorous) or 2.4 µmol L^{-1} (lenient).

  The Scheldt group needs DIP reduction for every target, but DIN reduction only if the 0-50m strip is the target.

The Figure 107 and Figure 108 illustrate on the case of a wide geographical target (the MSFD French and Belgian sub-regions) the possibility to accept high DIN concentrations in some marine meshes because of the lack of DIP in these meshes. However, under some circumstances, the “fully bioavailable” nutrients are not determined by the Redfield ratio exactly as phytoplankton internal N:P ratio may vary.

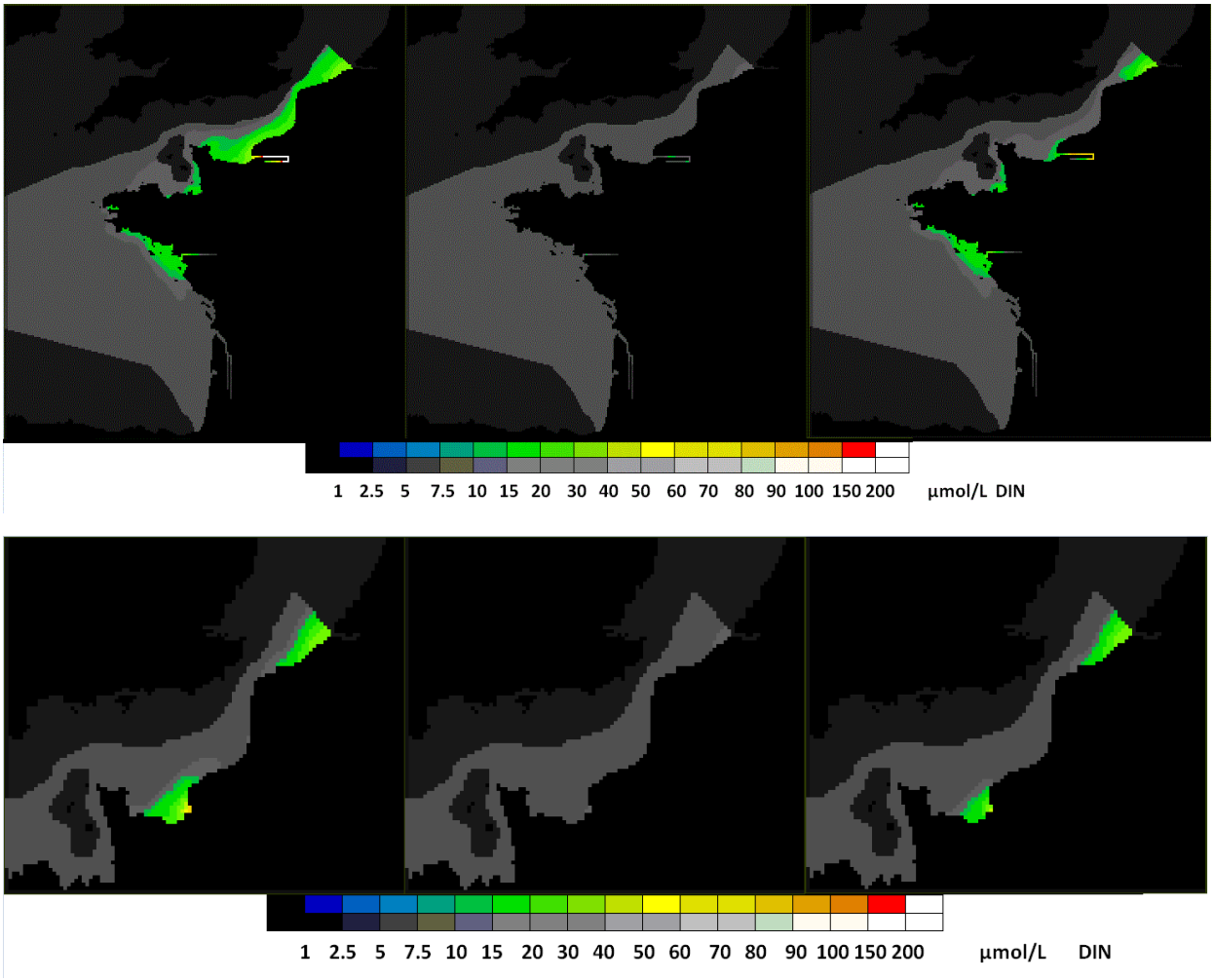

Figure 107: Maps of DIN concentration in the MSFD French and Belgian sub-regions from the ECO-MARS3D model (top) and MIRO&CO model (bottom), respectively for: the present situation (left), after "light and N/P free" optimization (middle) and after "light and N/P constrained" optimization (right). The color scale is used for concentrations above the GEnS threshold, the grey one for concentrations below the GEnS threshold.

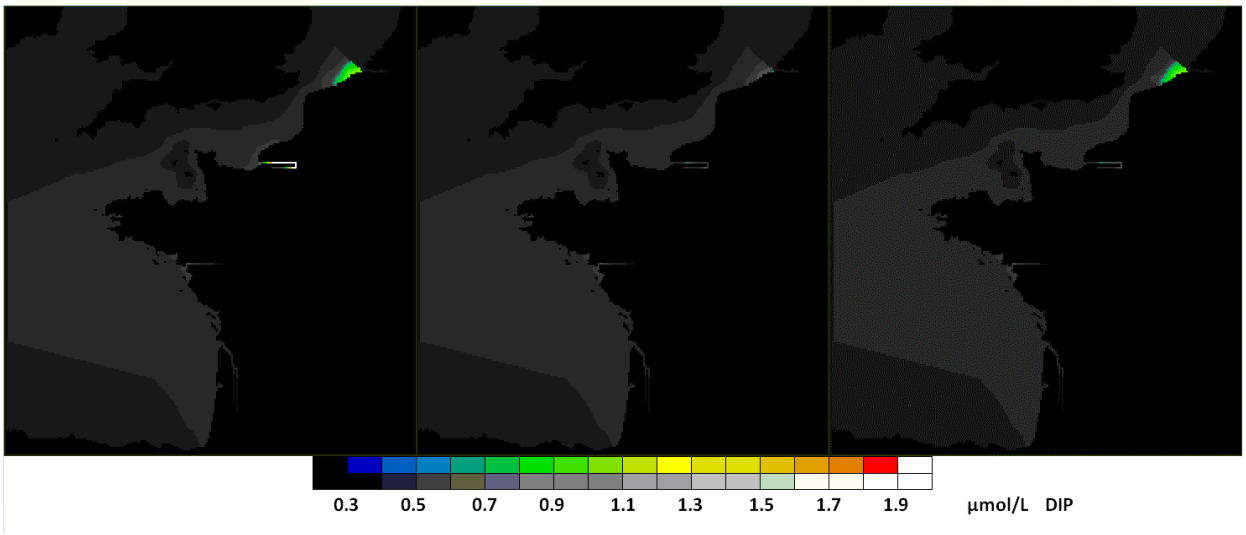

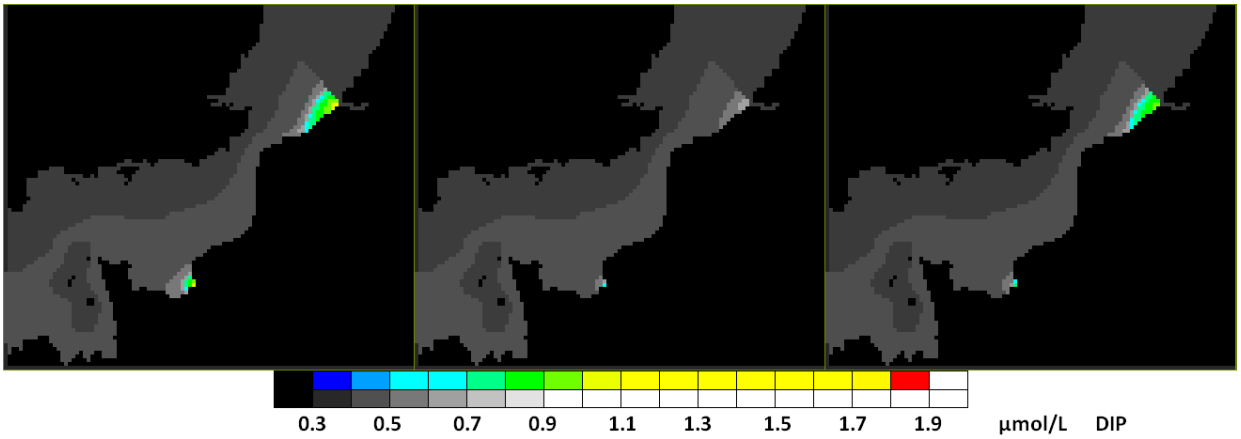

Figure 108: Maps of DIP concentration in the MSFD French and Belgian sub-regions from the ECO-MARS3D model (top) and MIRO&CO model (bottom), respectively for: the present situation (left), after "light and N/P free" optimisation (middle) and after "light and N/P constrained" optimisation (right). The color scale is used for concentrations above the GEnS threshold, the grey one for concentrations below the GEnS threshold.

Table 11: Mean 2000-2010 decadal DIN and DIP concentrations (µmol L^{-1}) in 4 groups of rivers (as defined for ECO-MARS3D and MIRO&CO respectively), in the present situation (from measured nutrient loads in ECO-MARS3D, from PyNuts nutrient loads in MIRO&CO) and after optimal reductions computed by the Simplex method for 3 different geographical targets and 2 levels of thresholds (rigorous and lenient). Cells in gray point to the nutrients which have been reduced in the Simplex optimization.

Region	0-50m_bathymetric_strip				WFD water masses together				MSFD sub-regions together			
Name of the tracer	DIN		DIP		DIN		DIP		DIN		DIP	
	N/P & light free	N/P & light constrained	N/P & light free	N/P & light constrained	N/P & light free	N/P & light constrained	N/P & light free	N/P & light constrained	N/P & light free	N/P & light constrained	N/P & light free	N/P & light constrained
ECO-MARS3D grid												
rigorous marine threshold (µmol/L)	9	9	0.56	0.56	9	9	0.56	0.56	9	9	0.56	0.56
above rigorous threshold, optimisable meshes	2636	330	581	334	834	4	97	4	1658	29	127	29
above rigorous threshold, discarded meshes	7	0	0	0	0	0	0	0	7	0	0	0
lenient marine threshold (µmol/L)	19.5	19.5	0.65	0.65	19.5	19.5	0.65	0.65	19.5	19.5	0.65	0.65
above lenient threshold, optimisable meshes	542	155	490	228	103	2	79	2	171	27	99	27
above lenient threshold, discarded meshes	0	0	0	0	0	0	0	0	0	0	0	0
UK PRESENT (µmol/L)	384	384	7.3	7.3	384	384	7.3	7.3	384	384	7.3	7.3
UK rigorously OPTIMISED (µmol/L)	127	384	7.3	7.3	136	384	7.3	7.3	384	384	7.3	7.3
UK leniently OPTIMISED (µmol/L)	384	384	7.3	7.3	384	384	7.3	7.3	384	384	7.3	7.3
Holland-Belgium PRESENT (µmol/L)	197	197	8.0	8.0	197	197	8.0	8.0	197	197	8.0	8.0
Holland-Belgium rigorously OPTIMISED (µmol/L)	21	28	1.4	1.4	38	28	2.8	3.1	46	197	3.1	8.0
Holland-Belgium leniently OPTIMISED (µmol/L)	63	61	1.7	1.8	129	124	3.9	4.2	159	197	4.2	8.0
France-East PRESENT (µmol/L)	431	431	3.2	3.2	431	431	3.2	3.2	431	431	3.2	3.2
France-East rigorously OPTIMISED (µmol/L)	10	76	0.6	0.6	75	431	3.2	3.2	10	76	0.6	0.6
France-East leniently OPTIMISED (µmol/L)	19	86	0.6	0.6	264	431	3.2	3.2	19	86	0.6	0.6
France-West PRESENT (µmol/L)	267	267	3.5	3.5	267	267	3.5	3.5	267	267	3.5	3.5
France-West rigorously OPTIMISED (µmol/L)	64	267	3.5	3.5	89	267	3.5	3.5	64	267	3.5	3.5
France-West leniently OPTIMISED (µmol/L)	218	267	3.5	3.5	267	267	3.5	3.5	218	267	3.5	3.5
MIRO grid												
rigorous marine threshold (µmol/L)	9	9	0.56	0.56	9	9	0.56	0.56	9	9	0.56	0.56
above rigorous threshold, optimisable meshes	649	46	254	47	220	4	99	4	317	1	65	1
above rigorous threshold, discarded meshes	0	0	0	0	0	0	0	0	0	0	0	0
lenient marine threshold (µmol/L)	19.5	19.5	0.65	0.65	19.5	19.5	0.65	0.65	19.5	19.5	0.65	0.65
above lenient threshold, optimisable meshes	219	49	174	16	77	2	63	2	87	1	41	1
above lenient threshold, discarded meshes	0	0	0	0	0	0	0	0	0	0	0	0
Scheldt PRESENT (µmol/L)	656	656	12.2	12.2	656	656	12.2	12.2	656	656	12.2	12.2
Scheldt rigorously OPTIMISED (µmol/L)	11	23	0.7	0.4	109	656	7.1	12.2	10	656	0.4	12.2
Scheldt leniently OPTIMISED (µmol/L)	28	10	0.9	0.4	384	656	9.4	12.2	10	656	0.4	12.2
Rhine PRESENT (µmol/L)	259	259	6.4	6.4	259	259	6.4	6.4	259	259	6.4	6.4
Rhine rigorously OPTIMISED (µmol/L)	25	104	1.6	2.4	23	109	1.5	3.4	60	259	4.0	6.4
Rhine leniently OPTIMISED (µmol/L)	79	118	2.1	3.1	71	204	1.9	4.5	211	259	5.3	6.4
Thames PRESENT (µmol/L)	1171	1171	45.0	45.0	1171	1171	45.0	45.0	1171	1171	45.0	45.0
Thames rigorously OPTIMISED (µmol/L)	49	336	3.2	13.9	163	1171	10.6	45.0	1171	1171	45.0	45.0
Thames leniently OPTIMISED (µmol/L)	164	746	4.1	18.5	579	1171	14.2	45.0	1171	1171	45.0	45.0
Seine PRESENT (µmol/L)	456	456	4.7	4.7	456	456	4.7	4.7	456	456	4.7	4.7
Seine rigorously OPTIMISED (µmol/L)	25	142	1.6	1.9	46	456	3.0	4.7	25	142	1.6	1.9
Seine leniently OPTIMISED (µmol/L)	76	92	2.0	2.4	154	456	3.9	4.7	76	239	2.0	2.4

4 DISCUSSION

4.1 Reaching the GEnS in the rivers and in the NEA

4.1.1 Necessary reductions to reach background: TBNT and DTT

4.1.1.1 TBNT: Sources and paths of anthropogenic nutrients

The source and path of anthropogenic nutrients are quite diverse within the NEA. The Iberian Peninsula does not experience transboundary exchanges in spite of occasional remote river influence in the sea. In the Bay of Biscay, the Loire river brings nutrient along the coasts of Brittany and up to the Bay of Seine. In the English Channel, the impact of the Seine and the Loire is significant. The English Channel and the Southern Bight of the North Sea (SBNS) show an eastward and northward water transport allowing recurrent patterns of TBNT between France, Belgium and The Netherlands that may lead to remote transboundary contamination. The rivers showing the most important transboundary influence in the Belgian coastal waters are the Rhine, Meuse and Scheldt and in the offshore waters the Seine and other smaller French rivers.

In Portugal, the region of riverine influence may extend far from the coast and considerably varies with seasons and with wet and dry years. The influence of rivers extends especially far in the sea during summer in wet year. Then, the nitrogen export to the ocean is maximum and follows a SW direction. Riverborne DIN concentrations of 1 µmol L^{-1} may be found at 400 km from the river outlet, which is a relatively high concentration as oceanic winter DIN concentrations are in the order of 0.4-0.5 µmol L^{-1} offshore the Iberian Peninsula. However, there is hardly any remote transboundary exchange of nutrients between the Iberian Peninsula and the French waters of the Bay of Biscay, because the highest Portuguese river influence occurs under a SW wind along the Portuguese coast.

ECO-MARS3D model shows that the nitrogen content of phytoplankton in the English Channel is influenced by the Seine group of rivers. Even the remote Loire river contributes to up to 10% of the nitrogen content of phytoplankton in the English Channel. In contrast, the riverine contribution to the phosphorus content of phytoplankton exhibits a much lesser spatial area of influence. This suggests that the actual phosphorus river loads contribute considerably less than nitrogen river loads to the nutrient enrichment of the coastal zone, due to the strong reduction of phosphorus wastes. In the ECO-MARS3D model, the atmospheric nitrogen counts for 10% to 20% in the nitrogen content of phytoplankton over the continental shelf in the Reference situation. A recommendation from this study is to reduce atmospheric N depositions in parallel with river loads, especially in "realistic" future scenarios like LocOrgDem.

One of the most striking results obtained by the TBNT simulation, illustrated in this report on the basis of MIRO&CO model results, is the scenario-dependent relative change of the Atlantic contribution to DIN concentration in the Belgian coastal waters (BCW), i.e. 20% in the Reference situation, 31% in the LocOrgDem scenario and 88% in the Pristine situation. When restricted the domain to Ecozone 1, the Atlantic contribution varies between 14% in the Reference situation, 24% in the LocOrgDem scenario and 80% in the Pristine situation. The atmospheric depositions of nitrogen are far from negligible in the

sea (see also Troost et al. 2013), and show an increasing relative contribution when riverine nutrient loads are reduced. It should be pointed out that the implementation of the proposed reduction scenarios could contribute to decrease the atmospheric depositions of nitrogen in the sea, even if that aspect was not calculated in the present study. The present analysis made with MIRO&CO shows that the relative contribution of nitrogen depositions increases in the BCW from 17% in Reference situation to 25% in the LocOrgDem scenario.

4.1.1.2 Distance to Target: mitigating eutrophication in marine areas

Reducing the transboundary contamination and mitigating eutrophication to reach the GEnS imply a dual-nutrient reduction (N,P) in the rivers. The DTT exercise provided useful information regarding the river load reductions necessary to reach the GEnS in target areas. Several target areas have been considered in the exercise and the extension of the target area influences the result of the DTT. The method applied in the present DTT study differs from previous studies (Los et al. 2014) in that the constraint to the optimization is not the mere reduction of DIN and DIP concentrations to their respective threshold levels. As DIN and DIP are not harmful, but phytoplankton may be, the optimization focused on the "fully bioavailable" nutrients, i.e. the DIN and DIP required for the bloom formation, which both depend on the phytoplankton internal N:P ratio (16 molN $molP^{-1}$) and on the light availability. This method is a considerable improvement to the previous ones as it estimates better the necessary nutrient reductions in the rivers (especially it does not conclude anymore to unnecessary reductions). However, under some circumstances, the "fully bioavailable" nutrients are not determined exactly by the Redfield ratio as phytoplankton internal N:P ratio may vary locally (Falkowski and Davis 2004). The dataset of Belgian and Dutch historical campaigns suggests that the spring bloom formation requires winter DIN:DIP ratios of about 30 molN $molP^{-1}$ in these coastal waters (Desmit et al. 2015). That DIN:DIP value of 30 molN $molP^{-1}$ also corresponds to the background winter DIN:DIP value found as the maximum coastal value in the pristine situation (see Results, section 3.2.2). Taking higher DIN:DIP ratios into account in the DTT exercise may lower the N reductions required in the rivers or conversely increase the required P reduction.

In this study, two distance-to-target exercises were tested to estimate the range between a "rigorous" and a "lenient" case. In the "rigorous" case, the "fully bioavailable" nutrients are estimated from the background Chl P90 (8 µgChl L^{-1}) and from an oceanic DIN:DIP ratio (16 molN $molP^{-1}$). In contrast, in the "lenient" case, the "fully bioavailable" nutrients are estimated from the Chl P90 recommended by WFD/MSFD in Belgian and French (north) coastal waters (15 µgChl L^{-1}) and from a DIN:DIP ratio more suitable to coastal zones (30 molN $molP^{-1}$, see 3.2.2). In the "rigorous" case, threshold values (8 µgChl L^{-1}, 9.0 µmol L^{-1} and 0.56 µmol L^{-1} for Chl P90, winter DIN and winter DIP, respectively) are representative of background values close to the pristine situation, and in the "lenient" case, threshold values (15 µgChl L^{-1}, 19.5 µmol L^{-1} and 0.65 µmol L^{-1} for Chl P90, winter DIN and winter DIP, respectively) are close to values recommended by the WFD/MSFD. The percentages of N and P riverine reduction needed to reach the marine thresholds (rigorous and lenient) have been computed from results obtained with the optimization Simplex method (see section 3.5, Table 11) and are presented in Table 12.

According to ECO-MARS3D model runs (using rivers loads from current observations), the necessary reductions to reach the marine thresholds in the WFD region are about 86% (rigorous) and 37% (lenient) in riverine N concentrations and about 61% (rigorous) and 48% (lenient) in riverine P concentrations in the Belgian-Dutch group of rivers (Rhine, Meuse, Scheldt) (see Table 12, "N/P and light constrained"). Considering the MSFD region, a reduction of N and P concentrations of about 80% in the French-eastern rivers (Seine river group) would be needed to reach the thresholds (rigorous and lenient). In the case of "N/P light free", that means without taking into account local light limitations, the riverine nutrient reductions needed to reach the thresholds concern more rivers. When the WFD region is the targeted area, riverine N concentrations have to be reduced by 65% (rigorous) in the UK rivers, by 81% (rigorous) and 35% (lenient) in the NL-BE rivers, by 83% (rigorous) and 39% (lenient) in the FR-East rivers and by 67% (rigorous) in the FR-West rivers. A P reduction of 65% (rigorous) and 51% (lenient) is needed in the NL-BE rivers. Considering the MSFD region, N concentrations have to be reduced for 3 river groups: the NL-BE (77% rigorous, 19% lenient), the FR-East (98% rigorous, 96% lenient) and the FR-West (76% rigorous, 18% lenient). P concentrations have to be reduced only in 2 river groups: the NL-BE (61% rigorous, 48% lenient) and the FR-East (81% rigorous and lenient).

According to MIRO&CO model runs (using PyNuts rivers loads), in the case of "N/P light constrained", the thresholds would be reached in the WFD region at the cost of reductions in the Rhine/Meuse river group of about 58% (rigorous) and 21% (lenient) for DIN and 47% (rigorous) and 30% (lenient) for DIP. In the MSFD region, a riverine reduction in the Seine river group of 69% (rigorous) or 48% (lenient) for DIN and 60% (rigorous) or 49% (lenient) for DIP is needed to reach the thresholds. In the case of "N/P light free", the riverine N and P reductions needed to reach the thresholds concern all river groups when the WFD region is the targeted area and all groups except UK if the target area is the MSFD one. Targeting the WFD area, the needed nutrient reductions range from 83% to 91% (rigorous) and 41% to 73% (lenient) for DIN, and from 36% to 77% (rigorous) and 17% to 70% (lenient) for DIP. Targeting the MSFD area, the needed nutrient reductions range from 77% to 98% (rigorous) and 19% to 98% (lenient) for DIN, and from 38% to 97% (rigorous) and 17% to 97% (lenient) for DIP.

Table 12: Mean 2000-2010 decadal DIN and DIP concentrations (µmol L^{-1}) in 4 groups of rivers (as defined for ECO-MARS3D and MIRO&CO respectively, see Table 11), in the present situation (from measured nutrient loads in ECO-MARS3D, from PyNuts nutrient loads in MIRO&CO) and percentage of optimal reduction (%) required to reach the 2 levels of thresholds (rigorous and lenient) computed by the Simplex method. Cells in gray point the nutrients which have been reduced in the Simplex optimisation.

Region	0-50 m bathymetric strip				WFD water masses together				MSFD sub-regions together			
Name of the tracer	DIN		DIP		DIN		DIP		DIN		DIP	
	N/P & light free	N/P & light constrained	N/P & light free	N/P & light constrained	N/P & light free	N/P & light constrained	N/P & light free	N/P & light constrained	N/P & light free	N/P & light constrained	N/P & light free	N/P & light constrained
Rigorous marine threshold (µmol/L)	9	9	0.56	0.56	9	9	0.56	0.56	9	9	0.56	0.56
Lenient marine threshold (µmol/L)	19.5	19.5	0.65	0.65	19.5	19.5	0.65	0.65	19.5	19.5	0.65	0.65
ECO-MARS3D grid												
above rigorous threshold, optimisable meshes	2636	330	581	334	834	4	97	4	1658	29	127	29
above lenient threshold, optimisable meshes	542	155	490	228	103	2	79	2	171	27	99	27
UK (Thames & small UK south) PRESENT (µmol/L)	384	384	7.3	7.3	384	384	7.3	7.3	384	384	7.3	7.3
UK (Thames & small UK south) rigorously OPTIMIZED (%)	-67	0	0	0	-65	0	0	0	0	0	0	0
UK (Thames & small UK south) leniently OPTIMIZED (%)	0	0	0	0	0	0	0	0	0	0	0	0
NL-BE (Rhine, Meuse & Scheldt) PRESENT (µmol/L)	197	197	8.0	8.0	197	197	8.0	8.0	197	197	8.0	8.0
NL-BE (Rhine, Meuse & Scheldt) rigorously OPTIMIZED (%)	-89	-86	-83	-83	-81	-86	-65	-61	-77	0	-61	0.0
NL-BE (Rhine, Meuse & Scheldt) leniently OPTIMIZED (%)	-68	-69	-79	-78	-35	-37	-51	-48	-19	0	-48	0.0
FR-East (Seine & small FR) PRESENT (µmol/L)	431	431	3.2	3.2	431	431	3.2	3.2	431	431	3.2	3.2
FR-East (Seine & small FR) rigorously OPTIMIZED (%)	-98	-82	-81	-81	-83	0	0	0	-98	-82	-81	-81
FR-East (Seine & small FR) leniently OPTIMIZED (%)	-96	-80	-81	-81	-39	0	0	0	-96	-80	-81	-81
FR-West (Loire & small FR) PRESENT (µmol/L)	267	267	3.5	3.5	267	267	3.5	3.5	267	267	3.5	3.5
FR-West (Loire & small FR) rigorously OPTIMIZED (%)	-76	0	0	0	-67	0	0	0	-76	0	0	0
FR-West (Loire & small FR) leniently OPTIMIZED (%)	-18	0	0	0	0	0	0	0	-18	0	0	0
MIRO&CO grid												
above rigorous threshold, optimisable meshes	649	46	254	47	220	4	99	4	317	1	65	1
above lenient threshold, optimisable meshes	219	49	174	16	77	2	63	2	87	1	41	1
UK (Thames) PRESENT (µmol/L)	1171	1171	45	45	1171	1171	45	45	1171	1171	45	45
UK (Thames) rigorously OPTIMIZED (%)	-96	-71	-93	-69	-86	0	-76	0	0	0	0	0
UK (Thames) leniently OPTIMIZED (%)	-86	-36	-91	-59	-51	0	-68	0	0	0	0	0
NL (Rhine & Meuse) PRESENT (µmol/L)	259	259	6.4	6.4	259	259	6.4	6.4	259	259	6.4	6.4
NL (Rhine & Meuse) rigorously OPTIMIZED (%)	-90	-60	-75	-63	-91	-58	-77	-47	-77	0	-38	0
NL (Rhine & Meuse) leniently OPTIMIZED (%)	-69	-54	-67	-52	-73	-21	-70	-30	-19	0	-17	0
BE (Scheldt & small BE) PRESENT (µmol/L)	656	656	12.2	12.2	656	656	12.2	12.2	656	656	12.2	12.2
BE (Scheldt & small BE) rigorously OPTIMIZED (%)	-98	-96	-94	-97	-83	0	-42	0	-98	0	-97	0
BE (Scheldt & small BE) leniently OPTIMIZED (%)	-96	-98	-93	-97	-41	0	-23	0	-98	0	-97	0
FR-East (Seine & small FR) PRESENT (µmol/L)	456	456	4.7	4.7	456	456	4.7	4.7	456	456	4.7	4.7
FR-East (Seine & small FR) rigorously OPTIMIZED (%)	-95	-69	-66	-60	-90	0	-36	0	-95	-69	-66	-60
FR-East (Seine & small FR) leniently OPTIMIZED (%)	-83	-80	-57	-49	-66	0	-17	0	-83	-48	-57	-49

The DTT technique based on numerical models offers a refined perspective on the necessary nutrient reductions in all rivers simultaneously. On the overall, the DTT optimization exercise shows differences between the percentage reduction requested to reach the marine thresholds according to the target region considered (0-50 m strip, WFD and MSFD regions). It emphasizes the importance of the choice of the area on which marine thresholds have to be reached. Also, the difference between the "rigorous" and the "lenient" cases is significant, and for some rivers it may result in halving the necessary nutrient reduction (e.g. DIN reduction in Rhine river group targeting the WFD water masses, see Table 12). The difference between "rigorous" and "lenient" gives a range of potential reductions that somewhat reflects the difference between reaching background values (i.e. close to the pristine situation) and reaching more realistic values (closer to the recommended WFD/MSFD thresholds). Finally, the results also show differences in nutrient reductions between the optimization that takes, or alternately that does not take, into account the light availability and the N/P ratio in the bioavailability of nutrients at sea (N/P & light constrained). The additional constraint of the light availability and the N/P ratio drastically reduces the bioavailable nutrients and, hence, the number of marine meshes being above the thresholds in the current situation. This, in turn, lowers considerably the nutrient reductions imposed to the rivers. For that same reason, the achievement of GEnS in WFD and MSFD areas sometimes only requires nutrient reductions in one group of rivers (respectively NL (Rhine/Meuse) or FR-East (Seine) in MIRO&CO, NL-BE (Rhine/Meuse/Scheldt) or FR-East (Seine) in ECO-MARS3D). Obviously, this result is challenging the common sense even if it is accepted that there is no need to reduce nutrient loads in low-light areas where photosynthesis does not occur.

The DTT results should be taken with caution for at least three reasons:

1/ For both ECO-MARS3D and MIRO&CO, in case of "N/P & light constraints", the number of cells above the thresholds that can be optimized is in some cases very low (values in red in Table 12) and the results calculated on this very low number of cells must be taken with caution.

2/ The refinement of the optimization technique in the present case focuses on the occurrence of light-limited phytoplankton production in nutrient-enriched areas. The light-limitation of phytoplankton production is a complex topic as it has been shown that some species are adapted to very low-light conditions, and that some species may acclimate to low-light conditions and perform net phytoplankton production in very turbid areas. Therefore, the concept of light-limited production may not be relevant for all coastal areas across the NEA, or at least it should not be implemented in a uniform way but it should instead take into account the natural variability of adaptation and acclimation mechanisms.

3/ Some rivers may be submitted to higher human pressures and, hence, higher nutrient loads than others due to the combination of the necessary land use and their natural capacity to filter the nutrients. The present study shows that, even in the LocOrgDem scenario, it is not yet possible to achieve "good" levels of nitrate concentrations (0.45-2.25 mgN L^{-1}) in some rivers (north of France, Belgium, The Netherlands and south of UK, see Figure 59). Theoretically, the optimization technique could also consider the practical feasibility of a nutrient reduction, or the economical and political constraints. Taking that into account could perhaps result in another repartition of the national efforts in nutrient reduction necessary to reach the GEnS.

4.1.2 Realistic future reductions: the scenarios

4.1.2.1 Effects of scenarios in the rivers

A first message learned from the prospective analyses carried out for the 174 river basins included in the EMoSEM case study is the limited room for improving water quality based on adding or upgrading wastewater treatment plants (WWTPs). The Urban Wastewater Directive (Directive 91/271/EEC) is actually almost fully implemented for most of EU Member States. With additional effort for reducing the use of phosphates and other phosphorus compounds in household laundry products, human emissions of phosphorous to the rivers are now reduced to their minimum. Improved nitrogen removal by WWTPs leads to only few noticeable improvements (very localized in the NEA domain), because agriculture is actually the major source of nitrogen contamination in most NEA rivers. The results obtain with the UWTD scenario (Figure 52 and Figure 53) confirm the limited impact on overall nitrogen loading of reducing point sources and emphasize the need to target diffuse sources to significantly reduce nitrogen contamination. Ongoing changes in European agricultural activities toward more reasoned practices (scenario GAP, including UWTD) appear as a very promising option for mitigating nitrogen emissions and exports. It allows to significantly reduce nitrate contamination in most of the NEA Rivers. However it does not enable to reach a generalized good quality status in the rivers (cf. GAP nitrogen map, Figure 55). Such achievement implies in-depth changes in the agro-food systems and reconnecting crop production and livestock farming, as well as agriculture and local human food consumption. These more radical options are included in the Local-Organic and Demitarian scenario (LocOrgDem, Figure 57) and should be considered as the most efficient measure to seriously reduce N contamination of water resources and nutrient fluxes to the sea.

4.1.2.2 Effects of scenarios in the sea

There are three messages that come out from the model results analysis. Firstly, the reduction scenario LocOrgDem appears as the most efficient scenario because of the significant N reduction implemented in the river and marine waters. Secondly, the indicator Chl P90 is not always sufficient to estimate the GEnS in the sea when nutrient reduction scenarios are applied, and the presence of undesirable species must be quantified. Thirdly, the WFD/MSFD thresholds for winter nutrients are only partially consistent with background levels derived from the pristine situation. More consistency could be achieved if, for instance, a ratio between winter DIN and DIP threshold values was set around 30 molN $molP^{-1}$ in the enriched coastal zones of the NEA (see below, section 4.2.2).

The nutrient reduction obtained with the LocOrgDem scenario mainly affects marine winter DIN concentrations, while winter DIP concentration is only marginally affected. The consequence of a significant DIN reduction is a modification of the DIN:DIP ratio and of the DIN:DSi ratio, which in turn changes the phytoplankton composition in the sea towards a more favorable status (i.e. a higher diatom:non-diatom ratio on average in the period Mar-Oct). On the other hand, the marginal DIP reduction resulted in only small changes in the Chl P90 along the coasts of the NEA, and was also reflected in the SBNS by the very low reduction achieved in the spring maximum of colonial *Phaeocystis*. This supports previous conclusions (Conley et al. 2009, Desmit et al. 2015) stating that a dual-nutrient reduction should be applied in coastal zones as a P-reduction will mostly reduce the spring peak of

chlorophyll *a* and a N-reduction (compared to P and Si) will mostly mitigate the development of undesirable species biomass. That conclusion is again supported by this study as only the pristine situation shows low levels of winter DIP compared to the Reference, and a concomitant reduction in Chl P90.

Even if the Chl P90 is not significantly reduced after the nutrient reduction in the rivers (LocOrgDem scenario) the phytoplankton composition changes toward less presence of undesirable species when nutrient reductions are applied. For instance, the LocOrgDem scenario reduces the mean (Mar-Oct) abundance of the undesirable colonial *Phaeocystis* while diatoms are maintained at comparable levels as in the Reference situation (in SBNS, see Figure 69 and Figure 70). This suggests that the assessment of the GEnS should not be made only on the basis of the Chl P90 but should also take into account the relative proportion of phytoplankton nuisance species. In this project, a new indicator NDAChl was proposed to gather all non-diatom species into one group. It must be pointed out that not all non-diatoms are nuisance species, or even undesirable species. But the NDAChl is an attempt at defining a more universal indicator that could eventually be applied across the NEA, even if the present study only shows results in the SBNS.

4.1.3 Requirements for GEnS vs. best future scenario

One of the main objectives in EMoSEM was to compare the necessary nutrient reductions to reach the GEnS (from DTT) and the "realistic" nutrient reductions potentially relevant in the future (from best scenario) in order to outline some advices to the end-users and support the decision. Table 13 indicates the achievable percentage reduction of DIN in each river group (red number). The numbers obtained in scenario LocOrgDem (best scenario) may be compared to the percentage reduction obtained for DIN with the DTT technique applied to ECO-MARS3D (largest domain, Table 12).

As explained above (section 4.1.1.2), the range of nutrient reduction estimated necessary by the DTT exercise to reach the GEnS depends on the target area and on the constraints applied to the optimization. The range of unconstrained ("N/P and light free") N reduction needed in the FR-West (Loire) river group is 0-67% (in WFD area, respectively for "lenient" or "rigorous" optimization) and 18-76% (in MSFD area, respectively for "lenient" or "rigorous" optimization), which matches well the 66.8% N reduction obtained with LocOrgDem ("Loire-Bretagne" group). In the FR-East river group (Seine and small FR rivers), the range is 39-83% (WFD) and 96-98% (MSFD), which must be compared to a 55.8% reduction in the LocOrgDem scenario ("Seine-Somme"). In the NL-BE river group (Rhine/Meuse/Scheldt), the needed N-reduction range is 35-81% (WFD) and 19-77% (MSFD), which is compared to 51% reduction in LocOrgDem ("Rhine-Scheldt"). And the UK river group ("Thames and small UK south") needs N reductions within the range 0-65% (WFD) and 0-0% (MSFD), which compares with 44.6% in LocOrgDem ("British Islands").

In most river groups, the N reductions obtained in the LocOrgDem scenario are within the range of necessary reductions, and even closer to the high values ("rigorous"), except in the Seine river group if the MSFD area is the target. This qualifies the LocOrgDem scenario as a potential solution to mitigate eutrophication in most NEA areas (here from the Bay of Biscay to the SBNS). And in the case of the "N/P & Light constrained" optimization (which should be taken with caution), the LocOrgDem also responds

to the needs in reduction, though not completely regarding the Seine river group (MSFD target area). Figure 59 shows that, even in the LocOrgDem scenario, a good quality status is hardly achievable in some French (north), Belgian, Dutch and UK rivers.

As DIP does not change much between scenarios, such a comparison was not made for that nutrient. It is, however, important to consider whether more DIP reductions could be achieved in order to specifically reduce the magnitude of the colonial *Phaeocystis* spring maximum in some eutrophied areas of the SBNS.

Table 13: Sum of N dry loads per river group for the pristine and reference situations and for the three scenarios. The respective percentage reduction in each river group is indicated for the three scenarios in red between brackets.

kgN/day	Pristine	Reference	UWTD	GAP	LocOrgDem
Spain - Portugal	130251	1267697	1221494 (-3.6 % ref)	1078426 (-14.9 % ref)	894313 (-29.5 % ref)
Bay of Biscaye	85800	850011	847037 (-0.3 % ref)	722877 (-15 % ref)	513675 (-39.6 % ref)
Loire - Bretagne	51484	872192	871966 (0 % ref)	727383 (-16.6 % ref)	289530 (-66.8 % ref)
Seine - Somme	31747	574621	539877 (-6 % ref)	395170 (-31.2 % ref)	253914 (-55.8 % ref)
Rhine - Schelde	121942	1647438	1642590 (-0.3 % ref)	1367291 (-17 % ref)	807399 (-51 % ref)
British Isles	47964	694266	652496 (-6 % ref)	641332 (-7.6 % ref)	384667 (-44.6 % ref)

4.2 Products of EMoSEM and Consistency in EU directives

4.2.1 Products of EMoSEM

Ecozones have been defined in this study as transboundary subareas across the NEA delimited on the basis of satellite-borne multiyear-averaged chlorophyll *a* P90. These Ecozones allowed us to measure the effects of nutrient reduction in similar area types (e.g. highly eutrophic vs. oligotrophic) across the NEA. There are four Ecozones determined on the basis of long-term average of RS Chl P90, with boundary values equal to 2 µgChl L^{-1}, 4 µgChl L^{-1} and 8 µgChl L^{-1}. By plotting the spatial frequency distribution (PDF) of indicators inside each Ecozone, the central and optimal tendencies were clearly identified for each indicator, which allowed comparing the effects of different scenarios. Also, matching the PDF of an indicator with its reference level allowed to compute the relative geographical area where the parameter shows higher values than the reference level.

Regarding the known indicator Chl P90, the maximum value of coastal Chl P90 in the pristine situation was proposed as a background value, i.e. 8 µgChl L^{-1}. Moreover, as it was concluded that Chl P90 should not be the only indicator used in the assessment of GEnS, an indicator reflecting the presence of undesirable species (NDAChl) was also proposed to measure the effect of nutrient reduction scenarios on marine eutrophication. NDAChl encompasses all non-diatom species, which show some risks of being undesirable species. In this study, the reference value 2 µgChl L^{-1} was defined for the haptophyte *Phaeocystis globosa* in the SBNS. Other reference values should be set for the other undesirable species.

4.2.2 Consistency between DIN and DIP background values

In the nutrient reduction scenarios, it has been shown that some background values could be derived from the maximum values obtained in the pristine situation. These background values are informative regarding the consistency between winter DIN and winter DIP threshold values used in the WFD/MSFD. Regarding the winter DIN:DIP ratio, the reference (global oceanic mean) value of 16 molN $molP^{-1}$ seems to be outmatched in most coastal areas of the NEA even under pristine conditions (Figure 68). Apparently, "natural" pristine levels of the winter DIN:DIP ratio may reach higher values than 16 molN $molP^{-1}$ (up to 32 molN $molP^{-1}$ in some coastal areas) due to river "natural" enrichment. This value of 32 molN $molP^{-1}$ is comparable to the ratio between the maximum pristine winter DIN and winter DIP (i.e. 15/0.5=30 molN $molP^{-1}$, Figure 77 and Figure 78), whereas the ratio of the respective WFD/MSFD thresholds gives much lower values (e.g. 15/0.8=18.75 molN $molP^{-1}$ for the Belgian coastal waters). This advocates for a harmonisation of the winter DIP and winter DIN thresholds of the MSFD, at least in some coastal zones where high ratios are found even under pristine conditions. If a threshold value is chosen for winter DIN or for winter DIP, then a ratio of 30 molN $molP^{-1}$ could link the two threshold values in all "naturally enriched" coastal areas. For instance, if the threshold value of DIN was set at 15 µmol L^{-1}, then the threshold value of winter DIP in the "naturally enriched" coastal areas should be set at 0.5 µmol L^{-1}. Inversely, if the threshold value of winter DIP was set at 0.8 µmol L^{-1} (i.e. the case of Belgian waters), then the threshold value of winter DIN could be levelled up to 24 µmol L^{-1}. In the latter case, the application of a winter DIN:DIP ratio of 30 to define the thresholds would result in winter DIN and winter DIP threshold values that are in very good accordance with the average coastal values obtained in the LocOrgDem scenario (i.e. winter DIP = 0.8 µmol L^{-1} compared to threshold 0.8 µmol L^{-1}, and winter DIN = 18.3 µmol L^{-1} compared to threshold 24 µmol L^{-1}). This reflection about the consistency between DIN and DIP threshold values is supported by the fact that higher DIN:DIP ratios than 16 molN $molP^{-1}$ may sometimes be compatible with good environmental conditions in coastal zones. For instance, Desmit et al. (2015) concluded that DIN:DIP ratio values equal to 34.4 molN $molP^{-1}$ would still be tolerable in Belgian coastal waters (and 28.6 molN $molP^{-1}$ in Dutch waters) with respect to the objective of mitigating undesirable levels of *Phaeocystis* colonies. Similar studies are still to be made for other coastal zones in the NEA.

5 GENERAL CONCLUSION

Nitrogen input to the sea remains a major issue preventing the good ecological status in most coastal zones of the NEA. Modelling tools have been developed and combined to describe the river-ocean continuum in the NEA continental seas. Three marine ecological models (BIOPCOMS, ECO-MARS3D, MIRO&CO) and one generic ecological model for European river-basins (PyNuts-Riverstrahler) have been developed and validated. By using these models, the eutrophication nuisances in marine regions from the Iberian shelf to the SBNS have been linked to anthropogenic inputs, and the source of eutrophication has been identified in the watersheds. The current agricultural practices are the main sources of nitrogen to the rivers and to the sea through diffuse pathways. It was shown that the implementation and upgrading of wastewater treatment plants required by the UWWTD were almost complete. As a result, the P reductions are currently close to their maximum as required by the WFD.

The current eutrophication status (i.e. the Reference situation) has been compared with a reconstructed natural status (i.e. the Pristine situation) to scale the effect of anthropogenic nutrient inputs into the sea. In the Pristine situation, the riverine nutrient inputs reached low levels and achieved the GEnS across the NEA. The TBNT study showed how the oceanic waters became in the Pristine situation the highest contributor to nutrient inputs in some currently eutrophied coastal zones (e.g. in the Pristine situation, 90% of the nitrogen present in the Belgian coastal waters is coming from the Atlantic compared to 20% in the current situation). This confirms that human activities in the river watersheds are the cause of the marine eutrophication. It was shown that in the Pristine situation, the DIN and DIP levels allowed a considerably low Chl P90 across the NEA compared to the current situation. A study of the PFT composition in the SBNS showed that, in the Pristine situation, the phytoplankton assemblage was dominated by diatoms, and that *Phaeocystis* abundance never reached the reference level (4×10^6 cells L^{-1}).

The mitigation of current eutrophication by river loads reduction requires to identify all contributive sources of nutrients in the target marine areas. The transboundary nutrient transport (TBNT) technique is a useful modelling tool to achieve that objective. The TBNT showed that along the Iberian Peninsula, significant river-borne nutrient transport may be observed in the coastal zones, though there is hardly any remote transboundary exchange of nutrients. It also showed, the large influence of Portuguese rivers on nitrogen concentrations in the sea during the wet season in summer, and a significant contribution of the Loire river nitrogen on the phytoplankton production along the coast of Brittany and up to the English Channel where it accounts for 10% of the production. The TBNT is generally high in the English Channel and the SBNS, due to the combination of high nutrient loads from the rivers and the patterns of water transport. The TBNT study emphasized the need to operate a reduction of the atmospheric N depositions in parallel to any future riverine nutrient reduction (no reduction in N depositions was tested in this study).

The distance-to-target (DTT) exercise provided useful information regarding the river load reductions necessary to reach the GEnS in target areas. A conclusion is that reducing the transboundary contamination and mitigating eutrophication to reach the GEnS imply a dual-nutrient reduction (N,P) in the rivers. Several target areas (0-50m bathymetric strip, WFD and MSFD) have been considered in the

exercise, and the extension of the target area influences the result of the DTT. The method applied in the present DTT exercise differs from previous studies and focuses on the "fully bioavailable" nutrients, which is a considerable improvement to previous studies as the necessary nutrient reductions are better estimated. Two DTT exercises were tested to estimate the range between a "rigorous" case (i.e. targeting background values of indicators) and a "lenient" case (i.e. targeting levels closer to the WFD/MSFD thresholds).

In parallel to the theoretical DTT study, three "realistic" scenarios have been tested to explore different options of nutrient emission reduction (upgrading wastewater treatment plants (UWTD), reasoned agricultural practices (GAP), conversion to local, organic farming and demitarian diet (LocOrgDem)). A conclusion of this study is that any significant change in the GEnS across the NEA will require a deep change in agricultural practices. Another conclusion is that most WWTPs required by the UWWTD are already operational in the contemporary situation as winter DIP was never significantly reduced in any scenarios. While the development of more reasoned agricultural practices (GAP scenario) significantly improves the ecological status of European rivers, it does not lead to the GEnS in the marine ecosystems. The most promising "realistic" scenario is the LocOrgDem, which implies in-depth cultural and technical changes. In this scenario, the marine winter DIN was significantly reduced, inducing a decrease in the DIN:DIP and the DIN:DSi ratios. This, in turn, resulted in a positive change in the phytoplankton composition of the SBNS, with a reduced presence of the undesirable species *Phaeocystis globosa*. In contrast, neither the winter DIP nor the Chl P90 were significantly reduced across the NEA in LocOrgDem compared to the current situation.

The theoretical river loads reduction required for the achievement of GEnS in the sea, and identified by the DTT exercise, were compared to the best "realistic" future river loads reduction, given by the LocOrgDem scenario. The comparison showed that the LocOrgDem scenario resulted in N reductions in the range of the required N reductions for each group of rivers, except for the Seine river group (MSFD area). This is explained by the fact that some rivers in the north of France would not always reach the good quality status regarding nitrogen, even in the LocOrgDem scenario. Still, the nutrient reductions in the LocOrgDem scenario are generally in the upper range ("rigorous" case) of the reductions calculated by the DTT, suggesting that the status of eutrophication might be significantly improved if a scenario like LocOrgDem was implemented in reality.

The EMoSEM project stimulated the rational to more universal and transboundary approaches to estimate the GEnS in large areas like the NEA, which encompasses several Member States. This led to design transboundary Ecozones across the NEA (i.e. sub-area determined on the basis of satellite-borne long-term averaged Chl P90). This is an attempt to measure the effects of nutrient reduction across the NEA, from the Iberian shelf to the North Sea, in sub-areas that present an ecological meaning (e.g. highly eutrophic vs. oligotrophic) instead of in sub-areas constrained only by political boundaries. During the project, some thoughts have also been devoted to the relevance of WFD/MSFD indicators and to the consistency between indicators threshold values. As Chl P90 did not change significantly in the three scenarios, whereas N reductions were observed, it was proposed to also take the PFT composition into account when assessing the GEnS in the sea. A novel indicator has been proposed to complement Chl P90, i.e. the non-diatom chlorophyll *a* (NDAChl). In the SBNS, a reference value for this indicator was

suggested equal to 2 µgChl L^{-1} based on the undesirable colonial haptophyte *Phaeocystis globosa*. The ratio between winter DIN and winter DIP in some coastal zones indicates some inconsistency in the threshold recommended by the WFD/MSFD in some coastal zones. The background value of the winter DIN:DIP ratio, taken as the maximum coastal value of DIN:DIP across the NEA in the pristine situation, is close to 30 molN $molP^{-1}$ whereas the ratio of winter DIN and winter DIP WFD/MSFD thresholds is closer to 18 molN $molP^{-1}$ (Belgian coastal waters).

EMoSEM has engaged many efforts in numerical modelling from all partner teams in order to reach an accurate estimate of the pristine and the current status of eutrophication across the NEA. This study allowed quantifying better the required nutrient levels to reach the GEnS in riverine and marine systems and to link them with precision to human activities. Changes in nutrient loads resulted in effects on the large-scale in the sea, which were identified and quantified. Finally, the project proposed realistic solutions to characterize and to improve the environmental status of the European western rivers and of the North-East Atlantic waters in the future.

5.1.1.1 Acknowledgements

This research was supported by the EMoSEM project, a two-year project (2013-2014) funded by the French National Research Agency (ANR) and the Belgian Science Policy (BELSPO, SD/ER/11) in the frame of EU FP7 ERA-NET Seas-era.

The EMoSEM consortium was supported by 3 “collaborators” from neighbor countries (GE, NL and UK) not eligible for funding, who shared their knowledge and data in the frame of the OSPAR ICG-EMO. Throughout the project, we had fruitful discussions with Hermann Lenhart (UHAM, GE), Tineke Troost (Deltares, NL) and Johan vander Molen (CEFAS, UK) who participated to annual and/or final project meeting. We also had useful discussions with Wendy Bonne (JPI Ocean) who participated in the Kick Off and the final meeting as a representative of End-Users.

Microwave OI SST data are produced by Remote Sensing Systems and sponsored by National Oceanographic Partnership Program (NOPP), the NASA Earth Science Physical Oceanography Program, and the NASA MEaSUREs DISCOVER Project. Data are available at www.remss.com. SeaWiFS, MODIS-Aqua, GSM V6 analyses used in this study were produced with the Giovanni online data system, developed and maintained by the NASA GES DISC. The GlobColour primary data set is part of the core data set of the Group on Earth Observations System of Systems (GEOSS) under reference: urn:geoss:csr:resource:urn:uuid:4e33fd81-d5cc-dc40-b645-ab961447d9d8. The atmospheric depositions of nitrogen (2000-2010) computed in the frame of the “European Monitoring and Evaluation Program (EMEP)” have been put at disposal of EMoSEM by Semeena Valiyaveetil and Jerzy Bartnicki (met.no). We also acknowledge the European Centre for Medium-Range Weather Forecasts (ECMWF) for the very efficient and friendly support that enabled us to perform the MIRO&CO simulations.

5.1.1.2 References

Allen JI, Holt J, Blackford J, Proctor R (2007). Error quantification of a high-resolution coupled hydrodynamic-ecosystem coastal-ocean model: Part 2. Chlorophyll-a, nutrients and SPM. Journal of Marine Systems 68: 381-404.

Alvarez I, Lorenzo MN, deCastro M (2012). Analysis of chlorophyll *a* concentration along the Galician coast: seasonal variability and trends. – ICES Journal of Marine Science 69: 728–738.

Aminot A, Guillaud JF, Kérouel R (1997). La baie de Seine: hydrologie, nutriments et chlorophylle _1978–1994. Edition IFREMER, Repères Océan 14, 148 pp.

Arzul G, Erard-Le Denn E, Belin C, N´ezan E (1995). Ichtyotoxic events associated with Gymonodinium cf. nagasakiense on the Atlantic coast of France. Harmful Algal News 2–3:8–9.

Baretta-Bekker JG, Baretta JW, Latuhihinc MJ, Desmit X, Prins TC (2009). Description of the long-term (1991–2005) temporal and spatial distribution of phytoplankton carbon biomass in the Dutch North Sea. Journal of Sea Research, 61: 50-59. http://dx.doi.org/10.1016/j.seares.2008.10.007.

Billen G, Dessery S, Lancelot C, Meybeck M (1989). Seasonal and interannual variations of nitrogen diagenesis in the sediments of a recently impounded basin. Biogeochemistry 8:73–100.

Billen G, Garnier J, and Hanset P (1994). Modelling phytoplankton development in whole drainage networks: the RIVERSTRAHLER Model applied to the Seine river system. Hydrobiologia 289: 119-137.

Billen G, Garnier J (2007). River basin nutrient delivery to the coastal sea: assessing its potential to sustain new production of non-siliceous algae, Mar. Chem., 106 : 148–160, doi:10.1016/j.marchem.2006.12.017.

Billen G, Garnier J, Silvestre M (2015). A generic algorithm for modelling benthic nutrient fluxes in river systems. Int. J. Limnol 51: 37-47. http://dx.do.org/10.1051/limn/201403.

Billen G, Servais P (1989). Modélisation des processus de dégradation bactérienne de la matière organique en milieu aquatique. In: Bianchi M, Marty D, Bertrand JC, Caumette P, Gauthier M (eds) Micro-organismes dans les écosystèmes océaniques. Masson, Paris, p 219–245.

Bowie GL, Mills WB, Porcella DB, Campbell CL, Pagenkopf JR, Rupp GL, Johnson KM, Chan PWH, Gherini SA and Chamberlin CE (1985). Rates, constants, and kinetic formulations in surface water quality modeling. U.S. Environmental Protection Agency.

Calens J, Silvestre M, Garnier J, Billen G (2010). Impact du changement climatique sur la qualité biogéochimique de la Loire et de ses affluents). Rapport final projet HYDROQUAL, Plan Loire Grandeur Nature, Septembre 2010, 31pp.

Campuzano FJ, Kenov I, Brito D, Juliano M, Fernandes R, Pinto L, Neves R (2014). Numerical evaluation of the river nutrients influence for the Western Iberian coastal region. 3.as Jornadas de Engenharia Hidrográfica, 24-26 June 2014, Lisbon, Portugal. Extended abstracts: 263-266.

Carletti A, Heiskanen AS (2009). Water Framework Directive intercalibration technical report. Part, 3, 240.

Chapelle A, Lazure P, Ménesguen A (1994). Modelling eutrophication events in a coastal ecosystem. Sensitivity analysis. Estuar., Coast. and Shelf Sci. 39: 529-548.

Cloern JE and Jassby AD (2010). Patterns and scales of phytoplankton variability in estuarine–coastal ecosystems. Estuaries and Coasts 33(2): 230-241.

Conley DJ, Paerl HW, Howarth RW, Boesch DF, Seitzinger SP, Havens KE, Lancelot C, Likens GE (2009). Controlling eutrophication: nitrogen and phosphorus. Science 323 (5917): 1014-1015.

Crespo BG, Teixeira IG, Figueiras FG, Castro CG (2008). Microplankton composition off NW Iberia at the end of the upwelling season: source areas of harmful dinoflagellate blooms. Marine Ecology Progress Series 355:31-43.

Daniel A, Soudant D (2010). Evaluation DCE mai 2010: Elément de qualité: nutriments, Document général pour les masses d'eaux de la France métropolitaine, hors lagunes méditerranéennes – Convention 2009 – Action 4. Onema, Ref. DYNECO/PELAGOS/10.03, http://archimer.ifremer.fr/doc/00019/12991/.

Danzig GB (1963). Linear Programming and Extensions. Princeton University Press, Princeton, N.J.

Daro M-H, Breton E, Antajan E, Gasparini S, Rousseau V (2006). Do *Phaeocystis* colony blooms affect zooplankton in the Belgian coastal zone? p. 61-72. In V. Rousseau, C. Lancelot and D. Cox [eds.], Current status of eutrophication in the Belgian coastal zone. Presses Universitaires de Bruxelles, Bruxelles.

Deleersnijder EL (1989) Upwelling and upsloping in three-dimensional marine models. Applied Mathematical Modelling, 13: 462-467. doi: 10.1016/0307-904X(89)90094-2.

Desmit X, Ruddick K and Lacroix G (2015). Salinity predicts the distribution of chlorophyll *a* spring peak in the southern North Sea continental waters. Journal of Sea Research 103:59-74.

De Vries W, Reinds GJ, Deelstra HD, Klap JM, Vel EM (1998). Intensive monitoring of Forest Ecosystems in Europe-1998 Technical report. Intensive monitoring of Forest Ecosystems in Europe: 1998 Technical report.

Drillet Y, Bourdalle-Badi R, Siefrid L, Le Provost C (2005). Meddies in the Mercator North Atlantic and Mediterranean Sea eddy-resolving model. Journal of Geophysical Research 110(C3): C03016.

Eckhardt K (2008). A comparison of baseflow indices, which were calculated with seven different baseflow separation methods. J. Hydrol. 352, 168–173.

Erard-Le Denn E, Belin C, Billard C (2001). Various cases of ichtyotoxic blooms in France. In: Arzul G., (Ed.), Aquaculture environment and marine phytoplankton. 21-23 May 1992, Brest (France).

Falkowski PG and Davis CS (2004). Natural proportions. Nature 431: pp.131.

Ferreira JG, Andersen JH, Borja A, Bricker SB, Camp J, Cardoso da Silva M, Garcés E, Heiskanen A-S, Humborg C, Ignatiades L, Lancelot C, Ménesguen A, Tett P, Hoepffnerm N, Claussen U (2011). Overview of eutrophication indicators to assess environmental status within the European Marine Strategy Framework Directive. Estuarine, Coastal and Shelf Science 93(2): 117-131.

Garcia HE, Locarnini RA, Boyer TP, Antonov JI, Baranova OK, Zweng MM, Johnson DR (2010a). World Ocean Atlas 2009, Volume 3: Dissolved Oxygen, Apparent Oxygen Utilization, and Oxygen Saturation. S. Levitus, Ed. NOAA Atlas NESDIS 70, U.S. Government Printing Office, Washington, D.C., 344 pp.

Garcia HE, Locarnini RA, Boyer TP, Antonov JI, Zweng MM, Baranova OK, Johnson DR (2010b). World Ocean Atlas 2009, Volume 4: Nutrients (phosphate, nitrate, silicate). S. Levitus, Ed. NOAA Atlas NESDIS 71, U.S. Government Printing Office, Washington, D.C., 398 pp.

Garnier J, Billen G, Coste M (1995). Seasonal succession of diatoms and Chlorophyceae in the drainage network of the river Seine: Observations and modelling. Limnol. Oceanogr. 40: 750-765.

Garnier J, Billen G, Hannon E, Fonbonne S, Videnina Y, Soulie M (2002). Modeling transfer and retention of nutrients in the drainage network of the Danube River, Estuar. Coast. Shelf Sciences 54: 285-308, doi: 10.1006/ecss.2000.0648.

Garnier J, Billen G, Palfner L (1999). Understanding the oxygen budget and related ecological processes in the river Mosel: the RIVERSTRAHLER approach, Hydrobiologia 410:151-166, doi: 10.1023/A:1003894200796.

Gohin F (2011). Annual cycles of chlorophyll-a, non-algal suspended particulate matter, and turbidity observed from space and in-situ in coastal waters, Ocean Sci. 7: 705-732, doi:10.5194/os-7-705-2011.

Gypens N, Lacroix G, Lancelot C (2007). Causes of variability in diatom and *Phaeocystis* blooms in Belgian coastal waters between 1989 and 2003: a model study. Journal of Sea Research 57: 19–35.

Hartmann M. (2011). Corporate Social Responsibility in the Food Sector. European Review of Agricultural Economics 38:297-324.

Holligan PM (1979). Dinoflagellate blooms associated with tidal fronts around the British Isles. Developments in marine biology.

Jickells TD (1998). Nutrient biogeochemistry of the coastal zone. Science, 281(5374): 217-222.

Jones KJ, Ayres P, Bullock AM, Roberts RJ, Tett P (1982). A red tide of *Gyrodinium aureolum* in sea lochs of the Firth of Clyde and associated mortality of pond-reared salmon. J. Mar. Biol. Assoc. U.K. 62: 771–782.

Jones RJA, Hiederer R, Rusco E, Loveland PJ and Montanarella L (2005). Estimating organic carbon in the soils of Europe for policy support. European Journal of Soil Science, October 2005, 56: 655-671.

Kirkby MJ, Jones RJA, Irvine B, Gobin A, Govers G, Cerdan O et al. (2004). Pan-European Soil Erosion Risk Assessment: The PESERA Map, Version 1 October 2003. Explanation of Special Publication Ispra 2004 No.73 (S.P.I.04.73) European Soil Bureau Research Report No.16, EUR 21176, 18pp. and 1 map in ISO B1 format. Office for Official Publications of the European Communities, Luxembourg.

Lacroix G, Ruddick KG, Ozer J, Lancelot C (2004). Modelling the impact of the Scheldt and Rhine/Meuse plumes on the salinity distribution in Belgian waters (southern North Sea). Journal of Sea Research 52: 149-163.

Lancelot C (1995). The mucilage phenomenon in the continental coastal waters of the North Sea. Science of The Total Environment 165 (1-3): 83–102.

Lancelot C, Billen G (1985). Carbon–nitrogen relationship in nutrient metabolism of coastal marine ecosystem. Adv Aquat Microbiol 3: 263–321.

Lancelot C, Billen G, Sournia A, Weisse T, Colijn F, Veldhuis MJW, Davies A, Wassmann P (1987). *Phaeocystis* blooms and nutrient enrichment in the continental coastal zones of the North Sea. Ambio 16: 38-46.

Lancelot C, Passy P and Gypens N (2014). Model assessment of present-day *Phaeocystis* colony blooms in the Southern Bight of the North Sea (SBNS) by comparison with a reconstructed pristine situation. Harmful algae 37:172-182.

Lancelot C, Veth C, Mathot S (1991). Modelling ice edge phytoplankton bloom in the Scotia–Weddell Sea sector of the Southern Ocean during spring 1988. J Mar Syst 2: 333–346.

Lancelot C, Rousseau V, Gypens N (2009). Ecologicaly based indicators for *Phaeocystis* disturbance in eutrophied Belgian coastal waters (Southern North Sea) based on field observations and ecological modelling. Journal of Sea Research 61: 44-49.

Lancelot C, Spitz Y, Gypens N, Ruddick K, Becquevort S, Rousseau V, Lacroix G, Billen G (2005). Modelling diatom and *Phaeocystis* blooms and nutrient cycles in the Southern Bight of the North Sea: the MIRO model. Marine Ecology Porgress Series 289: 63-78.

Lazure P, Dumas F (2008). An external–internal mode coupling for a 3D hydrodynamical model for applications at regional scale (MARS). Advances in Water Resources 31(2): 233-250.

Le Grand J (1994). Bilan du réseau de surveillance phytoplanctonique en Normandie _1989–1992. IFREMER, Rapport Ifremer/DEL/94.09, Port-en Bessin, 72 pp.

Lehner B, R-Liermann C, Revenga C, Vörösmarty C, Fekete B, Crouzet P, Döll P et al. (2008). High resolution mapping of the world's reservoirs and dams for sustainable river flow management. Frontiers in Ecology and the Environment. Source: GWSP Digital Water Atlas (2008). Map 81: GRanD Database (V1.0). Available online at http://atlas.gwsp.org.

Le TPQ, Garnier J, Billen G, Sylvain T, Van Minh C (2007). The changing flow regime and sediment load of the Red River, Viet Nam, Journal of Hydrology 334(1-2): 199-214, doi: 10.1016/j.jhydrol.2006.10.020.

Le Noé J, Billen G, Lassaletta L, Silvestre M, Garnier J (2015, revised). La place du transport de denrées agricoles dans le cycle biogéochimique de 1 l'azote en France : un aspect de la spécialisation des territoires. Cahier agri.

Loewe P (2003). Weekly North Sea SST Analyses since 1968. In: Hydrographie, O.d.a.h.b.B.f.S.u. (Ed.), D-20305 Hamburg, P.O. Box 301220, Germany.

Los FJ, Bokhorst M (1997). Trend analysis Dutch coastal zone. New Challenges for North Sea Research. Zentrum for Meeres-und Klimaforschung. University of Hamburg, 161-175.

Los FJ, Troost TA, Van Beek JKL (2014). Finding the optimal reduction to meet all targets—Applying Linear Programming with a nutrient tracer model of the North Sea. Journal of Marine Systems 131: 91-101.

Luu TNM, Garnier J, Billen G, Le TPQ, Némery J, Orange D, Le LA (2011). N,P and Si budgets for the Red River Delta (Northern Vietnam). How the delta affects river nutrient delivery to the sea?, Biogeochemistry.

Luyten P (2011). COHERENS — A Coupled Hydrodynamical-Ecological Model for Regional and Shelf Seas: User Documentation. Version 2.0. RBINS-MUMM Report, Royal Belgian Institute of Natural Sciences.

Lyard F, Lefevre F, Letellier T, Francis O (2006). Modelling the global ocean tides: modern insights from FES2004, Ocean Dynamics 56: 394-415.

Mateus M, Riflet G, Chambel P, Fernandes L, Fernandes R, Juliano M, Campuzano F, de Pablo H, Neves R (2012). An operational model for the West Iberian coast: products and services, Ocean Science 8: 713-732.

Ménesguen A (1990). Eutrophication along the French coasts. in : "Eutrophication-related phenomena in the Adriatic Sea and in other Mediterranean coastal zones", Bart H., Fegan L. (eds), Proc. Conf. 28-30 May 1990, Rome (Italie), C.E.C. Water Pollution Research Report 16: 63-82.

Ménesguen A, Cugier P, Leblond I (2006). A new numerical technique for tracking chemical species in a multisource, coastal ecosystem, applied to nitrogen causing Ulva blooms in the Bay of Brest (France). Limnology and Oceanography 51(1, part 2): 591-601.

Ménesguen A, Hoch T (1997). Modelling the biogeochemical cycles of elements limiting primary production in the English Channel. I. Role of thermohaline stratification. Mar. Ecol. Prog. Ser. 146: 173-188.

Muylaert K, Gonzales R, Franck M, Lionard M, Van der Zee C, Cattrijsse A, Sabbe K, Chou L, Vyverman W (2006). Spatial variation in phytoplankton dynamics in the Belgian coastal zone of the North Sea studied by microscopy, HPLC-CHEMTAX and underway fluorescence recordings. Journal of Sea Research 55(4): 253-265.

Neves R, 2013. The MOHID concept. In: M. Mateus & R. Neves (eds.). Ocean modelling for coastal management - Case studies with MOHID. IST Press, Lisbon, 1-11.

OSPAR Commission 2008. Second OSPAR Integrated Report on the Eutrophication Status of the OSPAR Maritime Area. OSPAR Eutrophication Series. 372/2008, London, 108pp.

OSPAR Commission 2013. "Distance to target" modelling assessment. OSPAR Eutrophication Series 599/2013, London, 80pp.

Passy P, Gypens N, Billen G, Garnier J, Thieu V, Rousseau V, Callens J, Parent J-Y, Lancelot C (2013). A Model reconstruction of riverine nutrient fluxes and eutrophication in the Belgian Coastal Zone (Southern North Sea) since 1984. Journal of Marine Systems 128: 106-122.

Perrot T, Rossi N, Ménesguen A, Dumas F, (2014). Modelling green macroalgal blooms on the coasts of Brittany, France to enhance water quality management. J. Mar. Sys. 132: 38-53.

Philippart CJM, Beukema JJ, Cadée GC, Dekker R, Goedhart PW, van Iperen JM, Leopold MF, Herman PMJ (2007). Impacts of nutrient reduction on coastal communities. Ecosystems 10(1): 96-119.

Prins TC, Desmit X, Baretta-Bekker JG (2012). Phytoplankton composition in Dutch coastal waters responds to changes in riverine nutrient loads. J. Sea Res. 73: 49-62.

Radach G, Lenhart HJ (1995). Nutrient dynamics in the North Sea: fluxes and budgets in the water column derived from ERSEM. Netherlands Journal of Sea Research 33(3): 301-335.

Redfield AC (1963). The influence of organisms on the composition of sea-water. The sea 26-77.

Riegman R, Noordeloos AA, Cadée GC (1992). *Phaeocystis* blooms and eutrophication of the continental coastal zones of the North Sea. Marine Biology 112(3): 479-484.

Rodriguez F, Fernandez E, Head R, Harbour D, Bratak G, Heldal M, Harris R, 2000. Temporal variability of viruses, bacteria, phytoplankton and zooplankton in the western English Channel off Plymouth. J. Mar. Biol. Ass. U. K. 80: 575–586.

Rossi V, Garçon V, Tassel J, Romagnan J-B, Stemmann L, Jourdin F, Morin P, Morel Y (2013). Cross-shelf variability in the Iberian Peninsula Upwelling System: Impact of a mesoscale filament, Continental Shelf Research 59: 97-114.

Rousseau V, Becquevort S, Parent J-Y, Gasparini S, Daro M-H, Tackx M, Lancelot C (2000). Trophic efficiency of the planktonic food web in a coastal ecosystem dominated by *Phaeocystis* colonies. Journal of Sea Research 43: 357-372.

Rousseau V, Park Y, Ruddick K, Vyverman W, Parent J-Y, Lancelot C (2006). Phytoplankton blooms in response to nutrient enrichment. In: Rousseau V, Lancelot C, Cox D (Eds.), Current Status of

Eutrophication in the Belgian Coastal Zone. Presses Universitaires de Bruxelles, Bruxelles, pp. 45-59.

Ruelland D, Billen G., Brunstein D, Garnier J (2007). SENEQUE 3: a GIS interface to the RIVERSTRAHLER model of the biogeochemical functioning of river systems, Science of the Total Environment 375: 257-273, doi: 10.1016/j.scitotenv.2006.12.014.

Sá C (2013). Ocean Colour off the Portuguese Coast: Chlorophyll a products validation and applicability. PhD Thesis. Universidade de Lisboa.

Sathyendranath S, Stuart V, Nair A, Oka K, Nakane T, Bouman H, Forget M-H, Maass H, Platt T (2009). Carbon-to-chlorophyll ratio and growth rate of phytoplankton in the sea. Marine Ecology Progress Series 383: 73-84.

Sferratore A, Billen G, Garnier J, Smedberg E, Humborg C, Rahm L (2008). Modelling nutrient fluxes from sub-arctic basins: comparison of pristine vs. dammed rivers, Journal of Marine Systems 73(3-4): 236-249. doi: 10.1016/j.jmarsys.2007.10.012.

Sirjacobs D, Alvera-Azcárate A, Barth A, Lacroix G, Park Y, Nechad B, Ruddick K, Beckers J-M (2011). Cloud filling of ocean color and sea surface temperature remote sensing products over the Southern North Sea by the Data Interpolating Empirical Orthogonal Functions methodology. J Sea Res 65(1): 114–130.

Strahler AN (1957). Quantitative analysis of watershed geomorphology, Transactions of the American Geophysical Union 38 (6): 913–920, doi:10.1029/tr038i006p00913.

Taylor K (2001). Summarizing multiple aspects of model performance in a single diagram. Journal of Geophysical Research-Atmospheres V106, D7.

Troost TA, Blaas M, Los FJ (2013). The role of atmospheric deposition in the eutrophication of the North Sea: A model analysis. Journal of Marine Systems 125: 101–112.

Vogt JV, Soille P, de Jager A, Rimaviciute E, Mehl W, Foisneau S, Bodis K, Dusart J, Paracchini ML, Haastrup P, Bamps C (2007). A pan-European River and Catchment Database. European Commission - Joint Research Centre (Report EUR 22920 EN) Luxembourg, 120 p.

Weisse T, Tande K, Verity P, Hansen F, Gieskes W (1994). The trophic significance of *Phaeocystis* blooms. Journal of Marine Systems 5(1): 67-79.

Appendix

A. Patterns of chlorophyll *a* variability: method

Cloern and Jassby (2010) decomposition model (annual, seasonal and residual components) was applied on Remote Sensing chlorophyll *a* (RS Chl) at several stations representative of phytoplankton dynamics (coastal vs. offshore, oceanic influence vs. river influence) in the EMoSEM national domains (BE, FR, PT). As an example, Figure A1 shows the decomposition of the RS chlorophyll *a* signal at station 330 in the Belgian Continental Shelf.

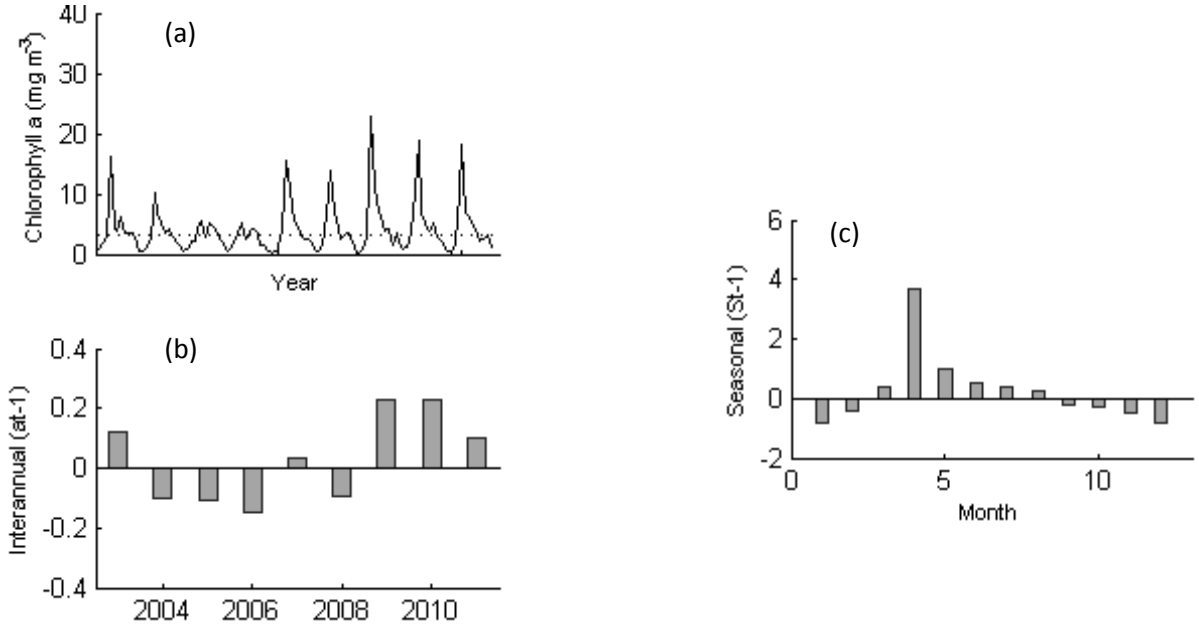

Figure A1: (a) RS Chl long-time series (MERIS 2003-2011) at station 330 in the BCS. The multiyear grand median is indicated with dashed line. (b) Interannual pattern over the period indicating years of high/low Chl. (c) Seasonal pattern averaged over the period 2003-2011.

The multiplicative decomposition model of Chl may be applied provided there is a log-log relationship between the seasonal variability and the annual mean of Chl, and a log-log relationship between the year-to-year variability and the long-term mean of Chl. These requirements are checked in Figure A2.

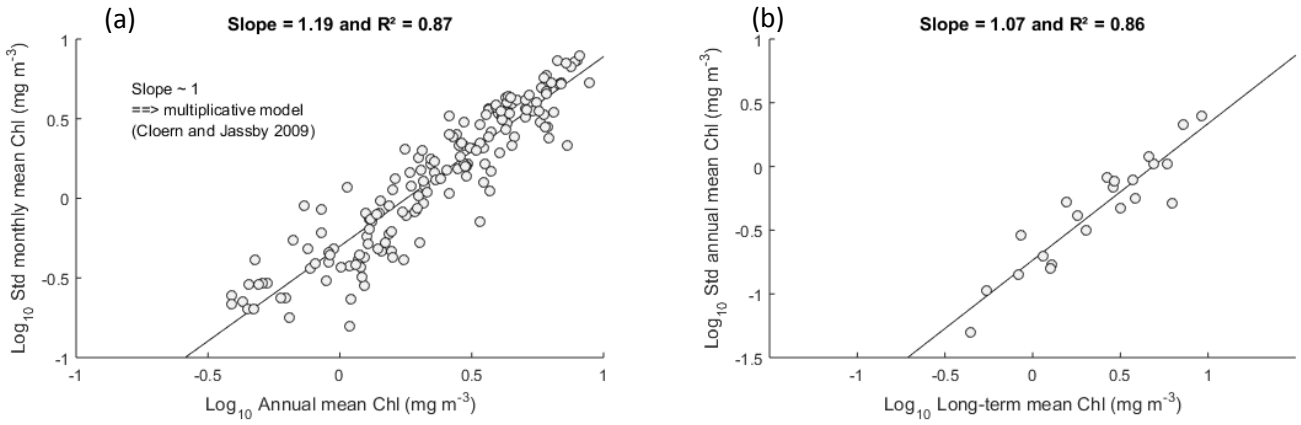

Figure A2: (a) Relationship between the seasonal variability and the annual mean of chlorophyll a for 22 stations meeting minimum data requirement (data coverage in time during the period >75%). (b) Relationship between year-to-year variability and long-term mean chlorophyll a for the same stations as in (a).

The decomposition of the long-time series of Chl allows to identify the annual, seasonal and residual components of the signal. This is illustrated for some stations in the NEA in Figure A3.

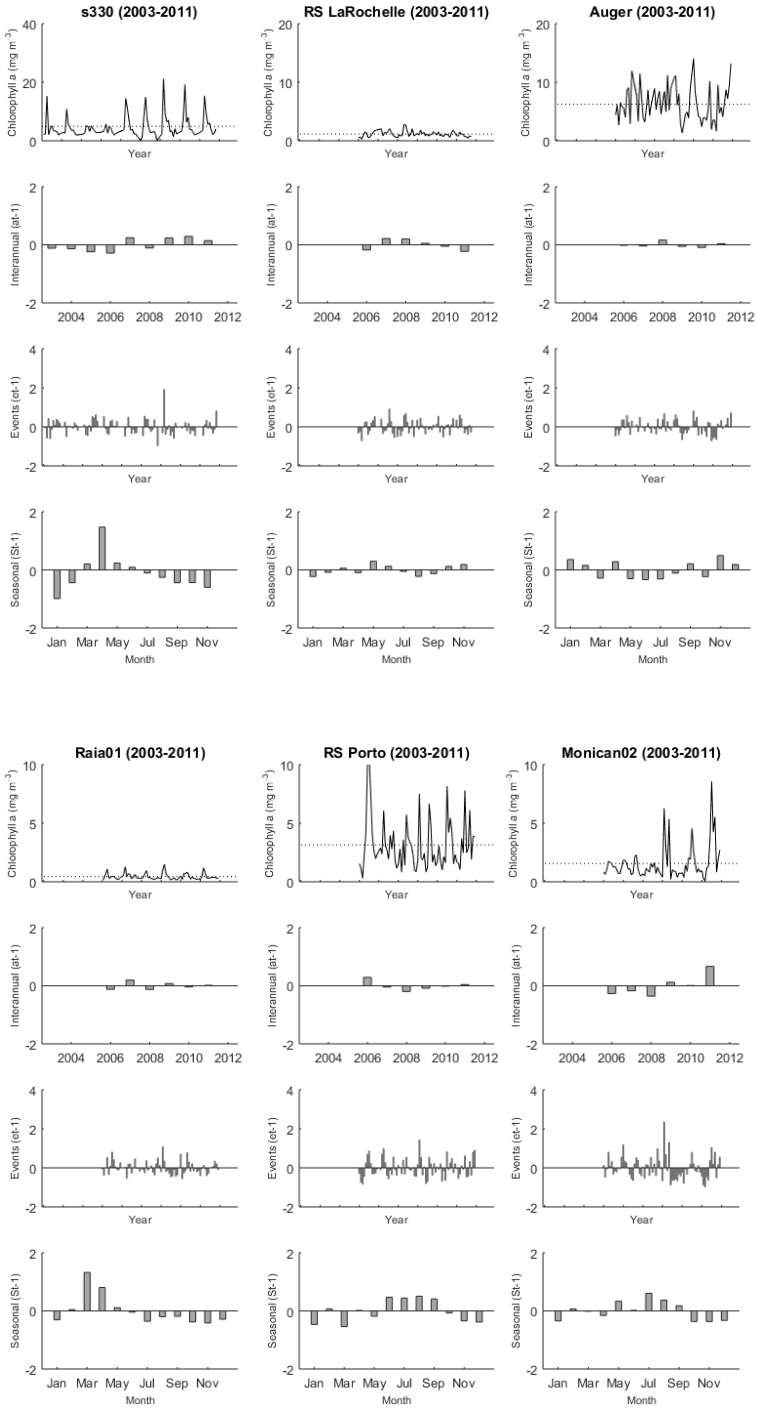

Figure A3: Decomposition in six stations across the NEA of the long-time series of Chl signal (top) into its annual component (middle top), its residual component (middle bottom) and its seasonal component (bottom).

B. Marine model results for the GAP scenario

The following maps exclude the Portuguese model results as these results have not yet been produced.

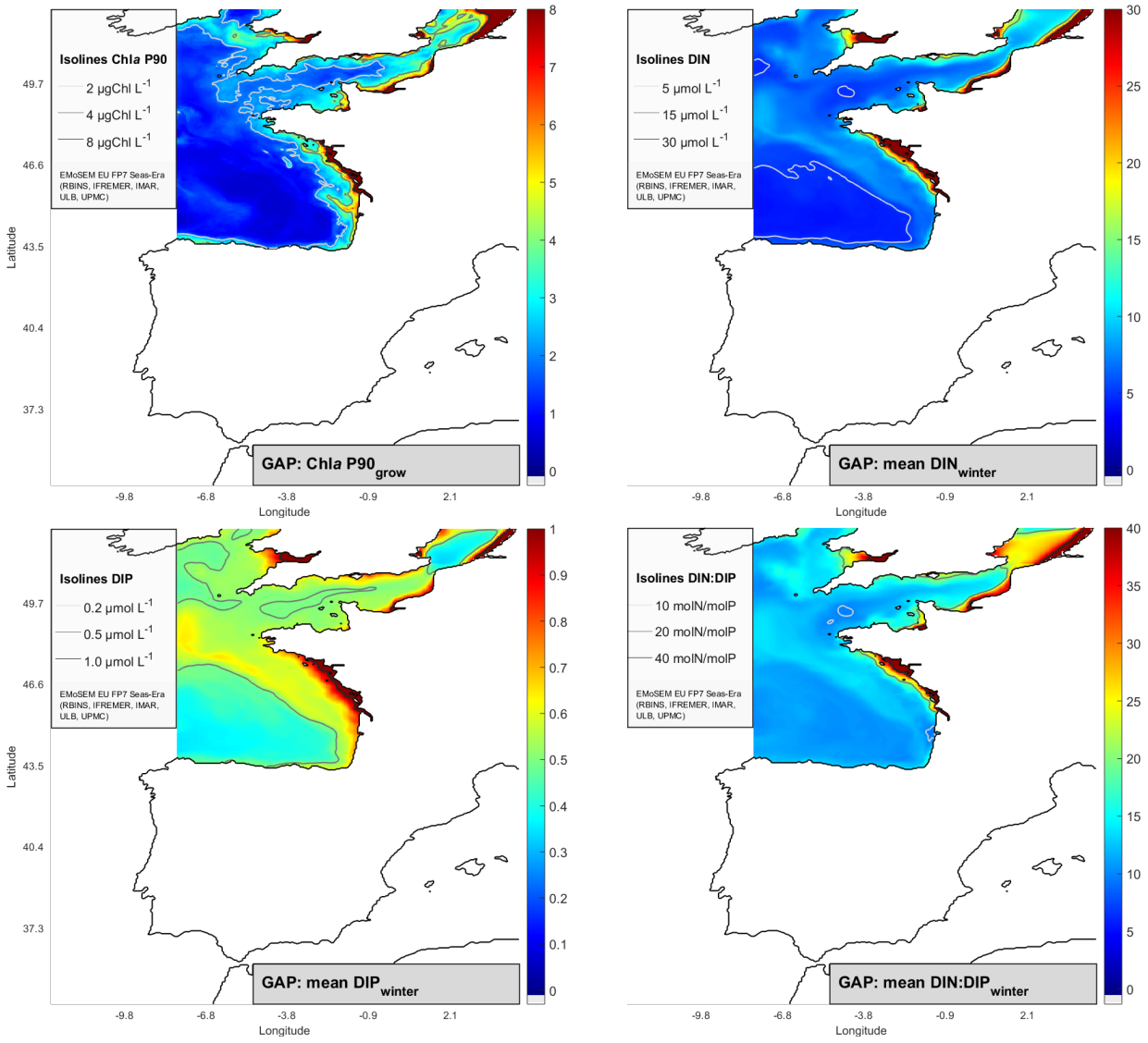

Figure A4: NEA-integrated contour maps of modelled Chl P90 (Mar-Oct), winter DIN (Jan-Feb), winter DIP and winter DIN:DIP ratio on a year with average meteorological conditions. Each graph represents a different parameter for the scenario GAP. Results from MIRO&CO, ECO-MARS3D and BIOPCOMS, with river inputs from PyNuts-Riverstrahler.

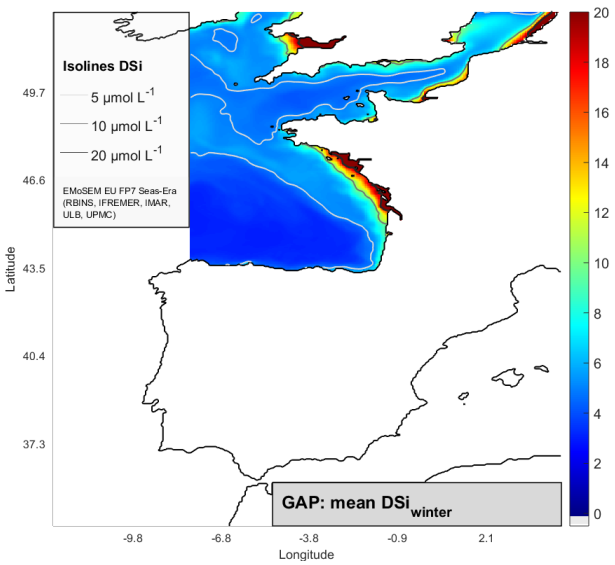

Figure A5: NEA-integrated contour map of modelled winter DSi (Jan-Feb) on a year with average meteorological conditions for the scenario GAP. Results from MIRO&CO, ECO-MARS3D and BIOPCOMS, with river inputs from PyNuts-Riverstrahler.

C. Dissemination

1. Publications

- Ascione Kenov I, Campuzano F, Franz G, Fernandes R, Viegas C, Sobrinho J, de Pablo H, Amaral A, Pinto L, Mateus M, Neves R (2014). Advances in Modeling of Water Quality in Estuaries, in: Finkl, C.W., Makowski, C. (Eds.), Remote Sensing and Modeling. Springer International Publishing, pp. 237-276.
- Billen G, Lasseletta L, Garnier J (2014). A biogeochemical view of the global agro-food system: Nitrogen flows associated with protein production, consumption and trade. Global Food Security, 3: 209-219.
- Billen G, Lassaletta L, Garnier J (2015) A vast range of opportunities for feeding the world in 2050: trade-off between diet, N contamination and international trade. Envir. Res. Letters 10: 025001. Doi:10.1088/1748-9326/10/2/025001.
- Billen G, Garnier J, Silvestre M (2015). A simplified algorithm for calculating benthic nutrient fluxes in river systems. International Journal of Limnology, 51: 37-47.
- Desmit X, Ruddick K, Lacroix G (2015). Salinity predicts the distribution of chlorophyll a spring peak in the southern North Sea continental waters. Journal of Sea Research 103: 59-74. Doi: 10.1016/j.seares.2015.02.007.
- Lancelot C, Passy P, Gypens N (2014). Model assessment of present-day *Phaeocystis* colony blooms in the Southern Bight of the North Sea (SBNS) by comparison with a reconstructed pristine situation. Harmful Algae 37: 172-182 & corrigendum (Fig. 7).
- Lassaletta L, Billen G, Grizzetti B, Anglade J, Garnier J (2014). 50 year trends in nitrogen use efficiency of world cropping systems: the relationship between yield and nitrogen input to cropland. Environ. Res. Lett. 9, 105011 (9pp).

2. Conferences

2.1 Session chair

- "Coastal ecosystem under anthropogenic pressure: impact on ecosystem structure and services". European Geosciences Union (EGU), General Assembly 2013, Vienna (Austria), 07-12 April 2013.
  Convener: N. Gypens, Co-Conveners: M. Grégoire, J. Bruggeman, S. Nelson.
- "Impacts of anthropogenic pressures on coastal ecosystem functioning and services". European Geosciences Union (EGU), General Assembly 2014, Vienna (Austria), 27 April – 02 May 2014.
  Convener: N. Gypens, Co-Conveners: M. Grégoire, A. Newton, A. Borja, C. Solidoro.
- ”Biogeochemistry of coastal seas and continental shelves and impacts of anthropogenic pressures on coastal ecosystem functioning and services”. European Geosciences Union (EGU), General Assembly 2015, Vienna (Austria), 12-17 April 2015.
  Convener: H. Thomas, Co-Conveners: A. V. Borges, N. Gypens, M. Grégoire.

2.2 Oral presentations

- Billen G, Garnier J, Silvestre M. A generic algorithm for modelling benthic nutrient fluxes in river systems. Soil and Water Assessment Tool (SWAT), Toulouse (France), 15-19 July 2013.
- Desmit X, Lacroix G. Rise and fall of classical ecological modelling. Innovative Approaches in Marine Environment Modelling (AIMEN), Brest (France), 19-23 August 2013.
- Ménesguen A. Noxious effects of the increasing eutrophication of coastal marine ecosystems: how far should we reduce the terrestrial nutrient loading? 7ème Symposium sur la Biodiversité marine. Fondation total, Porquerolles (France), October 2013.
- Ménesguen A. Influence en mer des apports nutritifs des fleuves : domaines d'influence et effets eutrophisants. 15 ans d'Ecoflux, Brest (France), 11 October 2013.
- Ménesguen A., Dussauze M., Dumas F., Lecornu F. *Using ecological modelling to assess the role of each French watershed in some eutrophication and HAB occurrences (Pseudo-Nitzschia, Karenia, Phaeocystis) in the Bay of Biscay and the English Channel. Estuarine Coastal and Shelf Science (ECSA 53), Shanghai (China), 13-17 October 2013.*
- Dulière V, Gypens N, Lancelot C, Luyten P, Desmit X, Lacroix G. Linking human activities to eutrophication along the river ocean continuum with an ecological model. VLIZ Young Scientist's Day, Brugge (Belgium), 07 March 2014. [2nd award]
- Lacroix G. Ecosystem Models as Support to Eutrophication Management in the North Atlantic Ocean (EMoSEM): first year report. SEAS-ERA Final Conference, Palma de Majorca (Spain), 8-9 April 2014.
- Dulière V, Gypens N, Desmit X, Lacroix G. Tracking nutrients in the southern North Sea. Joint Numerical Sea Modelling Group Conference (JONSMOD 2014), Brussels (Belgium), 12-14 May 2014.
- Lancelot C. Cultural eutrophication in the Greater North Sea: cause, symptoms, mitigation. Eutrophication of coastal waters – ISECA final conference, Boulogne-sur-Mer (France), 30 June – 01 July 2014. [Invited presentation]
- Dulière V, Thieu V, Gypens N, Lancelot C, Luyten P, Desmit X, Lacroix G. Linking human activities to eutrophication in the southern North Sea. Advances in Marine Ecosystem Research (AMEMR IV), Plymouth (UK), 30 June – 04 July 2014.
- Dulière V, Gypens N, Lancelot C, Thieu V, Luyten V, Lacroix G. Tracing back nutrients from southern North Sea eutrophicated areas up to the watersheds. European Geosciences Union (EGU), General Assembly 2014, Vienna (Austria), 27 April – 02 May 2014.
- Campuzano F., Brito D., Juliano M., Fernandes R., Neves R. Effect of the river discharge implementation in an operational model for the West Iberia coastal area. European Geosciences Union (EGU), General Assembly 2014, Vienna (Austria), 27 April – 02 May 2014.
- Thieu V, Silvestre M, Billen G, Garnier J, Passy P, Lassaletta L. Nutrient transfer in aquatic continuum and delivery to coastal zone: rising up the challenge of a generic application of the

Riverstrahler ecological model to the watershed domain of the European North Atlantic Ocean. I.S. Rivers International Conference, Lyon (France), 22-26 June 2015.

- Lacroix G, Dulière V, Desmit X, Gypens N, Lancelot C, Billen G, Garnier J, Thieu V, Silvestre M, Passy P, Lassaletta L, Ménesguen A, Thouvenin B, Dussauze M, Mateus M, Neves R, Sobrinho J, Ascione Kenov I, Campuzano F., Pinto L., Garcia C. Ecosystem Models as Support to Eutrophication Management in the North Atlantic Ocean (EMoSEM). World Conference on Natural Resource Modeling (RMA 2015), Bordeaux (France), 29 June – 01 July 2015.
- Desmit X, Billen G, Thieu V, Passy P, Silvestre M, Garnier J, Dulière V, Ménesguen A, Pinto L, Gypens N, Campuzano F, Ramiro N, Lancelot C, Lacroix G. Reducing marine eutrophication needs a paradigmatic change. Marine and Human Systems (IMBER IMBIZO IV), Trieste (Italy), 26-30 October 2015.

2.3 Posters

- Lacroix G, Billen G, Desmit X, Garnier J, Gypens N, Lancelot C, Lenhart H, Los H, Mateus M, Ménesguen A, Neves R, Troost T, Van der Molen J. Ecosystem Models as Support to Eutrophication Management in the North Atlantic Ocean (EMoSEM). European Geosciences Union (EGU), General Assembly 2013, Vienna (Austria), 07-12 April 2013.
- Lacroix G, Billen G, Desmit X, Dulière V, Garnier J, Gypens N, Lancelot C, Lenhart H, Los H, Mateus M, Ménesguen A, Neves R, Troost T, Van der Molen J. Ecosystem Models as Support to Eutrophication Management in the North Atlantic Ocean (EMoSEM). *Estuarine Coastal and Shelf Science (ECSA 53), Shanghai (China), 13-17 October 2013.*
- Lacroix G, Desmit X, Dulière V, Gypens N, Lancelot C, Billen G, Garnier J, Thieu V, Silvestre M, Passy P, Lassaletta L, Guittard G, Théry S, Ménesguen A, Thouvenin B, Dussauze M, Mateus M, Neves R, Sobrinho J, Ascione Kenov I, Garcia C, Lenhart H, Los H, Troost T, Van der Molen J. Ecosystem Models as Support to Eutrophication Management in the North Atlantic Ocean (EMoSEM). VLIZ Young Scientist's Day, Brugge (Belgium), 07 March 2014.
- Lancelot C, Passy P, Gypens N. How significant are *Phaeocystis* colony blooms in the present-day southern North Sea compared to a reconstructed pristine situation: a model study. European Geosciences Union (EGU), General Assembly 2014, Vienna (Austria), 27 April – 02 May 2014.
- Gypens N, Passy P, Thieu V, Lancelot C. Present-day and projected magnitude of *Phaeocystis* colony blooms in southern North Sea. Advances in Marine Ecosystem Research (AMEMR IV), Plymouth (UK), 30 June – 04 July 2014.
- Ménesguen A., Dussauze M. Designing optimal scenarios of nutrient loading reduction in a WFD/MSFD perspective by using passive and active tracers in a biogeochemical-3D model of the English Channel/Bay of Biscay area. Advances in Marine Ecosystem Research (AMEMR IV), Plymouth (UK), 30 June – 04 July 2014.

3. Science policy support

- **ISC/PA4b**
  Communication: Lacroix G, Billen G, Desmit X, Garnier J, Gypens N, Lancelot C, Lenhart H, Los H, Mateus M, Ménesguen A, Neves R, Thieu V, Troost T, Van der Molen J. Ecosystem Models as Support to Eutrophication Management in the North Atlantic Ocean (EMoSEM). International Scheldt Commission, PA4b Coastal and transitional waters, Antwerpen (Belgium), 25 March 2013.
- **OSPAR ICG-MSFD**
  Participation of Geneviève Lacroix to the "Monitoring Workshop", Brussels (Belgium), 06 June 2013.
- **OSPAR ICG-EUT**
  1. Communication in the session "Dialogue ICG EUT – ICG EMO on modelling needs": Lacroix G, Lancelot C. Combining river catchment model and marine ecosystem models: lessons learned from EMoSEM. OSPAR ICG-EUT Workshop, Paris (France), 3-5 February 2014.
  2. Participation of Christiane Lancelot & Geneviève Lacroix to the session "JOINTLY Testing Eutrophication Common Indicators and new elements of updated Common Procedure". "*Phaeocystis*" test case. OSPAR ICG-EUT Workshop, Paris (France), 3-5 February 2014.
- **OSPAR ICG-EMO**
  Follow up of the ICG-EMO activities by Geneviève Lacroix and Alain Ménesguen.
  Regular exchanges with Herman Lenhart (chair), Johan Van der Molen, Tineke Troost et al. to identify synergies between EMoSEM and ICG-EMO.
- Participation of Wendy Bonne to the EMoSEM final project meeting and discussion about the **WFD intercalibration** study.
- **MONIT.BE**
  Participation of Geneviève Lacroix to the Steering group MONIT.Be (topic eutrophication).
- **"Rapport fédéral en matière d'environnement 2004-2008"**
  Participation of Geneviève Lacroix to the report update (topic eutrophication).
- **A Policy brief** at the intention of policy makers will be prepared and send to local authorities after the project.

4. Communication products

- **Leaflet.** Project presentation widely distributed
  http://odnature.naturalsciences.be/assets/users/emosem/flyer_emosem_july2013.pdf
- Lancelot C (2014). Fiche "eutrophication" (Institut Océanographique Monaco)
  http://institut-ocean.org/images/articles/documents/1412071686.pdf

5. Project website

http://odnature.naturalsciences.be/emosem/